The 2015 AIAA/Cessna Aircraft Company/Raytheon Missile Systems Design/Build/Fly Competition Flyoff was held at TIMPA Field in Tucson, AZ on the weekend of April 10-12, 2015. This was the 19th year the competition was held. Of the 100 entries this year, 84 teams submitted written reports to be judged and were eligible to participate in the flyoff. Sixty-five (65) teams attended the flyoff, all of which completed the technical inspection. Over 650 students, faculty, and guests were present. The weather was excellent allowing for non-stop flying. Of the 262 official flight attempts, 121 resulted in a successful score with 56 teams achieving a flight score (a new record!). Twenty-three (23) teams successfully completed all three missions. The quality of the teams, their readiness to compete, and the execution of the flights continues to improve each year.

The contest theme this year was a Remote Sensor Delivery and Drop System. The first mission was a Ferry Flight with no payload to see how many laps each team could fly in 4 minutes. The second mission was a Sensor Package Transport Mission with a 5 lb internal payload with the time to fly three laps as the score. The third mission was a Sensor Drop Mission in which the externally carried payload (12" whiffle balls) were dropped on each lap with the score being the number of laps with a successful drop. A ground mission was also required consisting of a timed loading of the payloads for mission 2 and 3. As usual, the total score is the product of the flight score and written report score. More details on the mission requirements can be found at the competition website: http://www.aiaadbf.org .

First Place went to the University of Ljubljana, the first time an international team has won DBF, Second Place went to University of California Irvine and Third Place went to Georgia Institute of Technology. A full listing of the results is included below. The Best Paper Award, sponsored by the Design Engineering TC for the highest report score, went to Georgia Institute of Technology with a score of 98.50.

We owe our thanks for the success of the DBF competition to the efforts of many volunteers from Cessna Aircraft, Raytheon Missile Systems, and the AIAA sponsoring technical committees: Applied Aerodynamics, Aircraft Design, Flight Test, and Design Engineering. These volunteers collectively set the rules for the contest, publicize the event, gather entries, judge the written reports, and organize the flyoff. Thanks also go to the corporate Sponsors: Raytheon Missile Systems and Cessna Aircraft Company, and also to the AIAA Foundation for their financial support. Special thanks go to Raytheon Missile Systems for hosting the flyoff this year.

Finally, this event would not be nearly as successful without the hard work and enthusiasm from all the students and advisors. If it weren't for you, we wouldn't keep doing it.

Russ Althof
For the DBF Governing Committee

UNIVERSITY OF LJUBLJANA

Faculty of Mechanical Engineering

2015 DESIGN – BUILD – FLY COMPETITION

EDVARD RUSJAN SLOVENIAN TEAM

AIRPLANE DESIGN REPORT

Table of Contents

1 Executive Summary

This report details the design, testing and manufacturing of the Edvard Rusjan Slovenian Team's EDA 2015 for the 2014/2015 AIAA Student Design/Build/Fly (DBF) Competition. The team's aim is to produce an airplane that maximizes the score according to the rules [1] provided by the contest organizers. There are ground mission and three flight missions required for the airplane to load quickly and fly successfully.

1.1 Design Process

The primary objective for EDA 2015 is good result. This would be achieved through a thorough analysis of the competition rules [1]. At the beginning the team considered most of known basic designs but then, considering past years' experience concluded that a classic low wing airplane would be our best choice. The design was then further analyzed using figures of merit to reflect important mission variables. This included stability and control, lifting area, weight, drag, transportability, speed, reliability and manufacturability. The team find out that the empty weight, number of servos, number of balls and maximum speed were the key mission requirements for which the airplane needs to be optimized. Based on all analysis and previous experience the team found out that a tractor propeller low passive (no ailerons) wing tail dragger airplane is the best solution for the 2015 year competition due to the accessible cargo bay, lightweight undercarriage and low number of servos.

1.2 Design and Performance Highlights

The chosen airplane is low wing design with spacious fuselage. The wing is sized to 6.56 ft (2.0 m) wingspan, 0.656 ft (0.2 m) chord and a total wing area of 4.30 ft^2 (0.4 m^2) with aspect ratio of 10. The NACA 6514 low drag high lift airfoil was selected for the wing. The empty weight (without payload) of the airplane was estimated to 2.86 lb (1.3 kg) and the maximum take-off weight to 7.86 lb (3.57 kg). The motor chosen for the airplane was Peggy Pepper 2221/16 with gearbox Micro Edition 5:1. The battery pack is 16 cells XCell 1600 mAh and the propellers are APC 15×8 and 14×10. The wing is made of balsa wood and light cover. The top speed in horizontal flight is about 46 kt (85 kph) and the number of complete laps is 8 in 4 minutes. The number of balls taken is 2. Time for three 3 laps is 110s.

2 Management Summary

The 2015 Edvard Rusjan Slovenian Team consists of 20 members of whom 13 are seniors others are juniors at University of Ljubljana, Faculty of Mechanical Engineering, Slovenia, EU.

2.1 Team Organization

The team used a hierarchical structure to establish leadership and responsibility amongst its members. The team was led by the Program Manager with the help of Mentor, who was responsible for overall team

productivity and progression. However, the hierarchy served as an outline only, as all team members collaborated extensively to reach deadlines, exchange opinions and many ideas, all for the good of producing a better airplane. The work was divided into 5 design phases/groups as shown in Figure 2.1.

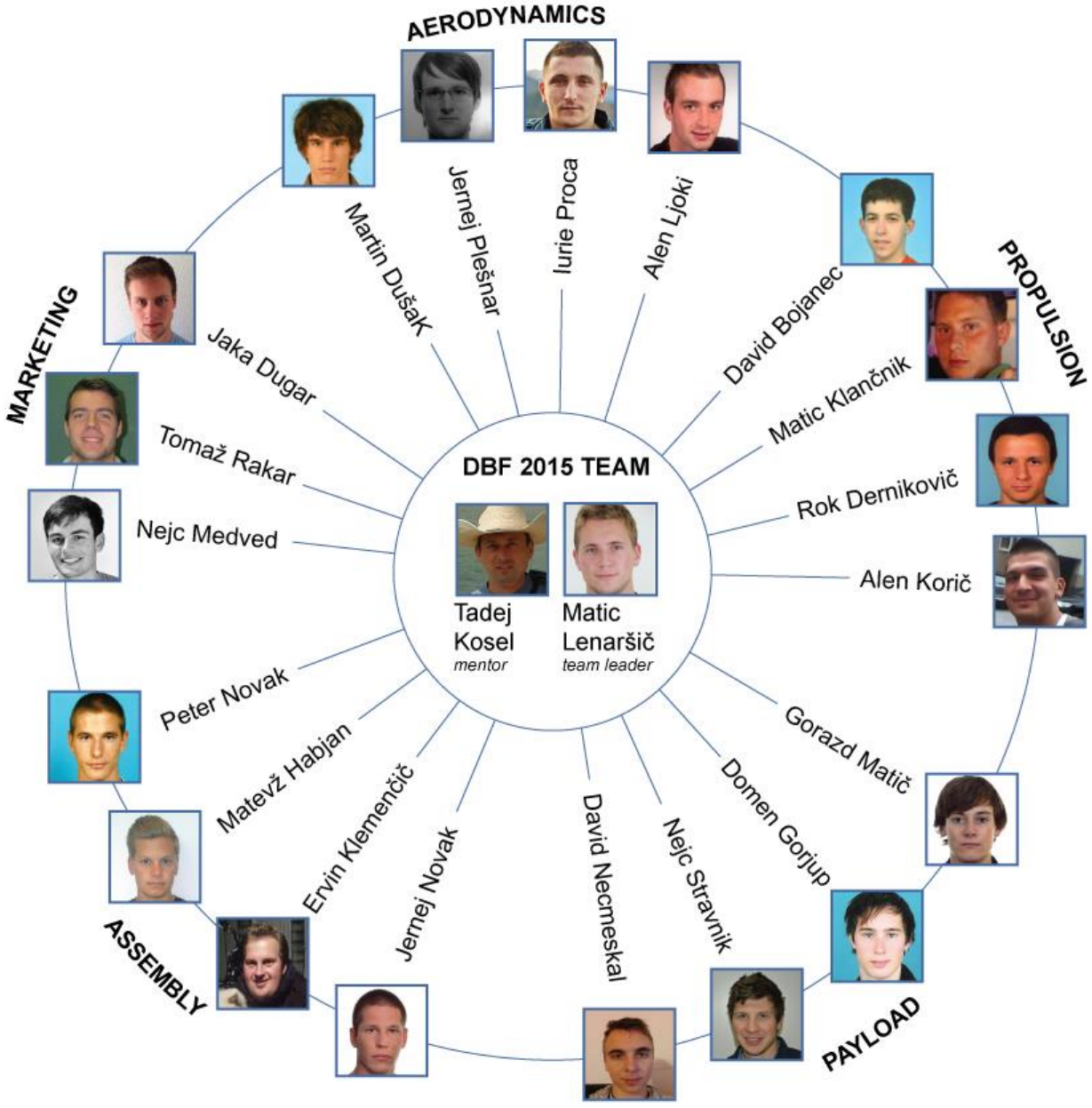

Figure 2.1: Team organization

Working groups are as follows:

- **Aerodynamics:** Optimize the airplane size, airfoil selection, aerodynamic calculations, control surface sizing and stability and control analysis.
- **3D Design:** Laying out the overall airplane's internal and external design, and to provide 3D design by using 3D software. Working out a manufacturing scheme, selecting materials, structural and material testing.
- **Propulsion:** Selecting appropriate propulsion system, the analysis of power requirements for each mission, and also for testing these propulsion systems in wind tunnel.
- **Payload:** Optimization of cargo space and cargo distribution in the cargo bay.
- **Promotion & Report Writing:** Writing the report and analysis of testing results. Providing finances, project promotion, sponsorship and travel organization.

2.2 Milestone Chart

The design project was conducted over two semesters at University of Ljubljana. Within this time frame, the implementation of a structural design schedule throughout the two semesters is vital to develop a competitive design of the airplane and report for successful participation in the competition. The development schedule is shown in Figure 2.2 and outlines the sequences of critical tasks for successful project completion.

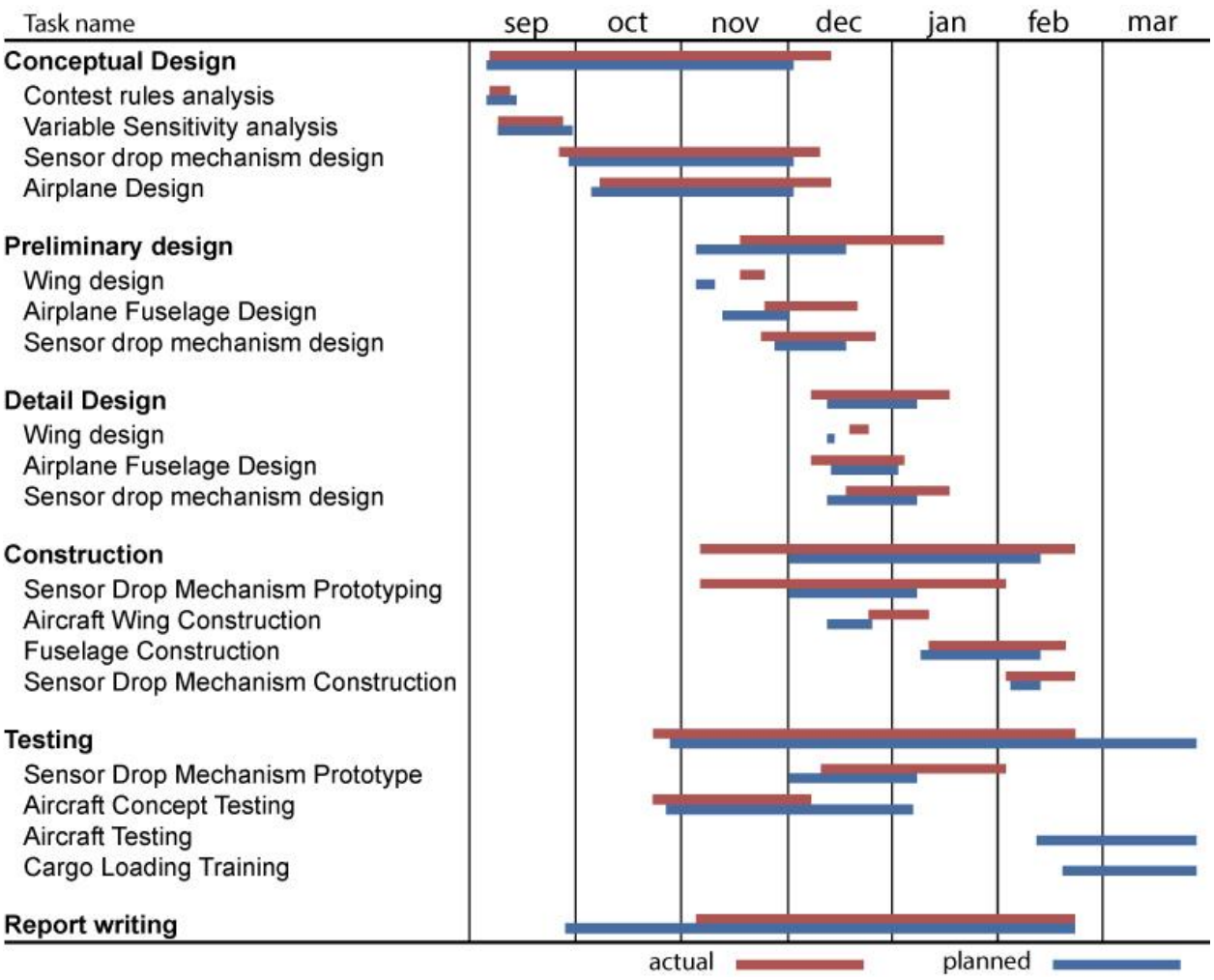

Figure 2.2: Development schedule

3 Conceptual Design

This section describes in detail the conceptual design for the team's airplane. Possible airplane configurations were explored with morphological matrices. Many of these configurations were eliminated by the team's quality assessment. The remaining configurations were evaluated by the Figure of Merit (FOM) analysis. These FOM were weighted to reflect various features affecting the missions: weight, loading and flight time of the airplane. Process of conceptual design methodology is shown in Figure 3.1

Figure 3.1: Conceptual design methodology

3.1 Mission Requirements for Backcountry Rough Field Bush Plane

The airplane and its systems must meet several performance, propulsion, structural and payload requirements. The competition features ground mission and three flight missions. The ground mission and the flight missions score is normalized across all airplanes that successfully complete each mission. The total mission score (TMS) is the weighted sum of flight scores. General specifications and missions specifications are listed below:

- Maximum take-off distance for all missions is 60 ft (18.3 m).
- Airplane must support multiple payloads (internal and external). Internal cargo (stack of boards) weight is 5 lb (2.27 kg) in the second mission, while in the third mission cargo weight is not specified and consists of Champro 12" Plastic Balls.
  Number of balls must be at least one ($n \geq 1$).
- Battery pack(s) maximum weight limit is 2.0 lb (908 g).
- Maximum current limit is not specified (per motor and battery pack). Fuse is strongly advise.
- Payload loading and check out must be completed in less than 5 minutes.

Mission		Description	Payload	Measure	Score
Payload Loading Mission	**0**	Payload Loading	Stack of Boards Champro Balls	Loading Time	$GS = T_{\text{Fast Load}}/T_{\text{Team Load}}$ or $GS = 0.2$
Ferry Flight	**1**	No. of Laps in 4 min	Empty	No. of Laps	$M_1 = 2 \cdot (N_{\text{Laps Team}}/N_{\text{Laps Max}})$
Sensor Package Transport Mission	**2**	3 Laps	Stack of Boards	Flight Time	$M_2 = 4 \cdot (T_{\text{Fast}}/T_{\text{Team}})$
Sensor Drop Mission	**3**	Ball Drop Laps	Champro Balls	No. of Laps	$M_3 = 6 \cdot (N_{\text{Laps Team}}/N_{\text{Laps Max}})$

Table 3.1: Mission summary

3.1.1 *Ground Mission (Payload Loading Time)*

The team will be required to load the payload for mission 2 and mission 3 in the airplane. Mission starts with the empty airplane and all hatches closed. Crew loads payload for Mission 2, re-close airplane as required to secure for flight then crew leaves the loading area. Timing is paused to verify airplane is secure then timing is restarted. Crew removes mission 2 payload and installs mission 3 payload. Hatches must be re-closed as required to secure for flight. Number of Champro balls will be the maximum number declared during tech inspection. Crew leaves the loading area after that timing is stopped. Airplane will be verified that is secured for flight. Ground Score is:

$$GS = \frac{T_{\text{Fast Load}}}{T_{\text{Team Load}}}$$

If ground mission has not been completed, then Ground Score is:

$$GS = 0.2$$

The mission must be completed within five minutes from the start.

3.1.2 Flight Mission One Requirements (Ferry Flight)

Mission 1 requires the airplane to complete maximum number of laps in a 4 minute flight time. The airplane without payload has to fly as fast as possible. The score M_1 depends on the team's completed laps:

$$M_1 = 2 \cdot \frac{N_{\text{Laps Team}}}{N_{\text{Laps Max}}}$$

Time starts when the throttle is advanced for the (first) take-off (or attempt). A lap is complete when the airplane passes over the start/finish line in the air. Mission score is normalized over all teams successfully completing this mission ($N_{\text{Laps Max}}$).

3.1.3 Flight Mission Two Requirements (Sensor Package Transport Mission)

Mission 2 requires the airplane to complete three laps with internal cargo. Internal cargo (simulated Sensor Package) is one stack of three standard 2×6 wooden pine boards (dimensional lumber), 10" (254 mm) long (i.e. wooden block). The nominal overall size of payload is 4.5"×5.5"×10" (114.3×139.7×254.0 mm) and nominal weight 5 lb (2.27 kg). Dimensional tolerance is ± 1/8" (± 3.175 mm) in all directions. The score M_2 depends on time of flight for three laps:

$$M_2 = 4 \cdot \frac{T_{\text{Fast}}}{T_{\text{Team}}}$$

Mission score is normalized over all teams successfully completing this mission (T_{Fast}).

3.1.4 Flight Mission Three Requirements (Sensor Drop Mission)

Mission 3 requires the airplane to remotely drop a Champro 12" plastic ball during each lap. The drop shall occur in a "drop zone" parallel to runway away from spectators in upwind leg. Nominal weight for each ball is approximately 1 oz (28.35 g). A lap will only count if a single ball is dropped within the drop zone. Multiple drops in the zone on a single lap will invalidate that lap. No other part of the airplane or payload mounting system may drop with the ball. The score M_3 depends on number of laps:

$$M_3 = 6 \cdot \frac{N_{\text{Laps Team}}}{N_{\text{Laps Max}}}$$

Time starts when the throttle is advanced for the (first) take-off (or attempt). Time ends when the airplane passes over the finish line (in the air) at the completion of the last lap. Number of laps $N_{\text{Laps Max}}$ is the maximum number of laps for all teams successfully completing this mission.

3.2 Score Calculation

Score (S) will be computed from Written Report Score (WRS), Flight Score (FS), Total Mission Score (TMS), Rated Aircraft Cost (RAC) and Ground Score (GS) using the formula:

$$S = WRS \cdot TMS$$

TMS is the product of the Ground Score and Flight Score:

$$TMS = \frac{GS \cdot FS}{RAC}$$

FS is the sum of the individual flight mission scores:

$$FS = M_1 + M_2 + M_3$$

The RAC (Rated Airplane Cost) is product of the Empty Weight (EW) and Number of Servos used in the airplane (N_{Servo}) of the airplane:

$$RAC = EW \cdot N_{\text{Servo}}$$

Empty Weight will be measured after each successful scoring flight:

$$EW = \text{Max}(EW_{\text{Mission 1}}; EW_{\text{Mission 2}}; EW_{\text{Mission 3}})$$

EW is the post flight weight with the payload removed.

3.3 Translation of Mission Requirements into Design Requirements

A score sensitivity study is conducted to evaluate the effect of mission scoring parameters on the competition score. The most important scoring parameter is RAC which depends on the empty weight (EW) of the airplane in lb and number of servos (N_{Servo}). The influence of the empty weight and number of servos on the $1/RAC$ is shown in Figure 3.2. We can see that the influence is gaining towards the zero empty weight and zero number of servos. The empty weight is the most challenging design requirement of the competition and must be as small as possible and all efforts must be used to reduce it.

Mission/Scoring Requirement	Design Requirement
60 ft (18.3 m) Ground Roll	High Motor Thrust, High Wing Area, Low Weight
High Speed	High Motor Power, Low Drag, Low Weight, Low Wing Area
High Load Capability	High Lift Airfoil, High Wing Area
Internal Cargo	Internal Bay, Spacious Fuselage
External Cargo	Retractable Pylons
Low Weight	Efficient Monocoque Structure
Simplicity	Low Number of Servos, No Flaps, No Ailerons

Table 3.2: Design requirements

For design point we used empty weight 2.86 lb (1.3 kg) and three servos. Three servos (elevator, rudder, motor controller) are minimum possible number of servos for powered fully defined remote control airplane. Theoretically the remote controlled airplane can be controlled only by two motors (two servos) about all three axes (pitch, roll, yaw), but this configuration is not applicable for the completion due to lack of controllability of the airplane in all phases of flight. The $1/RAC$ must be maximized as much as possible to get the maximum score.

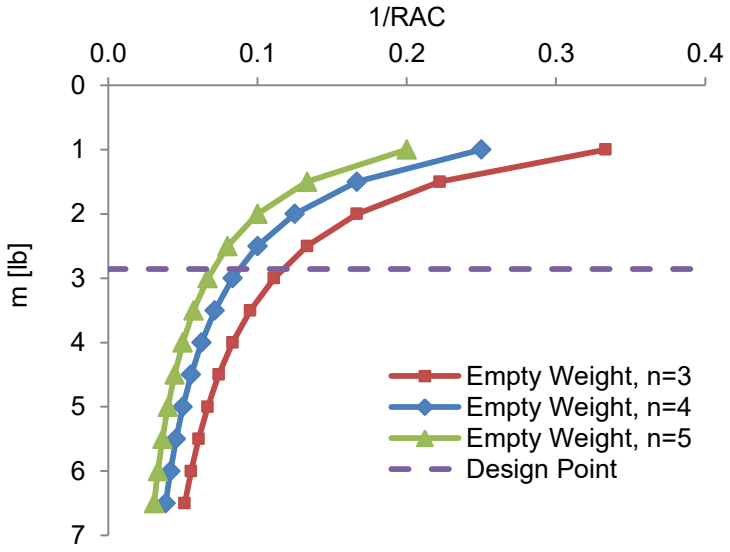

Figure 3.2: Influence of empty weight and number of servos on the $1/RAC$

From Figure 3.2 we can see how the number of servos influences on the $1/RAC$. If we increase the number of servos from 3 to 4, we lose 25% of final score and if we increase the number of servos from 3 to 5, we lose 40% of final score. So the number of servos has huge influence on the final score.

Influence of the number of laps, number of dropped balls and time of flight on the flight mission score is shown in Figure 3.3. We can see that the largest impact on the score of flight missions has mission 3 which depends on the number of dropped balls. We estimate that we will make 8 laps with average flight speed of 49 kt (90.8 kph) in the mission 1, 102 s flight time for 3 laps in mission 2 with average speed of 48.3 kt (89.4 kph) and drop 2 balls in the mission 3. We conclude that the number of balls is the most important mission requirement after RAC factor. For mission score calculations we assumed the maximum 8 laps, 2 balls and 102 s of flight time as best of all team score due to simplicity. The score of other teams is hard to predict. On the other hand large number of balls means complex airplane and complex drop mechanism and larger empty weight.

Very important factor is also ground mission time for loading/unloading of mission 2 and mission 3 payload. Ground mission score is multiplied with flight mission score. Its maximum value is 1 for the fastest team. If the fastest team loading/unloading time is 5 s, then one second more (6 s) mean 20% score loss and double time mean 50% score loss.

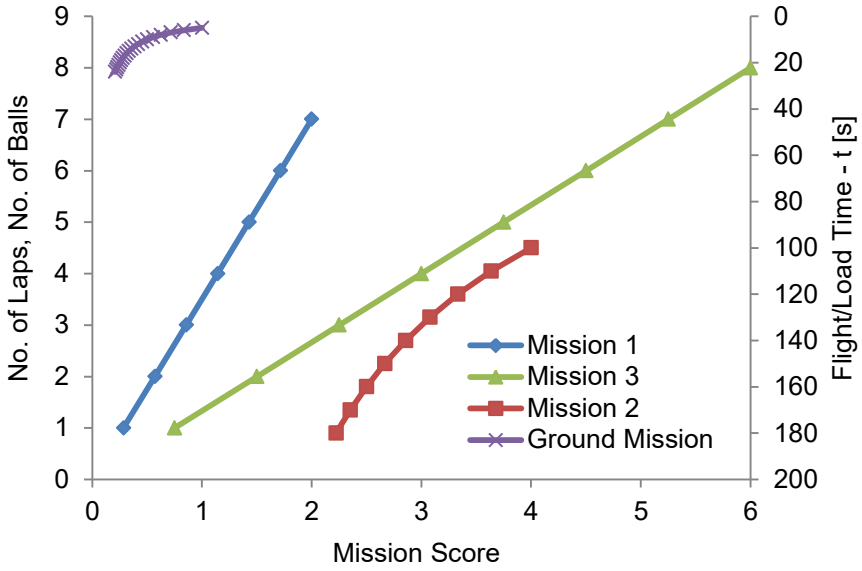

Figure 3.3: The influence of the number of laps, number of balls and time of flight on the mission score

We can see that increasing or decreasing the number of laps for one lap in the mission 1 gives ±0.286 to the total mission score. Increasing or decreasing the number of external balls for one ball in the mission 3 gives ±0.8 to the total mission score and increasing or decreasing the flight time for 10 s in the mission 3 gives approx. ±0.2 to the total mission score. While the ±0.5 lb (227 g) change in weight contributes approx. 0.01 multiplication factor to the total flight score and each servo ±0.02 multiplication factor. We can see that the number of balls in the mission 3, empty weight and number of servos have the largest impact to the total flight score around the design point. Design point was selected on the basis of experience from the past seven years and by weighting all airplane components. We calculated that the empty weight cannot be less than 2.86 lb (1.3 kg) for take-off distance of 60 ft (18.3 m) for payload about 5.0 lb (2.27 kg). The wing area was calculated to 4.3 ft^2 (0.4 m^2).

The team concluded that design solution must be lightweight, simple (lowest possible number of servos and reasonable number of balls (as low as practical)) and must fulfill next objectives and requirements:

- **Ground Mission: Payload Loading Time** – The internal payload bay must be easy accessible, payload bay doors must be very simple to operate and the latch must be simple for quick open/close operations during loading and unloading of payload. Pylons for external payload must

be simple to perform quick loading and securing. During flight in mission 1 and mission 2 must generate as low as possible drag. Pylons must be lightweight and retractable.

- **Mission 1: Ferry Flight** – The main requirement is high flight speed. To fulfill this requirement we need small wing area, low airplane drag and low weight. This can be achieved by low drag airfoil, fuselage aerodynamic shape, lightweight materials and powerful propulsion to reach high speed in flight to perform high number of laps in 4 min.
- **Mission 2: Sensor Package Transport Mission** – Require powerful propulsion system which will provide take-off run (ground roll) less than 60 ft (18.3 m), fast flight and short time for 3 lap flight with wooden block of 5 lb (2.27 kg). The high average flight speed is important for the final score. To fulfill this requirement we need large wing area, low airplane drag, low weight and powerful propulsion system.
- **Mission 3: Sensor Drop Mission** – The team must decide the number of Champro balls. The minimum number is one ball of 1 oz (28.35 g). The maximum weight of balls may not exceed the payload weight in mission 2, which is 5 lb (2.27 kg), for optimal design. The number of balls equals the weight of mission 2 payload is 89. This is huge number of balls therefore the number of carried balls will not influence the size of the wing. The number of balls will slightly influence on the empty weight of the airplane due to larger pylon. The reliable drop mechanism is very important to drop a ball over drop zone and not to drop more than one ball at the time. Larger number of balls requires more complex mechanism which has negative influence to the airplane weight.

3.4 Review of Considered Solution Concepts and Configurations

According to mission/scoring requirements we considered multiple airplane configurations as shown in Table 3.3. Due to internal payload airplane needs to have spacious fuselage with large payload bay and according to RAC the lightweight structure. The empty weight cannot be independently controlled; it is result of the airplane size. Airplane size depends on payload weight and take-off distance. Size of the airplane is growing with increasing payload weight and with decreasing required take-off distance.

	Options		
General Configuration	**Conventional Monoplane**	Flying Wing	Lifting Body
	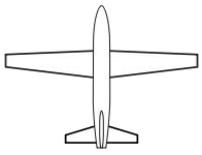	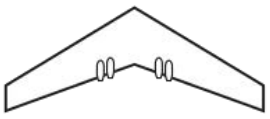	

Wing Configuration	**Monoplane**	Biplane	Triplane
		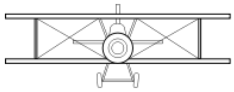	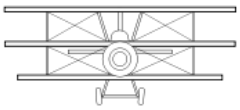
Monoplane Configuration	**Low Wing**	Mid Wing	High Wing
			

Table 3.3: Possible airplane configurations [9]

These solutions for each design configuration were then compared qualitatively against each other for advantages and disadvantages [2].

3.4.1 General Airplane Configuration

Using the qualitative assessment, the team ended up with three designs for further analysis:

- **Conventional Monoplane**

  Advantages: Design with tractor propulsion is simple and very predictable in terms of construction and aerodynamic performance. It has effective high aspect ratio wing with low induced drag and compact fuselage which has enough space for large payload bay. It can be composed of more small parts which is vital for transportation.

  Disadvantages: Large wing span, high profile drag and interference drag due to multiple aerodynamic surfaces.

- **Flying Wing**

  Advantages: Design with tractor style propulsion was considered for the fact that it would eliminate the fuselage components of the airplane. It has low interference and profile drag because there is only wing which all produces lift and there are no other components except undercarriage. It is easy to manufacture and can be made all in one part.

  Disadvantages: It has aerodynamically less efficient wing due to S-shaped airfoil and elevons. It has more complex stability characteristics and narrow allowable center of gravity shift. The payload bay is limited by the shape of the wing and is quite small.

- **Lifting Body**

  Advantages: All body produces lift and the body/fuselage is spacious for payload bay. It can be lightweight because the whole body is compact. All stresses are carried by the skin and the main spar is not needed for required strength. Only ribs are required to maintain the shape of the body. Due to long chord of the body the center of gravity shift can be large. This is good for different payload arrangements and types.

Disadvantages: It is applicable only for high speed flight and has high stall speed. It is not appropriate for short take-off. The body is not aerodynamically efficient due to low aspect ratio and high induced drag. It has possible stability problems.

Team decided to use *conventional monoplane configuration design* which is the most appropriate configuration for this year's rules.

3.4.2 *Conventional Airplane Wing Configuration*

- **Wing Configuration** – There are many possibilities of wing configuration for conventional design. The conventional design means that we have fuselage, one or more wings and empennage. Wing span must be as large as practical due to low induced drag. Therefore we decided to have one high aspect ratio wing (monoplane).
- **Monoplane Configuration** – There are three basic monoplane configurations: low wing, mid wing and high wing. High wing is good for ground clearance, but the access to payload bay is difficult. Mid wing configuration is not practical because the main spar intersects cargo bay. The low wing configuration is the best option if ground clearance is not a problem and if we need quick and easy access to the payload bay. The payload bay is accessible from the top.

For the final design we have chosen a configuration which incorporates advantages of conventional low wing monoplane with conventional fuselage. We decided to have two main wheels and tail skid due to lower weight of undercarriage. The nose wheel is much heavier than the tail wheel or skid. Advantage of this configuration is that the wing is from beginning of take-off run under high angle of attack, slightly less than stall angle of attack therefore the pilot can only wait for airplane to take-off without intervention around lateral axes. Wing is also close to the ground and can benefit from ground effect which reduces induced drag and enlarge lift due to higher pressure under the wing and low induced drag.

3.5 Final Concept

During the conceptual design the advantages and disadvantages helped us to converge to final concept. This is low wing airplane, tractor propulsion system, two main wheels landing gear and tail skid as shown in Figure 3.4. Tail skid is not steerable. Compromise was made between number of balls and complexity of the pylon and ball release system. We find out that two balls are quite easy to release using rudder servo. More balls means more complex drop system which must care about dropping only one ball at the time, more complex balls loading procedure and heavier pylon. We used rule: as low as practical number of balls. We will have a benefit of lower empty weight of the airplane and lower RAC.

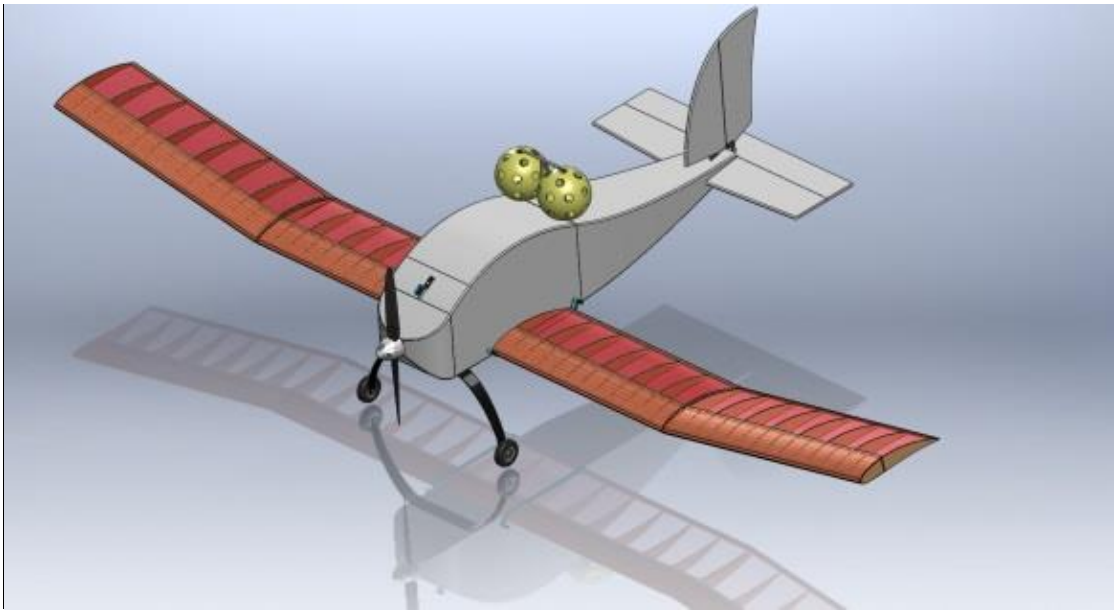

Figure 3.4: Final concept design of EDA 2015

4 Preliminary Design

After the conceptual design was selected, five design groups were formed: Aerodynamics, 3D-design, Propulsion, Payload and Promotion & Report writing. The first step was initial sizing of major components. Each group had formed critical parameters that were later used in the design process.

4.1 Design and Analysis Methodology

Having the conceptual design of the airplane chosen, it is important to obtain further insight into the concept capabilities in order to determine airplane gauge for the detail design sequence of the airplane development process. Therefore mission requirements and design constraints imposed by the DBF rules were modeled. Details of the modeling process are presented in the following chapters. Modeling mission requirements and design constraints yielded estimates of the airplane mission performance as a function of wing area. Furthermore general knowledge in terms of power required by the propulsion system was also obtained. Design/trading studies were performed based on these results. In order to fully quantify the design parameters for the detailed design sequence, coupled aerodynamic and stability analysis of the airplane was executed. Aerodynamic characteristics of the airplane such as airplane polar, wing polar, airfoil polar, neutral point and elevator effectiveness were calculated by a numerical simulation of the airplane (SolidWorks Flow Simulation). For proper airfoil selection and comparison of different airfoils from airfoil data base the Martin Hepperle's JavaFoil [3] was used. Proper propulsion system was selected using DriveCalc [8] which has a database of most common electric motors, cells, ESC's and

propellers and produces reliable data. After obtaining the required and available characteristics of the airplane, the model was built in Excel. Using this airplane model, influence of different parameters to the score was calculated. The most important parameter is wing area which has to be determined first. Wing area is a function of payload mass and take-off distance. Size of fuselage depends on size of payload and length of the fuselage (empennage position) depends on stability requirements of the airplane.

4.2 Mission Analysis

Mission model is composed of three parts corresponding to first, second and third mission respectively. Mission model was also designed to take constraints prescribed into account as well.

4.2.1 *Constraints*

There are four primary and four secondary constraints imposed by the rules [1] and mission requirements as shown in Table 4.1. Maximum battery pack weight dictates the maximum available power of propulsion. On the other hand runway length and payload mass constraints the minimum wing area of the airplane. The wing area should be large enough to reach take-off speed before the end of the runway (60 ft). Wing load is dictated by payload weight and empty weight of the airplane. The external payload is not exactly defined and can be chosen by the team but it is not affecting maximum take-off weight.

Primary Constraints		Secondary Constraints	
Constraint	**Value**	**Constraint**	**Value**
Electric Current	No Limit	**Flight Duration**	> 4 min
Runway Length	60 ft (18.3 m)	**Battery Capacity**	> 1500 mAh
Battery Pack Weight	2.0 lb (908 g)	**Payload Weight**	> 5 lb (2.27 kg)
Payload Bay Size	4.5"×5.5"×10" (114.3×139.7×254.0 mm)	**External No. of Balls**	> 1 ball

Table 4.1: Primary and secondary constraints

Maximum electrical power is limited by the maximum weight of the batteries and maximum current. Batteries are allowed to weigh max. 2.0 lb (908 g) and the electric current is officially not limited but it is limited by batteries to 24 A, so maximum output power cannot roughly exceed 864 W (36 cells, 1V/cell under load). It is important to keep in mind that this is a theoretical limit due to different losses. Efficiency of the propulsion system is roughly 85%. Expected maximum useful power on the propeller output is about 734 W if we use maximum number of cells and appropriate battery capacity. Properties of some appropriate batteries are shown in Table 5.7. We have to have in mind that the powerful propulsion system has high weight and we need to find a compromise between wing area and power of propulsion system.

Flight duration must be at least 4 minutes or 240 s in mission 1. For maximum number of laps the electric current must be close to 24 A, therefore the capacity of batteries must be at least 1600 mAh. There are no flight duration limits in mission 2 and 3. However in order to complete the second and the third mission successfully an airplane have to complete three complete laps on the course in the second mission and theoretically unlimited number of complete laps in the third mission. This means an airplane has to carry enough energy to complete three laps fully loaded with payload that is 5 lb (2.27 kg) of payload and enough energy to drop all balls. In the third mission the speed is not important factor therefore slow flight can be performed and duration of flight can be extended over 4 min.

4.2.2 Design and Sizing Trade-Offs

Since the final score is weighted with RAC it was necessary to optimize airplane in such way that it offers maximum performance with the lowest possible weight. This year's competition rules are very open about the maximum size of the airplane because it does not have to fit into a box and score does not depends on size of the airplane. The minimum airplane size is determined by the size of the internal cargo [1] and take-off distance. Both of these constraints were taken into account when determining the optimum size of the airplane.

4.2.3 Mission Model

In order to assess mission performance of the selected design concept it was decided to use the scoring system prescribed by the contest organizer. Total Mission Score (TMS) is calculated using the following expression:

$$TMS = \frac{GS \cdot (M_1 + M_2 + M_3)}{RAC}$$

For the sake of analysis it was assumed that EW would not change for different missions. The RAC (Rated Airplane Cost) is defined as:

$$RAC = EW \cdot N_{\text{Servo}}$$

EW is the post flight weight with the payload removed and N_{Servo} is number of servos.

If we assume that the number of servos is 3 and empty weight constant in all three flight missions the Total Mission Score reduces to the equation:

$$TMS = \frac{GS \cdot (M_1 + M_2 + M_3)}{3 \cdot EW}$$

To get the Total Mission Score mission functions must be divided by $EW \cdot N_{\text{Servo}}$. Influence of EW and N_{Servo} is shown in Figure 3.2. We can see that score increases with number of completed laps in the first mission, by increasing the number of external balls in the third mission and increases with decreasing the flight time in second mission. Expected range for the first mission is 8 completed laps in 4 min, number of balls is 2 in the third mission and expected range for three laps is 102 s in the second mission. All three

scores for mission 1, 2 and 3 depend on other team's score which is hard to predict. We used 8 laps, 2 balls and 102 s. If we compare all three curves in Figure 3.2 we can see that EW and N_{Servo} are the most powerful factors. If we compare all three curves in Figure 3.3 we can see that number of balls is the most powerful factor compared to the number of laps and flight speed. Wing area was selected as a reference measure for airplane size. It turns out to be a convenient parameter since most of the aerodynamic quantities such as lift and drag depend on it. Another important geometrical parameter influencing aerodynamic efficiency of the wing is its aspect ratio.

4.2.4 *Mission Performance Analysis*

We have predicted that the airplane cannot be lighter than 2.86 lb (1.3 kg) (EW) for a 5 lb (2.27 kg) payload and 60 ft (18.3 m) runway as a result of past years' experience for the selected design. With tractor propeller configuration we gained lightweight undercarriage and powerful propulsion system. Selecting powerful and lightweight propulsion system was a challenge which is described later. Selected propulsion system gives maximum 326 W on the propeller output. The only still undefined parameter is wing area. On the basis of our Excel mission model we made two graphs as shown in Figure 4.1. The left graph shows how the take-off distance depends on wing area. The take-off strip is 60 ft (18.3 m) long. The optimum wing area is defined on the basis of this maximum distance. The take-off distance not depends only on wing area but also depends on maximum take-off weight.

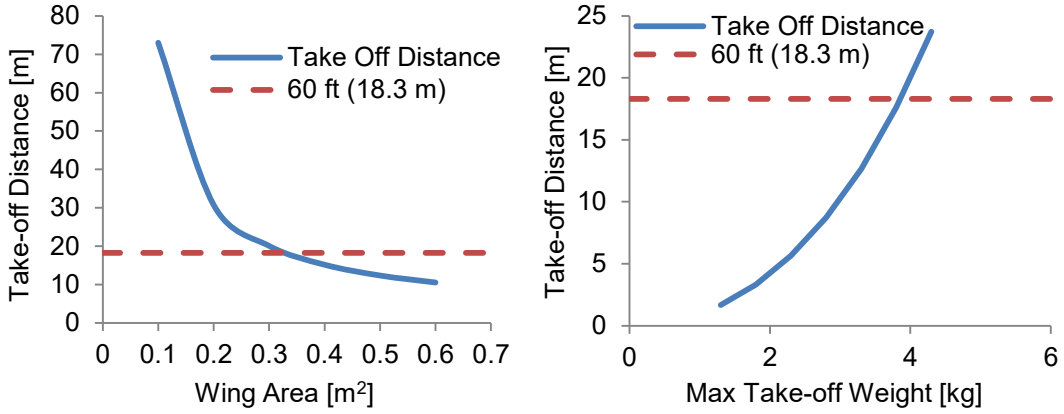

Figure 4.1: Influence of wing area on take-off distance (left) and MTOW on take-off distance (right)

4.3 Airfoil Selection

The goal of airfoil selection was to select an airfoil which would have a high lift coefficient, low drag coefficient and low pitching moment characteristics. The airfoils were looked up in the UIUC Airfoil Data Site [4] in the high lift airfoil category. The team chose between Eppler 560, Eppler 422, NACA 6514 and Martin Hepperle MH 114 airfoils. The Reynolds number was estimated to be around 150 000 so attention was paid to airfoils marked as low Reynolds number airfoils. Airfoils are shown in Figure 4.2.

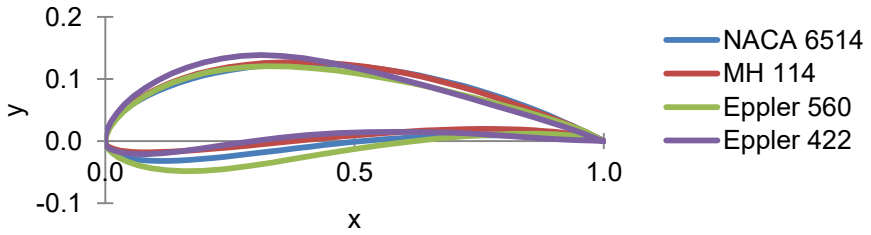

Figure 4.2: Promising airfoils for the wing

For airfoil evaluation, the software made by Martin Hepperle named JavaFoil [3] was used, which gave us an aerodynamic characteristic of airfoils. Four airfoils were compared, and on the basis of the requirements the NACA 6514 airfoil was chosen to best fit our requirements for the wing design. NACA 6514 has a high lift-to-drag ratio, high lift coefficient, low drag coefficient at high angles of attack and acceptable moment coefficient compared to other airfoils. The NACA 6514 airfoil was therefore selected for wing design and was used for the whole wing from root to tip. Lift and drag characteristics of selected airfoil are shown in Figure 4.3.

Parameter	NACA 6514	MH 114	Eppler 560	Eppler 422
Thickness [%]	**14**	13	16	14
Max. Thickness @ [%]	**30**	30	24	23
Camber [%]	**6**	6.5	4.3	7.3
Max. Camber @ [%]	**50**	50	51	23
Max. Lift Coefficient	**1.97**	2.02	1.92	2.06
Min. Drag Coefficient	**0.0153**	0.0145	0.0128	0.0177
Critical Angle of Attack [deg]	**13**	11	14	15
Lift Slope [deg^{-1}]	**0.115**	0.115	0.115	0.115
Max. Lift-to-Drag Ratio	**90.3**	90.9	80.9	76.6
Zero Lift Angle [deg]	**-7.5**	-8.7	-7.1	-6.6
Moment Coefficient @ 0.25 Chord	**-0.18**	-0.20	-0.17	-0.12
Aerodynamic Center Position [%]	**26.5**	26.5	26.5	26.0

Table 4.2: Characteristics of airfoils calculated using JavaFoil

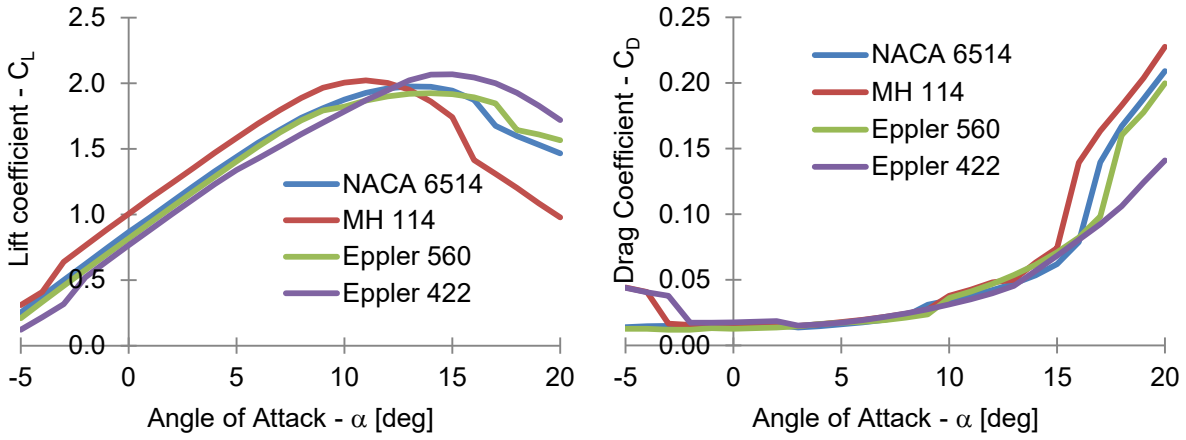

Figure 4.3: Lift and drag coefficient of NACA 6514

4.4 Aerodynamic Performance of Airplane

On the basis of selected airfoils the airplane was designed using Solid Works software [7]. The team performed numerical CFD analysis using Solid Works Flow Simulation (SWFS) from -4 to 20 deg angle of attack (AOA) of the right half of the airplane at Reynolds number of 150 000 and for the selected airfoil NACA 6514. The aerodynamic characteristics of the entire airplane and airfoil were established. The airplane has a maximal lift coefficient of 1.1 at 14 deg AOA and the airfoil 1.57 at 12 deg AOA, which is much less than analytically calculated. We can write down an airplane polar for mission 1 and mission 2:

$$C_D = 0.103 \cdot C_L^2 - 0.00906 \cdot C_L + 0.0665$$

and for mission 3:

$$C_D = 0.103 \cdot C_L^2 - 0.00906 \cdot C_L + 0.07$$

Airfoil polar is:

$$C_D = 0.00915 \cdot C_L^2 - 0.00437 \cdot C_L + 0.02321$$

The airplane polar is for airplane clean configuration for mission 1 and mission 2. There is external payload in mission 3; therefore the polar is not the same for all configurations and all three missions. The minimum drag coefficient of airplane is 0.0665 in mission 1 and mission 2 and 0.07 for mission 3. On the basis of airplane polar, we estimated the required power (P_r) and force (F_r) and available power (P_a) and force (F_a) for the whole velocity range. We tested two propellers with a brushless electric motor, APC 15×8 and 14×10. The maximal available electric power is 384 W for the selected electric motor and cells. Maximal power on the propeller is 326 W as shown in Table 4.4. Available static thrust is 22.7 N and 19.3 N for 15×8 and 14×10 propeller respectively with 16 NiMH cells.

Parameter	Symbol	Airfoil	Airplane Mission 1, 2	Airplane Mission 3
Max. Lift Coefficient	$C_{L\,max}$	1.57	1.10	1.10
Max. Angle of Attack	α_{max} [deg]	12	14	14
Lift Gradient	a [deg^{-1}]	0.10	0.06	0.06
Zero Lift Angle	α_n [deg]	-5.0	-5.0	-5.0
Min. Drag Coefficient	$C_{D\,min}$	0.023	0.0665	0.07
Lift-to-Drag Ratio	L/D_{max}	41.4	7.4	6.5
Aerodynamic Center	AC [%]	25	25	25

Table 4.3: Airfoil and airplane aerodynamic characteristics as calculated by SWFS

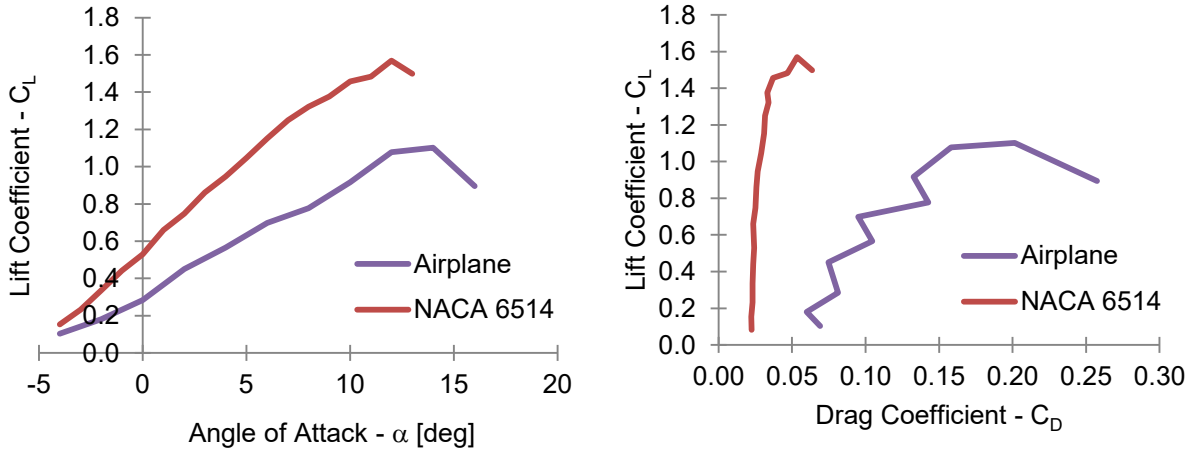

Figure 4.4: Lift and drag characteristics of airfoil NACA 6514 and airplane as calculated by SWFS

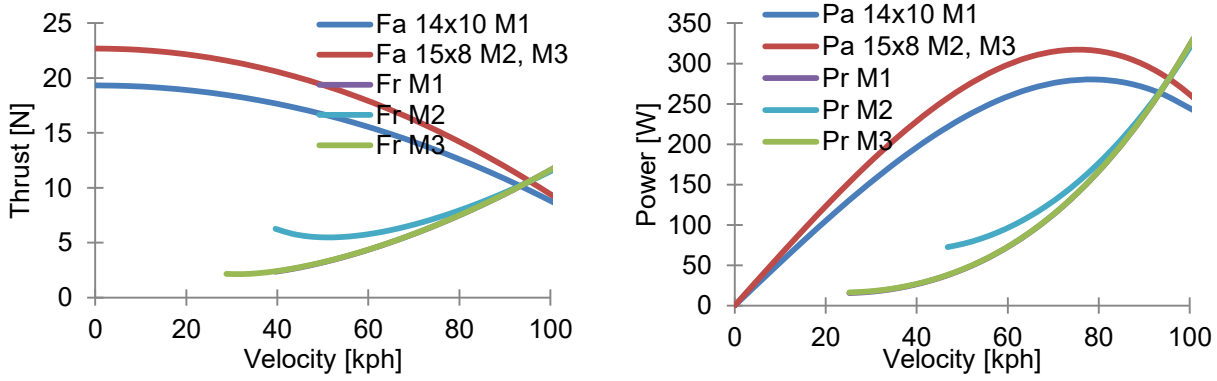

Figure 4.5: Required and available power and thrust for flight weight 2.86 lb (1.3 kg) and 7.86 lb (3.57 kg)

		Mission 1	Mission 2	Mission 3
Parameter	**Symbol**	**1.3 kg/14×10**	**3.27 kg/15×8**	**1.35 kg/15×8**
Max. Available Power	$P_{a\ max}$ [W]	344	384	384
Max. Available Thrust	$F_{a\ max}$ [N]	19.3	22.7	22.7
Max. Excess Power	dP_{max} [W]	189.6	202.3	227.6
Min. Required Power	$P_{r\ min}$ [W]	15.47	68.88	16.31
Min. Required Thrust	$F_{r\ min}$ [N]	2.06	5.48	2.14
Max. Climb Speed	W_{max} [m/s] (ft/min)	14.86 (2925)	5.78 (1137)	17.18 (3381)
Max. Airplane Speed	V_{max} [kph] (kt)	93.4 (50.4)	95.4 (51.5)	95.4 (51.5)
Min. Airplane Speed	V_{min} [kph] (kt)	25.3 (13.6)	41.9 (22.6)	25.7 (13.8)
Speed @ Zero Available Thrust	V @ F=0 [kph] (kt)	135.7 (73.3)	130.7 (70.6)	130.7 (70.6)
Pitch Speed	PS [kmh] (kt)	90.5 (48.8)	68.1 (36.7)	68.1 (36.7)
Take-off Distance	$L_{T/O}$ [m](ft)	2.0 (6.5)	15.19 (49.8)	1.8 (5.9)

Table 4.4: Calculated power and force characteristics of the airplane

In Figure 4.5 the available thrust and power are calculated using DriveCalc. The required power is estimated using SWFS. We can see that the maximum available power is about 384 W and minimum required power about 15.5 W for empty airplane and about 69 W for a fully loaded one.

From Table 4.4 we can see the performance of the empty and fully loaded airplane. The airplane has very promising characteristics with selected propulsion system and wing area. Using two different propellers the airplane performance for each mission is optimized. In the first mission the airplane must be as fast as possible, so we chose small diameter with high pitch (14x10). In the second mission the loaded airplane should take-off on 60 ft (18.3 m) long runway and fly three laps, so we chose higher diameter and lower pitch (15x8). In the third mission the airplane must fly three laps and speed is not important if we take two balls so we also chose large diameter propeller with low pitch (15x8).

4.5 Stability and Control

The airplane must be longitudinal, lateral and yaw statically and dynamically stable in all phases of flight. The goal of stability and control analysis is to determine the horizontal tail volume, vertical tail volume, front center of gravity (CG) limit, aft CG limit and position of neutral point (NP) of the airplane. Sizing of the vertical and horizontal tail volume was based on the previous experience with the same category of airplanes. The CG position was calculated and then evaluated through a series of test flights of the prototype. The necessary criteria for static longitudinal stability is that gradient must be negative ($\partial C_{m\,cg}/\partial C_L < 0$) and $C_m = 0$ (trim point) must be at positive lift coefficients. Data required for stability calculation are shown in Table 4.5. Let us suppose the position of CG at 2.52 in (64 mm) from the wing root leading edge for calculations.

Parameter	Symbol	Wing (w)	Horizontal Tail (h)	Vertical Tail (v)
Apex	Ap_x [mm](in)	93 (3.66)	670 (26.4)	670 (26.4)
Mean Aerodynamic Chord	MAC [mm](in)	200 (7.87)	155 (6.1)	155 (6.1)
X Position of AC	X_{AC} [mm](in)	143 (5.6)	718 (28.3)	718 (28.3)
Y Positon of AC	Y_{AC} [mm](in)	0	122 (4.8)	0
Z Position of AC	Z_{AC} [mm](in)	0	51 (2)	122 (4.8)
Area	S [dm^2](ft^2)	40 (4.3)	7.7 (0.82)	3.8 (0.82)
Lift Gradient	a [deg^{-1}]	0.06	0.035	0.035
Aspect Ratio	AR	10	3.2	1.5
Taper Ratio	TR	1	0.88	0.88
Incidence Angle	i [deg]	2.2	0	0
Zero Lift Angle	α_n [deg]	-5.0	0	0
Moment Coefficient @ AC	$C_{m\,ac}$	0	0	0

Table 4.5: Data required for stability calculation

With stability analysis and the following equations we found out the position of the neutral point (NP), which is at 3.66 in (93 mm) from the wing root leading edge, i.e. at 46.5% MAC. The recommended static margin for longitudinal static stability is from 5% to 15% mean aerodynamic chord (MAC). From flight tests we found out that a 5% static margin is marginal sufficient for stabile flight, but not enough for reliable flight. Therefore the far aft allowable position of the CG is 3.26 in (83 mm) from the wing root leading edge, i.e. at 41.5% MAC.

4.5.1 Wing Effect on Static Longitudinal Stability

The moment curve for wing's static longitudinal stability is defined as [6]:

$$d = x_{cg} - x_{ac} = 14\ \text{mm}$$

$$C_{m\,cg} = C_{m\,ac} + \frac{d}{c_w} \cdot C_L = -0.106 + 0.07 \cdot C_L$$

Where d is a distance between CG and AC, c_w wing's mean aerodynamic chord (MAC), $C_{m\,ac}$ moment coefficient about wing's AC and $C_{m\,cg}$ moment coefficient about airplane CG. The wing, made from cambered airfoil NACA 6514, destabilizes the airplane.

4.5.2 Horizontal Tail Effect on Static Longitudinal Stability

The purpose of the horizontal tail, made of flat thin airfoil, is to stabilize the airplane. The tail is influenced by the wing downwash. The downwash gradient is calculated from the following equation:

$$\frac{d\epsilon}{d\alpha} = \frac{2 \cdot a_w}{\pi \cdot \lambda} \cdot \frac{180}{\pi} = 0.2188$$

Tail volume of horizontal tail is calculated as:

$$\bar{V} = \frac{S_h \cdot x_h}{S_w \cdot c_w} = 0.53$$

The moment coefficient about airplane CG due to horizontal tail is:

$$C_{m\,cg} = -\eta \cdot \bar{V} \cdot a_h \cdot (\alpha_n - i_w + i_h + \tau \cdot \delta) - \eta \cdot \bar{V} \cdot \frac{a_h}{a_w} \cdot \left(1 - \frac{d\epsilon}{d\alpha}\right) \cdot C_L = 0.1269 - 0.2294 \cdot C_L$$

Where a_w is lift coefficient gradient, λ aspect ratio, S_h horizontal stabilizer area, S_w wing area, x_h distance between CG and horizontal tail AC, η air velocity reduction ratio at tail, a_h lift coefficient gradient of horizontal tail, α_n angle of attack of zero lift, i_w angle between wing chord and longitudinal axis (wing incidence angle), i_h angle between horizontal tail chord and longitudinal axis (tail incidence angle), ϵ downwash angle at tail, τ effectiveness of elevator and δ elevator deflection. Effectiveness of elevator is 0.5 and maximal deflection is ± 30 deg.

4.5.3 Airplane Static Longitudinal Stability

We can write the stability equation as a sum of wing and horizontal tail equation together as:

$$C_{m\,\mathrm{cg}} = 0.0209 - 0.1594 \cdot C_L$$

From the equation and Figure 4.6 we can see that airplane is statically stable. The trim point is at positive lift coefficient. This means that zero deflection of the elevator trim the airplane. With stability analysis using the presented equations we found out the position of the neutral point (NP), which is at 3.66 in (93 mm) from the wing root leading edge, i.e. at 46.5% wing root chord. The recommended static margin (SM) for longitudinal static stability is from 5% to 15% mean aerodynamic chord (MAC). The far aft allowable position of the CG is 3.26 in (83 mm) from the wing root leading edge, i.e. at 41.5% wing root chord and the front recommending position of the CG is 1.97 in (50 mm) from the wing root leading edge, i.e. at 25% wing root chord as shown in Figure 4.7. For forward CG position near forward limit we need more elevator authority to reach minimum velocity (stall speed).

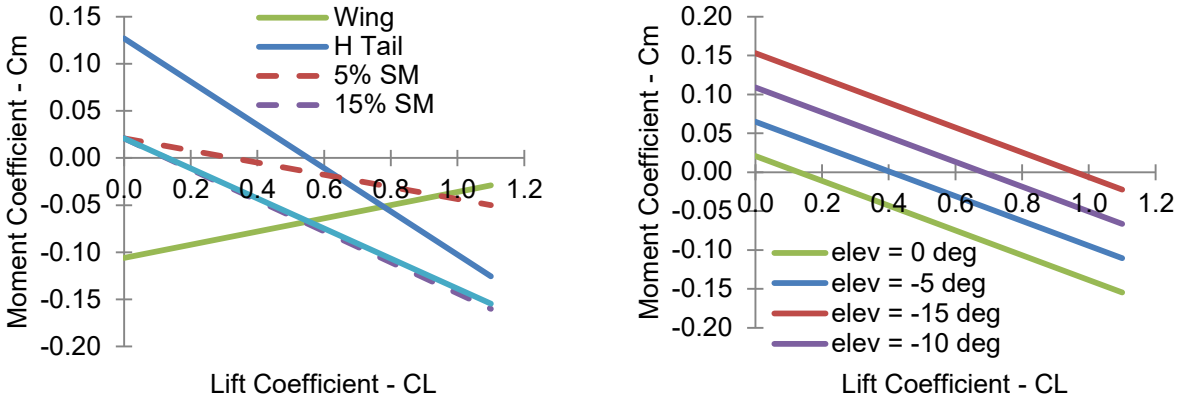

Figure 4.6 Airplane moment curve represents airplane static longitudinal stability

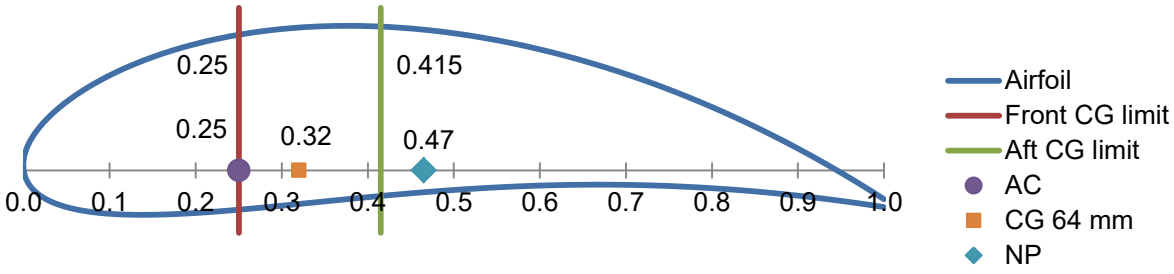

Figure 4.7: Front and aft limit position of airplane CG

4.5.4 Directional Static Stability

The vertical stabilizers volume defines the static directional stability of the airplane. The vertical stabilizer volume is defined as:

$$V_v = \frac{S_v \cdot x_v}{S_w \cdot b_w} = 0.051$$

Where S_v is vertical stabilizer area, x_v distance between vertical stabilizer aerodynamic center and center of gravity of the airplane, S_w is wing area and b_w wing span. For good directional stability the vertical tail volume should be from 0.02 to 0.04 [5]. The tail volume is 0.051 which means the airplane has oversized directional stabilizers. The vertical stabilizer is made of flat airfoil. We designed the large stabilizer due to better maneuverability during flight, because we do not have ailerons and we turn the airplane only by using rudder.

4.5.5 Lateral Static Stability

For improved lateral static stability the dihedral angle of the wing is used. We find out that we need the dihedral angle of the wing because we have low wing airplane. We used 10˚ dihedral angle on outside part of the wing.

4.6 Propulsion Selection

After aerodynamic analysis was complete, it was time for propulsion analysis and selection. To find suitable propulsion for this year's competition, we first looked at the mission profiles to see what kind of propulsion is required. The first mission requires a propulsion that provides enough available power to achieve as high pitch speed as possible. The second mission requires both: a lot of thrust and good pitch speed that the airplane can take-off in 60 ft and fly fast. The third mission can be performed using propeller from mission 2 and is not critical.

4.6.1 Motor Selection

From previous experience in DBF competition we concluded the propulsion should include a gear-box since that enables use of smaller motors with larger propeller because there is more torque on the shaft. Table 4.6 shows the results of static thrust estimation. We selected Peggy Pepper 2221/16 with gearbox Micro Edition 5:1 and controller YGE 30.

Motor	Mission 1	Mission 2, 3
No. of Cells	16	16
Propeller	14×10	15×8
Current [A]	21.5	24.0
Voltage [V]	16	16
Thrust [N]	19.3	22.7
RPM [min^{-1}]	5940	5591

Table 4.6: Static thrust estimation of motor

4.6.2 Battery Selection

The only two battery technologies allowed by the rules are NiMh and NiCd. We chose the former since they don't have memory effect and are lighter than NiCd which is very important from the RAC standpoint. Maximum allowed weight for the propulsion pack is 2 lb (908 g). This weight translated into maximum installed power on the airplane with regard to 24 A of maximum current draw equals to 384 W. The score analysis showed us that 16 cells is the optimal installed power for this year's competition and since RAC is very important we chose XCell 1600 2/3A cells. This type of batteries is optimal from the standpoint of

RAC. They can handle current up to 25 A and are lightweight. If current draw stays under 25 A, 1600 mAh provides enough endurance for all three missions. Changing number of cells between missions is not advisable because the gain in score is heavily undermined by gain in RAC.

4.6.3 *Propeller Selection*

Now, with the motor and batteries selected it was time to select optimal propeller. For the first mission we had to have a high pitch speed propeller and high thrust-to-weight ratio. First (high pitch speed) parameter is important because it imposes a limit on how fast the airplane can fly. The second (high thrust-to-weight ratio) parameter is important because it limits how fast the airplane will accelerate out of a turn into a straight flight to maximum speed. Therefore thrust-to-weight ratio must be at least 1 or preferably more. Second mission requires lots of thrust because airplane is heavily loaded. It is loaded with wooden block in the second mission. Therefore we chose APC 14×10 propeller which produce 19.3 N of static thrust at 21.5 A for the first mission, APC 15×8 propeller which produce 22.7 N of static thrust at 24 A for the second and the third mission. In Figure 4.8 we can see how the propellers pitch influences to the difference between available and required power. Excess power is important for climbing and accelerating of the airplane. The airplane reaches maximum flight speed where the excess power is zero and maximum climb speed where excess power reach maximum.

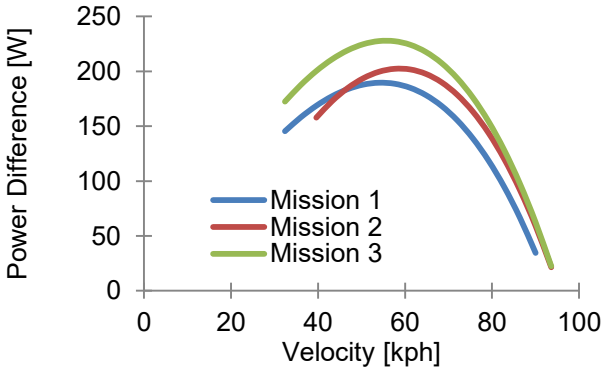

Figure 4.8: Power difference

4.7 Estimates of the Airplane Mission Performance

There are one ground and three flight missions with the following characteristics:

- **Mission 0: Payload Loading Time** – Loading/unloading payload of mission 2 and 3.
- **Mission 1: Ferry Flight** – Empty airplane, maximum number of laps in 4 min.
- **Mission 2: Sensor Package Transport Mission** – internal wooden block, three laps.
- **Mission 3: Sensor Drop Mission** – external cargo, n laps ($n \geq 1$).

For the ground mission flying performances of the airplane are not important. Important is accessible payload bay and simple mechanism for ball mounting and securing. From the required (P_r) and available (P_a) power we can calculate maximum velocity in the different phases of flight and different bank angles during one lap. From the bank angle during the turn we can calculate the turn radius and turn path. Each leg is 500 ft (152.4 m) long. The take-off acceleration and climbing are neglected in calculation. In Figure 4.9 are shown two graphs for mission 1 and in Figure 4.10 two graphs for mission 2. Mission 3 is not critical therefore the graphs are not present.

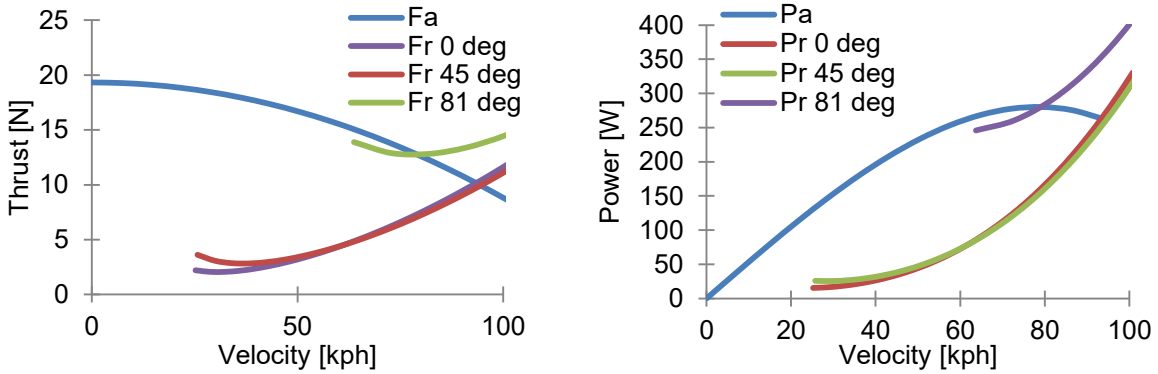

Figure 4.9: Required (P_r, F_r) and available power and thrust (P_a, F_a) in turns for FW 2.86 lb (1.3 kg)

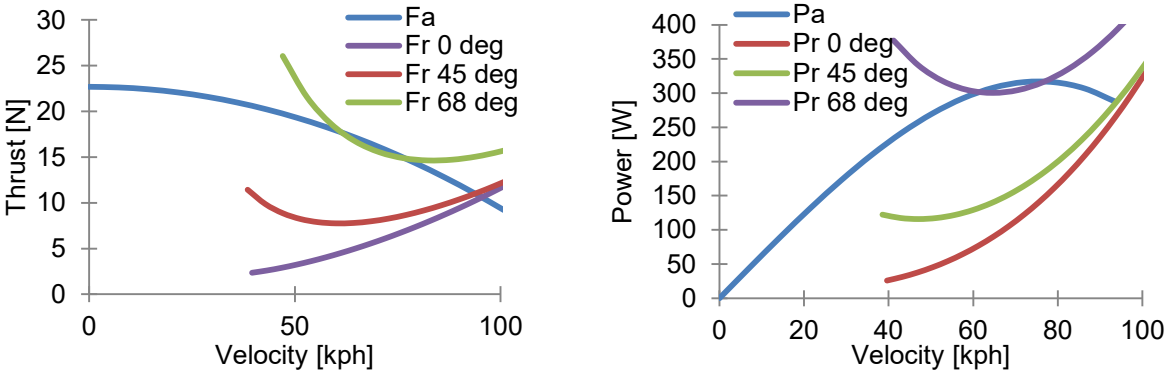

Figure 4.10: Required (P_r, F_r) and available power and thrust (P_a, F_a) in turns for FW 7.86 lb (3.57 kg)

4.7.1 Mission 0 (Ground Mission) - Payload Loading Time

For payload loading time minimization is important simple and accessible payload bay. We made cargo door on the upper side of the fuselage with hinge on forward side and magnetic latch on the rear side. Estimated time for loading of mission 2 payload is 2.5 s. The pylon for ball mounting is also very simple and easy to load. Estimated time for unloading of mission 2 payload and loading the mission 3 payload is 2.5 s. Total loading/unloading estimated time is 5 s. The ground score is estimated as $GS = 1$.

4.7.2 Mission 1

From Table 4.7 we can see that with the selected propulsion we can complete 8 laps. Lap is defined in Figure 4.11. Take-off velocity is 14.1 kt (26.2 kph) and distance 6.6 ft (2 m). For 8 laps we spend 1320 mAh of energy. Estimated Mission 1 score divided by RAC = 8.59 is 0.233.

Lap	Velocity [kph]	Distance [m]	Time [s]	Energy [mAh]
Cruise #0	94.7	152.4	5.79	34.6
Turn #1 (180 deg)	79.1	24.5	1.12	6.7
Cruise #1	94.7	152.4	5.79	34.6
Turn #2 (360 deg)	79.1	49.0	2.23	13.3
Cruise #2	94.7	152.4	5.79	34.6
Turn #3 (180 deg)	79.1	24.5	1.12	6.7
Cruise #3	94.7	152.4	5.79	34.6
Average / Total	**92.2**	**707.6**	**27.6**	**165.0**

Table 4.7: Mission 1 profile – TOW 2.86 lb (1.3 kg) (Turn bank is assumed to be 81 deg)

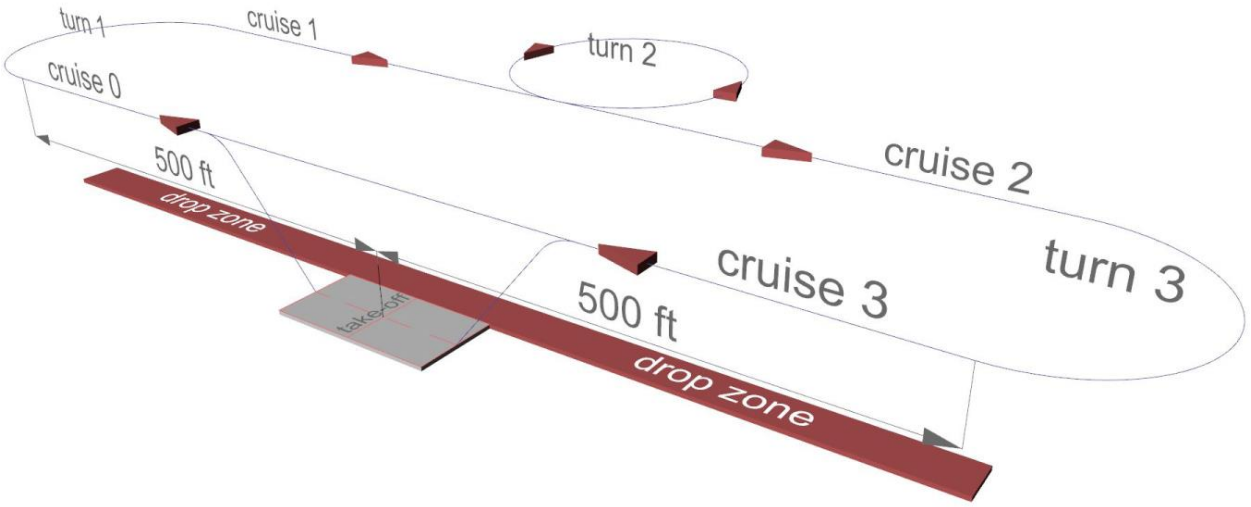

Figure 4.11: One lap legs definition

4.7.3 Mission 2

From the Table 4.8 we can see that with selected propulsion we can complete 3 laps in 1 min 42.1 s and spend 609.6 mAh of energy. Take-off velocity is 23.3 kt (43.2 kph) and distance 49.8 ft (15.2 m). Estimated Mission score divided by RAC = 8.59 for two wooden block on board is 0.465.

Lap	Velocity [kph]	Distance [m]	Time [s]	Energy [mAh]
Cruise #0	95.5	152.4	5.74	34.3
Turn #1 (180 deg)	76.8	58.9	2.76	16.5
Cruise #1	95.5	152.4	5.74	34.3
Turn #2 (360 deg)	76.8	117.8	5.52	33.0
Cruise #2	95.5	152.4	5.74	34.3
Turn #3 (180 deg)	76.8	58.9	2.76	16.5
Cruise #3	95.5	152.4	5.74	34.3
Average / Total	**89.4**	**845.2**	**34.0**	**203.2**

Table 4.8: Mission 2 profile – TOW 7.86 lb (3.57 kg) (Turn bank is assumed to be 68 deg)

4.7.4 Mission 3

From the Table 4.9 we can see that we will fly using half throttle in mission 3 with 32.4 kt (60 kph) because the speed is not important. Important is that we will drop a single ball each lap. We will drop only 2 balls so we will spend small amount of energy that is 589.4 mAh. Take-off velocity is 14.4 kt (26.7 kph) and take-off distance 3.7 ft (1.8 m). Estimated Mission score divided by RAC = 8.59 is 0.698.

Lap	Velocity [kph]	Distance [m]	Time [s]	Energy [mAh]
Cruise #0	60.0	152.4	9.14	54.6
Turn #1 (180 deg)	60.0	53.2	3.19	19.1
Cruise #1	60.0	152.4	9.14	54.6
Turn #2 (360 deg)	60.0	106.4	6.38	38.1
Cruise #2	60.0	152.4	9.14	54.6
Turn #3 (180 deg)	60.0	53.2	3.19	19.1
Cruise #3	60.0	152.4	9.14	54.6
Average / Total	**60.0**	**822.4**	**49.3**	**294.7**

Table 4.9: Mission 3 profile – TOW 2.97 lb (1.35 kg) (Turn bank is assumed to be 60 deg)

We expect the flight score for all three missions 1.396.

5 Detail Design

5.1 Dimensional Parameters of Final Design

During conceptual design we selected low wing concept with tractor propeller. The airplane (airplane system) is composed of the following parts:

- **Wing (no ailerons)**
- **Fuselage**
- **Undercarriage**

- **Vertical Tail with rudder**
- **Horizontal Tail with Elevator**
- **Propulsion System**
- **Control System**
- **Internal Payload Bay**
- **Pylon for External Payload**

The main dimensional parameters and performances are shown in Table 5.1 and Table **5.2**. Dimensional parameters for airplane parts are shown and discussed about the following chapters.

Parameter	Unit	Wing	Vertical Tail	Horizontal Tail
Airfoil	-	NACA 6514	Flat Airfoil	Flat Airfoil
Span	[mm] (ft)	2000 (6.56)	250 (0.82)	500 (1.64)
Area	[dm^2] (ft^2)	40 (4.31)	3.1 (0.33)	7.75 (0.83)
Root Chord	[mm] (ft)	200 (0.65)	165 (0.54)	165 (0.54)
Tip Chord	[mm] (ft)	200 (0.65)	145 (0.47)	145 (0.47)
Sweep Distance	[mm] (ft)	0	20 (0.065)	20 (0.065)
Aspect Ratio	AR	10	3.2	3.2
Volume	-	-	0.051	0.53
Taper Ratio	-	0	0.87	0.87
Control Surface	-	-	Rudder	Elevator
CS Area	[dm^2] (ft^2)	0	3.25 (0.35)	1.3 (0.14)
Deflection Angle	[deg]	0	± 30 deg	± 30 deg

Table 5.1: Basic dimensional parameters of wing, vertical and horizontal tail

Parameter	Unit	Value
Airplane Length	[m] (ft)	0.977 (3.2)
Airplane Height	[m] (ft)	0.467 (1.53)
Airplane Span	[m] (ft)	2.0 (6.56)
Maximum Take-off Weight	[kg] (lb)	3.57 (7.86)
Empty Weight	[kg] (lb)	1.3 (2.86)
Payload to MTOW Ratio	[%]	63
Payload to EW Ratio	[%]	174
Wing Load	[kg/m^2] (lb/ft^2)	8.9 (1.82)
Power Load	[W/kg] (W/lb)	107.5 (48.8)
Stall Speed (EW)	[kph] (kt)	25.3 (13.6)
Stall Speed (MTOW)	[kph] (kt)	41.9 (22.6)
Design Load Factor	[g]	2.5

Table 5.2: Basic dimensional parameters and performance of airplane

5.1.1 Wing

Wing is made of balsa wood covered by Oralight cover. Span of the wing is 78.74 in (2000 mm) and chord 7.87 in (200 mm). Wing has no ailerons. The wing is made of 31 ribs which are 2.75 in (70 mm) apart and made of 0.078 in (2.0 mm) thick balsa wood. The first rib, the last rib and two inner ribs which connect the wing sections are made of 0.078 in (2 mm) plywood. In the leading edge in front of the main beam there are 60 ribs for D-box shape stability. The wing has one main beam made of balsa wood web and carbon fiber flanges. The upper flange of the main beam is made of unidirectional (UD) carbon band (Graupner) dimensions 0.12×0.04 in (3×1 mm) and the lower flange of 0.12×0.02 in (3×0.5 mm). The thicker flange must be on the compression side of the beam due to flange compression stability issue. The beam web is made of 0.12 in (3 mm) balsa wood. The beam is made of one part for central wing part. Wing tips are not subjected to high stresses therefore the balsa wood will be enough for flanges. The main beam carries the flexural stresses. In front of the beam is a D-box made of 0.04 in (1 mm) balsa sheet wrapped around the front ribs and carrying the torsion stresses. The central part of the wing is mounted on the bottom of the fuselage using rubber band. Wing incidence angle is (+2.2 deg). Wing tips are mounted at 10 deg angle to central part with mounts which are protruding to main beam at the central part and at the wing tips. We found out that this type of wing construction is far more lightweight compared to other techniques of wing construction.

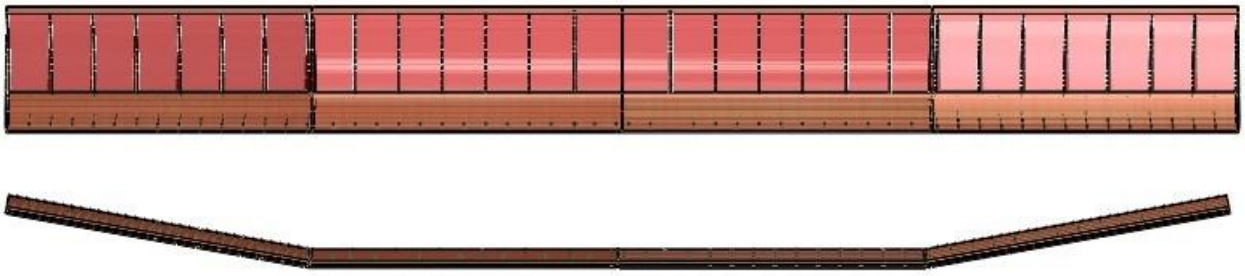

Figure 5.1: Entire wing made from 3 sections (central section and two tip sections)

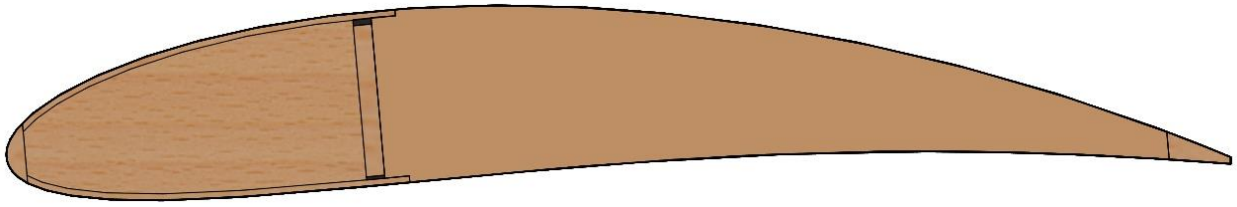

Figure 5.2: Wing cross section

Main Beam Stress Analysis

We made a bending test on the Zwick testing machine of the main beam dimensions 0.94×0.12 in (23.9×3 mm). The upper flange of the main beam is made of a unidirectional (UD) carbon band (Graupner) dimensions 0.12×0.04 in (3×1 mm) and the lower flange of 0.12×0.02 in (3×0.5 mm). The beam web is made of 0.12 in (3 mm) balsa wood cut in such way that fibers are perpendicular to the beam axis for better carry of shear stresses. We assume that the bending moment in the beam supports only flanges.

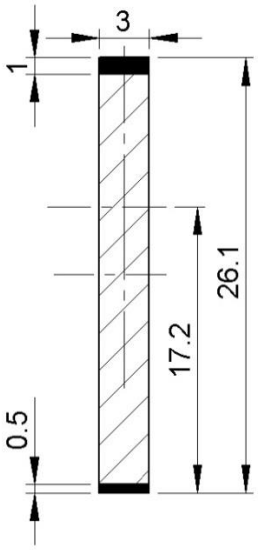

Parameter	Value
Area of Upper Flange (Compression) [mm^2]	3.0
Area of Lower Flange (Tension) [mm^2]	1.5
Neutral Axis of Beam Cross Section [mm]	17.2
Moment of Inertia [mm^4]	482.0
Moment of Resistance [mm^3]	28.0
Center of Eliptic Distribution of Lift (43.4%) [mm]	325.5
Moment [Nmm]	3193.1
Flange Stress [MPa]	114.0
Ultimate Flange Stress [MPa]	900.0
Young's Modulus [MPa]	500000
Airplane Weight [kg]	2.0
Ultimate Load Factor [g]	7.9
Limit Load Factor (1.5 Safety Factor)	5.2
Main Beam Weight [g/m]	24

Table 5.3: Main beam mechanical properties

5.1.2 Fuselage

Fuselage is made of Depron, which is suitable material for construction of this year airplane's fuselage. The fuselage has rectangular cross section with internal payload bay. Size of the fuselage was constructed around the payload shape. Depron is lightweight material with density of 2.2 lb/ft^3 (35 kg/m^3). It has enough strength to construct the entire fuselage. We used 0.24 in (6 mm) and 0.12 in (3 mm) Depron thickness. The 0.24 in (6 mm) Depron was used for stressed parts and 0.12 in (3 mm) Depron for non-stressed parts. We made some reinforcement for firewall, undercarriage mounting points and wing mounting points using 0.04 in (1 mm) plywood. We made two ribs in the fuselage, one in front of the payload and the second in the back. Between firewall and the first rib is place for battery pack, RC receiver and main electric switch.

5.1.3 Undercarriage

The airplane has undercarriage, which consists of one main leg in the front of CG as shown in Figure 5.3 and a tail skid under the tail. It is made of unidirectional (UD) carbon fiber composite. Fiber rowing is composed into 1 in (25 mm) wide tape which is easily to handle during manufacturing. Carbon fibers are Torayca T300J 200 tex (3k).

Figure 5.3: Undercarriage

Undercarriage Stress Analysis

We made calculation to get the number of required layers in the composite to withstand 200 ft/min (1 m/s) vertical speed during landing without damage. This equals to the load factor of 6.3 g at the loaded airplane with heaviest payload, which is 5.0 lb (2.27 kg) and elastic modulus of composite 180 GPa. The result is 20 layers plus one additional layer on the each side of the carbon fabric +45/-45 due to torsional stiffness. The flexural shift at this load is 0.11 in (2.8 mm). Results of calculation are shown in Table 5.4.

Parameter	Value
Airplane Weight [kg]	3.57
Vertical Speed [m/s] (ft/min)	1.0 (200)
Load Factor [g]	6.31
Undercarriage Width [mm]	25
Cantilever Distance [mm]	100
Moment of Inertia [mm^4]	86.0
Moment of Resistance [mm^3]	37.8
Ultimate Stress [MPa]	600
Limit Stress (1.5 Safety Factor) [MPa]	400
Young's Modulus [GPa]	180
Limit Force at One Leg [N]	102.1

Number of UD Carbon Layers	20
Thickness of UD Carbon Layer [mm]	0.15
Flectural Shift Under Load [mm]	2.78
Undercarriage Weight [g]	43

Table 5.4: Undercarriage mechanical properties

5.1.4 Vertical Tail with Rudder

Vertical tail is made of 0.24 in (6 mm) Depron and has flat airfoil; only the leading edge is rounded. Geometrical data for tail are in Table 5.1. It has one servo motor to move the rudder. Due to high span we made carbon fiber reinforcement between stabilizer and rudder using 0.24×0.02 in (6×0.5 mm) unidirectional (UD) carbon band. The band increases bending stiffness. The vertical tail is shark fin shape due to esthetic impression.

5.1.5 Horizontal Tail with Elevator

Horizontal tail is made of 0.24 in (6 mm) Depron and has flat airfoil; only the leading edge is rounded. Geometrical data for tail are in Table 5.1. It has one servo motor to move the elevator. Due to high span we made carbon fiber reinforcement between stabilizer and elevator using 0.24×0.02 in (6×0.5 mm) unidirectional (UD) carbon band. The band increases bending stiffness.

5.1.6 Propulsion System

The propulsion system consists of motor, propeller, motor regulator and NiMH cells. Propulsion must provide enough energy and power to drive the airplane during all three missions. During the first and the second mission the airplane must fly as fast as possible. We reach high static thrust in the mission 2 using a large propeller diameter with low pitch, and high speed flight in mission 1 using a small propeller diameter with high pitch. So we decided to use two propellers one for ferry flight and the other for payload flight. We selected propulsion systems as shown in Table 5.5. There are two limitations of the propulsion system, batteries must be NiCd or NiMH and maximum weight of the battery pack is 2 lb (908 g). Maximum allowed electric current is not specified. We have selected 24 A electric current limit due to selected cell current limit. In practice the voltage of battery pack drops at 20 A current for 0.2 V per cell, from 19.2 V to 16 V.

Part	Propulsion	Weight [g]	Weight [lb]
Motor	Peggy Pepper 2221/16	86	0.1608
Gear Box	MicroEdition 5:1	18	0.0396
Motor Regulator	YGE 30	31	0.0682
Propeller (Mission 1)	14×10	35	0.0771

Propeller (Mission 2, 3)	15×8	38	0.0837
Battery Pack	16 XCell 1600 mAh	400	0.8810
Total Weight	Entire propultion system	**570**	**1.2555**

Table 5.5: Contents of selected propulsion systems with weights

Motor

From the motors on the market we have chosen out-runner Peggy Pepper 2221/16. Characteristics are shown in Table 5.6. We used Peggy Pepper (Scorpion) motor which has very good thrust-to-weight ratio. For selection of proper motor we have to tune weight of the motor, motor RPM, redactor reduction, number of cells and propeller. These five parameters must fit together that the motor works in RPM and electric current range with maximum efficiency.

Parameter	Peggy Pepper 2221/16 + Micro Edition 5:1
Rotation Type	Out-runner
Kv [RPM/V]	2010 / 5 = 402
Max. Cont. Current [A]	28
Max. Voltage [V]	21 (17 NiMh)
Max. Power [W]	400
RPM Reduction	5:1
Shaft Diameter [mm]	3.17 / 6

Table 5.6: Basic characteristics of brushless electric motor

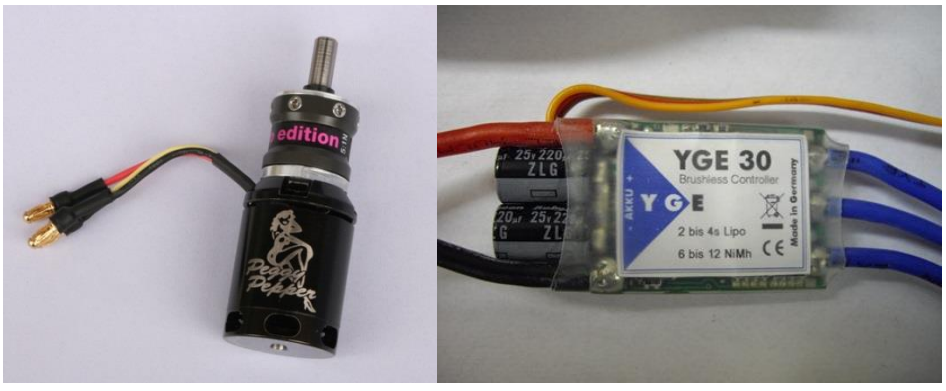

Figure 5.4: Brushless electric motor Peggy Pepper 2221/16 with Micro Edition 5:1 gearbox and controller

Cells

Cells are the main source of energy. There is not very much choice on the market. We calculated that we need 1433 mAh of energy for 4 min flight at 21.5 A in the first mission, so the cell capacity of 1500 mAh is enough. We chose between Elite, Kan and Xcell cells as shown in Table 5.7.

Parameter	Elite	Kan	XCell
Battery Type			
Size [mm] (2/3A)	29/17	29/17	29/17
Cell Weight [g]	23	21	22
Cells in Pack	10	10	10
Pack Weight [g]	230	210	220
Nominal Pack Voltage [V]	12.0	12.0	12.0
Pack Voltage @ 15A [V] (U = 1 V)	10.0	10.0	10.0
Capacity [mAh]	1500	1100	1600
Available Power @ 15 A [W]	150	150	150
Discharge Time @ 15 A [min:sec]	6:00	4:24	6:24
Specific Capacity [mAh/g]	65.2	52.4	72.7
Specific Energy Stored [Wh/kg]	78.3	62.8	**87.3**

Table 5.7 Battery packs comparison

Figure 5.5: XCell racing 1600 NiMh cell and blade type fuse in socket

Between each battery pack and motor controller is blade type fuse on the positive battery pole. It is not required by the rules but will be used as safety device to disengage the power electric circuit during airplane handling on the ground. We choose the XCell due to low weight, high capacity and good time characteristic. It has maximum specific capacity and specific energy of all three available cells. There are more different possible types of packs. Due to available space we will use two rows of cells (2×8=16) as shown in Figure 5.6.

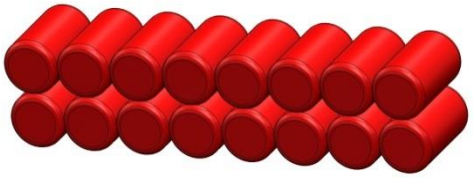

Figure 5.6: Used battery pack consisting of 16 XCell cells

Propeller

The propeller produces thrust and drives the airplane. We decided to use fix APC propellers because it has better efficiency than folding Aeronaut propellers. We chose APC E (electric) tractor propellers. The APC propellers are very efficient and lightweight. For the selected motor we chose two propellers: 14×10 for the first mission and 15×8 for the second and third mission. We used DriveCalc for calculation of motor-propeller characteristics. Results are shown in Table 5.8. We have to keep in mind the fact that actual performance of the propulsion system would be worse than predicted. The difference between theoretical and actual propeller characteristics is roughly 10%.

Propeller	14×10	15×8
Rotational Speed [rpm]	5940	5591
Thrust [N]	19.3	22.7
Electric Current [A]	21.5	24.0

Table 5.8: Static thrust of propellers

5.1.7 Control System

The control system consists of a radio control (RC) transmitter, RC receiver, receiver's own power supply, two servo motors, motor controller, cables and switch. We have used a Futaba T12FG 12-channel 2.4 GHz transmitter, Futaba R6014HS 12-channel receiver, five NiMH KAN 350 mAh 2/3AAA size batteries soldered in pack, two Hyperion ATLAS 09 AMD digital servos and thin wires 0.08 mm^2. The weight of the receiver is 21 g, battery pack 40 g, servo 10 g and switch 10 g. Between the battery pack and the receiver is switch on outside the airplane to switch on and off the control system. Control system is shown in Figure 5.7.

Parameter	KAN
Battery Type	
Size [mm] (2/3AAA)	29/10
Cell Weight [g]	8
Cells in Pack	5
Pack Weight [g]	40
Nominal Pack Voltage [V]	6.0
Capacity [mAh]	350
Available Power @ 1 A [W]	6
Discharge Time @ 1 A [min:sec]	21:00
Specific Capacity [mAh/g]	43.8
Specific Energy Stored [Wh/kg]	52.5

Table 5.9: NiMH KAN 350 mAh 2/3AAA size batteries

Figure 5.7:, Transmitter, receiver, servo motor, switch and receiver battery pack

5.1.8 Payload

This year's payload is composed of different types of cargo as shown in Figure 5.8. There are two different types of cargo:

- One wooden block 4.5×5.5×10 in (114.3×139.7×254.0 mm), weight 5 lb (2.27 kg). Simulated sensor package is one stack of three standard 2×6 wooden pine boards (dimensional lumber), 10

in long. Dimensional tolerance will be ± 1/8 in (3.175 mm) in all directions. The payload during the competition will be provided by contest officials.

- Team-selected number of Champro 12 in Plastic Balls (12 in Circumference "Softball" size). A sample of 12 balls from the full population of 240 were measured for size and weight. Nominal weight for each ball is approximately 1 oz (28.35 g). All of the balls fit through an opening that was 3.759 in (95.48 mm) wide (All Go) and none of the balls fit through an opening that was 3.623 (92.02 mm) in wide (No Go). The payload during the competition will be provided by contest officials.

Payload is internal and external. Tolerance of internal cargo dimension is ±1/8 in (3.175 mm). We sized the cargo bay for maximal possible payload size that there is no doubt to fit the cargo into the cargo bay. We also sized pylons to balls maximum possible size that all balls can fit on the pylon.

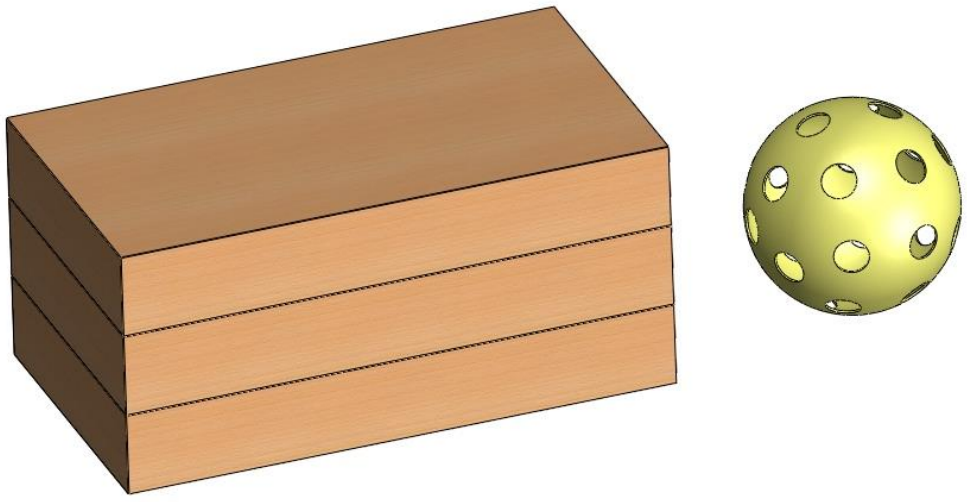

Figure 5.8: Internal and external payload

Mission 2 Payload (Sensor Package Transport Mission)

Internal cargo in the second mission is wooden block as shown in Figure 5.9. Nominal and maximal/minimal dimensions are shown in Table 5.10.

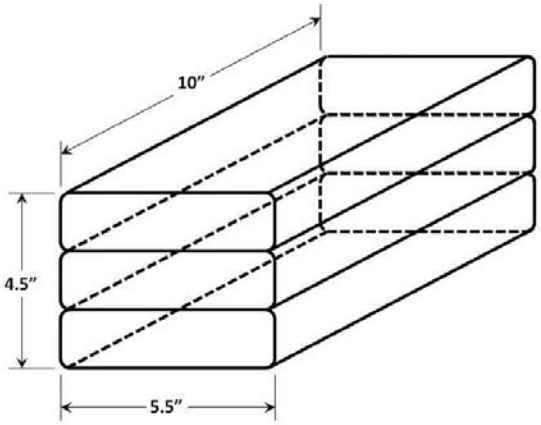

Figure 5.9: Wooden block payload for mission 2.

Dimensions	Length [in/mm]	Width [in/mm]	Height [in/mm]	Mass [lb/g]
Nominal	10 / 254.0	4.5 / 114.3	5.5 / 139.7	5 / 2.27
Maximal	10.125 / 257.2	4.625 / 117.5	5.625 / 142.9	N/A
Minimal	9.875 / 250.8	4.375 / 111.1	5.375 / 136.5	N/A

Table 5.10: Internal cargo nominal, maximal and minimal dimensions

Mission 3 Payload (Sensor Drop Mission)

Payload for mission 3 is shown in Figure 5.10. The number of balls may not be zero and may not exceed number demonstrated in tech inspection. Nominal and maximal/minimal dimensions are shown in Table 5.11. We decided to take only 2 balls because of simplicity of the pylon, simple and lightweight drop mechanism and short loading time.

Dimensions	Diameter [in/mm]	Mass [oz/g]
Nominal	3.82 / 97.0	1 / 28.35
Maximal	3.759 / 95.48	N/A
Minimal	3.623 / 92.02	N/A

Table 5.11: External cargo nominal, maximal and minimal dimensions

Figure 5.10: Champro ball as external payload for mission 3

Internal Payload Bay

Figure 5.11 shows payload bay which fulfill entire central part of the fuselage. For easy and quick loading and unloading of wooden block there is a cut in the each side of the fuselage to grasp it during unloading. On the top of fuselage are door for quick access during loading/unloading. Latch on the door is made of small neodymium magnet for quick lock/unlock. The wooden block is secured by fuselage walls and door in all three directions for safe normal (not aerobatic) flight.

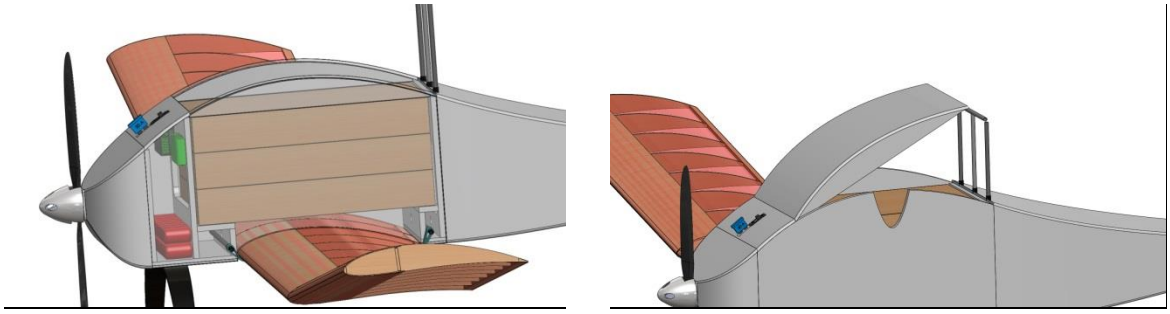

Figure 5.11: Internal payload bay shape for wooden block in mission 2 with grasp cut and door

Pylons for External Payload

We made two pylons using two hollow carbon poles which can protrude into fuselage during ball drop. In the middle between the pylons is ball holder which holds ball in position during flight. During ball loading holder is turned in longitudinal direction (parallel to longitudinal airplane axis) as shown in Figure 5.13 (left) and after loading holder is turned to positon perpendicular to the longitudinal direction as shown in Figure 5.12. Release mechanism is hidden in the fuselage. It consists of rubber and pin which holds the pylon in position during flight. Pin is controlled with rudder servo. Pin is connected with servo using thin cord. The rudder can be operated with no effort between ±25˚ due to flexible cord, but when it riches the angle about ±30˚ the pin is pulled out of the pole and rubber retracts the pole into the fuselage. For rudder

deflection of 30˚ right the left ball is release and vice versa. In the first and second mission the pylons are retracted into the fuselage for less airplane drag.

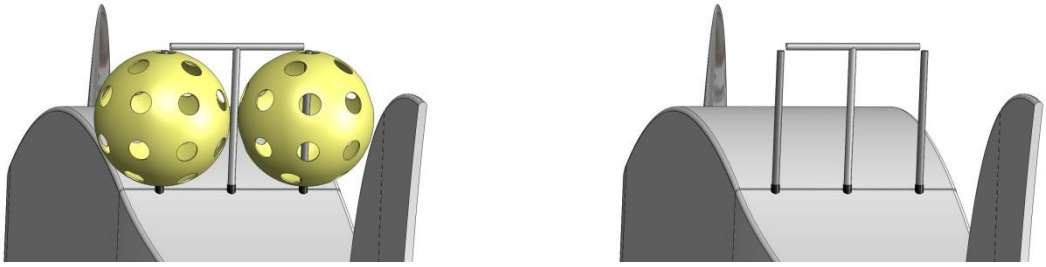

Figure 5.12: Pylon for two external balls; loaded (left), unloaded (right)

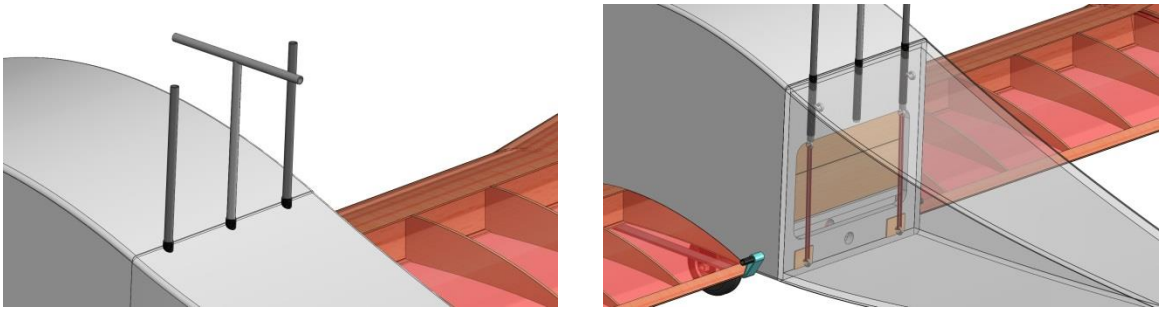

Figure 5.13: Ball holder in ball loading position (left) and release mechanism in the fuselage (right) (cord connection to the rudder servo is not shown)

5.2 Weight and Balance

Position of the center of gravity (CG) is very important for static longitudinal stability of the airplane. We found out that the CG must lie from 50 mm (25.0% root chord) to 83 mm (41.5% root chord) from the wing root leading edge. Front side of firewall was used for weight and balance pivot plane. From Table 5.12, Table 5.13 and Table 5.14 we can see the airplane components position and weight.

Mission 1	Weight [g]	Arm [mm]	Moment [gmm]
Wing	214	174	37236
Airframe	359	326	117034
Motor + Prop. + Contr.	170	-8	-1360
Main Battery Pack	400	32	12800
Control System	101	186	18786
Main Landing Gear	56	26	1456
Sum / CG Position	**1300**	**143**	185952
CG Position from Wing LE	**-**	**50**	-

Table 5.12: Weight and balance calculation for empty airplane (mission 1)

Mission 2	Weight [g]	Arm [mm]	Moment [Nmm]
Airplane	**1300**	**143**	185952
Payload	2270	183	415410
Sum / CG Position	**3570**	**168**	463872
CG Position from Wing LE	**-**	**75**	-

Table 5.13: Weight and balance for mission 2

Mission 3	Weight [g]	Arm [mm]	Moment [Nmm]
Airplane	**1300**	**143**	185952
Payload	56	325	18200
Sum / CG Position	**1356**	**150**	204152
CG Position from Wing LE	**-**	**57**	-

Table 5.14: Weight and balance for mission 3

We cannot predict the exact weight of produced parts, especially wing and fuselage. For fine tuning of the airplane CG position we will shift the receiver battery pack backward or forward inside the fuselage. Pivot plane is at the front wall of the firewall. Distance between firewall and wing root leading edge is 3.6 in (93 mm). We made a design of airplane in a way that the CG is forward of aft limit because we cannot exactly estimate the weight and CG of the fuselage. If the fuselage CG will be more aft of predicted value the airplane CG will not drop out of the CG limits. In the design level we can tune the position of CG on the wing by mowing the wing backward and forward. CG position for all three missions is shown in Figure 5.14.

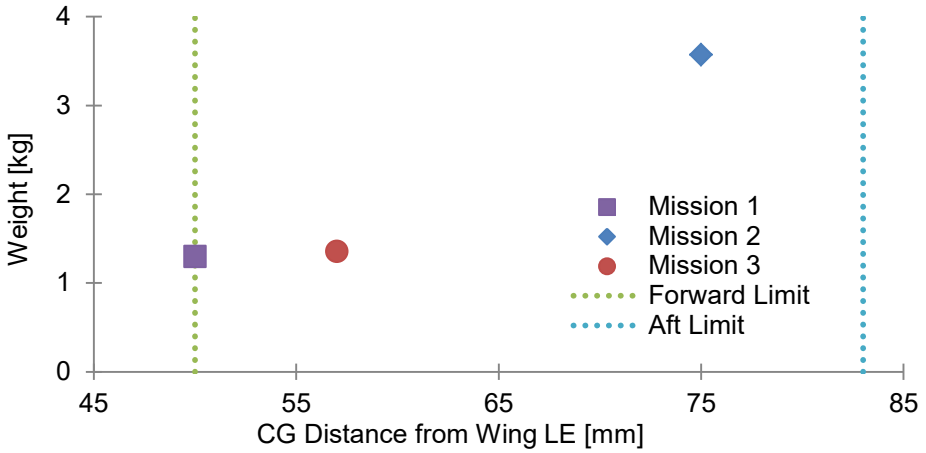

Figure 5.14: CG position for all three missions

We can see CG is inside the limits. The airplane is designed in such way that the empty airplane has CG forward compared to fully loaded airplane.

5.3 Flight Performance for Final Design

Predicted flight performances of final design of the airplane are shown in Table 5.15. Selected design is top performance and has a lot of chance to win. Maneuvering envelope for the empty and fully loaded airplane is shown in Figure 5.15. All flight loads must be all the time inside the envelope for safe flight of the airplane. Limit load factors are estimated from wing strength (beam strength).

Parameter	Mission 1	Mission 2	Mission 3
Max. Speed [kph]	93.4	95.4	95.4
Max. Speed (Turn) [kph]	76.9	76.8	82.4
Speed at Max. Excess Power [kph]	54.0	57.3	60.3
Max. Turn rate [deg/s]	166.2	65.1	155.0
Stall Speed [kph]	25.3	41.9	25.7
Max. Bank Angle [deg]	81	68	60
Thrust-to-Weight Ratio [N/N]	1.5	0.63	1.68
Power-to-Weight Ratio [W/kg]	145.8	56.6	168.6
Max. Climb Speed [m/s]	14.8	5.8	17.1
Max. Climb Angle [deg]	44.6	19.9	48.7
Take-off Distance [m]	2.0	15.2	1.8

Table 5.15: Predicted flight parameters

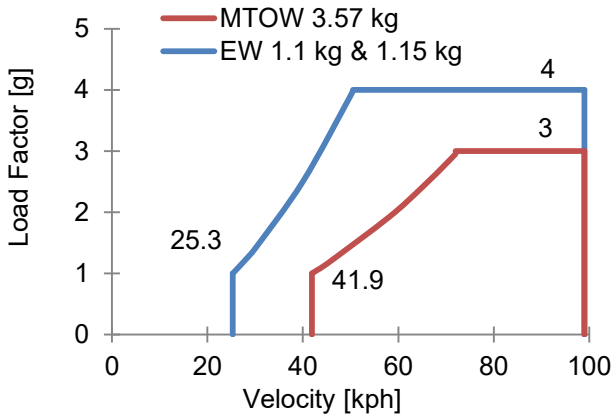

Figure 5.15: Maneuvering envelope (V-n)

5.4 Mission Performance for Final Design

In the Table 5.16 we can see mission performance for final design. We expect to get 1.396 points for total mission score. Assembly time of the airplane is not limited this year, only loading time. Our design allows quite simple and fast loading and unloading of payload. Our expected loading time is 5 s for mission 2 and 3 payload. We expect 8 laps in 4 min in mission 1, flight time 102 s in mission 2 and two laps in mission 3.

	Result	Score
Empty Weight	2.86 lb (1.3 kg)	-
No. of Servos	2+1=3	-
RAC	2.86·3=8.59	8.59
Ground Mission	5 s	1
Mission 1	No. of laps = 8	2
Mission 2	3 Laps Time = 102 s	4
Mission 3	No. of Dropped Balls = 2	6
Total Mission Score (TMS)		**1.396**

Table 5.16: Mission performance for final design

5.5 Drawing Package

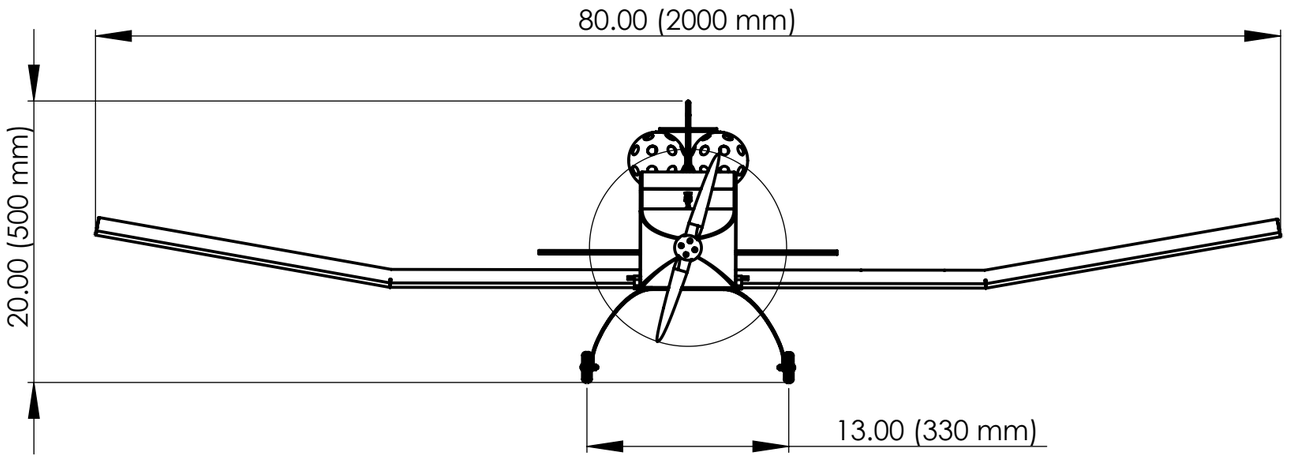

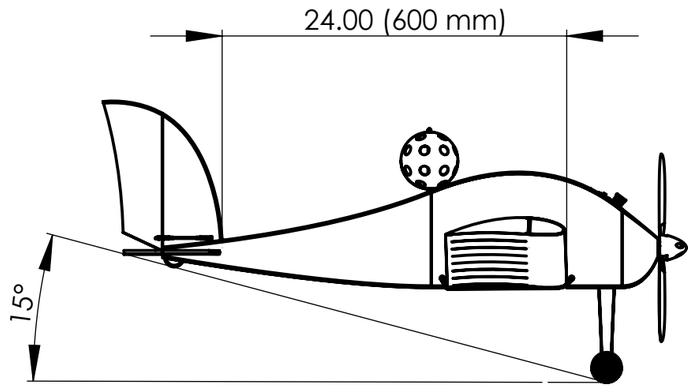

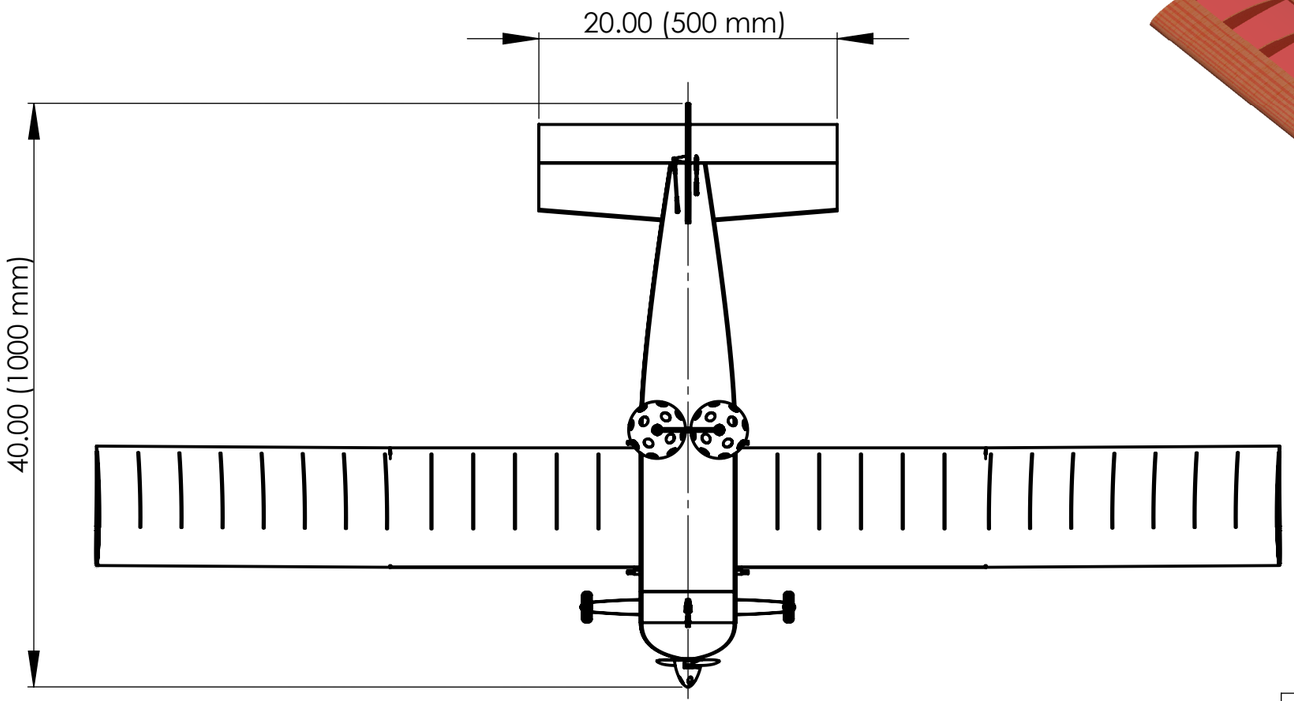

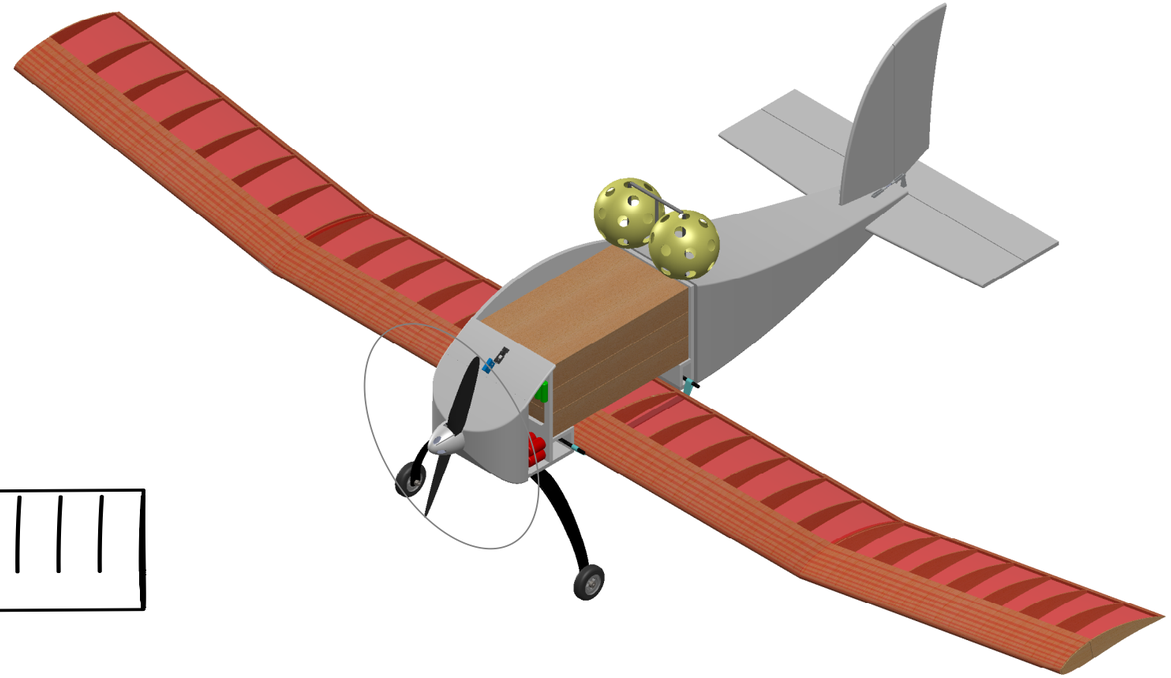

Dimensions are in inches							Scale: 1:10	Masa: kg
No.	Change	Date	Name		Date	Name	Title:	
				Drawn	18.1.2015	A. Ljoki	3-View drawing	
				Chk'd	18.1.2015	T. Kosel		
				Appv'd				
Design, Build, Fly 2015				University of Ljubljana Faculty of Mechanical Engineering Aškerčeva 6, SI-1000 Ljubljana, Slovenia			Edvard Rusjan Slovenian Team	Page 1/4 1 St. 11"x17"

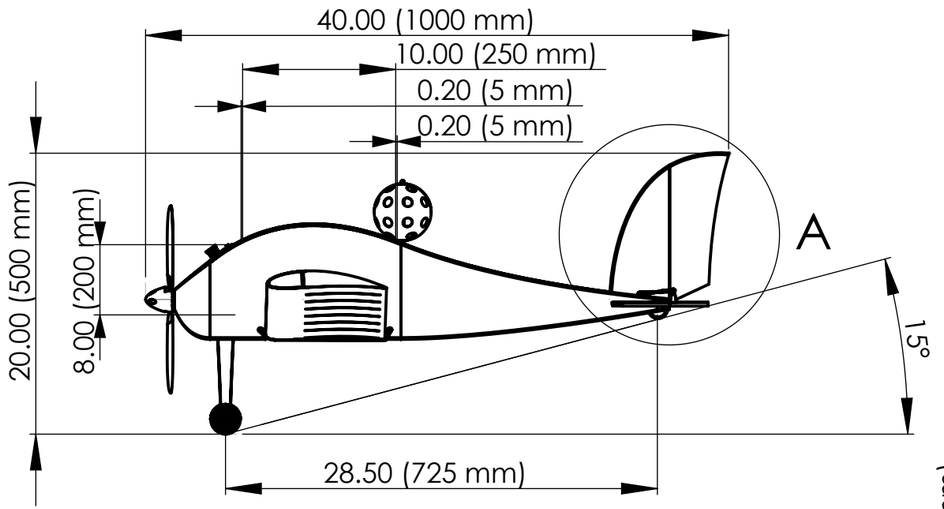

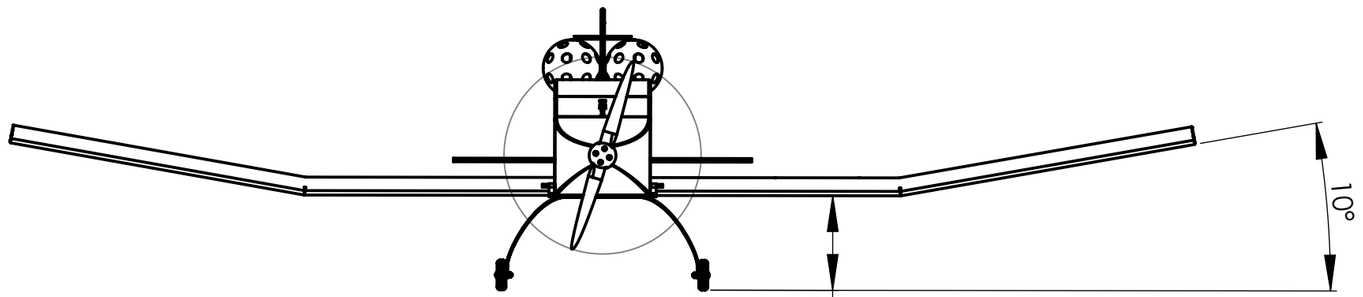

SECTION B-B
SCALE 1 : 2

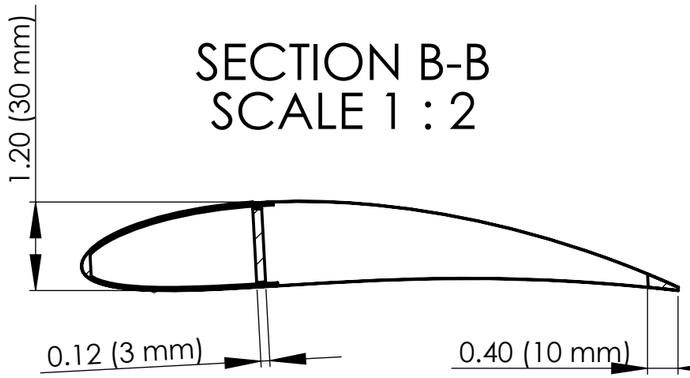

DETAIL C
SCALE 1 : 5

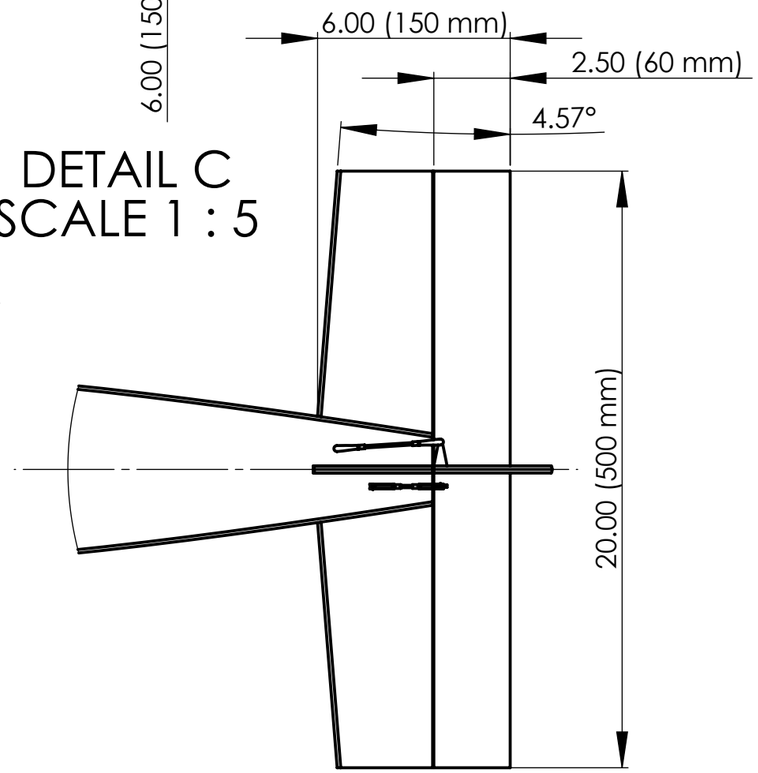

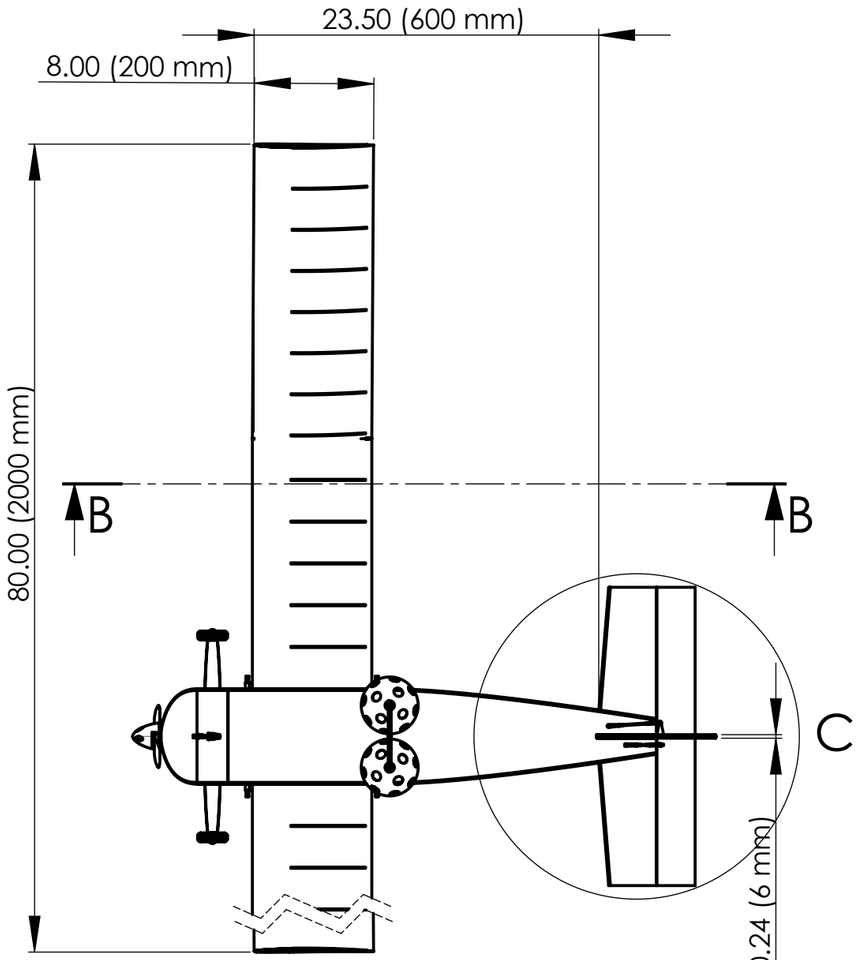

DETAIL A
SCALE 1 : 5

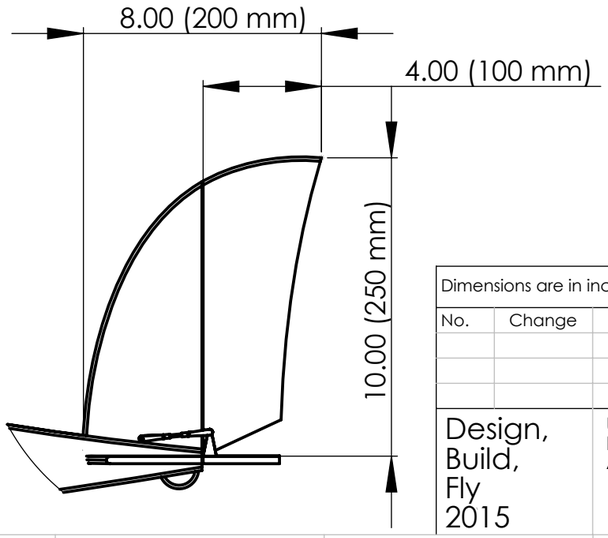

Dimensions are in inches						
No.	Change	Date	Name		Date	Name
				Drawn	18.1.2015	A. Ljoki
				Chk'd	18.1.2015	T. Kosel
				Appv'd		

Design, Build, Fly 2015

University of Ljubljana
Faculty of Mechanical Engineering
Aškerčeva 6, SI-1000 Ljubljana, Slovenia

Scale: 1:10 | Masa: kg

Title:

Structural arrangement

Edvard Rusjan Slovenian Team

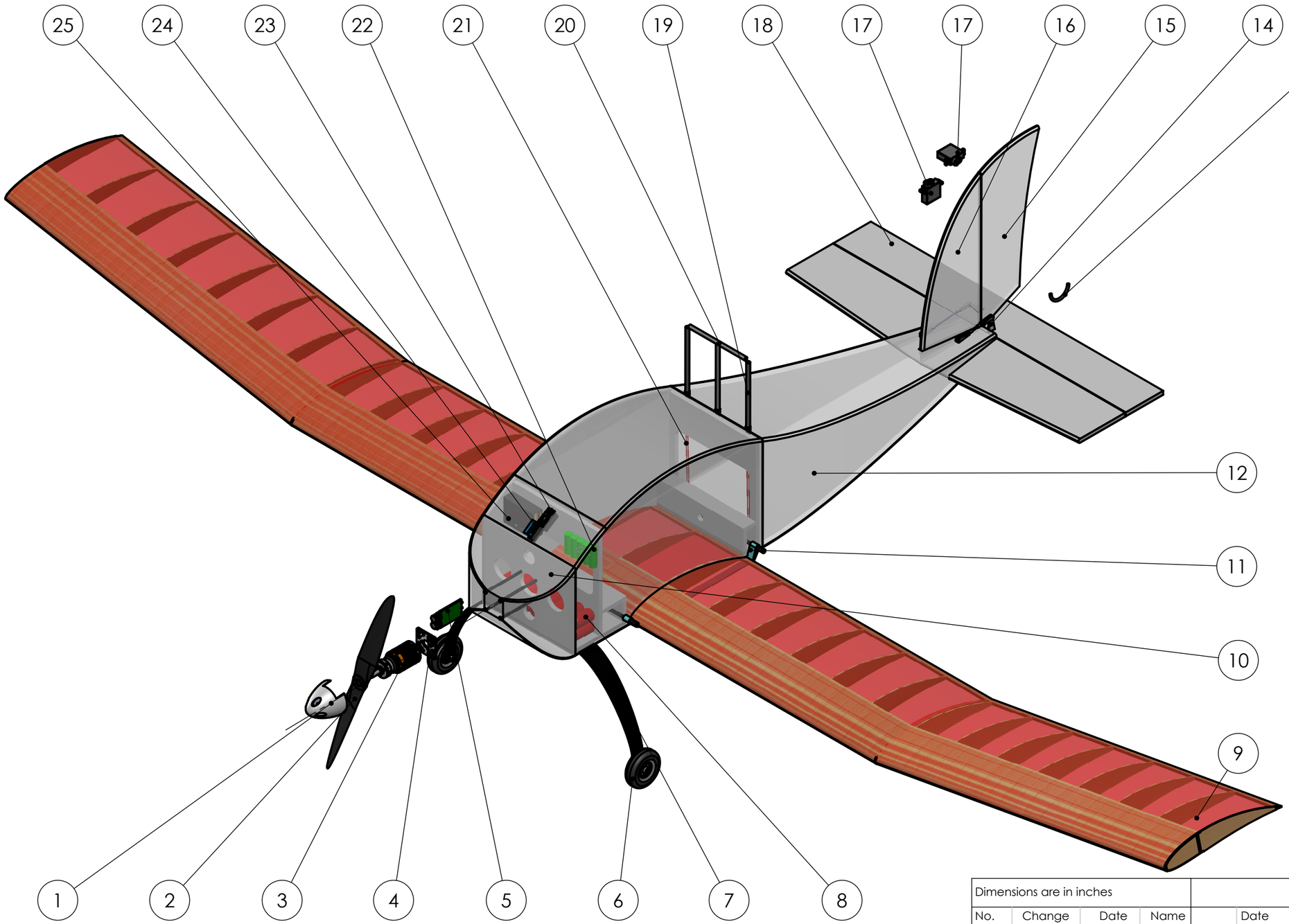

ITEM NO.	PART NUMBER	QTY.
25	Receiver	1
24	Fuse	1
23	Main switch	1
22	Receiver battery pack	1
21	Rubber band - small	2
20	T coupler	1
19	Ball holder	2
18	Elevator	1
17	Servomotor	2
16	Vertical tail	1
15	Rudder	1
14	Lever for Servomotor	2
13	Skid	1
12	Fuselage	1
11	Rubber band - large	2
10	Firewall	1
9	Wing Assembly	1
8	Main battery pack	1
7	Undercarriage	1
6	Main wheel	2
5	Speed controller	1
4	Motor mount	1
3	Motor Assembly	1
2	Propeller	1
1	Spinner	1

Dimensions are in inches

No.	Change	Date	Name		Date	Name
				Drawn	18.1.2015	A. Ljoki
				Chk'd	18.1.2015	T. Kosel
				Appv'd		

Scale: 1:5 | Masa: kg

Title:

Systems layout/location

Design, Build, Fly 2015

University of Ljubljana
Faculty of Mechanical Engineering
Aškerčeva 6, SI-1000 Ljubljana, Slovenia

Edvard Rusjan Slovenian Team

Page 3/4

1 St.

11"x17"

Mission 2 Payload (Stack of three standard 2x6 wooden pine boards):

Scale: 1:5

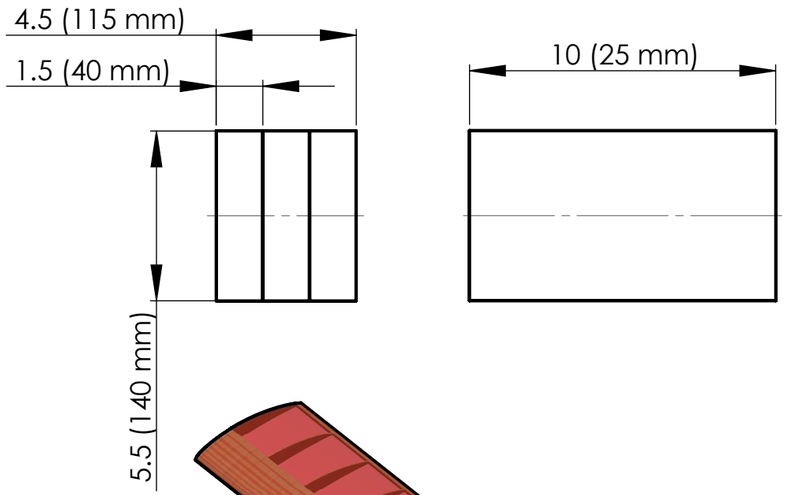

Mission 3 Payload: Champro 12" Plastic Ball

Scale: 1:5

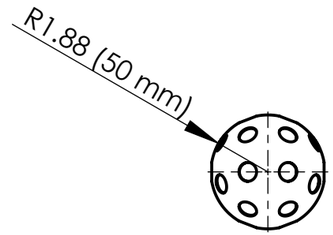

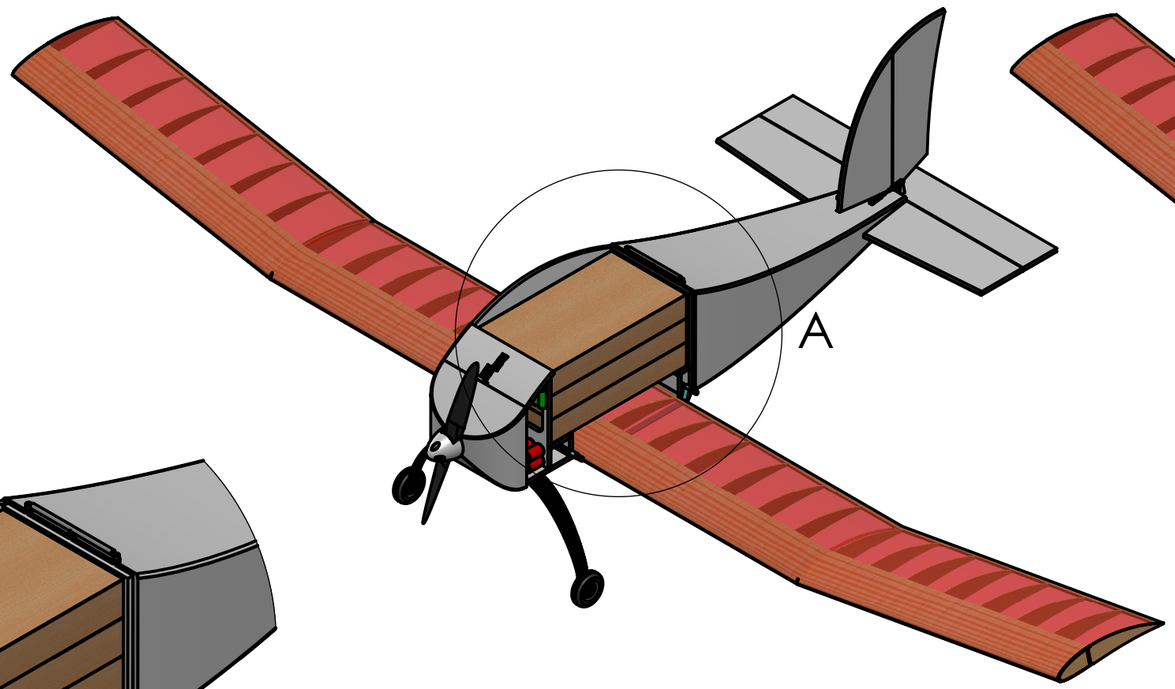

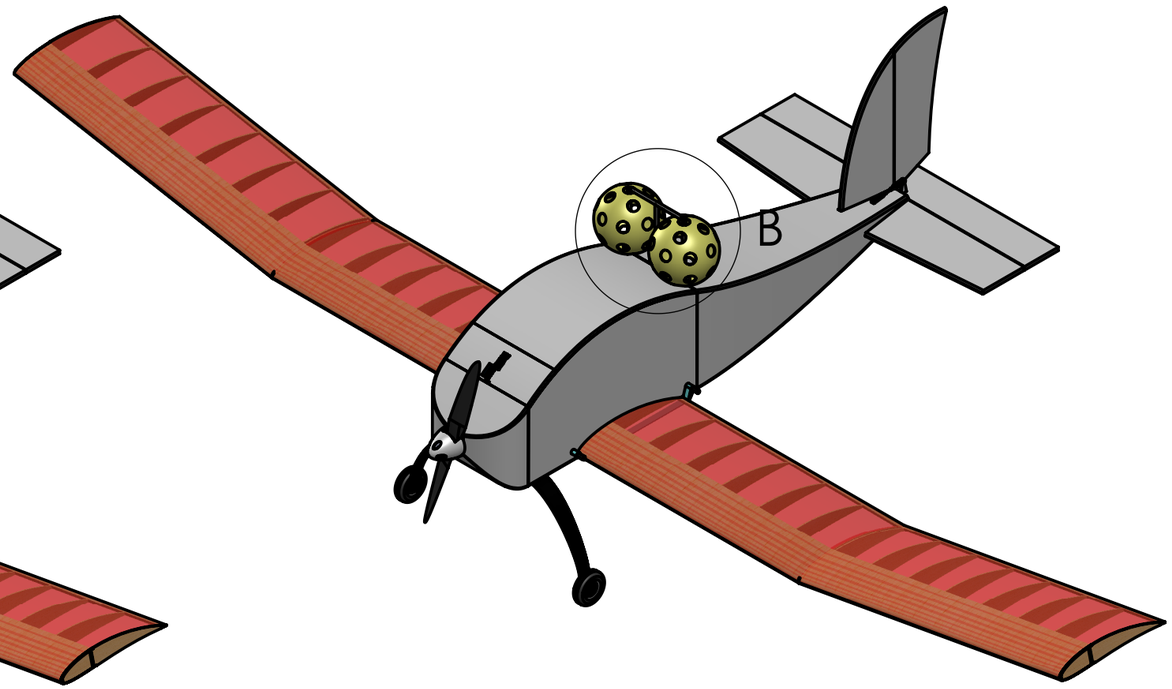

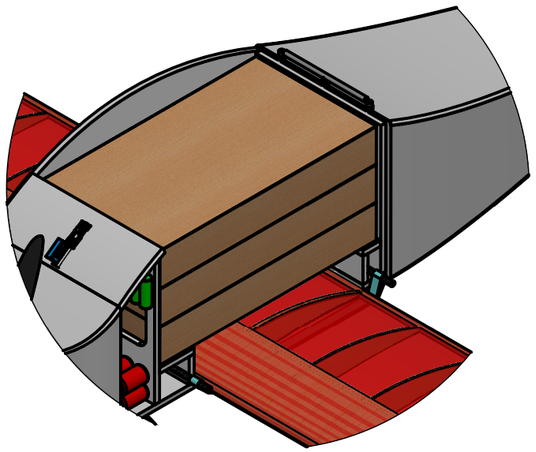

DETAIL A
SCALE 1 : 5

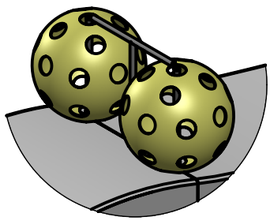

DETAIL B
SCALE 1 : 5

Dimensions are in inches							Scale: 1:10	Masa: kg
No.	Change	Date	Name		Date	Name	Title:	
				Drawn	18.1.2015	A. Ljoki	Payload accommodation	
				Chk'd	18.1.2015	T. Kosel		
				Appv'd				
Design, Build, Fly 2015	University of Ljubljana Faculty of Mechanical Engineering Aškerčeva 6, SI-1000 Ljubljana, Slovenia						Edvard Rusjan Slovenian Team	Page 4/4 1 St. 11"x17"

6 Manufacturing Plan and Processes

All parts of the airplane were designed using Solid Works [7]. There are two major airplane production techniques:

- **Classic Technique** – Used many years for airplane model building using balsa wood, glue and thin cover. We used this technique for wing.
- **Depron Technique** – Is a classic technic using depron instead of wood. We used this technique for fuselage.

6.1 Process Selected for Manufacture

We decided to use both techniques. The parts are made by CNC milling process were needed. All fuselage sides, empennage, all plywood reinforcements and wing ribs are CNC machined. Using these two methods we built the whole airplane.

6.2 Wing

The wing is made of balsa wood covered by Oralight cover. There are 31 ribs in the entire wing which are 2.75 in (70 mm) apart and made of 0.078 in (2 mm) thick balsa wood as is shown in Figure 6.1. The first and the last rib in each wing segment are made of 0.078 in (2 mm) plywood. In the leading edge in front of the main beam there are 60 ribs for shape stability. The wing has one main beam made of balsa wood and carbon fiber bars. The upper flange of the main beam is made of unidirectional (UD) carbon bar (Graupner) dimensions 0.12×0.04 in (3×1 mm) and the lower flange of 0.12×0.02 in (3×0.5 mm). The thicker flange must be on the compression side of the beam due to flange compression stability issue. The beam web is made of 0.12 in (3 mm) balsa wood. The beam is also from three parts and is adapted to mount in one integrated beam. The main beam carries the flexural stresses. In front of the beam is D-box made of 0.02 in (1 mm) balsa sheet wrapped around the front ribs and carries the torsion stresses. The central section of the wing is mounted on the bottom of the fuselage using rubber. Wing upper side shape is adapted to fuselage shape and positioned for a proper wing incidence angle (+2.2 deg). We found out that this type of wing construction is far more lightweight and stiff compared to other techniques of wing construction.

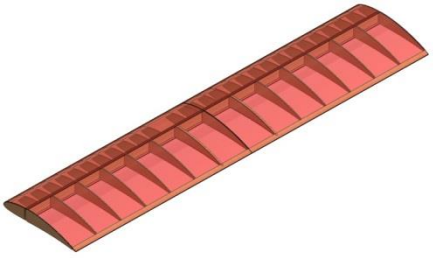

Figure 6.1: Ribs and construction of the central wing

6.3 Undercarriage

Undercarriage is made out of the simple mold. Mold material is Necuron 540 and was milled on CNC machine. We used carbon ribbon 25 mm wide which is made of 20 carbon threads. Ribbon was cut on 20, 500 mm long segments, impregnated by epoxy resin and laid into the mold. Vacuum was applied after that and it was cured on room temperature for 24 hours. After curing we expose undercarriage to 80˚ C for 8 hours to get the final strength of epoxy resin.

6.4 Manufacturing Milestone

Manufacturing schedule and milestones are shown in Figure 6.2.

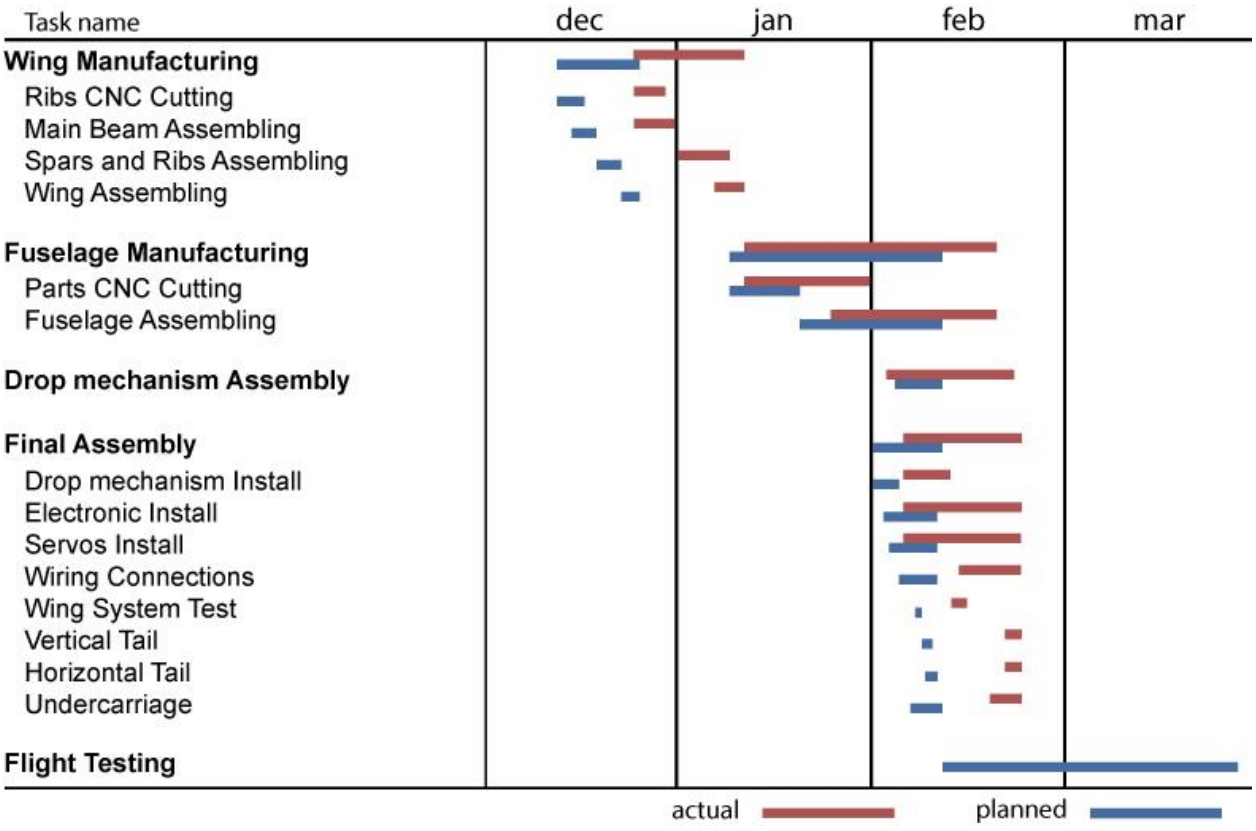

Figure 6.2 Manufacturing schedule and milestone

7 Testing Plan

To ensure our final design and building process was good enough to withstand conditions at the competition; a thorough testing plan had to be made. We tested the structural and propulsion elements for durability and endurance and to get actual strength of the materials used.

7.1 Detail Testing Objectives and Schedules

The objectives presented in the following tables were determined to be the most important properties to get tested. Conforming to the set objectives should ensure a highly competitive airplane.

7.1.1 *Propulsion Tests*

To see that the appropriate propulsion system was selected for the airplane, we set the objectives for batteries, propeller and motor. The objectives are presented in Table 7.1. We performed tests of Peggy Pepper 2221/16 brushless motor.

Part	Objective	Description
Propeller Test	Get actual data of two different propellers	Measuring shaft torque, thrust and RPM
Motor Test	Get actual performance of brushless motor	Measuring output power, current, voltage and RPM
Battery Cycle Charge/Discharge	To find good and bad (low capacity) cells before soldering into pack	Measuring charging and discharging capacity
Motor/Propeller System Test	To select optimal combinations motor-propeller for different missions	Measuring static and dynamic (progresive velocity) thrust, current and voltage

Table 7.1: Propulsion test objectives

Motor and Propeller Test

We tested combination of motor and propeller on static and dynamic thrust in the laboratory for all three missions as shown in Figure 7.1. We used stabile electrical source and battery packs.

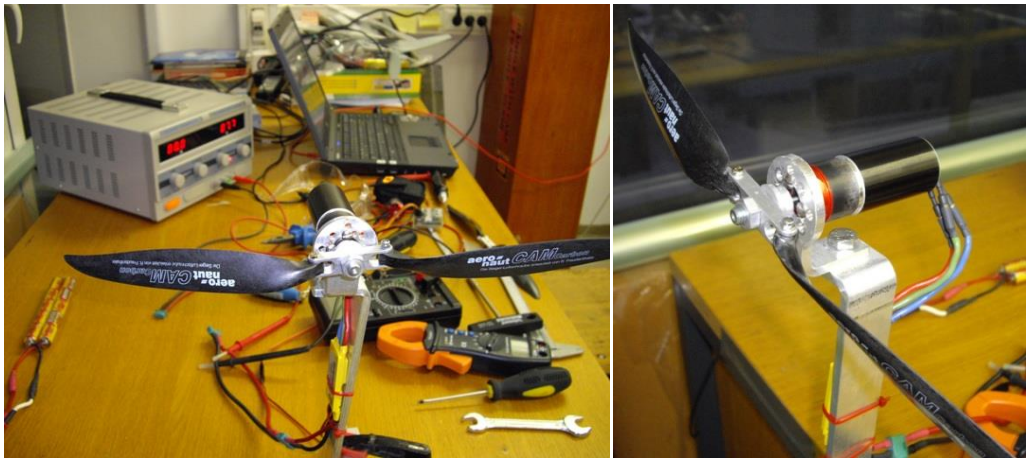

Figure 7.1: Propeller static thrust test

Battery Test

NiMh cells are the main source of energy. There is not so much choice on the market. We calculated that we need 1433 mAh of energy for 4 min flight at 21.5 A in the first mission, so the cell capacity of 1600 mAh is enough. We chose between Elite, and XCell cells. We made a pack of 16 cells; we filled them and waited for them to cool down. We measured thrust as a function of time as shown in Figure 7.2. We found out that the XCell cells have better characteristics because of more beginning thrust or voltage over time. We will get better characteristics if the cells will be warm at the beginning of the flight, then the initial thrust will be higher and more constant over time.

Batteries Elite 1500 and XCell 1600 were tested for capacity to determine which cells should form a single battery pack because it is important to have nearly identical capacities to form a reliable battery pack. The highest performing cells had a capacity around 1550 mAh, lower performing cells around 1450 mAh. Packs were also tested for reliability due high current draw (24 A) during flight. All battery packs became unusable after around 6 to 7 flights because one cell would die due to high temperature. High temperature about 70˚C is a result of high internal resistance of cells at 24 A current. To be on the safe side we then concluded it would be best to have fresh battery pack installed before each mission. We estimated voltage drop of one cell to 0.2 V. The conductivity of the cell depends on cell temperature. Warm cells are more “lively” and allow more electric current to go through. The optimal temperature for cell pack before take-off is 50˚ C. At that temperature they are high performance from beginning until end of capacity. Cold cells need some time to warm up. This is critical in the take-off phase, where fast acceleration is required. It is hard to predict when the airplane will take-off so the temperature will be lower or cells can be cooled down during take-off. Cool battery pack has low performance on the take-off therefore take-off distance (ground roll) is longer. We made all measurement at 50˚C cell temperature as nominal temperature. We found out that the ground roll can be up to 15% longer if the cells are cooled to 20˚C.

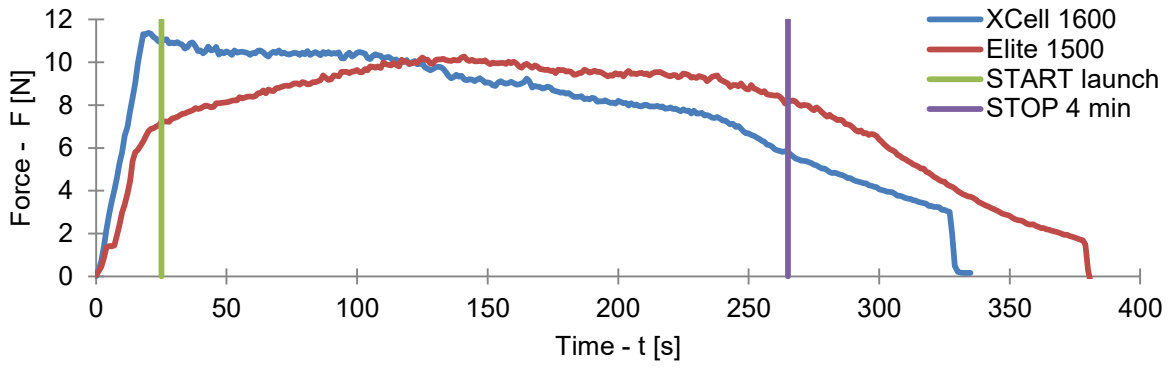

Figure 7.2: Propeller static thrust as function of time with Elite 1500 and Xcell 1600 cells

7.1.2 Ball Drop System

We tested ball drop system in wind tunnel at 46.6 kt (86.4 kph), very close to maximum speed flight. We found out that the system is working properly under air flow. Test is shown in Figure 7.3. Ball drop mechanism consists of pin and cord connected to servo. The pole retracts into the fuselage due to rubber band when the pin is removed. We were afraid that the drag force is so strong that the rubber band is not strong enough to retract the pole.

Figure 7.3: Testing of ball drop mechanism in wind tunnel

7.1.3 Flight Tests

The flight test objectives are shown in Table 7.2. We used a GPS logger (Figure 7.4) to acquire flight parameters as velocity, height, ground speed, course and position. We used this data to compare actual performances of the flight system and final design.

Test	Objective	Description
Flight Control Check	Confirm all controls working properly	Check for control surfaces deflecting as they should and that limits are not set too wide
Fale Safe Test	Test the control system for fale safe operation	Chek the control surfaces and throttle work at distance of 100 m.
Empty Flight	Determine airplane stability	Check for stall, maximum speed and handling
Weighted Flight	Determine maximum wing load and contolability	Add weight incrementally and checking for stall speed and controlability
Mission Flight	Training for mission flights	Pilot training for mission 1, 2 and 3
Ground Mission Loading/Unloading	Training for loading and unloading of cargo	Three members of the team load and unload the airplane and check the spend time

Table 7.2: Flight test objectives

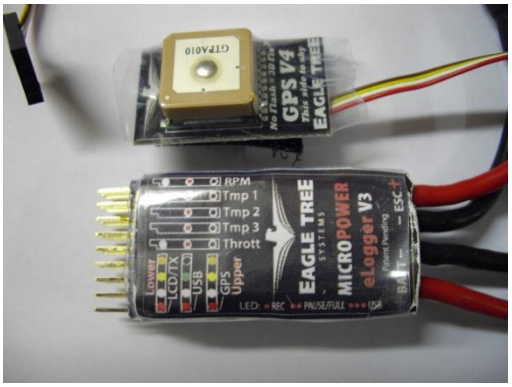

Figure 7.4: Eagle Tree V3 GPS logger (10 Hz) installed in airplane during flight tests

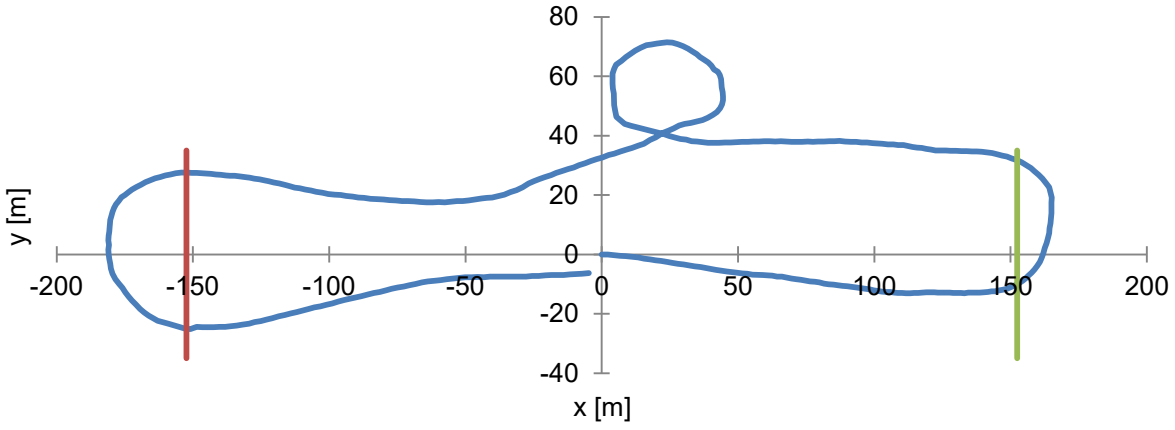

Figure 7.5: One lap logged by GPS logger

7.2 Check Lists

Preflight check lists were made with a reason to ensure safe flight tests and useful results, so that important procedures are not forgotten. Check lists are presented in Table 7.3.

Structural Integrity		Avionics and Controls	
Wing	• Check for damage • Screws are tightly screwed • Wing segments tightly connected	**Transmitter**	• Check the battery is fully charged
Internal Payload	• Insert into fuselage • Secured payload • Lock the lid	**Servo Wiring**	• Connect all servos
Empennage	• Check for damage	**Fuse**	• Check the fuse is removed and stored near transmitter
Control Surfaces	• Check for damage • Clear of obstructions	**Controls Test**	• Check all control surface for correct movement • Check maximum deflections
Receiver Battery	• Check the battery is fully charged • Insert battery into the airplane	**Failsafe**	• Test failsafe mode on the transmitter
External Payload	• Payload correctly installed on pylons • Secured payload by T holder	**Payload Door**	• Check that payload lid is fully closed and secured

Table 7.3: Check list

8 Performance Results

Test flights of prototype airplane proved our predictions. The airplane is maneuverable, stable and easy to control and without unpredictable behavior at low speeds. It has no tendency to spin.

Airplane speed and energy consumption were measured with a GPS logger. The acquired data showed us that during the first mission the airplane's average speed was 47 kt (87 kph) and completed 8 laps in 4 minutes as predicted with plenty of energy left if a go around were needed during landing. The number of laps was highly dependent of pilot's performance that is why we gave the pilot a task to train circuit flying as many days as possible until the competition. During the second and third mission the airplane's average speed was 46 kt (85 kph). The time of 1 lap was less than 30 seconds, which means that we are on the safe side concerning the battery capacity even in the event of a slight wind on the day of

competition because the motor did not exceed 24 A which was a critical limit for successful completion of the second and third mission.

8.1 Demonstrated Performance of Key Subsystems

There are two subsystems in the airplane: control system and propulsion system.

8.1.1 Propulsion System

The most important subsystem for all three missions is propulsion system. We can see in Table 5.8 that is predicted thrust about 10% overestimated for given revolutions per minute. Voltage drop per cell was correct estimated on 0.2 V or 3.2 V per pack. For performance calculation we used 16 V per pack. Measured value is 16.3 V per pack at 24 A.

8.1.2 Battery

Several charge discharge cycles have been made and documented on each cell. With that data we preselected cells that would form balanced packs and minimize the possibility of battery pack malfunction. Cycles were made at 1 A current and the results showed that there is quite a bit of difference between cells in term of charge capacity. It varies from 1450 mAh to 1550 mAh.

8.2 Demonstrated Performance of Complete Airplane

The demonstrated performances acquired during flight test are shown in Table 8.1, Table 8.2 and Table 8.3. For confirmation of the analysis results, we used the prototype airplane as shown in Figure 3.4. In order to acquire results that would have any significance in analysis, we installed Eagle Tree Telemetry into our airplane. It recorded propulsion pack current draw, propulsion pack voltage, airplane speed, course, location and altitude.

We had a bit of a problem with taking off a tail dragger airplane because we didn't pull enough back on the stick so that the tail gear was not in tight contact with the ground during ground roll. That resulted in failed attempts of take-off, it means running off the runway and very unstable take-off. After we fixed take-off technique, it was taking-off flawlessly. First, we flew the first mission and results were in line with the performance predicted in analysis – maximum speed of 48 kt (90 kph) at 23 A of current with a 14×10 APC E propeller. It also did 8 laps, as was predicted in the analysis. Next testing phase was to determine flight characteristics during second and third mission. Here, the primary objective was to measure the take-off ground roll distance and to compare it with predicted value. Secondary objective was to determine the flight time of 3 laps. In this case we simulated the mass of wooden block with lead blocks which were duct-taped into the airplane. We used 15×8 APC E propellers to achieve greater thrust. The

take-off weight of the airplane was 7.86 lb (3.57 kg) and with it the take-off distance was 52.5 ft (16 m). It is longer as was predicted in the analysis. Flight time in the second mission was 95 s. This is also very close to prediction.

As we can see in Table 8.1, Table 8.2 and Table 8.3 that the estimated and actual data are very close. Actual propulsion efficiency is even better than estimated.

Mission 1	Estimated	Actual
Max. Speed [kph]	93.4	87.1
Stall Speed [kph]	25.3	25.4
No. of Laps	8	8
Max. Climb Rate [m/s]	14.8	15.3
Take-off Distance [m]	2.0	3.2

Table 8.1: Estimated and actual data for mission 1

Mission 2	Estimated	Actual
Max. Speed [kph]	95.4	85.2
Stall Speed [kph]	41.9	35.3
Max. Climb Rate [m/s]	5.8	5.1
Time for 3 Laps [s]	102	110
Take-off Distance [m]	15.2	16.3

Table 8.2: Estimated and actual data for mission 2

Mission 3	Estimated	Actual
Max. Speed [kph]	95.4	88.4
Stall Speed [kph]	25.7	26.2
Max. Climb Rate [m/s]	17.1	18.2
Take-off Distance [m]	1.8	2.5

Table 8.3: Estimated and actual data for mission 3

Stability and control during testing was satisfactory with aft allowable CG position and the airplane was easy to control without ailerons which is very important since it removes a bit of pressure from the pilot during competition that can then focus all of his attention to flying the circuit correctly. The pilot technique is very important to get good score.

We are satisfied with the airplane performance and low weight. It was designed to fly on “the edge” and pose a serious opposition to this year’s competitors.

References

[1] DBF Rules and Vehicle Design: http://www.aiaadbf.org/2014_files/2014_rules.htm

[2] Jan Roskam, Airplane Design, Part 1 – Preliminary sizing of airplanes, 1989, University of Kansas

[3] JavaFoil, http://www.mh-aerotools.de/airfoils/index.htm

[4] UIUC Airfoil Coordinates Database, http://www.ae.illinois.edu/m-selig/ads/coord_database.html

[5] Warren F. Phillips, Mechanics of Flight, 2004, John Wiley & Sons, Inc.

[6] Courtland D. Perkins and Robert E. Hage: Airplane Performance Stability and Control, John Wiley & Sons, Inc.

[7] Solid Works: http://www.solidworks.com/

[8] Drive Calculator, http://www.drivecalc.de/

[9] Wing configuration, http://en.wikipedia.org/wiki/Wing_configuration/

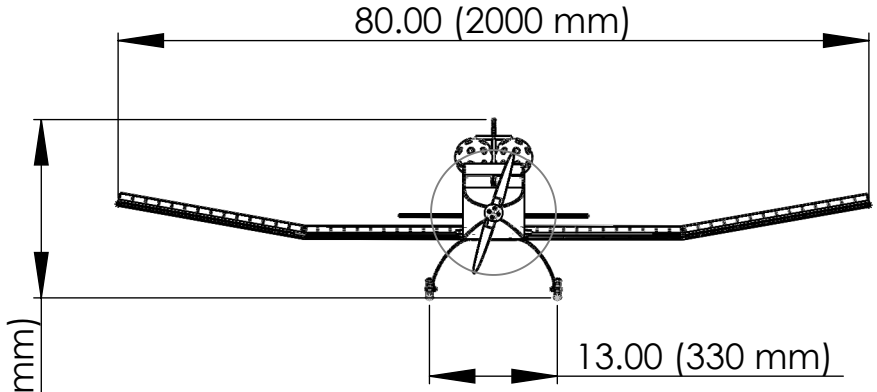

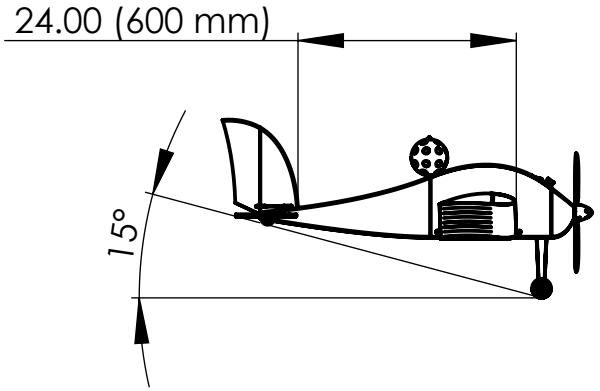

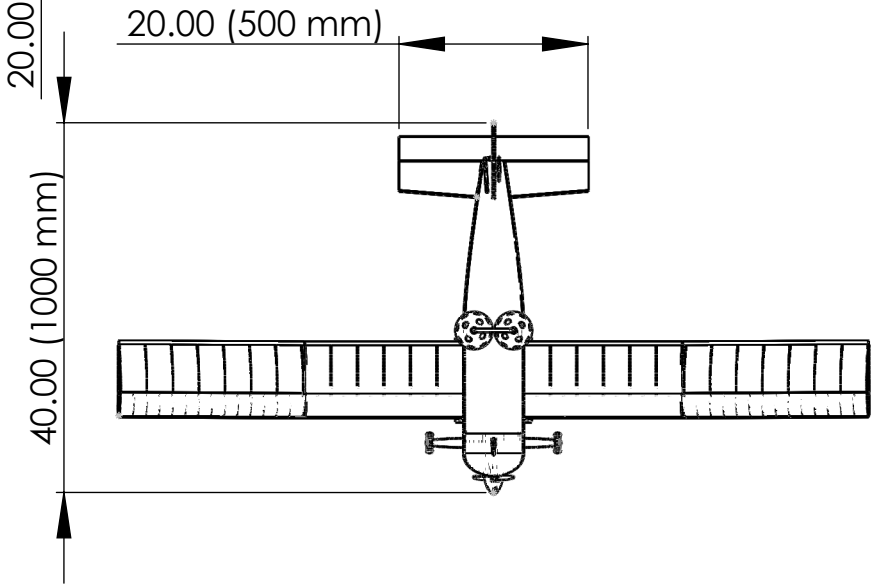

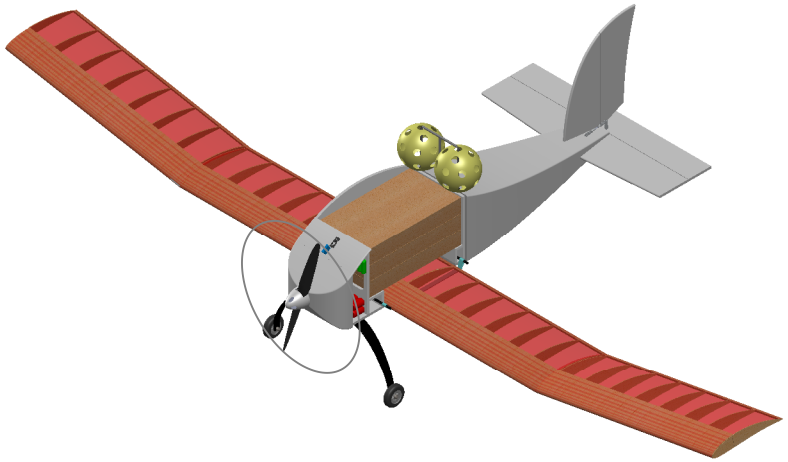

Dimensions are in inches						
No.	Change	Date	Name		Date	Name
				Drawn	18.1.2015	A. Ljoki
				Chk'd	18.1.2015	T. Kosel
				Appv'd		

Scale: 1:20 | Masa: kg

Title:

3-View drawing

Design, Build, Fly 2015

University of Ljubljana
Faculty of Mechanical Engineering
Aškerčeva 6, SI-1000 Ljubljana, Slovenia

Edvard Rusjan Slovenian Team

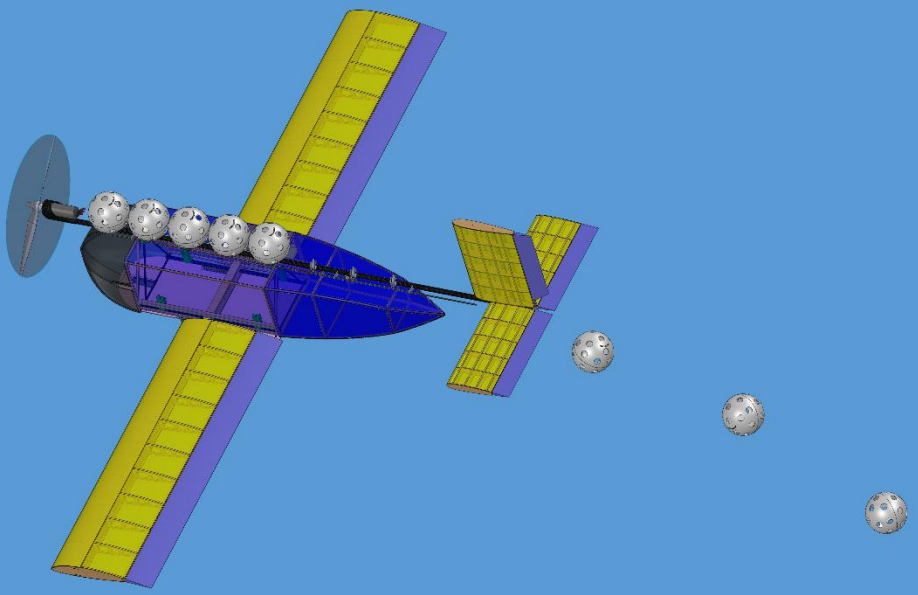

DESIGN/BUILD/FLY

Cessna/Raytheon AIAA Design/Build/Fly Competition 2014-2015

UC Irvine | The Henry Samueli School of Engineering

Table of Contents

1.0 Executive Summary

This report documents the design, analysis, manufacturing processes, and testing conducted by the University of California, Irvine (UCI) Design/Build/Fly team, for the development of their aircraft entry in the 2014-2015 AIAA/Cessna/Raytheon Design/Build/Fly competition. The objective of the competition is to produce an electric remote controlled aircraft; that will not only meet the mission requirements but will receive the highest total score: a combination of the written report score, total flight score, and rated aircraft cost (RAC).

The theme of this year's competition is Remote Sensor Delivery and Drop System [1]. The goal of the aircraft is to be as light as possible while carrying two types of payload: for mission 2, an internal 5-lb payload made of plywood and for mission 3, an external payload consisting of 3.75-in diameter wiffle balls. The aircraft must be capable of completing a ground mission as well as three flight missions. These flight missions will test the aircraft's performance speed, handling of the sensor package, and efficiency when releasing a ball each lap. The ground mission requires three crewmembers to load and unload the payload for mission 2, then load the payload for mission 3 as fast as possible. The objectives of the flight missions are as follows: fly a maximum number of laps in a four-minute period without a payload, fly three timed laps with a 5-lb wooden payload, and fly as many laps as possible while releasing one 3.75-in diameter wiffle ball per lap.

Through score analysis, the team determined that the winning aircraft would be one built with the lightest possible empty weight while still being able to complete all four missions. Focusing only on weight or one mission alone would not help engineer a winning airplane. A major challenge is taking off within a 60-ft runway, while meeting the propulsion limitation of a 2-lb maximum battery weight. In addition, the need to be able to release one 3.75" wiffle ball per lap adds further complexity to the design. To address the challenges posed by each mission, the team identified the driving design requirements: high speed for flight mission 1, high thrust for mission 2, and high number of wiffle balls for flight mission 3. After considering several aircraft configurations, a conventional aircraft design consisting of a low wing, conventional tail, tail dragger landing gear, and a single tractor motor was selected as the optimal design.

With maximized performance in mind, the team chose a low kV motor and opted to increase the voltage and propeller diameters for each mission in order to gain enough thrust for takeoff while staying within the 60-ft takeoff requirement. The battery pack was sized accordingly to provide enough energy for all missions while minimizing weight. The aircraft's wing was sized specifically for the takeoff portion of mission 2 due to the additional 5-lb payload. This meant that the wing was overbuilt to fly mission 1, which allowed it to pull high G turns to reduce the turn radius and lap time. The aircraft optimization revealed that the number of external payloads should match the weight used in mission 2.

Constraints on how to position the payload drove the fuselage design. The cross section of the fuselage was minimized to fit the payload for mission 2 longitudinally and enclosed a central carbon rod

that ran from the motor to the tail. The landing gear was attached to the fuselage floor, allowing loads to be transmitted from the landing gear to the central carbon rod through the fuselage structural members. To minimize structural weight, the fuselage section was constructed mainly of balsa strips and carbon rods with Microlite™ covering as skin. The payload release mechanism was mounted to the central carbon rod so that the length was efficiently used to carry as many 3.75" plastic wiffle balls.

The aircraft was tested to its performance limits, while the design of the aircraft and its components were being improved and optimized, eliminating weight when possible. Through thousands of simulations and multiple prototypes, the team was able to produce an aircraft to satisfy all mission objectives. The average times and results for each mission are as follows: 30-sec for the ground mission, 6 laps for mission 1, 157-sec for mission 2, and 8 laps for mission 3.

2.0 Management Summary

The UCI team implemented an organizational structure and design timeline that focused on maximizing efficiency and team collaboration.

2.1 Team Organization

The team follows a hierarchical structure similar to those found in industry, which places responsibility on members to perform their requested tasks. Figure 2.1 shows the team's organizational chart.

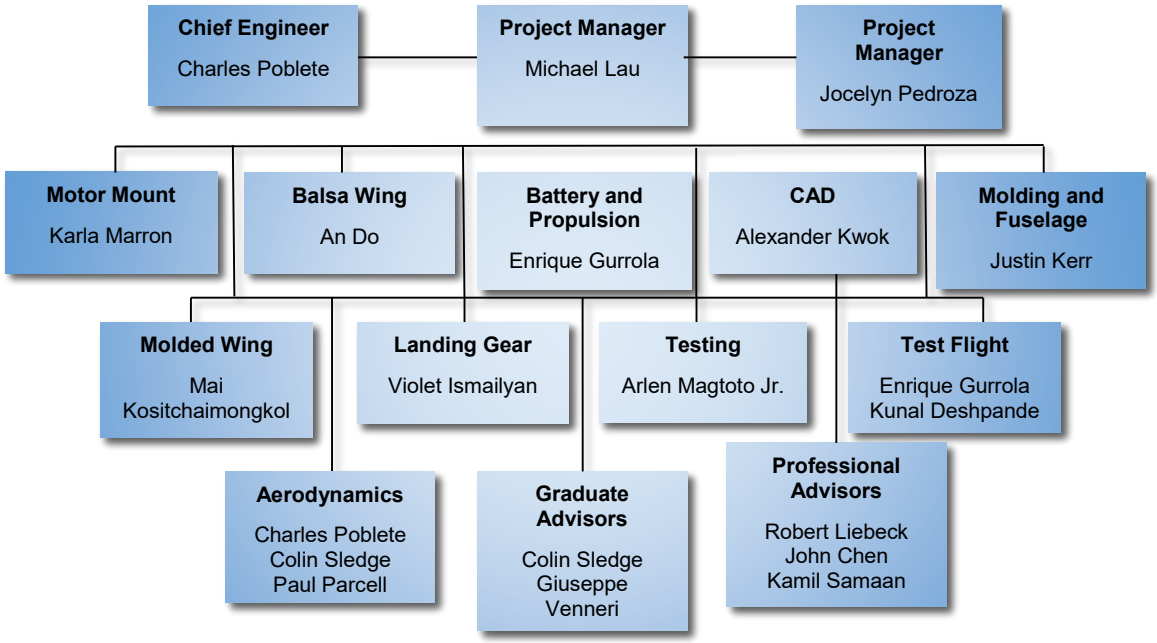

Figure 2.1: Team Organizational Chart

The Project Managers are responsible for facilitating productivity in all areas of the project by acquiring material, scheduling, managing logistics, keeping a budget portfolio, and leading team meetings. The Chief Engineer steers the design effort and facilitates the communication between design groups. All three individuals lead the team project, which is further supported by the following teams:

- **Aerodynamics** computes the flight characteristics and necessary wing dimensions. This team also ensures that the aircraft meets certain control and stability standards, and uses numerical modeling to predict flight performance.
- **Balsa Structures** experiments with new manufacturing methods for the wings and fuselage in order to decrease the overall weight while maintaining structural integrity.
- **Battery and Propulsion** analyzes and tests the propulsion system to find the best motor, propeller, and battery combination for the aircraft.
- **CAD** creates detailed drawings of every component of the aircraft system and aids in the rapid visualization of possible aircraft solutions.
- **Fuselage and Payload** designs and builds fuselage, fairings, and payload restraint mechanisms.
- **Motor Mount** focuses on fabricating motor mounts that attach to the fuselage boom.
- **Landing Gear** designs and fabricates landing gears integrated with the fuselage floor.
- **Testing** fabricates test apparatuses and conducts load testing for manufactured parts while collecting data for documentation purposes.
- **Test Flight** organizes and conducts test flights, performs preflight/post-flight inspection and collects flight data.
- **Wing** manufactures the wing, tails, and control surfaces using proven methods.
- **Graduate and Professional Advisors** guide and provide insightful suggestions with constructive criticism. Graduate Advisors look over aerodynamic performance aspects of the design and are more accessible than professional advisors. Professional Advisors offer manufacturing tips from previous and current industry experience.

The team held a large-scale recruitment event at the beginning of the year to attract new members in order to satisfy the 1/3 underclassmen rule. New members were placed under the supervision of various team leaders and tasked with learning manufacturing processes as well as their respective team's duties and objectives. With over 40 dedicated members, the team benefits from the enthusiasm and wealth of fresh ideas from new members as well as the experience from returning members.

2.2 Project Milestone Chart

Due to the demand for a competitive aircraft, an organized schedule was set up at the beginning of the year with the use of a Gantt chart. Both Project Managers maintained a master schedule that tracked the various phases of the design, testing, and important milestones of the project. The planned and actual schedules are shown in Figure 2.2.

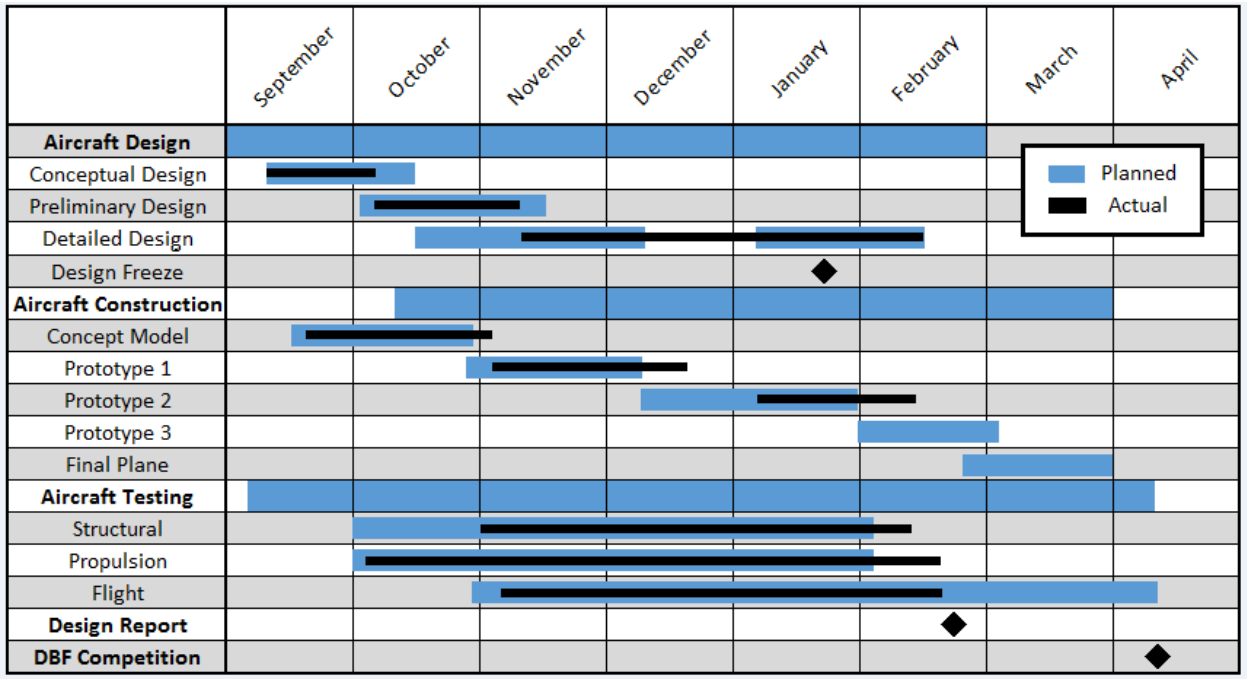

Figure 2.2: Gantt chart with planned and actual timelines

3.0 Conceptual Design

The objective of the conceptual design process is to obtain possible solutions that would satisfy the given design request. Possible solutions are compared and analyzed using figures of merit (FOM) extracted from the analysis of the mission goals, requirements, and the design constraints provided in the contest rules. The result of this process is a high performance design that maximizes the overall flight score.

3.1 Design Constraints

The team analyzed the contest rules in order to determine the important design limitations. The main requirements for the Design/Build/Fly competition this year were as follows:

- The weight of the propulsion battery must not exceed 2.0-lb
- The mission 2 payload must be carried internally
- The mission 3 payload must be carried externally, defined as being exposed to free stream flow from three sides excluding the front and back
- The aircraft must be designed to fly all three missions
- The ground rolling takeoff for every mission must take place within a 60-ft runway distance
- All batteries must be either nickel cadmium (NiCad) or nickel metal hydride (NiMH).
  During flight, payloads must be secured sufficiently to ensure safe flight without possible variation of the aircraft's center of gravity (CG) beyond the design limits.

3.2 Scoring Formula

The AIAA Design/Build/Fly competition for 2015 consists of one ground mission, three flight missions, and one written report. The total score is contingent on the mission scores, the rated aircraft cost (RAC), and the report score. The formula to determine a team's score is shown below:

$$Total\ Score = \frac{Total\ Mission\ Score * Written\ Report\ Score}{Rated\ Aircraft\ Cost}$$

$$Total\ Mission\ Score = GS * FS$$

$$Flight\ Score = FS = M1 + M2 + M3$$

$$Ground\ Score = GS = \frac{Fastest\ Loading\ Time}{Loading\ Time}$$

$$Rated\ Aircraft\ Cost\ (RAC) = EW_n * N_{servo}$$

$$Empty\ Weight = EW_n = Max(EW_1, EW_2, EW_3)$$

EW_n is the heaviest measured weight of the aircraft after any flight with the payload removed

3.3 Mission Sequence

The competition consists of a ground mission and three flight missions. The ground mission may be completed at any time when the flight line is open. However, all three flight missions must be flown in order; a new mission cannot be attempted until a score has been received for the previous mission. The aircraft must first pass the wing tip load test with the largest payload loading intended to fly for any mission; the maximum load will be recorded and cannot be altered after tech inspection. For the ground mission, the aircraft will enter the assembly area with no payload and the team will then have 5 minutes to load the payloads for missions 2 and 3. After each payload is secured,, time is stopped and the aircraft systems are checked for safety. The team cannot work on the aircraft after loading/checkout time, meaning no compartment on the aircraft will be re-opened. The staging box is only for the pilot, pilot assistant and assembly crew members. After checkout, the crew members may be swapped out. The aircraft is limited to a 60-ft takeoff length. The pilot will have unaided visual control of the aircraft at all times. For the first turn on any mission, the turn will not be permitted until the judge gives a signal. Finally, to receive a score on any mission, the plane must successfully land.

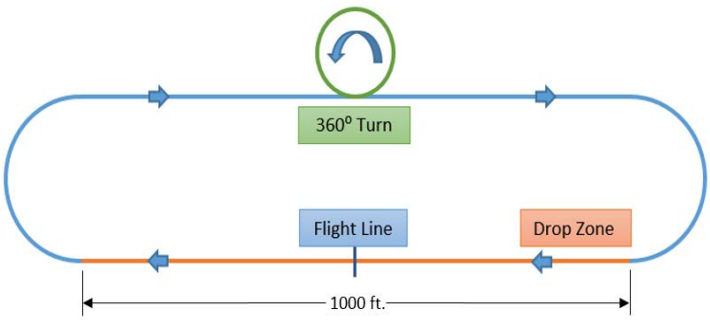

Figure 3.1: Course Layout

3.3.1 Ground Mission – Payload Loading Time

The ground mission is a timed mission of how quickly payloads for mission 2 and 3 can be installed and secured; which commences with an empty airplane and closed hatches. Mission 2 payload is installed internally and secured. After the crew leaves the loading area, time is stopped to verify that the aircraft is secured at which point the time is restarted. When time is restarted, mission 2 payload must be unloaded and mission 3 payloads must be installed and secured. Once again the crew leaves the loading area and time is stopped so that the judges can verify that the airplane is secure. The score is determined by the following equation:

$$GS = \frac{Fastest\ Loading\ Time}{Loading\ Time}$$

Note: If ground mission has not been completed, then GS=0.2 will be used for intermediate scoring calculations.

The fastest loading time by any team is divided by the loading time of your team

3.3.2 Mission 1 – Ferry Flight

This mission has no payload and has a 60-ft takeoff requirement. The goal is to complete as many laps as possible within the time limit of 4 minutes. Time is started during throttle for takeoff. The laps are measured when the aircraft passes the start/finish line. The aircraft must land successfully to get a score. The score is determined by:

$$M1 = 2 * \frac{Number\ of\ laps\ flown}{Maximum\ number\ of\ laps\ flown}$$

The number of laps flown by the team is divided by the maximum number of laps flown by any team competing.

3.3.3 Mission 2 – Sensor Package Transport Mission

In Mission 2, the payload must be secured internally, meaning no component of the load can be exposed to free-stream air. The mission consists of 3 timed laps with the provided sensor package payload. The payload is a 5-lb stack of three 10-in long 2x6 wooden pine boards.

- The overall size will be 4.5" x 5.5" x 10".
- The weight will be ~5lb.
- Dimensional tolerance will be +/-1/8" in all directions.

Time starts when the aircraft throttles for takeoff and ends when the aircraft passes the finish line. A successful landing must occur to get a score. The score is determined by:

$$M2 = 4 * \frac{Fastest\ Time\ Flown}{Time\ Flown}$$

3.3.4 Mission 3 – Sensor Drop Mission

This mission requires the payloads to be loaded externally; defined as being exposed to air on three or more sides, excluding front and back. The load is a team-selected quantity of Champro 3.75-in diameter wiffle balls. Each ball weighs approximately 2.4-oz. For each lap, the aircraft will drop a ball in the designated area while airborne. A lap will count only if one ball is dropped; multiple or no balls drops per lap will invalidate that lap. No other part of the aircraft besides the ball can be dropped. The aircraft must land successfully to get a score:

$$M3 = 6 * \frac{Number\ of\ Laps\ Flown}{Maximum\ of\ Laps\ Flown}$$

The maximum of laps flown is determined by any team competing. The number of laps flown is the number of laps flown by your team.

3.4 Sensitivity Analysis

The score equations were first analyzed to see the level of impact that each parameter had on the competition's final score.

3.4.1 Extreme Cases

Several aircraft designs were considered when looking at extreme cases. The goal was to determine if it was possible to exploit a single parameter in order to achieve a very high score.

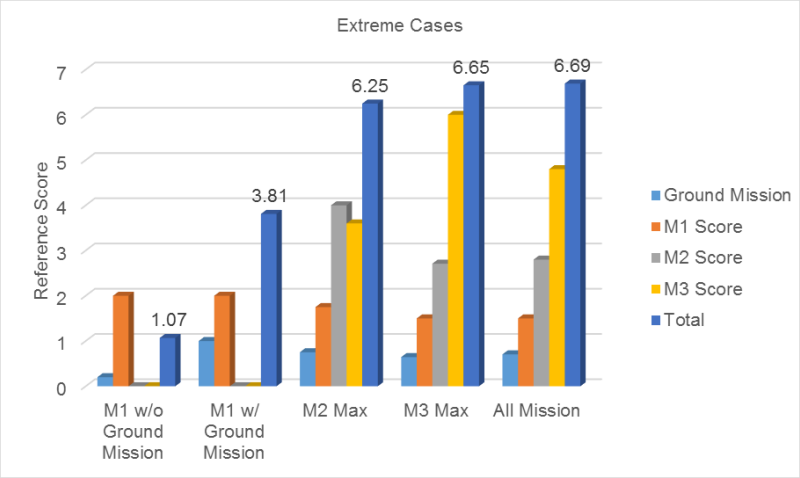

Figure 3.2: Extreme Case Scores

The first case that was considered is an aircraft that is only capable of flying mission 1. This aircraft would be very lightweight but would not be capable of storing the payload for mission 2 or mission 3; this case was only considered as a reference for the other cases. The second case was an aircraft that is also lightweight and was capable of statically holding the payloads for mission 2 and mission 3. The third case is an aircraft that is designed to have a very high mission 2 score; for this case, the weight of the aircraft increases dramatically compared to the first two cases, because the propulsion system for the

aircraft must be large to be capable of taking off with the 5-lb payload of mission 2. Since this case was capable of flying mission 2, it would have enough power to fly mission 3 as well. So in the case of maximizing the score for mission 2, the aircraft must also be capable of obtaining a decent mission 3 score. The fourth case was an aircraft that is designed for endurance; this aircraft would not fly very fast, but was capable of staying in the air long enough to release the maximum number of whiffle balls. The last case was a balanced aircraft that performs well in each mission. The chart above shows that the highest score is achieved by performing well in every mission.

3.4.2 Sensitivity Analysis

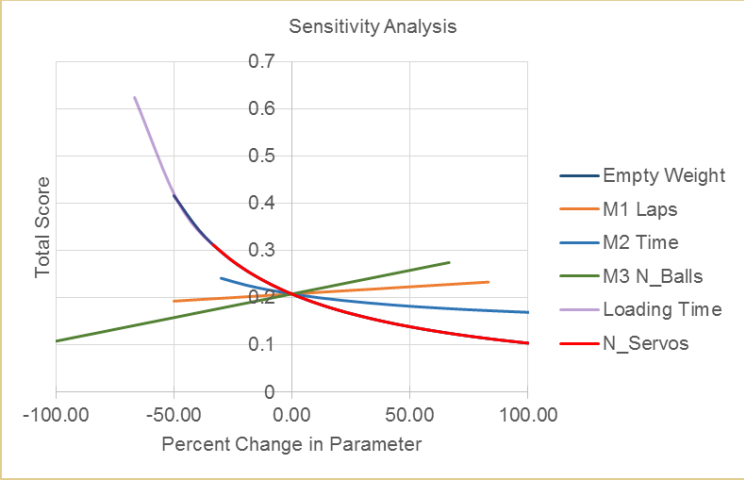

Figure 3.3: Sensitivity Analysis

The score equations were first analyzed to see the level of impact that each parameter had on the score. Part of the initial analysis included analyzing extreme cases. This analysis confirmed the necessity of performing well in every mission in order to achieve a high score. From here, further analysis was conducted using MATLAB to show how sensitive the score was to changes made to each parameter. Empty weight, number of servos, and loading time equally had the greatest effect on the total score compared to other parameters. In order to conduct these analyses, estimates were made using past years' competition data. The estimated best mission scores were 8 laps for mission 1, 105 seconds for mission 2, 10 balls dropped for mission 3, and 20-sec for the ground mission. The estimated values for an average team were 3.80-lb empty weight, 6 laps for mission 1, 150 seconds for mission 2, 6 balls for mission 3, and 60 seconds for the ground mission.

3.5 Configuration Selection

3.5.1 Configuration Figures of Merit (FOM)

During the configuration selection process, each part was scored independently using a set of scoring parameters to find the best configuration for this year's competition. Based on the scoring analysis, more emphasis was given to specific areas. The scoring parameters were:

- **System Weight (50%):** The most important parameter considered was system weight, which consisted of the aircraft weight without the motor, servos, and payload. Since a lighter aircraft would score higher, weight was were given the most consideration in determining the aircraft configuration.
- **Ease of Payload Loading (20%):** The extreme cases analysis showed that having a quick loading time for the loading mission is critical to achieving a high score.
- **Lift to Drag Ratio (L/D) (20%):** The L/D ratio is a basic function of the aircraft and can be used as an evaluator of flight performance. Choosing a configuration that maximizes the L/D ratio ensures that the aircraft can travel longer distances by accelerating more efficiently.
- **Manufacturability and Reparability (10%):** The ease and consistency of which the aircraft could be manufactured and repaired was also taken into consideration during the design process. The ability to design and build specific configurations was determined from experienced members. The aircraft required a simplistic design that would ease assembly and repairs.

3.5.2 Configuration Selection

Several different aircraft configurations were evaluated as possible options for this year's design. They were evaluated according to how well they could accomplish missions as dictated by the sensitivity analysis. The conventional configuration was used as a baseline for comparison.

- **Conventional:** The benefits of a conventional aircraft are that it is proven and is relatively easy to design and build. However, most components only serve a single purpose, so it would not be the most efficient design when weight and materials are considered.
- **Flying Wing:** This type of aircraft offers a greater L/D than the conventional design. However, the major drawback of this configuration is its inability to carry the mission 2 payload without requiring a substantial increase in size. Its ground handling also suffers because it lacks a fuselage to mount steerable landing gear on.

  Biplane: The biplane configuration offers greater wing area per span, allowing for a smaller planform; however, it also requires additional structure to connect the wings together, which adds weight and drag. The interaction between the wings also generally reduces the efficiency of each wing.

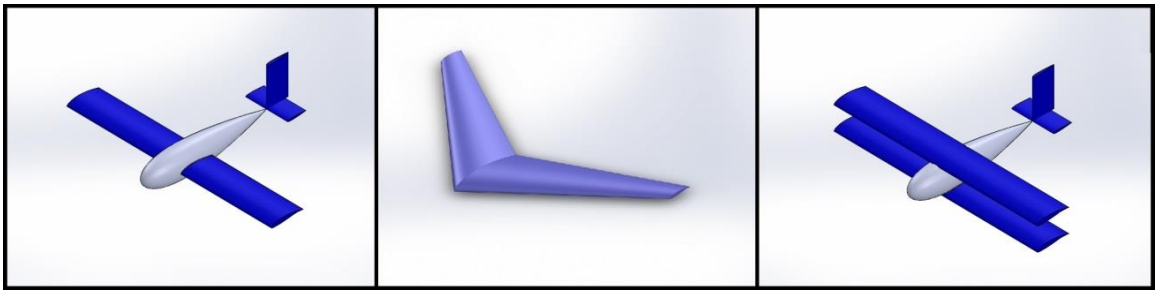

Figure 3.4: Aircraft Configurations

FOM	Weight	Conventional Aircraft	Flying Wing	Biplane
Aircraft Weight	50	0	0	-1
L/D	20	0	1	-1
Manufacturability	20	0	-1	-1
Handling	10	0	-1	0
Total	100	0	-10	-90

Table 3.1: Aircraft Configuration Figures of Merit

Based on the FOM chart, a conventional aircraft scored the best. The greater handling and manufacturing aspects supersede the flying wing design and the biplane design.

3.6 Sub-systems Selection

After a conventional configuration was selected, the major sub-system components, which include the motor, tail, and landing gear, were analyzed. A figure of merit chart was used, comparing several configurations for each subsystem and scoring each based on a number of characteristics.

3.6.1 Motor Configuration of Merit

The team investigated the placement and number of motors, which affects the aircraft's efficiency and ability to carry payload. A figure of merit chart is used to gauge the different propulsion methods, using the single tractor as the baseline for comparison. The scoring parameters are:

- **Number of Servos (40%):** Because this year's competition score depends heavily on the number of servos used, which includes the speed controller, this section was given the most weight.
- **System Weight (25%):** System weight was given the second most weight because the RAC significantly affects the total score.
- **Structural Weight (15%):** Structural weight was given the third highest weight since this also affects the RAC, which again, significantly affects the total score.
- **System Efficiency and Structural Efficiency (10% each):** System efficiency was weighed significantly less since the differences in this aspect were small.

3.6.1.1 Motor Configurations

- **Single Tractor:** This configuration is lightweight and is less likely to have propeller strikes on takeoff and landing than a pusher configuration. Forward-mounted propellers have high efficiency because they act on undisturbed air. If high thrust is desired, a geared motor is used to decrease the current, which in turn increases the system weight.
- **Double Tractor:** Two motors of reduced size can use smaller propellers to attain takeoff speed. The battery voltage may be split between two motors while preserving the current limit set by the batteries, so a gearbox may be avoided. The system's weight including electronic speed controllers is greater than that of a single motor system. A double tractor configuration would also

increase the servo count due to the extra required speed controller. The aircraft's wing must also be reinforced to withstand the loads of the motors.

- **Single Pusher:** Mounting a single motor aft of the aircraft would allow better air flow around the airframe, reducing scrub drag. Likewise, it would also suffer from the additional weight of a gearbox needed to obtain high thrust, and the propulsive efficiency is reduced as the propeller operates in the wing and fuselage wake. Finally, a significant disadvantage would be the necessity of more weight or a longer moment arm of the battery in front to balance the aircraft.

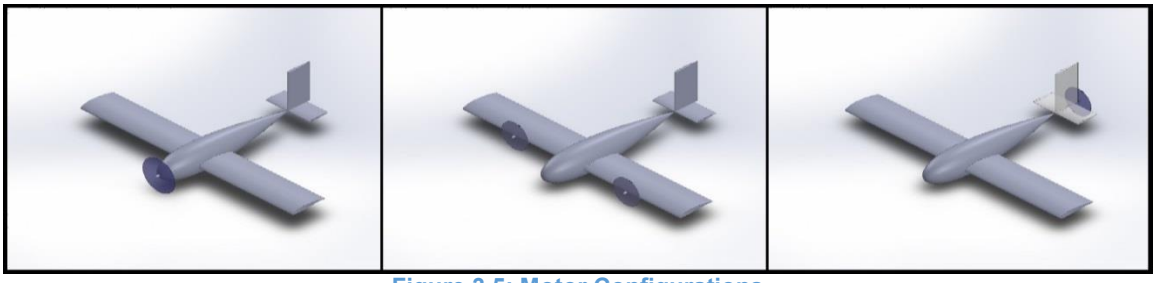

Figure 3.5: Motor Configurations

FOM	Weight	Single Tractor	Double Tractor	Single Pusher
# of Servos	40	0	-1	0
System Weight	25	0	-1	0
Structural Weight	15	0	-1	-1
System Efficiency	10	0	0	-1
Structural Efficiency	10	0	0	1
Total	100	0	-80	-15

Table 3.2: Motor Configuration Figures of Merit

The motor configuration FOM chart shows that the baseline setup, single tractor, is the best setup. Since servo count was highly weighted in this year's competition, double tractor would significantly lower the total score. Single pusher setup was also ruled out due to the lack of efficiency and weight. A strong propulsion setup is required for the mission 2 takeoff, and propeller efficiency had to be maximized.

3.6.2 Tail Figures of Merit

The tail provides stability and allows the aircraft to make high performance turns. The scoring parameters for the tails were:

- **System Weight (35%):** System weight was deemed the most important because it affects the RAC, which affects the overall score significantly.
- **Number of Servos (35%):** The number of servos was also deemed equally important since the number of servos significantly affects the overall score.
- **Stability and Control (20%):** Stability and control was weighted the third highest since greater flight control yield better flight times.
- **Drag (10%):** Drag was weighted the lowest since it is not as important since all of the designs compared have similar drag.

3.6.2.1 Tail Configurations

- **Conventional:** This configuration is simple to install and provides sufficient stability and control.
- **T-tail:** It is effective at high angles of attack, but placing the horizontal stabilizer on top of the vertical stabilizer will increase its structural weight.
- **V-tail:** Two surfaces form a "V" with the tail boom and provide both elevator and rudder control. Control authority is reduced in both yaw and pitch, but weight can be reduced.

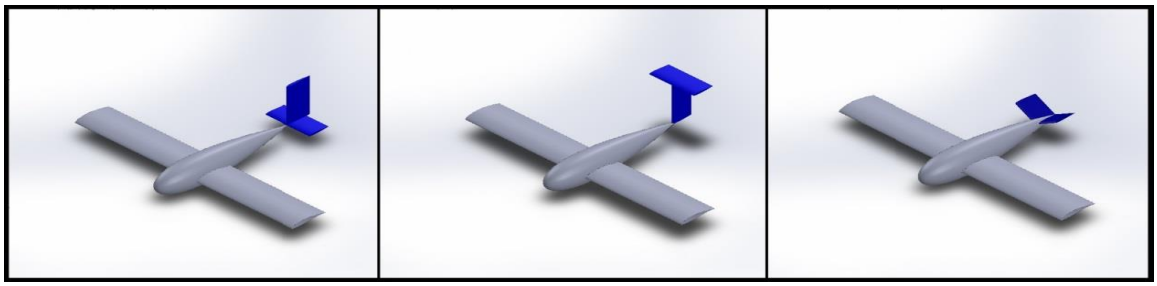

Figure 3. 6: Tail Configurations

FOM	Weight	Conventional	T-Tail	V-Tail
System Weight	35	0	-1	0
# of Servos	35	0	0	0
Stability and Control	20	0	0	-1
Drag	10	0	0	-1
Total	100	0	-35	-30

Table 3. 3: Tail Configurations Figures of Merit

The FOM chart showed that baseline, conventional, tail was the best setup as it required less structure in comparison to the T-tail and provided better control than the V-tail.

3.6.3 Landing Gear Figures of Merit

Takeoff and landing are very critical for the successful completion of all missions. The challenge at takeoff is to maintain sufficient control during the ground roll until the aircraft attains sufficient speed. For this year's competition, the takeoff roll will be short, so precise control and quick rotations are crucial. Naturally, during the landing portion, the landing gear must withstand the load from the ground impact. The scoring parameters were:

- **System Weight (40%):** The most important characteristic evaluated for the landing gear was system weight since it directly affects the RAC of the airplane, meaning that the total overall mission score is divided by the RAC.
- **Drag (30%):** Drag was given the second highest weight since the drag created by the wheels and landing gear structure create substantial pressure drag
- **Handling (15%):** Handling was given the third highest weight since good handling is critical to the completion of each mission.
- **Durability (15%):** Durability was given the same weight as handling since the landing needs to be durable especially when landing fully loaded with the 5 lb payload from mission 2.

3.6.3.1 *Landing Gear Configuration*

- **Tricycle:** This configuration has main wheels under the wing and a nose wheel for steering. The nose wheel is exposed to the propeller wake, causing a significant drag penalty. However, the nose wheel allows for excellent ground handling on flat terrain.
- **Bicycle:** This configuration has two centerline wheels and two wing tip wheels. The landing gear can be significantly reduced as the main loads are transferred through the center wheel, but the configuration adds more components, which add drag.
- **Tail Dragger:** This configuration has two main wheels under the wing and one smaller wheel under the tail of the aircraft. This configuration does not have good ground handling in the presence of a crosswind, but it does have less drag than a tricycle configuration. Its ground footprint is also larger, effectively reducing the takeoff field length.

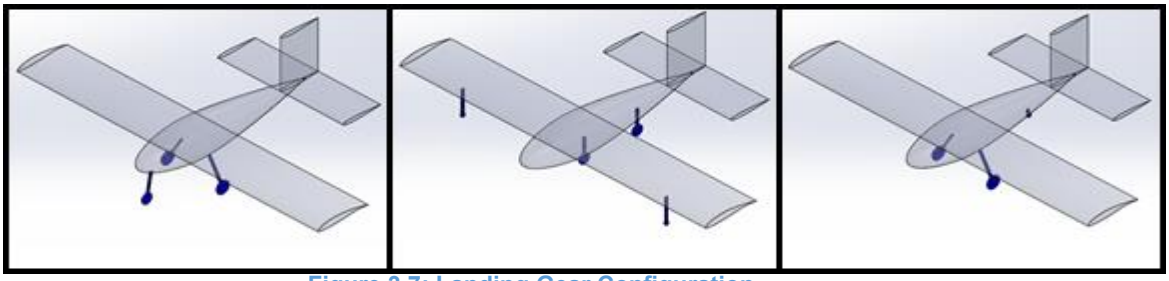

Figure 3.7: Landing Gear Configuration

FOM	Weight	Tricycle	Bicycle	Tail Dragger
Aircraft Weight	40	0	1	1
Drag	30	0	-1	1
Handling	15	0	-1	0
Durability	15	0	-1	0
Total	100	0	-20	70

Table 3.4: Landing Gear Configuration Figures of Merit

The tail dragger setup worked the best because it optimized the least amount of landing gear drag and the aircraft weight. Though the conventional, tricycle, would have worked well, the reduced handling of the Tail dragger in the end was still worth choosing.

3.6.4 Payload Release System

The payload release mechanism for mission 3 was selected according to these parameters:

- **Installment time (35%):** The most important characteristic was deemed to be the installment time since loading time significantly affects the ground score, which is then multiplied to the overall mission score.
- **System Weight (25%):** System weight was deemed the second highest weighted characteristic because weight contributes to the RAC, which is used to divide your overall mission score.
- **Reliability (20%):** Reliability was deemed third most important because the balls need drop specifically when commanded otherwise mission three score becomes invalid.

- **Drag (15%):** Drag is important to the overall performance of the airplane, and the different configurations change the drag significantly. The least amount of drag is wanted so that the airplane has less to overcome when in flight.
- **CG (5%):** There is not much change in the CG when a ball is released making it the least weighted parameter.

3.6.4.1 Payload Release Mechanism Configuration

- **Clips:** This configuration has the lowest system weight and drag. The clips have the smallest change in CG since the design allows for balls to be released strategically so that the CG does not change. This system is also reliable because if one ball fails to drop it will not affect the other balls. Loading fast takes practice though.
- **Rail:** This configuration is the easiest to load from all the designs, without much practice. However, this configuration has a greater system weight, drag, and CG change.
- **Skewered:** This configuration has a carbon rod going through the wiffle balls. The installment time is greater than the other two configurations since the carbon rod has to be put completely through a wiffle ball. This configuration also has a higher system weight, drag, and change in CG compared to the clip payload system.

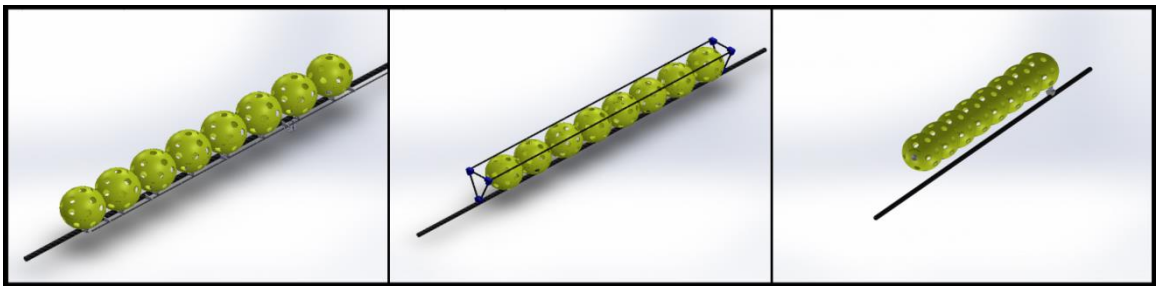

Figure 3. 8: Payload Release Configuration

FOM	Weight	Clips	Rail	Skewered
Installment Time	35	0	0	-1
System Weight	25	0	-1	-1
Drag	20	0	-1	-1
Reliability	15	0	1	0
CG	5	0	-1	-1
Total	100	0	-35	-85

Table 3.5: Payload Release Mechanism Figures of Merit

The clip system, based on the FOM chart, ended up being the best choice. Though kinks had to be worked out to get it to work correctly, the drag build-up, weight, and CG change of the other two system negatively affected the score, and as such weren't the best possible choices.

3.7 Conceptual Design Summary

The finalized conceptual design is a conventional aircraft powered by a single tractor propeller, that features a tail dragger landing gear, and a conventional tail which provides adequate ground control. This final concept reflects the qualities that the team deemed important in order to obtain a high score at the competition.

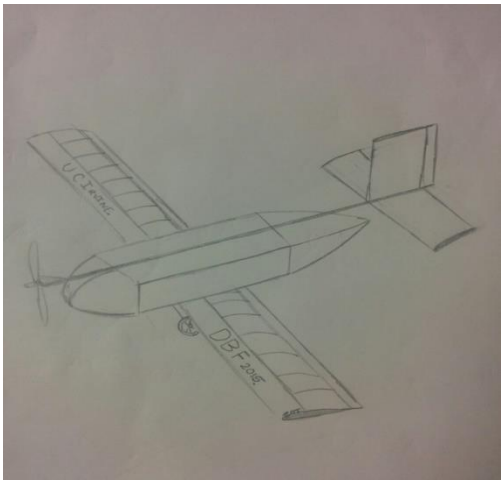

Figure 3.9: Conceptual Sketch

4.0 Preliminary Design

Preliminary design took the configuration proposed during the conceptual design phase and applied it to a mission model that would output several aircrafts. This section shows how the sizing and optimization of each subsystem was done to converge on an aircraft that would score the highest at the competition

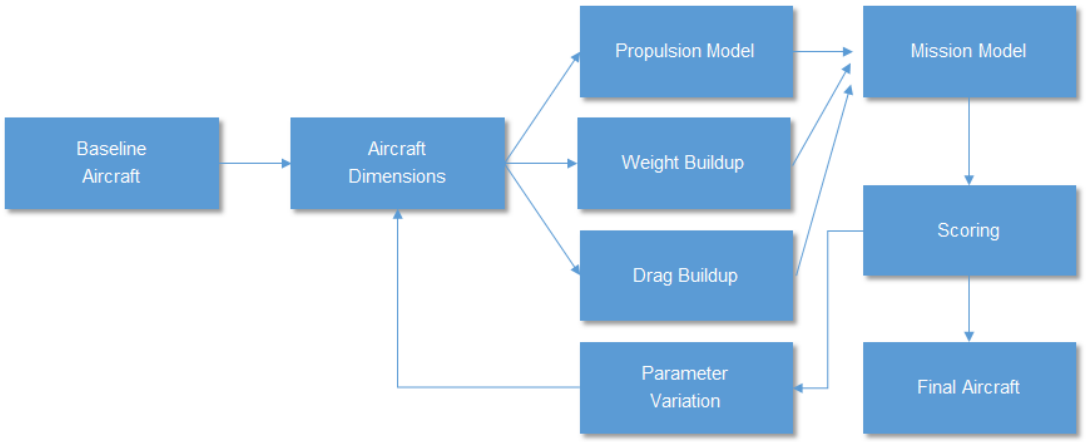

Figure 4.1: Optimization Program Flow Chart

4.1 Design and Analysis Methodology

Taking the initial configuration proposed during the conceptual design phase, a MATLAB code was written to model the aircraft size and performance parameter to generate a total score. The program

iterates varying the size of each component while holding everything else constant and computes the total score the aircraft would receive. This method leads to an optimal design with the maximum flight score. In terms of calculating a total score, this code did not take into account the report score or the ground missions score. It is assumed that the aircraft would pass the ground mission therefore, the value of the total score is only a reference value and not the actual score the aircraft would receive.

The program is composed of 4 distinct parts: weight buildup, drag build up, propulsion model, and mission model. The weight build up is calculated by knowing the materials used and the corresponding density of each material. For complex parts, estimates were made using empirically obtained data for each component. Ratios such as weight per linear foot and weight per square foot were estimated then verified in order to improve the accuracy of the weight build up simulation. After calculating the weight of the aircraft, the drag build up makes use of wind tunnel data along with parasitic drag equations developed for small- scale aircrafts to calculate the coefficient of drag when lift equals zero (CD_0). The aerodynamic characteristics for the entire aircraft are calculated in this section of the program. The drag model took into consideration the airfoil properties obtained from XFOIL, a program created by Mark Drela at MIT, and the wing dimensions in conjunction with the parasite drag estimations. After the CD_0 for the aircraft is calculated, the program then attempts to model the propulsion system.

The propulsion model and the mission model aspect of the code uses more complex methods to estimate the outcomes. Using digitized charts of APC propeller data, the propulsion model is able to find the propeller thrust and pitch speeds. With this data, along with empirical battery voltage data and airspeed inputs, the mission model is able to predict the performance of the propulsion system. The mission model relies on the aircraft characteristics defined by the weight buildup, the drag buildup, and the propulsion model to compute the flight times, the energy consumption during flight, and the takeoff distances. The key features and limitations of the mission model are described in Section 4.2.

4.2 Mission Model

The mission model was used to estimate the power and energy requirements for each mission. It simulates each of the basic flight segments. The aircraft is modeled as flying at full throttle to achieve minimum flight time along with ensuring the battery energy capacity will not be exceeded in real life. No headwind or crosswind is assumed. Any aircraft which was unable to complete all three missions either due to insufficient energy or not accomplishing takeoff in 60 ft. was disregarded.

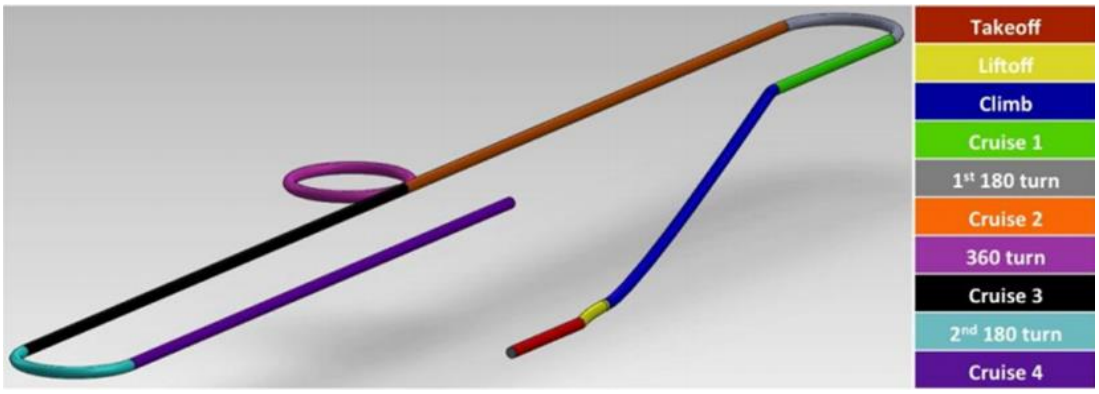

Figure 4. 2: Mission Model Sequence

Flight Segment	Constraints	Description
Takeoff	Constant angle of attack ; Rotate at $V=1.2*V_{stall}$	The aircraft accelerates on the ground until rotation.
Liftoff	Constant altitude	The aircraft accelerates to ideal climbing speed.
Climb	Constant load factor	The aircraft climbs to cruise altitude of 50-ft.
Cruise	Constant altitude	The aircraft maintains a 50-ft. altitude.
Turn	Constant load factor	The aircraft turns without overloading the wings.

Table 4.1: Flight constraints and description

The load factor represents a 3G loading for the heaviest mission.

4.3 Design and Sizing Trades

4.3.1 Aerodynamic Trade-offs

Airfoil

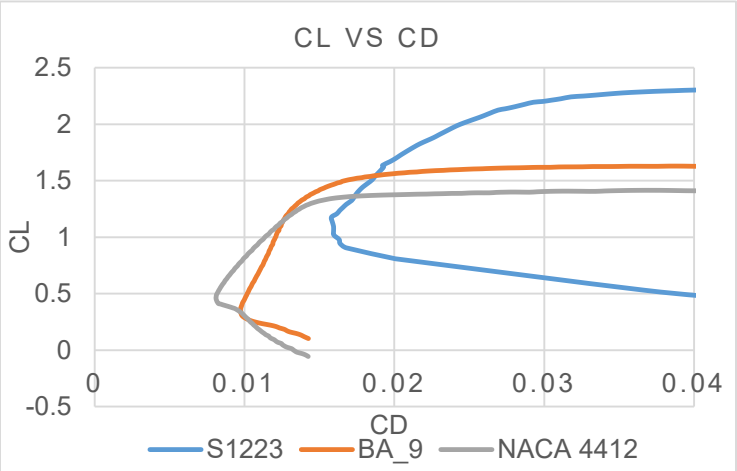

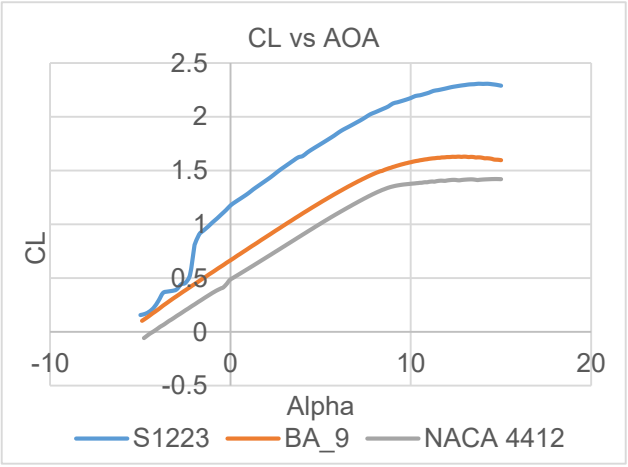

Figure 4.3: Airfoil Polars

Several airfoils were studied and modeled to determine the ideal choice. Due to the 60 ft. runway and the heavy payload of mission two, cambered airfoils were mainly considered because of their high maximum coefficient of lift ($C_{L\ max}$). With previous year's performance data backed with test flight data, an average velocity of 65 ft. /s was assumed. The Reynolds number used to compare these airfoils lie in the 300,000 range. To narrow down the selection process, three airfoils were chosen which have the desired characteristics at low Reynolds numbers. The desired characteristics include a high $C_{L\ max}$ for takeoff and a low drag coefficient at low angles of attack for maximum cruise speed. The airfoils are shown below.

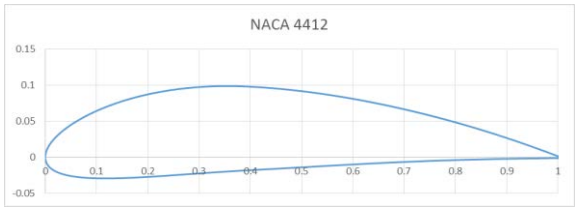

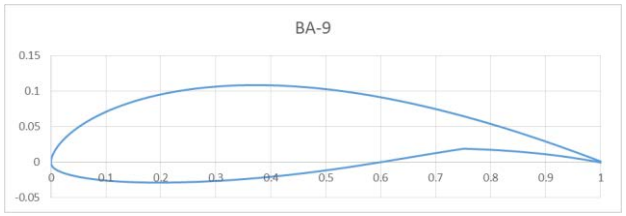

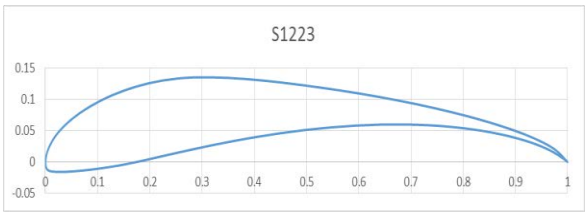

	NACA 4412	BA-9	S1223
Cl_{max}	1.422	1.630	2.308
Max t/c	12.0	13.3	12.1
CD @ CL=.5	0.0084	0.0111	0.0163

Figure 4.4: Airfoil profiles and characteristics

Overall, the BA-9 produces the highest score. The NACA 4412 consistently produces less drag than the BA-9 but its Cl_{max} is relatively low. On the other hand, the S1223 has a high Cl_{max} but the drag increases substantially, relative to the BA-9, as the angle of attack increases. The BA-9 was chosen because it has a high Cl_{max} while maintaining a large drag bucket. The BA-9 also has a greater average thickness. The thicker airfoil allows for lighter internal structure.

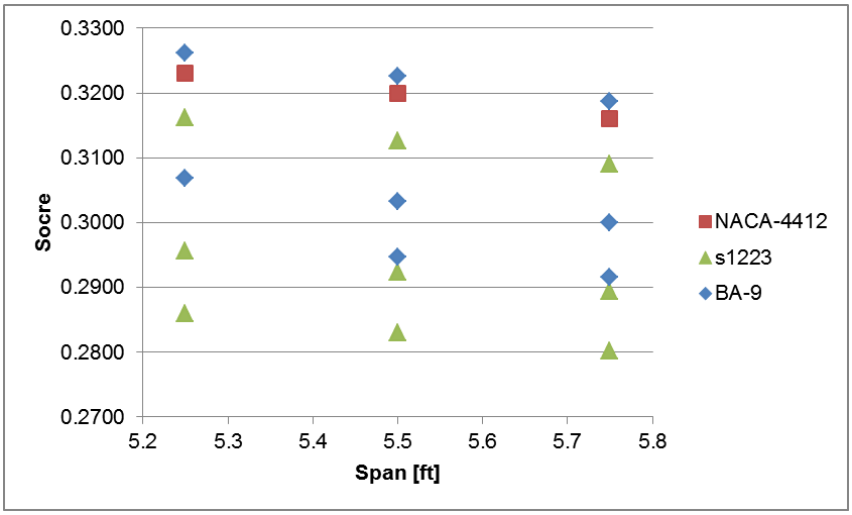

Figure 4.5: Score vs. Span

Chord

To minimize induced drag, the wing span should be maximized according to the induced drag equation.

$$D_i = \frac{\left(\frac{L}{b}\right)^2}{\pi q e}$$

For the low Reynolds number airfoils that were considered, the wing drag increases dramatically when the Reynolds number is below 300000. To maintain this Reynold number at takeoff for mission 2 where flight speed is approximately 60 ft/s, the chord must be at least 10 inches. It is also important to note that wing construction and wing structure become bigger issues when the wing thickness decreases.

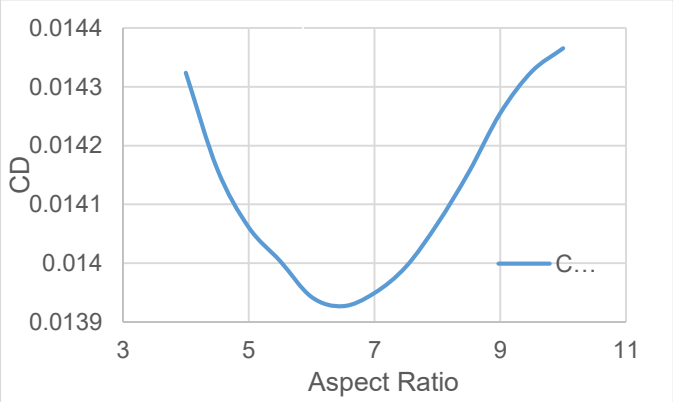

Figure 4.6: CD vs Aspect Ratio

A code was written to compare the effects on the drag of the wing to the aspect ratio. With an estimated empty weight of 4.51 lbs and a flight speed of 55 ft/s for mission 3, the lowest CD for the wing is obtained with an aspect ratio of approximately 6.6.

Sweep and Taper

Due to low flight speed, no wing sweep was implemented. Wing taper was not used because the gain in efficiency by tapering is outweighed by the complexity of building the wing. Tapering also increases the probability of tip stalls.

4.3.2 Propulsion System Trade – Offs

Motor

For this year's competition, since there was no fuse limit, the motor selection was not driven by low current draw. However, a motor capable of over 600-W was required to achieve expected flight performance which was calculated by allowing for a safety factor of 75-W/lb. Based on a MATLAB takeoff code, thrust of over 7-lb static was required in order to take off under 60-ft. This motivated the use of a gearbox to spin a propeller with larger pitch and diameter. Brushless outrunner motors were considered, but they were heavier than equivalent geared inrunner motors because the outrunners did not have a low enough kV with the required power output.

Inrunners with the lightweight Maxon 4.4:1 gear reduction drive were initially considered, but were ruled out because its maximum power rating was 500 watts. Inrunners with the P29 gearbox were considered next because the P29 offered a higher gear ratio of 6.7:1 with a maximum power rating of 3000 watts. The P29 also weighs the same as the Maxon. An optimization code was run with each motor considered, varying the props and battery combinations. The battery selection varied the number of cells, keeping the type constant, Elite NiMH batteries. Motors from Hacker and Neu were considered. Neu motors were more efficient across the range considered, as they have much lower resistance, while also weighing considerably less for a given power to weight ratio.

Motor	kV (RPM/V)	Weight (oz)	Rm (Ω)	Max RPM	Max Watts (W)	Max Voltage (V)	Specific Power (W/oz)
Neu 1105/2.5Y/P29	3800	4.96	0.028	60K	400	15	81
Neu 1107/6D/S/4.4	1900	5.59	0.058	60K	600	28.5	107
Neu 1110/3Y/S/6.7 P29	1512	6.66	TBD	60K	1000	36	150
Hacker A40-14L	355	9.59	0.032	16K	1100	20	115
Hacker A40-14S	530	7.34	0.021	16K	900	18	123

Table 4.2: Propulsion Configuration

The 1105 Neu motor, though lighter, was found to not have enough torque to spin the large propellers at the desired 6000 RPM to produce the greater than 7 lbs of thrust required to meet takeoff with the mission 2 payloads. The current draw from the motor to be able to spin such a large diameter prop was deemed too high for the batteries to handle. A parallel battery setup was considered, but the total number of cells required to meet the power output turned out to be the same amount required by the 1110 motor. Though the 1105 made takeoff, it was with feet to spare, so there was no safety factor. Also, the current draw, even with a much smaller prop that was optimized for mission 3, was still not low enough to drop all the balls. As such the 1105 was ruled out, since the effective kV was too high and as such the current draw was too high.

The 1107 motor was also considered. Though its current draw was low enough that parallel battery packs were not required, it was still not low enough to optimize mission 1 and mission 3. The cells required, after the voltage drop, to provide enough RPM to achieve enough thrust for mission 2 takeoff was not that much less (24 cells vs. 28 cells) than what an 1105 and a 1110 motor required. It also didn't provide enough of an energy safety factor for completing mission 1 and mission 3. As such, this motor was also ruled out.

The 1110 Neu motor was deemed to be the most optimized motor for all three missions. It provided enough of a mission 2-takeoff safety factor. And, due to its low effective kV, it is able to provide excellent performance for mission 1, where a small diameter, high pitch prop is required because little thrust is required in comparison to high pitch speed. Its low current draw was also able to maximize mission 3.

Battery Selection

A selection of battery cells were analyzed to determine which could provide enough power for mission 2 takeoffs and which could provide sufficient energy to complete mission 1 and mission 3. Higher capacity cells have the advantage of providing more energy for longer flights, and their low internal resistance allows a consistent power output. Smaller capacity cells have a small advantage in less weight, but they experience a power output drop at high loads. The power output is more significant than minimal weight in battery cell. Therefore, keeping with a consistent battery pack for all missions is favorable, for design and performance purposes.

Battery	Capacity (mAh)	Mean Current (A)	Weight (oz)
Elite 2000	2000	20.7	1.058
Elite 1500	1500	17.2	0.988

Table 4.3: Battery Selection

Two battery types were considered, an Elite 2000 and Elite 1500. Choosing a battery with lower than 1500 mAh would come at a disadvantage of increased internal resistance. The Elite 1500 was chosen because they provided sufficient energy and power for mission laps. Elite 2000 also provided sufficient performance, but they had excess energy and added extra weight for no advantage. They also didn't experience a significant power loss at burst current, which was at takeoff. The Elite 2000 cells do not outweigh the Elite 1500 cells because the increased capacity isn't utilized in the completion of all the missions, making the increased weight for capacity cost more of a hindrance than a benefit.

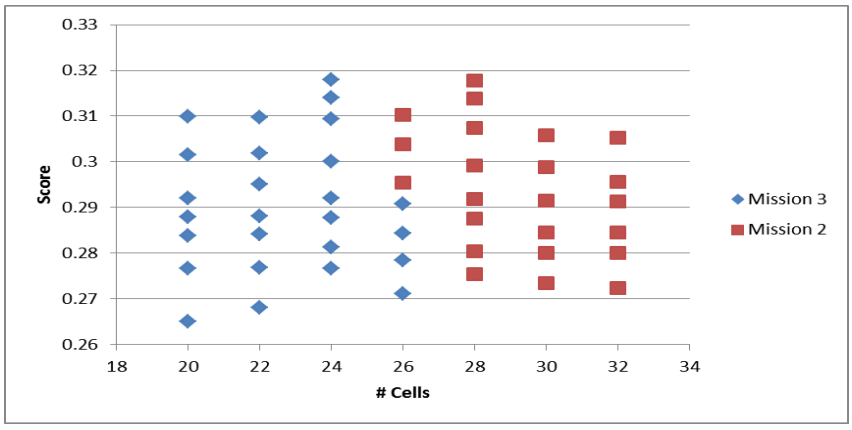

Figure 4.7: Score vs. Number of Cells

4.3.3 Final Optimized Aircraft

Airfoil	Motor & Gearbox	Battery	Mission 3 Payload
BA-9	Neu 1110 3Y 6.7:1	24 Cell Elite 1500	8

Table 4.4: Optimized Aircraft Selections

The final aircraft configuration, as shown in Table 4.4, represents a combination of features which maximize the total flight score. A high lift, low drag airfoil and a propulsion system that balance weight with performance represent the optimal aircraft. The propeller choices below maximize mission

performance by accommodating the different loading scenarios. A span of 66-in. was chosen to ensure takeoff occurred within the 60-ft. distance with the optimized propulsion system.

Propeller choices are shown in Table 4.5. Mission 1 uses a small diameter, high pitch prop to generate a pitch speed that allows the aircraft to reach maximum airspeed. Mission 2 maximizes thrust to accomplish takeoff with the stack of payload. Mission 3 achieves optimal efficiency to successfully drop one ball per lap.

	Mission 1	Mission 2	Mission 3
Propeller	12x12	16x10	13x10

Table 4.5: Propeller Choice for each mission

4.4 Lift, Drag, and Stability Characteristics

The aircraft drag polar, L/D vs C_L, and thrust & drag vs velocity are shown below in Figures 4.8-4.10 Mission 1 has the lowest C_L because it is a speed mission. Mission 2 is the heaviest mission, but mission 3 has the highest C_D and C_L because of the drag caused by the wiffle balls in flight. The addition of the wiffle balls significantly changes the geometry of the aircraft, thereby increasing its drag profile and requiring a separate drag polar. Mission 3 also does not consider speed because it focuses on efficiency. Mission 2 and mission 3 have approximately the same L/D.

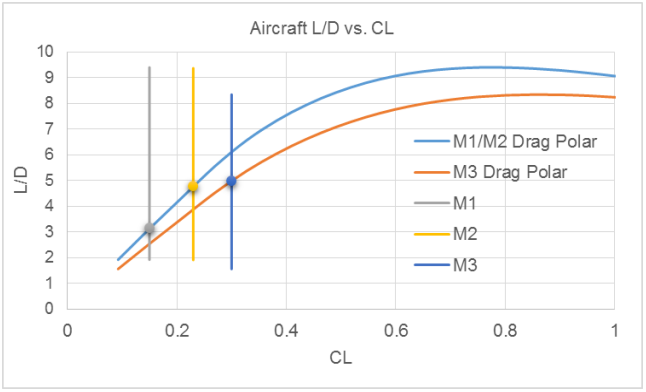

Figure 4.8: Aircraft L/D vs. CL

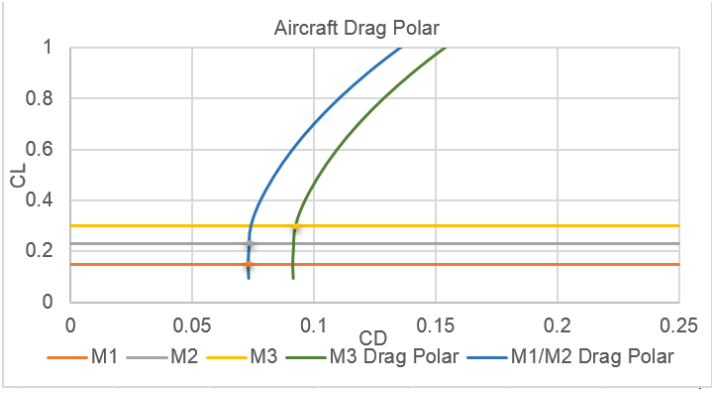

Figure 4.9: Aircraft Drag Polar

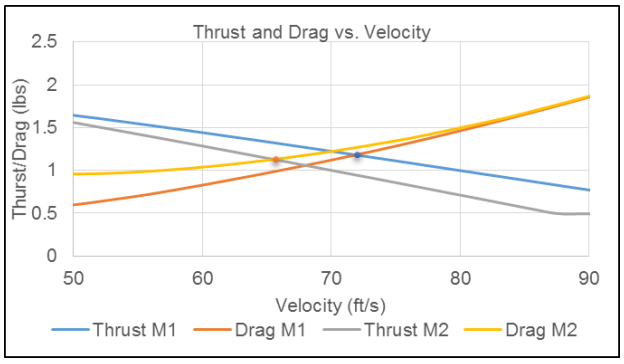

Figure 4.10: Score vs. Number of Cells

The drag buildup for each mission is shown in Figure 4.10. The fuselage contributes the highest percentage of drag for each mission, with the wing being the next biggest contributor. The induced drag for all the missions are relatively low because the plane was designed to fly fast. Having excess power ensures that the plane is capable of making takeoff for mission 2 without any headwind. The induced drag is relatively higher for mission 3 because the plane is flying slower in order to increase efficiency. The balls increase the drag dramatically in mission 3 since they are exposed to air and are positioned directly behind the propeller. Star-CCM+, a computational fluid dynamics software provided by CD-Adapco, was used calculate the delta cd for the wiffle ball arrangement.

Mission 1 and 2 maximum flight speeds are shown above. Mission 3 does not emphasize speed completion; therefore, it is not included in the thrust & drag vs velocity plot.

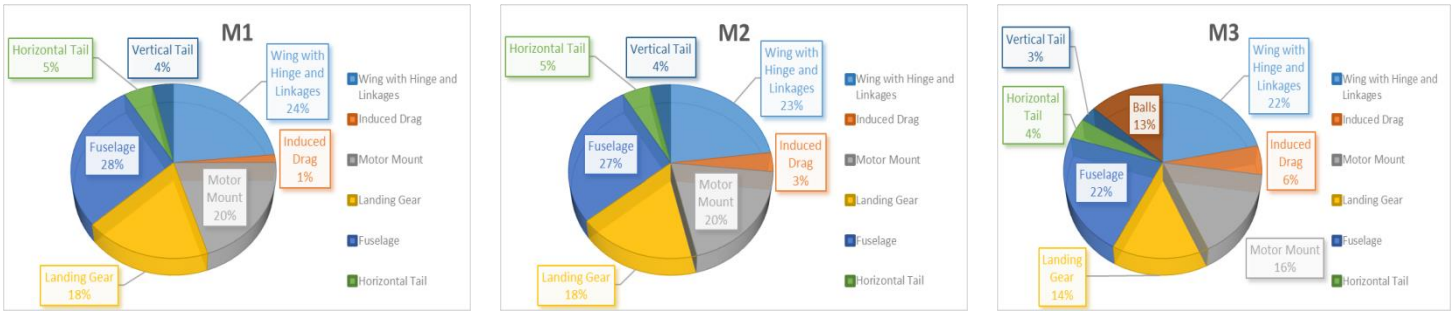

Figure 4.11: Drag Buildup

4.4.1 Stability and Control

The aircraft's C_L is highest for mission 2. A Trefftz plot, shown in Figure 4.12, was created with the geometry input in Figure 4.13, with the Athena Vortex Lattice (AVL) program, which was developed by Mark Drela and Harold Youngern at MIT [2]. This plot verified the peak C_L occurred within 50% of the semi-span and that any section, specifically the wingtips, C_L's did not exceed $C_{L\,max}$.

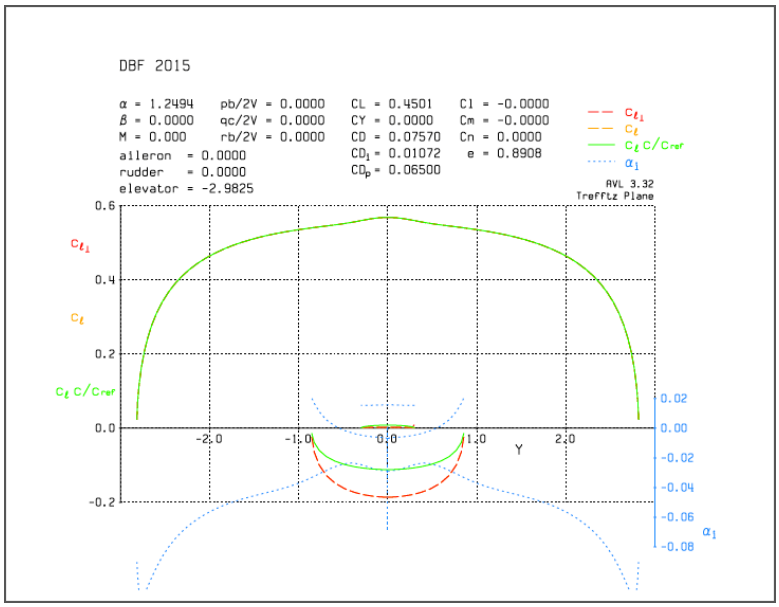

Figure 4.12: Trefettz Plot

Flight conditions for mission 2 were evaluated in the AVL program in order to assess the effects of increased loads and slower speed assessed in mission 2. The geometry input model is shown in Figure 4.13 Using preliminary weights and drag build-up, the simulation was conducted, providing an estimate for C_{Dp} the mass properties, and inertia of the aircraft.

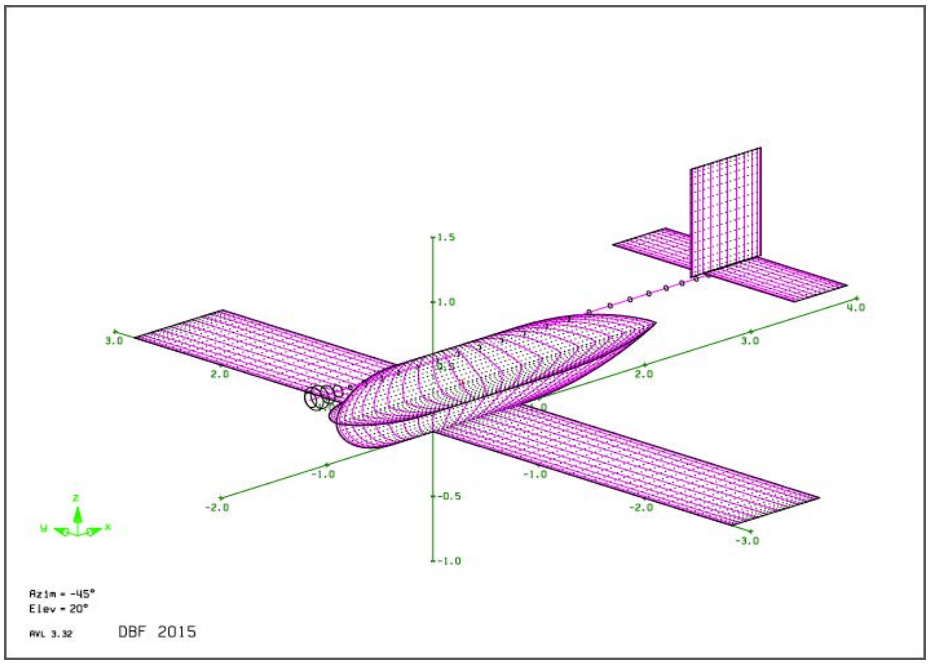

Figure 4.13: AVL Geometry Input

AVL takes the input geometry and uses an extended vortex lattice method to calculate the aerodynamic performance as well as the stability and control derivatives for the augmented aircraft. Figure 4.14 shows the resulting pole-zero map of the eigenvalues calculated by the program.

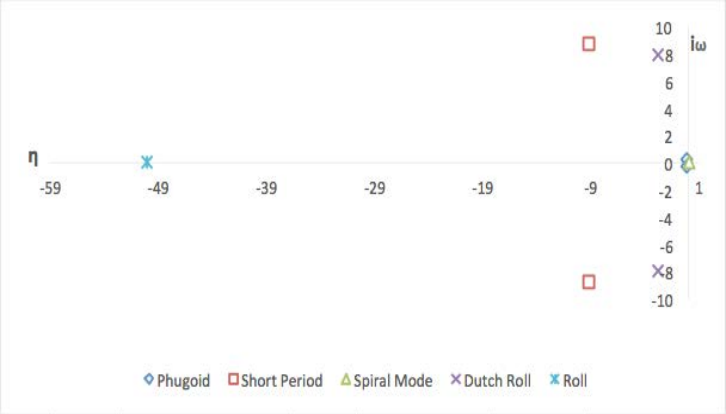

Figure 4.14: Pole-Zero Diagram

All modes achieve level one criteria for a class I plane per MIL-SPEC 8785C [2] with two exceptions. The only unstable mode was the spiral with a slight divergence. However, it satisfies level one handling qualities with a time-to-double of 18.4 seconds. In addition, the Control Anticipation Parameter satisfies the level two handling qualities criteria, having an η/α of 8.76 G's/rad with a short period natural frequency of 7.95 rad/sec. As discussed by Cook [2], level two handling qualities are stated as, 'Flying qualities adequate to accomplish the mission flight phase, but with an increase in pilot workload,' thus not requiring augmentation for mission performance. Upon conducting further research, it was found that the recommendations in MIL-SPEC 8785C are applicable to small-scale Unmanned Aerial Vehicles (UAVs) as discussed by Tyler Foster of Brigham Young University [3].

4.5 Predicted Mission Performance

	M1	Time (s)	Energy (KJ)
1st Lap	Takeoff	1.7	0.47
	Liftout	3	0.87
	Climb	5.1	1.51
	Cruise 1	10.1	2.75
	1st 180° turn	12.5	3.35
	Cruise 2	19.5	5.06
	360° turn	24.2	11.83
	Cruise 3	31.3	7.88
	2nd 180° turn	33.6	8.43
	Cruise 4	40.8	10.09
2nd through 6th Lap	…		
	1st 180° turn (Lap 6)	206.2	45.24
Landing	End of mission	235.8	51.24

Table 4.6: Mission 1 Predictions

	M2	Time track (s)	Energy (KJ)
1st Lap	Takeoff	3.1	2.04
	Liftout	4.9	3.14
	Climb	8.0	4.98
	Cruise 1	10.5	6.08
	1st 180° turn	17.5	9.11
	Cruise 2	23.5	11.60
	360° turn	37.1	31.66
	Cruise 3	43.2	7.88
	2nd 180° turn	49.8	8.43
	Cruise 4	55.9	10.09
2nd and 3rd Lap	…		95.01
	Cruise 4 (Lap 3)	150.4	45.24
Landing	End of Mission	156.9	51.24

Table 4.7: Mission 2 Predictions

	M3	Time track (s)	Energy (KJ)
1st Lap	Takeout	4.6	0.43
	Liftout	6.0	0.56
	Climb	21.4	2.07
	Cruise 1	22.0	2.10
	1st 180° turn	23.2	2.27
	Cruise 2	40.1	3.17
	360° turn	42.6	6.85
	Cruise 3	59.4	4.42
	2nd 180° turn	60.7	4.59
	Cruise 4	77.5	5.50
2nd through 7th Lap	…		31.96
	Cruise 4 (Lap 3)	298.0	18.45
Landing	End of Mission	523.8	31.20

Table 4.8: Mission 3 Predictions

5.0 Detail Design

Following the optimization process and mission profile predictions, the aircraft dimensions was finalized. The prototype of the final design was then built and tested to confirm the mission profile predictions.

5.1 Lift, Drag, and Stability Characteristics

Wing Area	
Span	67.6"
Chord	10"
Aspect Ratio	6.78
Wing Area	606 in^2
Airfoil	BA9
Static Margin	31.30%

Fuselage	
Length	36"
Width	6"
Height	6"

Rudder	
Span	10"
Chord	2.5"
Defection	0°

Electrical System	
Speed Controller	Castle Creations HV Lite 40
Radio Receiver	Futaba R617FS
Number of Servos	2
Servo Type	

Elevator	
Span	20.1"
Chord	1.5"
Defection	0°

Horizontal Stabilizer	
Airfoil	NACA0012
Span	20.1"
Chord	6"
Area	120 in^2
Incidence	±20°

Vertical Stabilizer	
Airfoil	NACA0012
Span	10"
Chord	8"
Area	80 in^2
Incidence	±20°

Motor	
Type	Neu 1110-3Y
Kv	1512 rpm/v
Gear Box	P29 6.7
RPM_max	60000
Io	
R_m	
P_m	1000
Propellers	13x13, 16x10, 13x10

Batteries	
Types	Elite 1500
Capacity	1500 mAh
R	0.016
V	1.2V
I_max	30A
Number of Cells	12, 14
Pack Energy	100.44 kJ, 117.18 kJ
R_pack	0.192, 0.224
V_pack	14.4, 16.8

Aileron	
Span	30.13"
Chord	2.50"
Deflection	±20°

Table 5.1: Dimensional Parameters

5.2 Structural Characteristics and Capabilities

The sensitivity analysis revealed that weight was the most important factor in the total score. Therefore, designing an aircraft to be as light as possible was the driving focus of the overall design. Before a formal detailed design could be finalized, an analysis of the loads along the wing and fuselage were made in both flight and landing scenarios. Figure 5.1 shows the shear and moment diagram for the maximum aircraft weight.

The fuselage structure consists of a central boom surrounded by a nonstructural fuselage fairing. All loads during takeoff and landing transmit from the landing gear through the fuselage to the boom. This particular setup creates a lightweight landing gear with built-in suspension. Coupled with the lightweight wing and tails, all major components combine to make a lightweight aircraft that can effectively compete for the highest score.

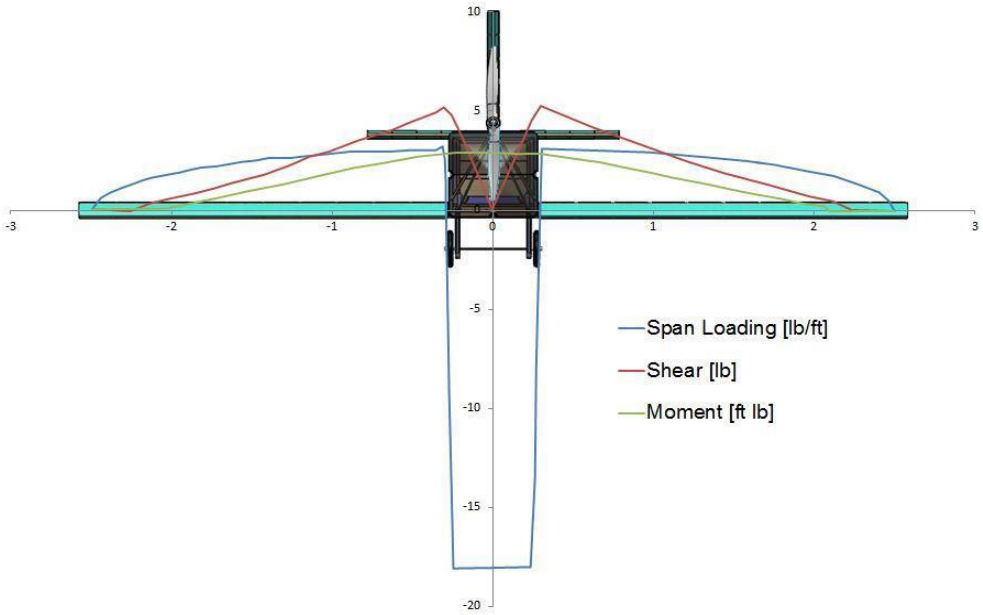

Figure 5.1: Shear, Moment Diagram

5.3 System Design and Component Selection/Integration

5.3.1 Wing

The wing was designed to be as light as possible, yet strong enough to withstand all the aerodynamic forces in flight: a balsa built-up wing, consisting of balsa ribs, sheeting, and a spar with unidirectional carbon fiber as structural reinforcement. Microlite covering was applied to the wing which gave it a smooth surface.

The two wing halves were attached through a solid balsa block and the airfoil shape is maintained with ribs. Lightening holes were laser cut in the wing ribs, which helped decrease the weight without hindering the structural integrity. Unidirectional carbon fiber was placed along the center spar to add reinforcement to the balsa spar caps. Moreover, the spar caps are thicker on the top to withstand compressive loads experienced in flight. Balsa sheeting provides torsional strength and helps to maintain the airfoil shape.

The tails share the same design as the wings; they were manufactured using balsa ribs. The tails differ from the wing in that two carbon rods act as the spars. Balsa stringers were embedded around the balsa ribs to maintain the airfoil shape. Microlite was used to cover the tails. This configuration provided the greatest weight savings while maintaining structural rigidity.

5.3.2 Motor Mount

The motor mount consisted of carbon fiber reinforced with epoxy resin. The mount uses multiple layers of unidirectional and bi-directional carbon fiber to take the electric motor's torsional loads. The

motor screws onto the faceplate to guarantee a flat mounting surface and help absorb motor vibrations. The mount is attached to the boom by a carbon fiber-reinforced sleeve that helps transfer the motor's forward momentum to the rest of the aircraft structure.

Figure 5.2: Front view

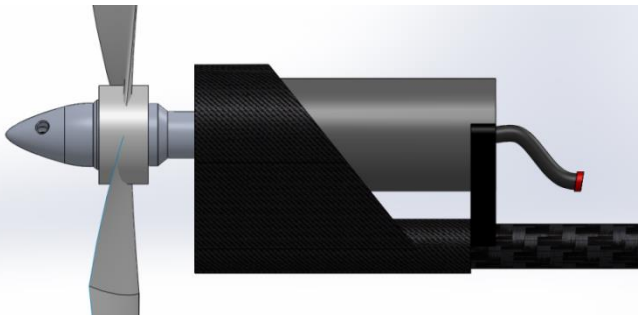

Figure 5.3: Side view of motor mount

5.3.3 Structural Boom

The central carbon boom acts as a major structural member connecting the motor, fuselage, and tails. The team has previous experience using this as a main structural member. Its significant weight advantages over a load bearing fuselage skin justifies its use.

5.3.4 Control Surfaces

The control surfaces, which include the ailerons, the elevators, and the rudder, were sized according to the need for adequate ground control and air maneuverability. Without the use of a steerable tail wheel, the rudder had to provide adequate directional control during the takeoff roll. The half span ailerons are used in order to reduce the amount of torque required for actuation. The elevator had to be sized in order to provide adequate pitch authority for all missions, especially for mission 3. It could not be too big such that it would cause a problem when dropping balls, since the elevator is coupled to the ball release mechanism. A pull-pull system was utilized to keep the number of actual servos at two. The ailerons and rudder were coupled together with a servo located behind the wing spar, with wires running through the wing and along the main boom.

5.3.5 Payload

The payload arrangement was chosen to minimize frontal area, allow for quick loading, and to satisfy the rules. The payload arrangement for missions 2 and 3 are shown respectively in Figure 5.4 below.

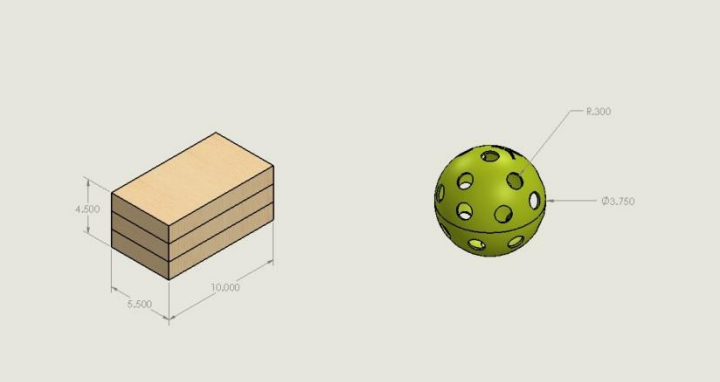

Figure 5.4: Payloads

5.3.5.1 *Mission 2 Payload Restraint*

Mission 2 specifies an internally-carried payload with dimensions of 10 x 5.5 x 4.5-in. The mission 2 payload is enclosed in the fuselage and secured using four 3D printed supports. The fuselage is composed of two parallel carbon rods connected to the main boom through a delta-frame. The supports for the mission 2 payload are attached to the carbon rods, restraining the motion of the payload horizontally and longitudinally in flight. To allow for quick loading of the payload, both sides of the fuselage open to allow an almost unobstructed access to the payload area.

5.3.5.2 *Mission 3 Payload Release*

The mission 3 specifications require that a payload of wiffle balls be carried externally and be released one at a time in a specified drop zone. A clip release system was chosen to carry and release the payload for mission 3 because it is very weight efficient, minimizes drag compared to other systems, and is very reliable after being refined. The system works by having a clip that locks open in a V-shape to secure the balls in place. Once a certain amount of down elevator input is applied to the servo, a ratchet actuates and pulls a fishing line. The fishing line is attached to a carbon rod with hooks that disengage the clips in a specific order to minimize CG change as balls are released. The clips disengage by snapping together allowing the balls to fall free of the aircraft.

5.3.6 Landing Gear

A shock-absorbing integrated landing gear was chosen because it can elastically deform to absorb some of the landing loads. The landing gear is integrated into the carbon structure, allowing for weight minimization and the force from landing impact to be absorbed. A continuous axle was added to prevent the landing gear from detaching due to possible cross wind landing impacts.

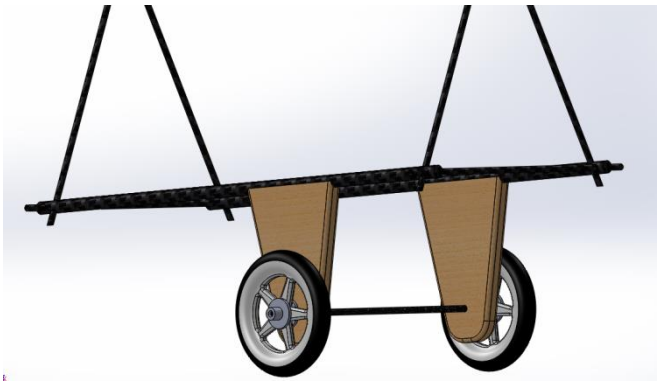

Figure 5.5: Landing Gear

5.3.7 Fuselage Fairing

The fuselage fairings were made non-structural to maximize weight savings. The cross section and shape constraint for the payload-carrying section of the fuselage was established by the intended cargo to be carried. The front and rear of the fuselage were gradually tapered for aerodynamic reasons. The top of the fuselage, which holds the wiffle ball release system, is open to satisfy the rules for the mission 3 payloads.

5.3.8 Tail Boom

The tail boom was sized based on a tail-sizing model, which varies the tail boom length, sizes the tails using a prescribed horizontal tail volume coefficient of 0.5, and accommodates the optimal number of balls. This resulted in a 25-in long tail arm from the wing quarter-chord to the horizontal tail quarter-chord.

5.3.9 Electronics

Servo Selection

The total score weighs heavily on the number of servos. Because our propulsion system already counts as a single servo, per the rules, there was a need to optimize the conventional “servo” count to complete all the actuation the aircraft required. An option of having only a rudder and elevator with dihedral in the wings was considered, but soon discarded because of the difficulty with manufacturing. There would also be a slight weight increase due to the additional wing structure required. The second option was to have only aileron and elevator actuation. But, since the aircraft is a tail dragger, we need the rudder to provide ground control steering. Weighing the options, we went with one servo controlling both the aileron and rudder, and another servo controlling the elevator and ball drop mechanism.

With each conventional servo having more than one actuation function, we had two criteria in choosing our ideal servo: the servo had to provide plenty of torque and be light enough so that it wouldn’t significantly increase our RAC. We found three servos that could be potential candidates for our application:

Servo	Torque (@4.8V oz-in)	Weight (g)	Dimensions (mm)
Hitec HS-65MG	25	11	23.6x11.6x24
Savox SH-0256	54.2	15.8	22.8x12x29.4
Hyperion HP-DS-11AMB	58.3	10.5	23.5x11.5x21

Table 5.2: Servo Selection

By analyzing the hinge moments from each surface using AVL, the Hyperion HP-DS-11AMB servo was chosen because it has enough torque to move both the rudder and ailerons. Though the HS-65MG had enough torque to move the elevator and ball drop system, the Hyperion servo proved to be more optimal because of its weight advantages. During testing, we discovered that the servo arm was not long enough to achieve sufficient control for aileron and rudder. Therefore, a longer 3D printed servo arm was designed and used.

Speed Controller Selection

This year's competition regulations do not limit the motor current. For the given continuous 36V limit of the 1110 motor, two battery packs in series are used to power the propulsion system. The speed controller must be able to withstand the voltage and current provided from these two packs. Therefore, its preferred rating is higher than 36V.

ESC	Continuous Current (A)	Voltsmax (V)	Weight (oz)	Resistance (Ω)
Phoenix HV 30	30	50	1.13	0.005
HobbyKing 50 SBEC	50	22.2	1.83	
Phoenix Edge Lite 50	50	29.6	2.05	0.025
Phoenix Edge Lite HV 60	60	44.4	3.3	0.0012

Table 5.3: ESC Selection

The Phoenix Edge Lite HV 40 was chosen because of its 44.4V and 40A rating, and low resistance.

Electronics integration

The receiver, motor, receiver battery are all mounted to the boom, the aileron and rudder servo is glued to the wing spar, the main propulsion battery is velcro-strapped to the underside of the fuselage underneath the spar and the ESC is double-sided taped to the triangle structure of the fuselage. A 400mAh receiver battery is used with an external switch to easily turn on/off the receiver in order to conserve energy while waiting in the flight line. The fuse is mounted on the exposed boom in between the motor and the first ball release for ease of attachment.

5.4 Weight and Balance

Aircraft weight, without the payload, was estimated to be 3.81-lb. A weight and balance table was computed for each mission based on weight estimates for the aircraft components. All measurements were made, from a point, 13 inches in front of the wing's center of gravity (CG). Components were placed

so that the CG would fall on the wing's quarter chord or slightly behind it. The mission 2 payload was placed at the aircraft's quarter chord.

The external payload system was placed such that after each ball is dropped, there would not be a significant change in the CG. The release system is setup such that the aircraft takes off slightly tail heavy and as the balls are dropped the aircraft becomes nose heavy. The first three balls drop from the tail end of the aircraft; once they are released, the moment the remaining balls produce, about the quarter chord, is zero. As the remaining balls are dropped the change in the CG is so little that it goes unnoticed. Essentially, the CG after the first three balls are released and the landing CG are identical.

Charts that show the weight and balance of the aircraft for each mission and how it alters for mission 3 are shown below:

	Components	Arm (in.)	Weight (oz)	Moment (oz-in)
Structure	Boom	21	1.96	41.16
	Vertical Stabilizer	42.5	0.5	21.25
	Motor Mount	2	0.3	0.6
	Horizontal Stabilizer	42.5	0.5	21.25
	Fuselage	14	0	0
	Rear Fairing	27.3	2	54.6
	Wing	13	6.25	81.25
Propulsions	Speed Controller	7	2.5	17.5
	Battery	16	27	432
	Propeller spinner nut	1	0.25	0.25
	Motor/Gearbox	2	5.8	11.6
	Propeller	1.5	1	1.5
avionics	Receiver Battery	14	1	14
	Receiver	19	0.24	4.56
	Elevator Servos	42.5	0.4	17
	Ailerons Servo	14	0.4	5.6
Landing Gear	wheels	12	2	24
	Main Gear	12	4	48
Total	Glue	0	5	0
	Aircraft	--	61.1	796.12
	Center of Gravity (in)		13.03	
	Center of Gravity (% chord)		25.05	

Table 5. 4: Aircraft center of gravity for mission 1

	Components	Arm (in.)	Weight (oz)	Moment (oz-in)
Aircraft	Aircraft without battery	10.68	34.1	364.12
	Battery	13	25.2	327.6
Payload	5 lb payload	15	80	1200
	Payload restraints	10.5	1	10.5
Total	Aircraft	--	140.3	1902.22
	Center of Gravity (in.)		13.56	
	Center of Gravity (% chord)		26.08	

Table 5. 5: Aircraft center of gravity for mission 2

	Components	Arm (in.)	Weight (oz)	Moment (oz-in)
Aircraft	Aircraft without battery	10.68	35	364.12
	Battery	15.5	25.2	390.6
Payload	Total balls carried	18.623	8	148.984
	Ball drop clip system	16	4	64
Total	Aircraft	--	72.2	967.704
	Center of Gravity (in.)		13.4	
	Center of Gravity (% chord)		25.77	

Table 5.6: Aircraft center of gravity for mission 3

	Components	Arm (in.)	Weight (oz)	Moment (oz-in)
Aircraft	Aircraft without battery	10.68	34.1	364.12
	Battery	15.5	25.2	390.6
Payload	After first 3 balls dropped	13	5	65
	Ball drop clip system	16	4	64
Total	Aircraft	--	68.3	883.72
	Center of Gravity (in.)		12.94	
	Center of Gravity (% chord)		24.88	

Table 5.7: Aircraft center of gravity during mission 3

	Components	Arm (in.)	Weight (oz)	Moment (oz-in)
Aircraft	Aircraft without battery	10.68	34.1	364.12
	Battery	15.5	25.2	390.6
Payload	After all balls are dropped	13	0	0
	Ball drop clip system	16	4	64
Total	Aircraft	--	63.3	818.72
	Center of Gravity (in.)		12.93	
	Center of Gravity (% chord)		24.87	

Table 5.8: Aircraft center of gravity after all balls are dropped in mission 3

5.5 Flight Performance Parameters

$C_{L,max}$	e	L/D max	Empty Weight (lbs)
1.275	0.85	8.23	3.82

	M1	M2	M3
Cells	24	28	24
Available energy (kJ)	155.52	181.44	155.52
$C_{L,cruise}$	0.15	0.23	0.30
C_{D_o}	0.10	0.12	0.26
$(L/D)_{cruise}$	1.46	1.85	1.13
W/S (oz/ft^2)	13.96	31.42	15.71
V_{cruise} (ft/s)	73	88	54.27
V_{stall} (ft/s)	24.50	78	26
TO distance (ft)	5	45	15
T/W (static)	0.68	0.54	0.89
Flight time (s)	270	170	450
Max G Loading	4.94	2.56	4.40
V_{max}	224.40	193.60	164.27
Turn rate (deg/s)	54.09	44.87	72.77
Energy required (kJ)	51.24	51.24	31.20
TOGW (lbs)	4	9	4.50
Cruise current (amps)	12	18	5.80

Table 5.9: Flight performance parameters

Mission 3 is shown to be more efficient because the aircraft is flown at lower V_{cruise}. However, the amount of balls loaded increases the parasite drag.

5.6 Predicted Mission Performance

Aircraft parameters and mission outcomes from the mission model were used to predict the estimated final competition score.

Ground Mission		Flight Mission 1		Flight Mission 2		Flight Mission 3	
Loading Time (s)	30	Laps Flown	6	Flight Time (s)	157	Laps Flown	8
Estimated Best (s)	20	Estimated Best (s)	8	Estimated Best (s)	105	Estimated Max.	10
		Empty Weight (lb)	3.24	Empty Weight (lb)	3.43	Empty Weight (lb)	3.22
		Number of Servos	3	RAC	10.29	Total Mission Score RAC	0.58

Table 5.10: Predicted Mission Performance

Ground Mission - Payload Loading Time

The loading time for the mission 2 and mission 3 payloads is recorded to determine the ease of loading for the aircraft. A crew of 3 is allowed to load the aircraft. Estimated times are determined through field test based on averages.

Flight Mission 1 - Ferry Flight

The main focus of mission 1 is to perform as many laps as possible within four minutes, after taking off from a 60-ft runway. The entire mission is flown at maximum speed. The aircraft is expected to complete 6 laps with a 30% safety margin on battery energy. The code will be further adjusted to reflect test data concerning propulsion system, performance, and components.

Flight Mission 2 - Sensor Package Transport Mission

The objective of mission 2 is to fly three laps as quick as possible while carrying a 5-lb payload. The takeoff weight of the aircraft with the mission 2 payload is 8.75-lb; therefore, producing enough thrust to make the 60-ft takeoff requirement is critical. Due to the fact that mission 2 is a timed mission, the energy consumption is high and mission lap times are very critical. As such, the aircraft is flown at maximum speed; keeping in consideration to not overstress the airframe. The predicted total flight time is 156.7-sec, which is competitive based on past competition data and mission 1 lap times.

Flight Mission 3 - Sensor Drop Mission

For mission 3, the aircraft flies eight laps while carrying eight wiffle balls; releasing a single ball each lap in the designated drop zone. The score is based on number of laps, not the time, so the aircraft is flown at a speed that optimizes the L/D to maximize endurance. The ability to successfully complete eight ball drops is predicted to be competitive for placing well based on previous years' experiences.

5.7 CAD Package

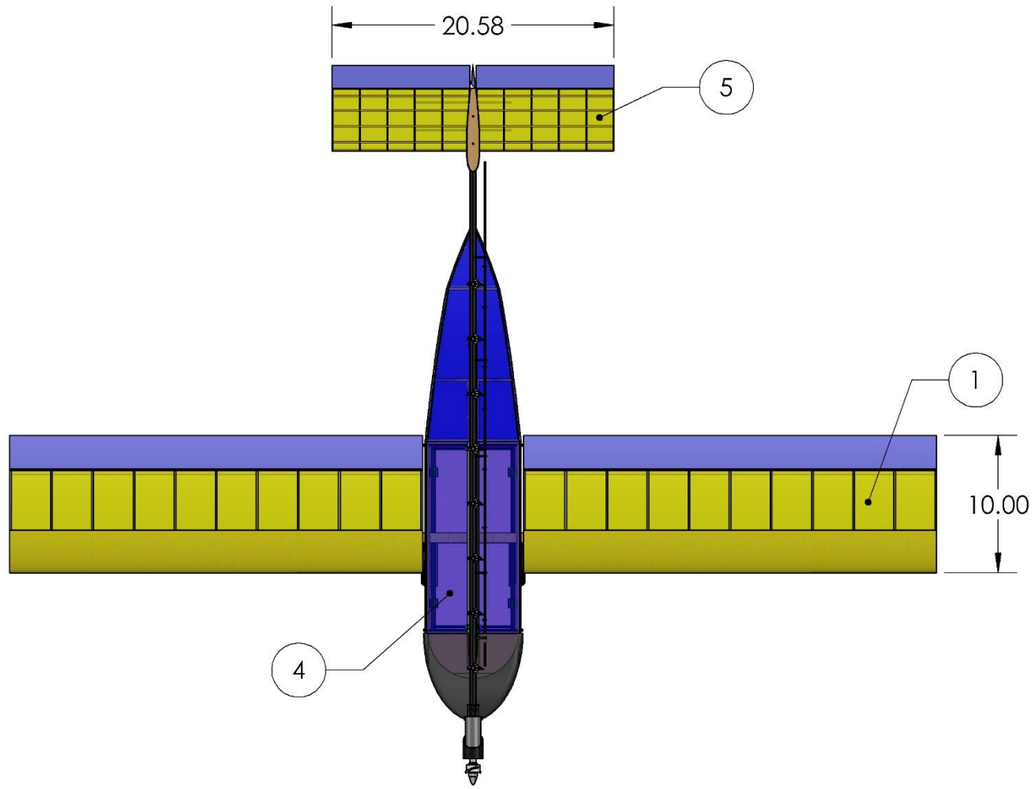

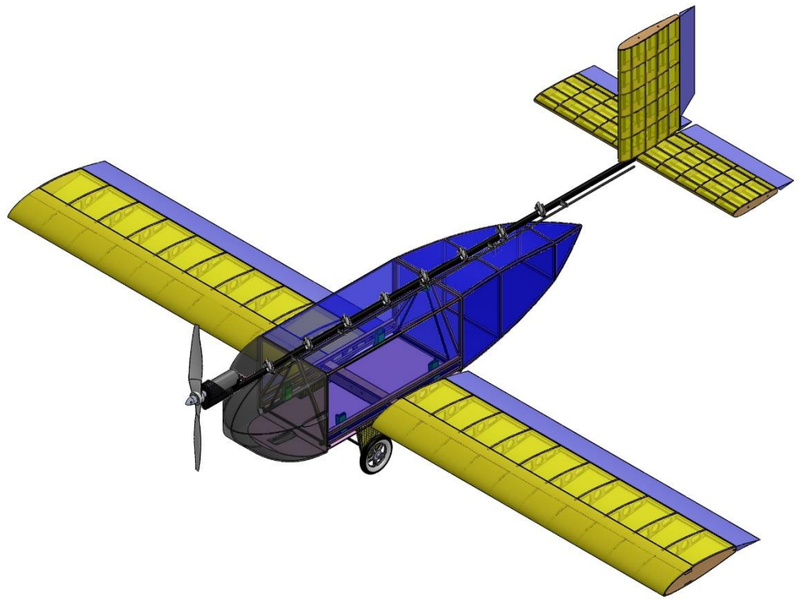

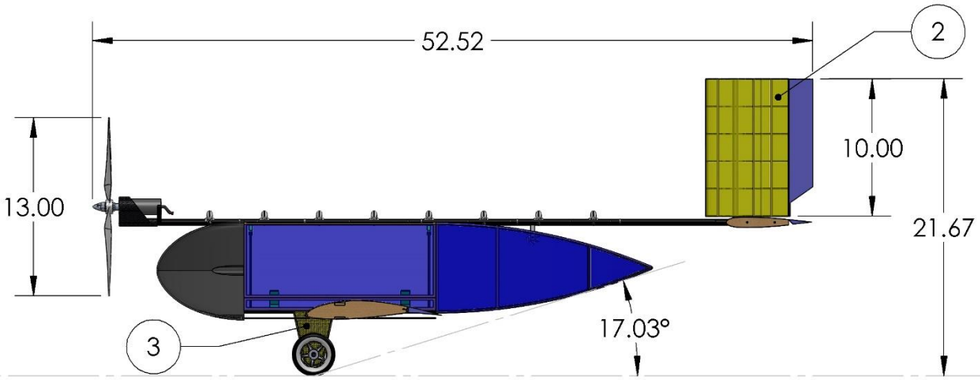

STATIC GROUND LINE

STATIC GROUND LINE

ITEM NO.	NAME
1	WING ASSEMBLY
2	VERTICAL STABILIZER
3	LANDING GEAR
4	FUSELAGE
5	HORIZONTAL STABILIZER

UNLESS OTHERWISE SPECIFIED:

DIMENSIONS ARE IN INCHES
TOLERANCES:
ANGULAR: BEND ± .5°
ONE PLACE DECIMAL ±.100
TWO PLACE DECIMAL ±.030
THREE PLACE DECIMAL ±.005

SAMUELI SCHOOL OF ENGINEERING, UNIVERSITY of CALIFORNIA - IRVINE

	NAME	DATE
DRAWN BY:	A. HE	2/21/2015
CHECKED BY:	A. KWOK	2/22/2015
CHIEF ENGINEER:	C. POBLETE	2/22/2015

UNIVERSITY OF CALIFORNIA IRVINE

CESSNA-RAYTHEON-DESIGN/BUILD/FLY 2014-2015

DOCUMENT TITLE: AIRCRAFT 3-VIEW

SIZE	APPROVAL DATE:	REPORT TITLE:	REV
B	2015-02-22	DRAWING PACKAGE	NC
	SCALE: 1:11	PAGE 1 OF 5	

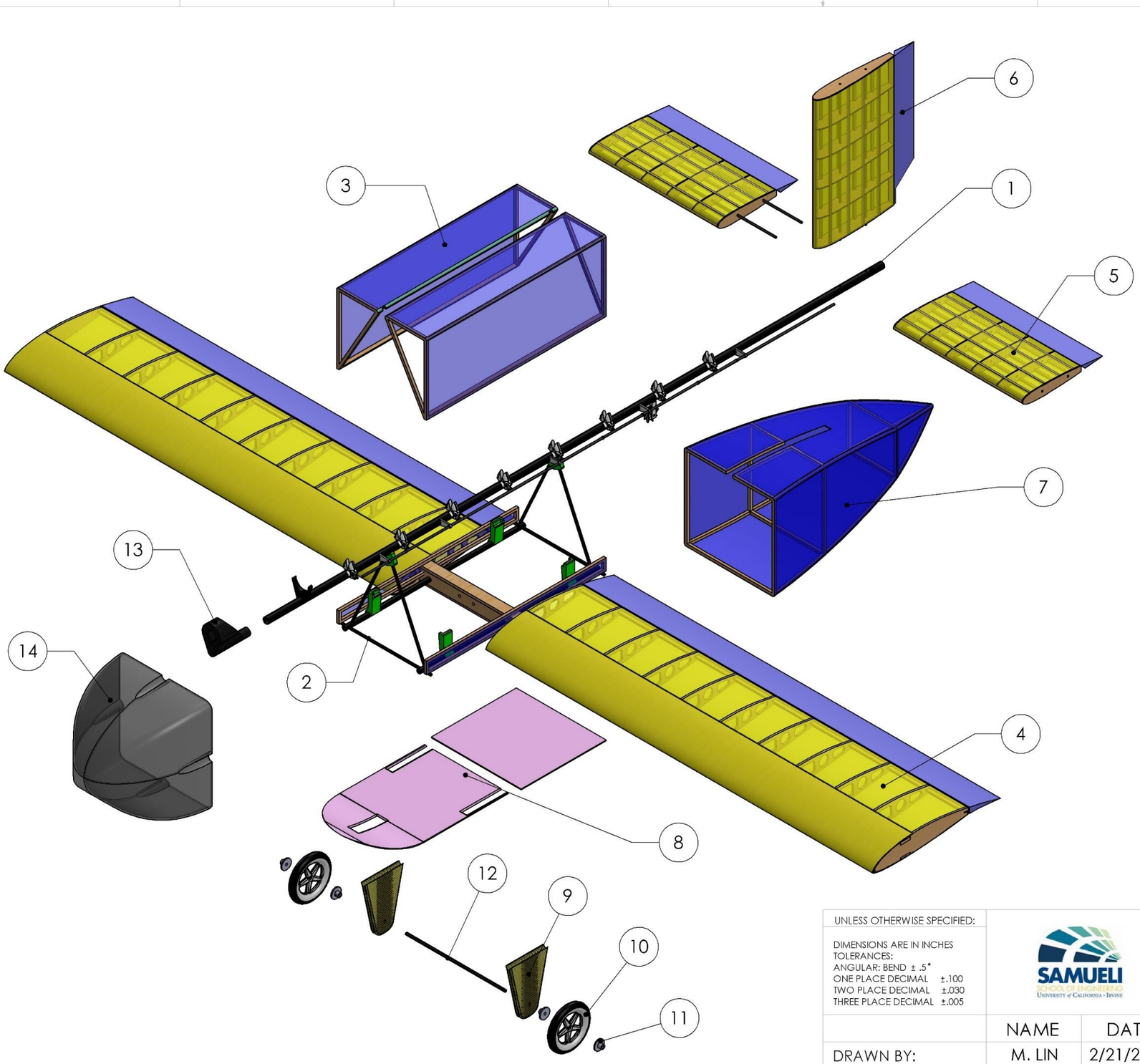

ITEM NO.	NAME	MATERIAL	QTY
1	BOOM	CARBON FIBER	1
2	FUSELAGE STRUCTURE	CARBON FIBER	1
3	FUSELAGE DOORS	BALSA - MICROLITE	1
4	MAIN WING ASSEMBLY	BALSA - MICROLITE - FOAM	1
5	HORIZONTAL STABILIZER	BALSA - MICROLITE - FOAM	1
6	VERTICAL STABILIZER	BALSA - MICROLITE - FOAM	1
7	REAR FAIRING	BALSA - MICROLITE	1
8	FUSELAGE FLOOR	FOAM	1
9	LANDING GEAR STRUT	BALSA - KEVLAR	2
10	LANDING GEAR WHEEL	PLASTIC - RUBBER	2
11	LANDING GEAR WHEEL WASHER	ABS PLASTIC	4
12	LANDING GEAR AXLE	CARBON FIBER	1
13	MOTOR MOUNT	CARBON FIBER	1
14	FRONT FAIRING	FIBERGLASS	1

UNLESS OTHERWISE SPECIFIED:

DIMENSIONS ARE IN INCHES
TOLERANCES:
ANGULAR: BEND ± .5°
ONE PLACE DECIMAL ±.100
TWO PLACE DECIMAL ±.030
THREE PLACE DECIMAL ±.005

SAMUELI SCHOOL OF ENGINEERING
UNIVERSITY of CALIFORNIA • IRVINE

	NAME	DATE
DRAWN BY:	M. LIN	2/21/2015
CHECKED BY:	A. KWOK	2/22/2015
CHIEF ENGINEER:	C. POBLETE	2/22/2015

UNIVERSITY OF CALIFORNIA IRVINE

CESSNA-RAYTHEON-DESIGN/BUILD/FLY 2014-2015

DOCUMENT TITLE:
STRUCTURAL ARRANGEMENT

SIZE	APPROVAL DATE:	REPORT TITLE:	REV
B	2015-02-22	DRAWING PACKAGE	NC
	SCALE: 1:6	PAGE 2 OF 5	

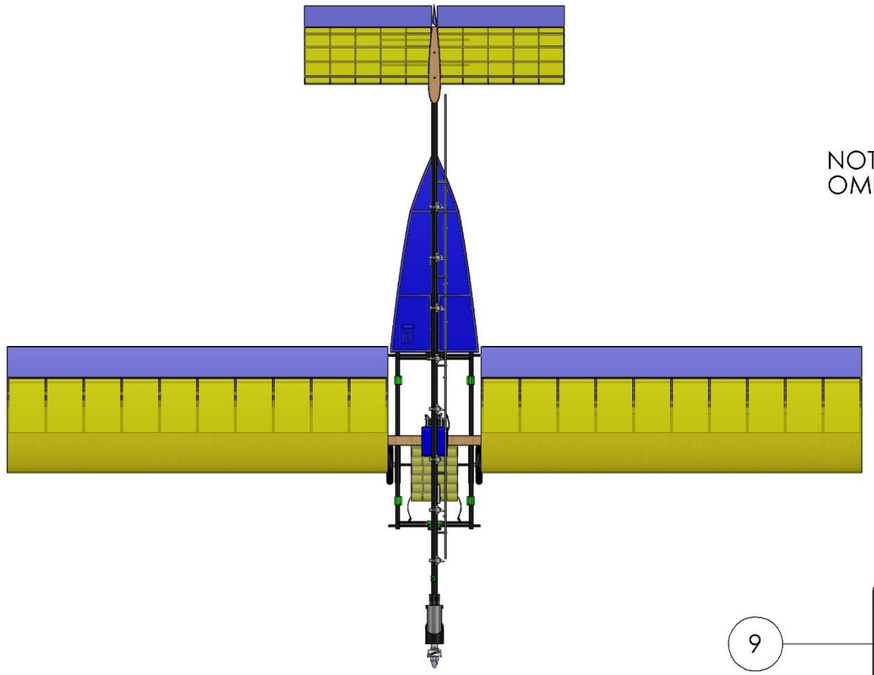

NOTE: FRONT FAIRING, FUSELAGE, AND FOAM FLOOR OMITTED FOR CLARITY

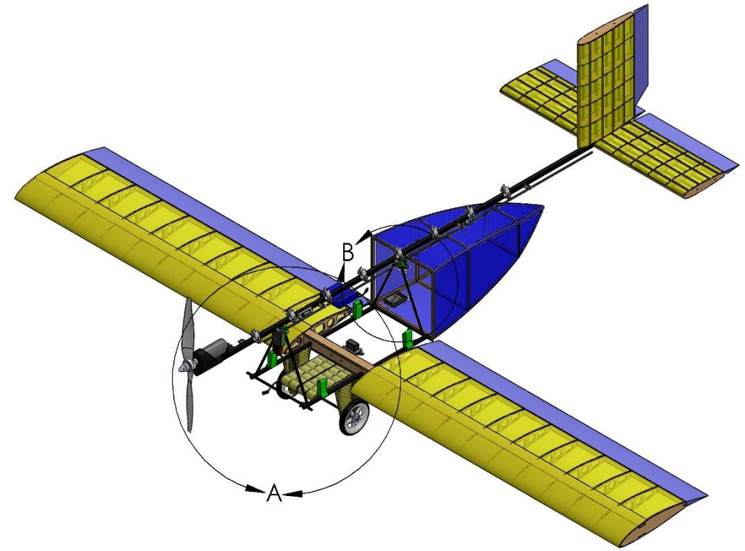

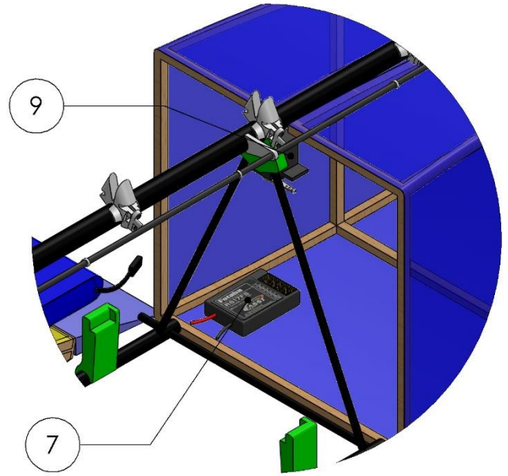

DETAIL B
SCALE 1 : 3

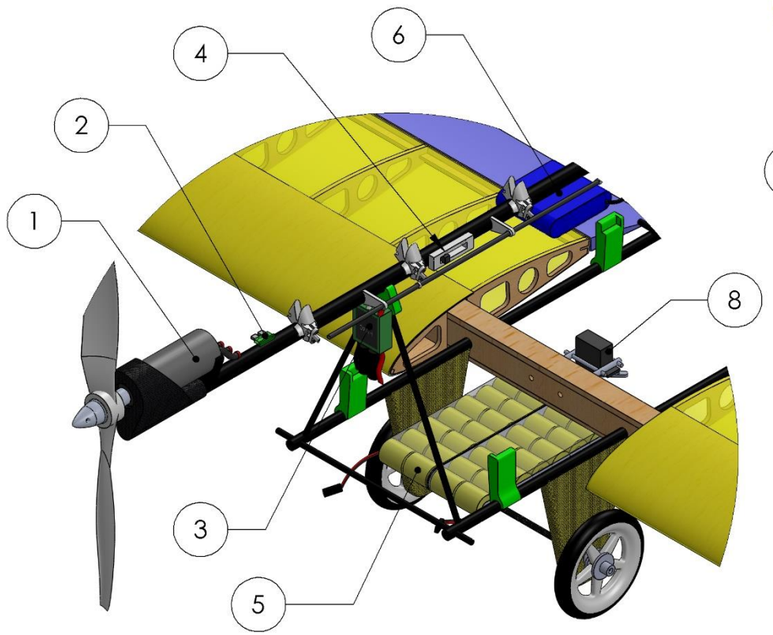

DETAIL A
SCALE 1 : 4

ITEM	NAME	MANUFACTURER	MODEL
1	MOTOR	NEU MOTORS	1110-3Y
2	FUSE	ALTRONIX	BF15
3	SPEED CONTROLLER	CASTLE CREATIONS	EDGE LITE HV-40
4	SWITCH	AIRTRONICS	96334
5	BATTERY	ELITE POWER PRODUCTS	ELITE 1500
6	RECEIVER BATTERY	FUTABA	NR4J
7	RECEIVER	FUTABA	R617FS
8	AILERON AND RUDDER SERVO	HYPERION	DS11AMB
9	ELEVATOR SERVO	HYPERION	DS11AMB

UNLESS OTHERWISE SPECIFIED:

DIMENSIONS ARE IN INCHES
TOLERANCES:
ANGULAR: BEND ± .5°
ONE PLACE DECIMAL ±.100
TWO PLACE DECIMAL ±.030
THREE PLACE DECIMAL ±.005

SAMUELI SCHOOL OF ENGINEERING, UNIVERSITY of CALIFORNIA · IRVINE

	NAME	DATE
DRAWN BY:	A. KWOK	2/21/2015
CHECKED BY:	C. SLEDGE	2/22/2015
CHIEF ENGINEER:	C. POBLETE	2/22/2015

UNIVERSITY OF CALIFORNIA IRVINE

CESSNA-RAYTHEON-DESIGN/BUILD/FLY 2014-2015

DOCUMENT TITLE:
SYSTEMS LAYOUT/LOCATION

SIZE	APPROVAL DATE:	REPORT TITLE:	REV
B	2015-02-22	DRAWING PACKAGE	NC
	SCALE: 1:12	PAGE 3 OF 5	

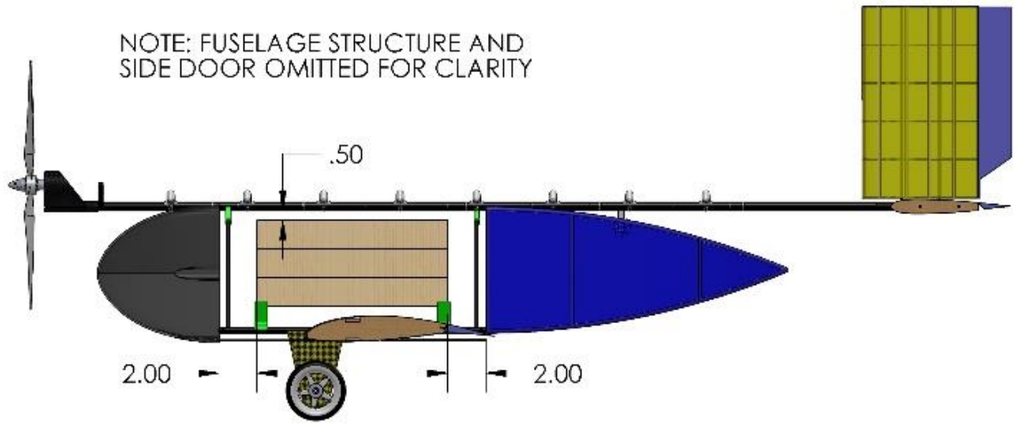

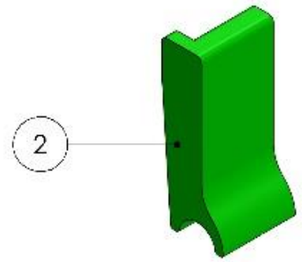

SCALE: 1:1

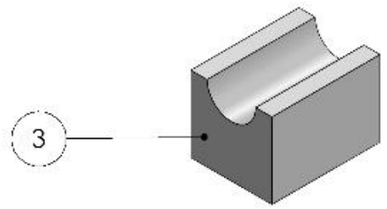

SCALE: 1:1

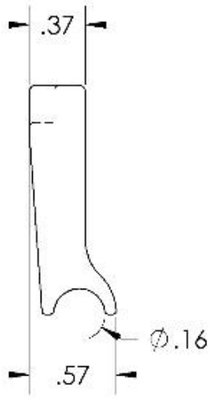

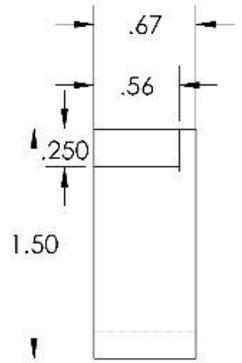

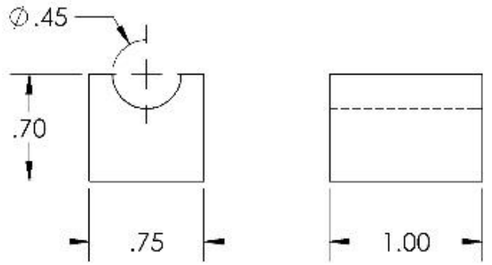

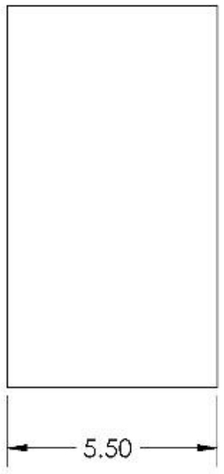

NOTE: PAYLOAD AND FUSELAGE BOTTOM
ISOLATED FOR CLARITY

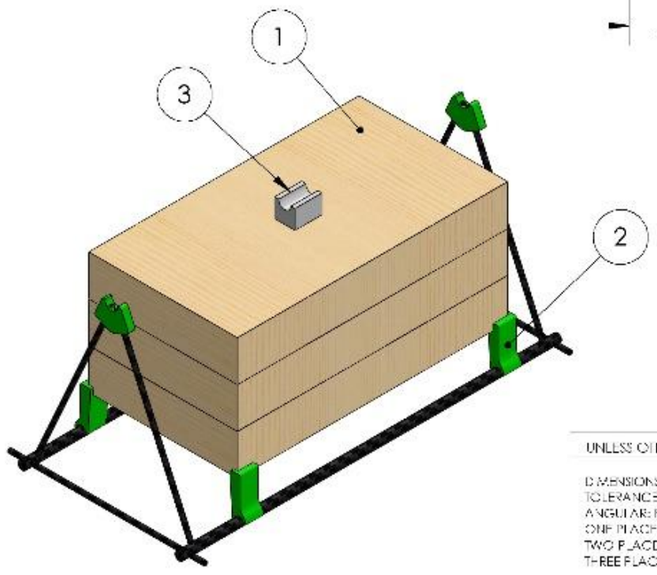

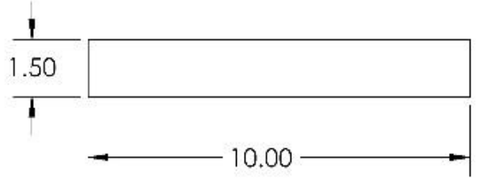

ITEM NO.	NAME	QTY.
1	INTERNAL PAYLOAD	3
2	PAYLOAD SUPPORTS	4
3	PAYLOAD RESTRAINT	1

UNLESS OTHERWISE SPECIFIED:
DIMENSIONS ARE IN INCHES
TOLERANCES:
ANGULAR: BEND ± .5°
ONE PLACE DECIMAL ± .00
TWO PLACE DECIMAL ±.030
THREE PLACE DECIMAL ±.005

	NAME	DATE
DRAWN BY:	A. KWOK	2/21/2015
CHECKED BY:	C. SLEDGE	2/22/2015
CHIEF ENGINEER:	C. POBLETE	2/22/2015

UNIVERSITY OF CALIFORNIA IRVINE

CESSNA-RAYTHEON-DESIGN/BUILD/FLY 2014-2015

DOCUMENT TITLE:
MISSION 2 PAYLOAD ACCOMODATION

SIZE B | APPROVAL DATE: 2015-02-22 | REPORT TITLE: DRAWING PACKAGE | REV NC

SCALE: 1:8 | PAGE 4 OF 5

NOTE: RELEASE MECHANISM AND BOOM
ISOLATED FOR CLARITY

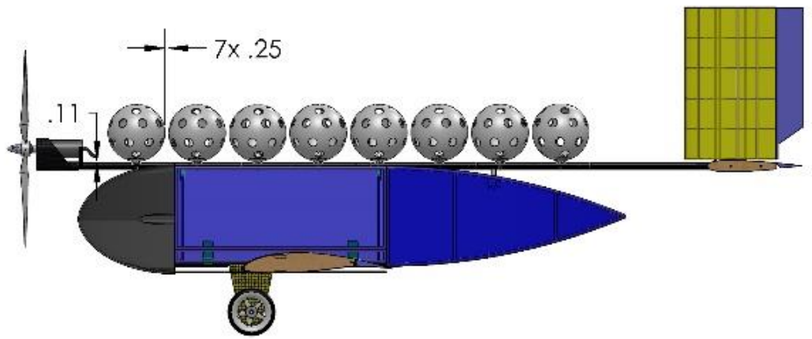

SCALE 1:10

NOTE: PAYLOAD AND BOOM
ISOLATED FOR CLARITY

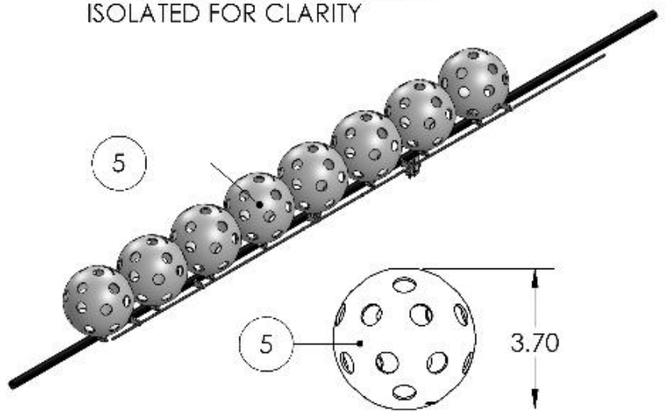

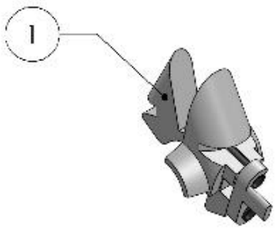

SCALE 1:1

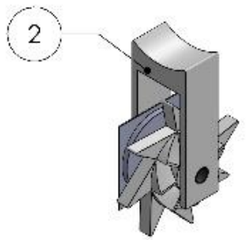

SCALE 1:1

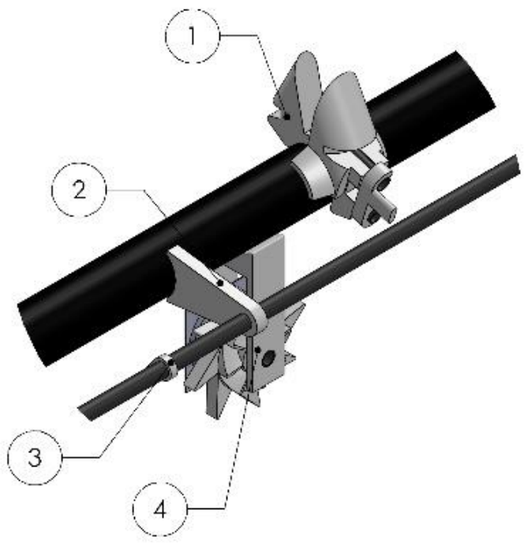

DETAIL A
SCALE 1 : 1

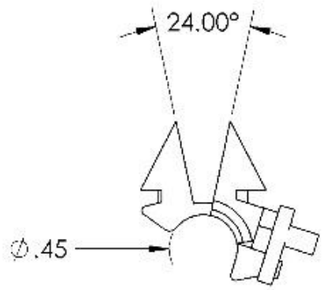

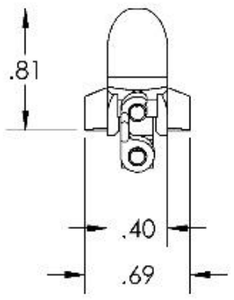

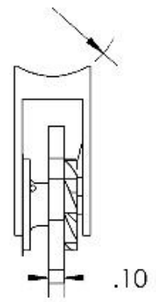

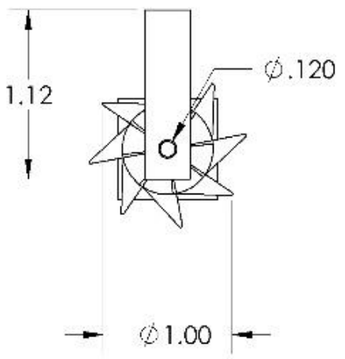

ITEM NO.	NAME	QTY.
1	RELEASE MECHANISM	8
2	GUIDE TAB	5
3	PAYLOAD TRIGGER	8
4	RATCHET SYSTEM	1
5	EXTERNAL PAYLOAD	8

UNLESS OTHERWISE SPECIFIED:
DIMENSIONS ARE IN INCHES
TOLERANCES:
ANGULAR: BEND ± .5°
ONE PLACE DECIMAL ± .100
TWO PLACE DECIMAL ± .030
THREE PLACE DECIMAL ± .005

	NAME	DATE
DRAWN BY:	A. KWOK	2/21/2015
CHECKED BY:	C. SLEDGE	2/22/2015
CHIEF ENGINEER:	C. POBLETE	2/22/2015

SAMUELI

UNIVERSITY OF CALIFORNIA IRVINE

CESSNA-RAYTHEON-DESIGN/BUILD/FLY 2014-2015

DOCUMENT TITLE:
MISSION 3 PAYLOAD ACCOMODATION

SIZE B | APPROVAL DATE: 2015-02-22 | REPORT TITLE: DRAWING PACKAGE | REV NC

SCALE: 1:8 | PAGE 5 OF 5

6.0 Manufacturing Plan and Process

6.1 Wings and Tails

The wings and tails are large volume components where manufacturing methods have a strong impact on weight reduction. The following methods were considered:

- **Foam Wings –** The foam wing shape was cut using a hot-wire CNC machine. The wing cores were then cut out using a hot-wire CNC machine. The wings are sanded to remove any defects from the hot-wire, bagged with composite fabrics, and hollowed out.
- **Balsa Wing –** Ribs were laser cut from CAD drawings for exact dimensions. The ribs were secured in a jig to ensure precise alignment and dimensions. Balsa spars were reinforced with unidirectional carbon fiber, which were then glued in place along the top and bottom cut out sections of the ribs. After securing the top and bottom spar caps, the assembled ribs were removed from the jig and the leading and trailing edge end pieces are glued in. Thin, flexible balsa was used to cover the leading edge to the spar caps to preserve the shape of the wing. The rest of the wing is covered with an iron-on skin: Microlite. Applying heat shrinks the material to a tight fit.

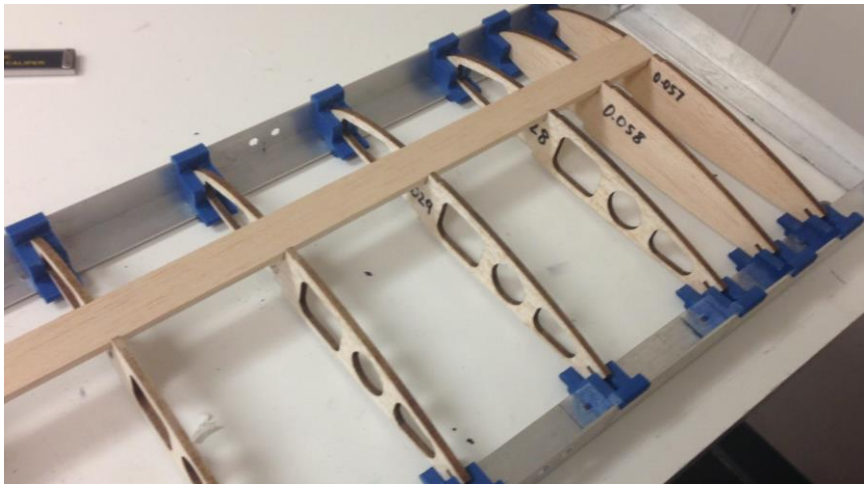

Figure 6.1: Balsa Wing

- **Balsa wings with molded leading edges** - The molded wing was similar to the balsa built-up wing, except the leading edge used composites instead of balsa sheeting. Kevlar was molded to the shape of the first 25% of the wing and glued in place. The Kevlar sheeting was manufactured using a foam mold. This guaranteed a precise and repeatable airfoil shape every time.

6.2 Fairings

The following methods were considered for the manufacturing of the fairings.

- **Female Molding** - A foam male plug that represents the final part was cut using an airfoil shape template, hand sanded to the desired shape, and then layered with composite materials. The female mold represents the negative of the part that was to be used on the aircraft. Tooling gel was applied to the plug, which then becomes the surface of the female mold. Once ready, it allows for rapid

prototyping of different lay-ups of the final parts that are optimized for variable criteria (i.e. stiffness, strength, etc.)

- **Male molding-** A male mold is made slightly smaller than the final part. This method is relatively easy to set up the mold, but the parts are not necessarily the exact desired size. If the part is made too thick it can no longer fit the aircraft because it is oversized.
- **Balsa structure-** A balsa structure was made using balsa strips and then covered with Microlite to seal the surface. Balsa construction is the quickest manufacturing method but is not easily repeatable because a whole new structure has to be manufactured to replace the old one. The balsa is also difficult to bend into a curved shape making it hard to replicate complex curves.
  While optimizing the aircraft design, the front fairing was manufactured using female molding while the rear fairing was designed to converge to a point using a 15 degree angle to allow for the adequate takeoff rotation angle corresponding to CL_{Max} using balsa structures.

Figure 6.2: Front Fairing Molds

6.3 Payload

6.3.1 Mission 2 Payload

The original payload design used the carbon frame from the landing gear, where Kevlar tow was placed across the payload area creating a platform for the Mission 2 payload to sit on. This design developed into 3D printed supports because the wing spar was found to come in the way of the Mission 2 payload floor. The 3D printed supports also provided longitudinal and lateral stability for the payloads.

The lengthwise member of the payload area is made of 0.31-in carbon tubes. Holes were drilled through these tubes at each end to allow 0.15-in carbon rods to be inserted to help construct the delta-frame structure. In order to obtain consistent angles for the delta-frame, a 3D printed jig was designed and used to facilitate the drilling of the guide holes. The delta-frame is completed at the top with a 3D printed joint that attaches the boom to the fuselage cage below. Carbon and Kevlar tow was then wrapped around all the joints in the delta-frame to reinforce them. Due to the low wing design of the aircraft, minor tensile loads were experienced during flights. The compressive loads during flight and landing were absorbed mostly by the carbon structure and transferred to the boom up the delta shape.

Figure 6.3: Mission 2 Payload

6.3.2 Mission 3 Payload

The ratchet system was configured in such a way that the ratchet advances only with significant down input from the elevator. This allows the pilot to decide when to trigger the system by choosing to pitch down and cause the ratchet to actuate. The ratchet system pulls on the control rod, which has incrementally spaced pins. A small hook locks the clips in the open position, keeping the ball secured through the hole. The pin on the carbon control rod unlocks the hook, triggering the clip to close due to the force of an elastic band.

The components for the clip payload release system were mainly 3D printed, allowing consistent parts to be rapidly produced. Having 3D printed parts also allowed minor adjustments to be easily made to the clips. When the clips are in the open position, the shape of the clips allows the balls to be inserted. The hook on the clips prevent the balls from falling out during flight, but do not restrain the balls when the clips are closed. The ball release mechanism is attached to the boom using cyanoacrylate glue.

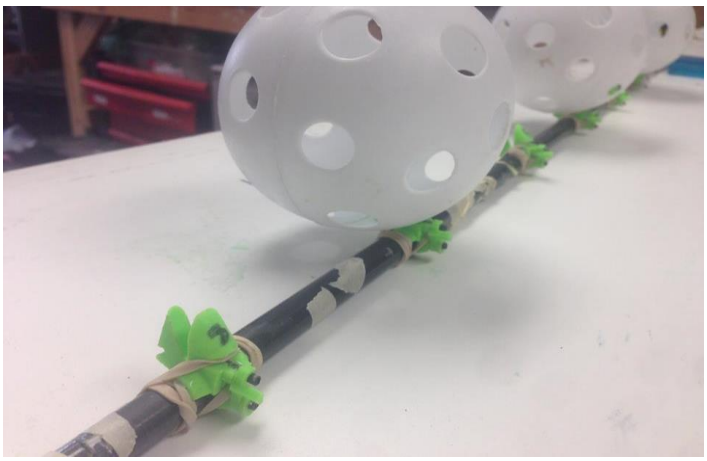

Figure 6.4: Mission 3 Payload with Clips System

6.4 Landing Gear

- **Conventional Landing Gear -** One option for a landing gear was a conventional configuration where a balsa core was bent on a mold and reinforced with bidirectional and unidirectional carbon fiber. This

configuration provides enough strength to support the aircraft's weight; however it would provide poor handling and add too much weight to the aircraft. Furthermore, this kind of landing gear showed to be too stiff during landing which can hinder the plane from landing safely. Due to these disadvantages, this landing gear option was not used.

The landing gear was therefore integrated with the payload system; making the manufacturing process unconventional when compared to traditional landing gears.

- **Landing Gear Struts** – For this structure a balsa wood block of .38 " was used and cut into the general shape of the struts. Slots were sanded into the balsa landing gears using a 3D printed jig in order to allow the integration of the .31'' carbon tubes of the payload and landing skids. After the struts were glued to the carbon rods they were reinforced by wrapping 45 degree bidirectional Kevlar. With this kind of manufacturing the landing gear was incorporated into the frame structure of the aircraft allowing us to minimize the weight of the aircraft and its drag.

Figure 6.5: Landing Gear and Wing

6.5 Motor Mount

Two methods of molding were considered in the manufacturing of the carbon fiber motor mounts. The goal was to manufacture mounts that were lightweight and durable.

- **3D Printed Female Mold** – A 3 piece mold was designed on SolidWorks and printed using ABS plastic. The mold was then prepared for manufacturing by sanding and waxing to obtain a smooth surface. The carbon fiber pieces were wetted out with epoxy and inserted into the mold. A piece of the structural boom is then placed inside to mold a carbon sleeve. The sleeve is used as the mount attachment. The mold is then placed in a vacuum bag and left to harden.

- **Foam Male Mold** - A male mold was cut out of foam using a CNC hotwire. The foam plug was then covered with several layers of carbon fiber that also wrap around the boom. The motor mount layup is then placed inside a vacuum bag, and left to harden.

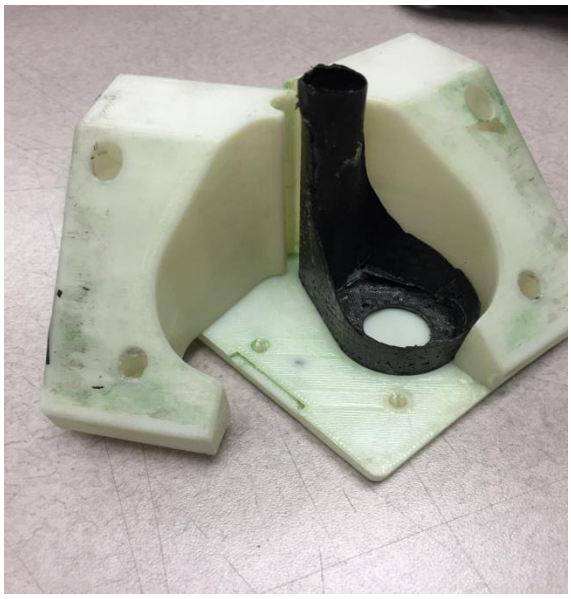

Figure 6.6: Motor Mount and 3D Printed Mold

7.0 Testing Plan

Components of the aircraft are tested to analyze performance of the design and note areas for improvement. Results of testing indicate areas for improvement or reduction to substitute for other advantages, such as reduced weight.

7.1 Objectives

Requirements or goals of each component are defined before testing. Current components are compared to past standards and manufacturing principles. The primary objective is a light aircraft that maintains consistent strength and reliability while flying all missions successfully.

7.1.1 Fuselage and Landing Gear

By design the fuselage was integrated into the landing gear and tested together for overall structural integrity. The initial test for the landing gear was a static load test to 8.75-lb to simulate the full load of the aircraft with the mission 2 payload. The landing gear was constrained to the ground and held in place. A load was then applied gradually and increased to a 43.75-lb. to simulate 5G acceleration.

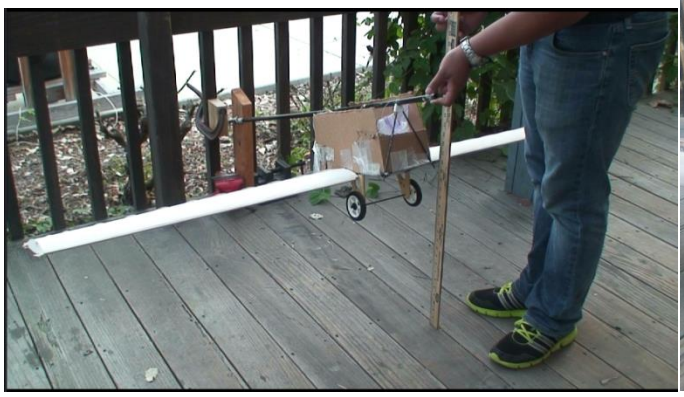

Figure 7.1: Langing gear drop test

Figure 7.2: Landing gear test failure

A drop test was conducted to insure that the landing gear would be able to carry the load of the aircraft during landing. This was done by attaching the boom to the landing gear frame and securing the boom at one end. The landing gear was loaded with the maximum weight the aircraft would carry and dropped from an initial height of 1ft. The drop height was then gradually increased until the point of failure. This type of test provided knowledge on the strength of the landing gear and insured its stability from the maximum height of landing. The drop test was conducted on a flat surface as well as at an angle to simulate a crosswind landing. The results of the drop test determined the energy transfer that the structure can handle in case of non-ideal landing or flight conditions.

7.1.2 Wing and Spar

The wing was modeled in SolidWorks during the design process. Some problems that may occur with this design of the wing could be due to torsion, load or vibrations. The wings are created using balsa wood which has an excellent strength to weight ratio; however in the radial or tangential directions the material becomes less stiff and weaker. In the air, the wings tend to experience some torque as the tips of the wings tend to flex up or down. This may cause some fatigue in the wings and cause them to break after continuous use. The balsa wings may also fracture by trying to support a large load. Each side of the wing should be able to withstand half of the weight of the aircraft's body. Taking into consideration all the needs and problems of the wing, the following testing options were decided upon to conduct a finite element analysis (FEA) on. The first test is a static test to determine whether the root of the wing, (the portion of the wing joining to the fuselage), can withstand the weight of the wing at rest. To verify this, the root of the part was restrained and the load was distributed along the wing Figure 7.3. The next analysis displays if the wing of the aircraft can withstand the weight of the aircraft when lifted from the tips. To simulate this the root of the aircraft was restrained and an upward force was applied on the tip equivalent to half the weight of the aircraft Figure 7.3.

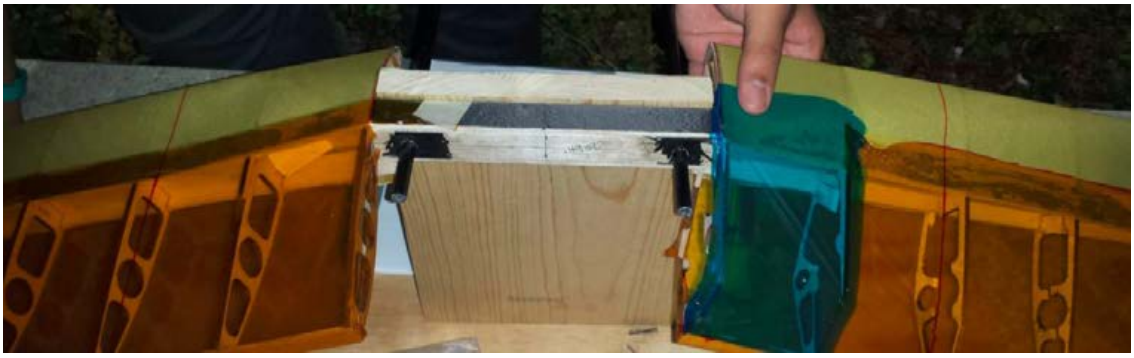

Figure 7.3: Wing stress under a distributed load

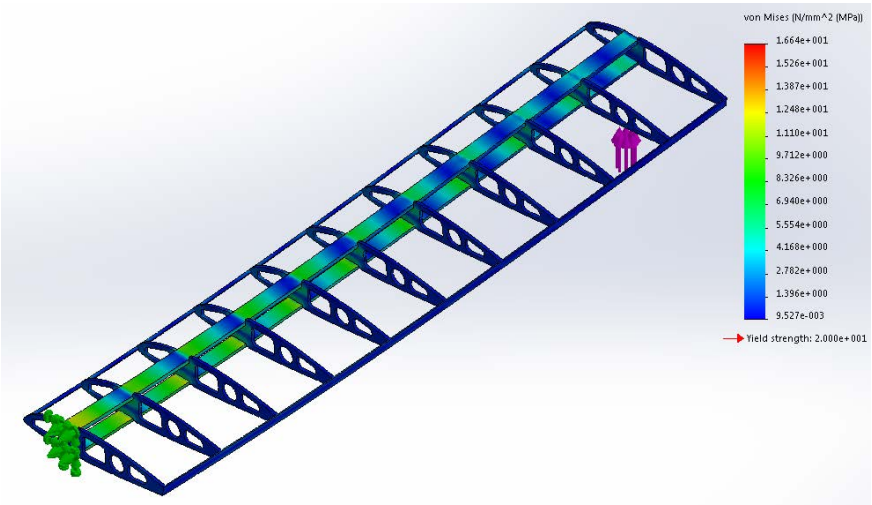

Figure 7.3: Wing stress under a distributed load

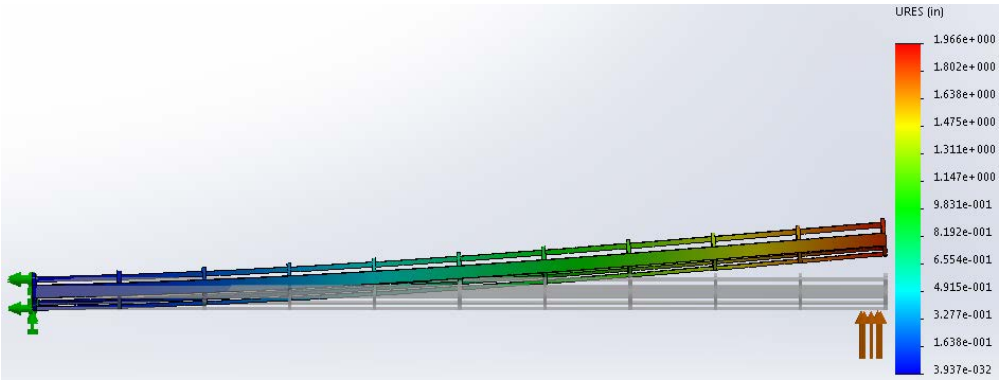

Figure 7.4: Wing deflection under a distributed load

The aircraft weighs 8.75-lb when loaded with the mission 2 payload. For the static loading analysis, a 17-N force was applied at the edge of the wing where the lift force has the most influence. A restraint was placed on the edge of the wing where it is connected to the fuselage of the aircraft. According to the stress plot produced based on the boundary conditions set, the FEA predicted that the

yield strength occurs at 20-MPa and the maximum stress the balsa wing experiences from the 17-N force is 16.6-MPa; therefore since the maximum stress is lower than the yield strength, the wing should not fail or yield when experiencing a 17-N load. A maximum displacement of 1.97-in also occurs at the end of the wing.

Furthermore, the wing and spar were tested for structural strength and the requirement to sustain a 5G turn while fully loaded. A static load test was conducted using an elliptical load distribution to simulate the in-flight load. Both halves of the wing were divided into five sections and loaded with sandbags starting from the center of the wing. The wing was tested until failure with notes taken on the types of failures and failure points.

7.1.3 Propulsion Testing

Propulsion testing was done to analyze the motor, battery, and propeller combination performance. Static tests were done with a thrust rig by varying one component and holding all others constant for comparisons

Motor & Propeller	Predicted Thrust (lb)	Actual Thrust (lb)	Predicted Current (A)	Actual Current (A)	Predicted Watts (W)	Actual Watts (W)	RPM
Neu 1105 14x7	5.57	4.60	35.40	34.70	437	452	6800
Neu 1105 16x8	7.03	5.35	55.20	45.93	584	514	5900
Neu 1110 16x8	5.91	5.08	17.37	14.92	433	385	5500
Neu 1105 16x10	7.39	6.10	85.87	48.30	908	555	6000

Static Errors			
Motor & Propeller	**Thrust %**	**Current %**	**Watts %**
Neu 1105 14x7	17.38505747	1.974906692	3.432494279
Neu 1105 16x8	23.89758179	16.79273276	11.98630137
Neu 1110 16x8	14.07307172	14.11157762	11.08545035
Neu 1105 16x10	17.43367623	43.75438117	38.87665198

Table 7.1: Static and predicted calculations for various propeller and motor combinations

7.1.4 Thrust Rig

Data is exported in real time using Medusa Research Inc. PowerPRO view program. Such data included voltage, amps, amp hours, watts, watt hours, temperature, prop rpm, thrust, etc. Components used to record the data were a temperature probe, rpm optical sensor, thrust cell, and a watt meter.

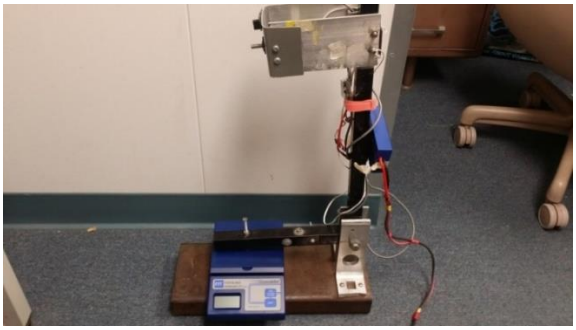

Figure 7. 5: Propeller Thrust Rig

7.1.5 Flight Test

Flight test performance data is recorded using an Eagle Tree telemetry system. A pre-flight checklist helps facilitate flight testing schedule and eliminate possible troubleshooting.

7.2 Master Test Schedule

Test	Objective	Start Date	End Date
Landing Gear	Verify gear meets bending stress and impact requirements to simulate landings	1/13/15	2/19/15
Payload Systems	Ensure no slippage, reliability, and ease of attachment/release	11/10/14	12/12/14
Propulsion System	Static thrust performance tests with motor, prop, and battery packs	11/15/14	2/15/15
Flight Testing	Compare flight measurements to calculated model	10/25/14	2/21/15
Payload Release Mechanism	Ensure the mechanism is firmly attached, and easy to load/release balls	10/26/14	2/21/15
Wings	Ensure wing is capable of withstanding aerodynamic load, bending, and torsion	11/20/14	1/30/15

Table 7.2: Master Test Schedule

7.3 Preflight Check List

Preflight Check List	
Structural Integrity – Visual inspection for damaged components	
☐ Control Surfaces / Linkages	☐ Horizontal/Vertical Stabilizers
☐ Payload Mounts	☐ Propeller
☐ Boom/All Fairings	☐ Landing Gear
☐ Wing	☐ Motor Mount
Avionics – Ensure all wires and electrical components are connected and performing properly	
☐ Servo Wiring	☐ Avionic Power Test
☐ Range Test	☐ Servo Test
☐ Receiver Properly Connected	☐ Receiver Battery Peaked
☐ Failsafe	☐ Main Battery Peaked
Propulsion – System should perform as desired	
☐ Motor Wiring	☐ Battery Connected
☐ Servo Wiring	☐ Battery Connected
☐ Motor Test	☐ Telemetry Connected
Final Inspection – Ensure safe, successful flight	
☐ Correct Control Surface Movement	☐ Mission/Objective Restated
☐ Ground Crew Clear	☐ Pilot and Spotter Ready

Table 7.3: Preflight Check List

7.4 Flight Test Plan

Flight Test Plan 2/20/15 Prototype 2	
☐ Acquire telemetry for all flights ☐ Live tracking of battery capacity, speed, current and altitude ☐ Ramp throttle to 100% before each flight on the ground	
First Flight: Trim flight **Battery: 20 cells 1500 mAh, Propeller: 12x12**	**First Flight: Mission 1 simulation** **Battery: 28 cells 1500 mAh, Propeller: 12x12**
☐ Trim plane	☐ Takeoff weight: 4-lbs
☐ Understand Behavior in straightaway and turns	☐ Cruise Speed: 70.4 ft/s ☐ Stall Speed: 24.5 ft/s
☐ Switch pilots and repeat	☐ Flight duration: 4 minutes
	☐ Fly the course with spotters.
First Flight: Mission 2 simulation **Battery: 28 cells 1500 mAh, Propeller: 16x10**	**First Flight: Mission 3 simulation** **Battery: 24 cells [x mAh], Propeller: 13x10**
☐ Takeoff weight: 9 lbs	☐ Takeoff weight: 4.56 lbs
☐ Cruise Speed: 80.7 ft/s ☐ Stall Speed: 36 ft/s	☐ Cruise Speed: 44 ft/s ☐ Stall Speed: 26 ft/s
☐ Flight duration: 2.75 minutes	☐ Flight duration: 7.5 minutes
☐ Fly the course with spotters.	☐ Fly the course with spotters.

Table 7.4: Flight Test Plan

8.0 Performance Results

Each set of components was tested to improve design and validate estimated predictions. The results allow for design corrections and fine tuning of components.

8.1 Performance of Key Subsystems

Wing and Spar Performance

The wing and spars were tested for bending moment and torsional stresses. Each wing was mounted upside down onto a test stand with two booms to simulate the same loading in flight. Sandbags were distributed symmetrically on each side of the wing, starting from the center. First, the wing was loaded until failure, and then analyzed to determine the cause of failure in order to obtain information for improvements. The initial tests determined that the first few sections from the center of the wing required more reinforcement because most of the load was concentrated towards the middle. Testing determined that the wing spar experienced more forces on the top cap due to compression, concluding that the top cap must be reinforced by using a thicker balsa piece. Figure 8.1 shows the balsa wing with a molded leading edge on the test stand during a test where the wing was only loaded to a factor of three. The results of the wing and spar tests are shown in the Table below.

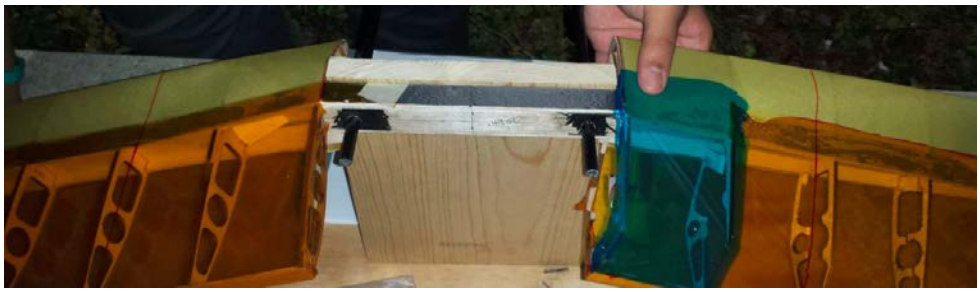

Figure 8. 1: Wing test failure

Wing	Load Factor Withstood	Notes	Weight (oz)
Fiberglass skin foam core	8	No warning before failure	12.11
Balsa Wing 1	4.5	Heard cracking before failure	5.26
Balsa Wing 2	4.5	Heard cracking before failure	5.14
Molded Balsa Wing	3	Heard cracking before failure	5.3
Balsa Wing 3	5	Performed up to expectation	5.4

Table 8.1: Results of Wing test

Landing Gear Performance

Two landing gear designs were considered: a conventional structure and an integrated landing gear. The conventional landing gear suffered from higher weight and poor landing performance due to rigidity. The integrated design was lighter in weight and resulted in more controlled landings. Moreover, the integrated landing gear is able to elastically deform, absorbing some of the landing loads.

The main landing gear was subjected to a static load test and a dynamic load test to confirm that it is structurally sound and capable of handling non-ideal landings. The static load test consisted of loading the main gear up to a safety factor of five times the total weight of the aircraft and payload. A dynamic load test was conducted with a consistent series of free fall drops with 8.75-lb in order to test the integrity of the landing gear in extreme conditions. These free fall drops increased in height with increments of 2-in until a maximum height of 18-in was recorded. In addition, a side load test was conducted to evaluate the performance of the landing gear under a one wheel touchdown condition.

The main landing gear was capable of handling a maximum drop height from 20-in on a flat surface with the mission two payload. Interestingly, the foam wheels and carbon rod attached to the landing gear absorbed a notable amount of the initial energy of the drop.

Landing Gear Design	Design Load (lb)	Static Test Results (lb)	Dynamic Test Results
Conventional Landing Gear	27	32	Survived 6 in drop; Failed side loading drop
Integrated Flexible Design	27	39	Survived 12 in drop; Failed side loading drop
2nd Integrated Flexible Design	27	42	Survived 16 in drop; Survived side loading drop
Final Design	27	42	Survived 20 in drop; Survived side loading drop

Table 8.2: Dynamic Drop Test Results

8.2 Complete Aircraft Performance

Eagle Tree Telemetry was used to record and monitor flight performance in real time. Data recorded included GPS, airspeed, volts, current, watts, rpm, temperature, and G forces. Test flight data was used to help optimize the aircraft for later iterations. The tables below show predicted propulsion data and field flight data obtained from telemetry.

Propeller	Predicted Thrust (lb)	Actual Thrust (lb)	Predicted Current (A)	Actual Current (A)	Predicted Watts (W)	Actual Watts (W)	RPM
12x12	2.54	1.5	11.78	11.5	345	360	6500
16x10	3.93	2.5	19.51	18	518	500	6000
13x10	1.30	0.9	5.51	5	113	120	4500

Flight Errors			
	Thrust %	Current %	Watts %
12x12	40.60433667	2.401744	4.347826087
16x10	35.95475256	7.7171089	3.474903475
13x10	33.68572094	9.1831602	6.194690265

Table 8.3: Flight data and predicted values for Neu 1110 motor

Mission 1

Speed is the primary focus of mission 1, where number of laps flown in four minutes goes into the mission score. Flights resulted in an average lap time of 50-sec and achieved takeoff within 5 feet. Average accelerations of 3.5 G's were experienced during the 180° turns and 4.94 G's were experienced during the 360° turns.

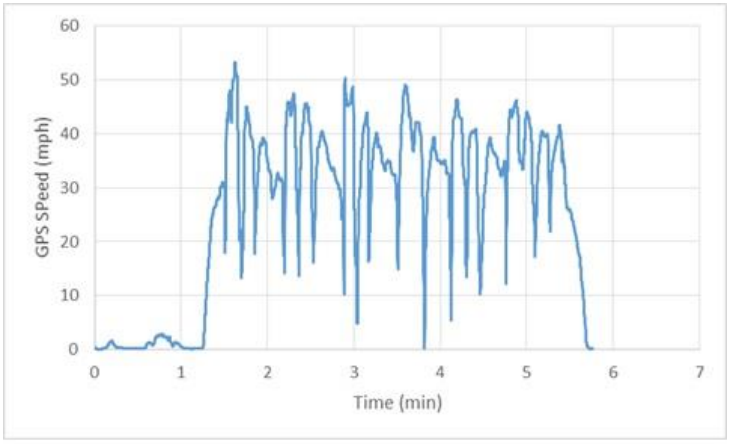

Figure 8.2: GPS speed during mission 1 using Neu 1105 motor

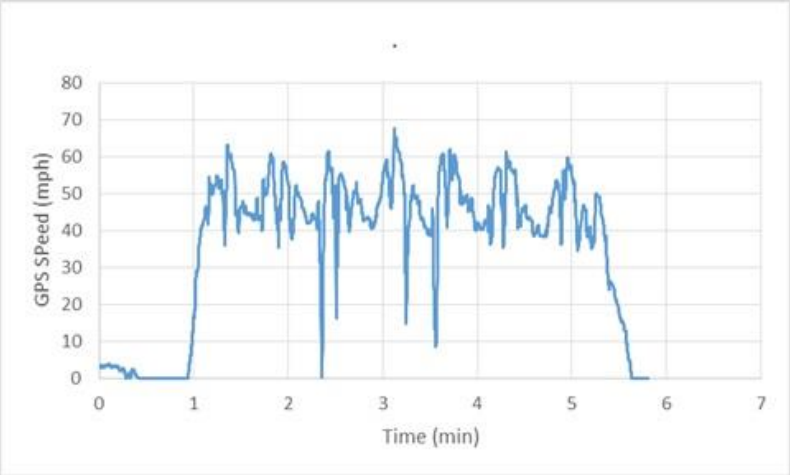

Figure 8.3: GPS speed during mission 1 using Neu 1110 motor

Mission 2

Mission 2 flies a 5-lb payload in addition to the aircraft's empty weight. Important parameters that needed to be recorded and monitored were the accelerations along the yaw axis, and propeller RPM during takeoff and cruise. The plane had a safety factor of 5 G's when being designed and built.

For accelerations, the G-Force expander was used to record the accelerations during takeoff, cruise, 180° turns, 360° turns, and landing. For mission 2, average acceleration experienced was 1.5-2 G's. The max occurred during landing at 2.6 G's.

Propeller rpm is calculated by measuring the motor rpm with a brushless rpm sensor and using the gearbox ratio. Considering the rpm measured from the propeller is important because it indicates the thrust that was produced by the propulsion system. The aircraft during mission 2 will have the heaviest payload when comparing to the rest.

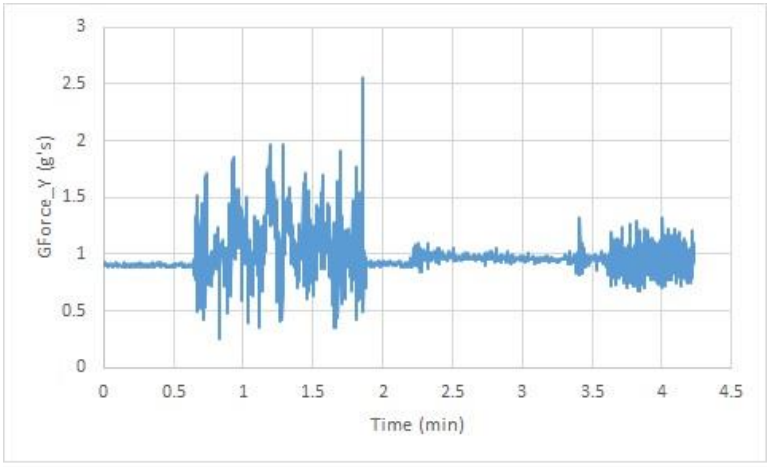

Figure 8.4: Accelerations along yaw axis during mission 2 using Neu 1105 motor

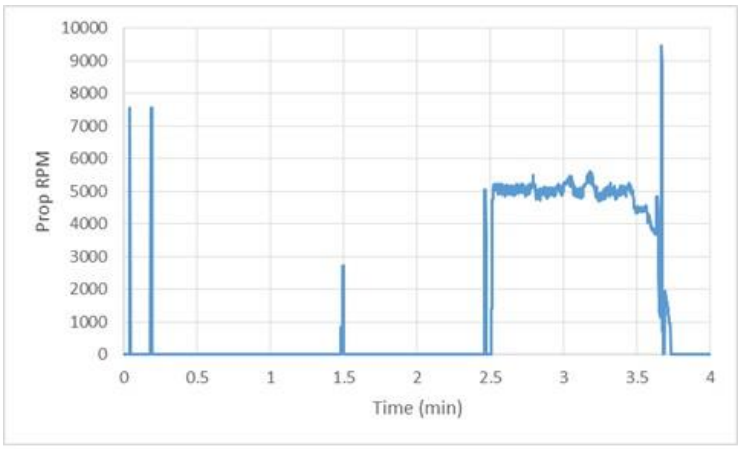

Figure 8. 5: Propeller RPM during mission 2 using Neu 1105 motor

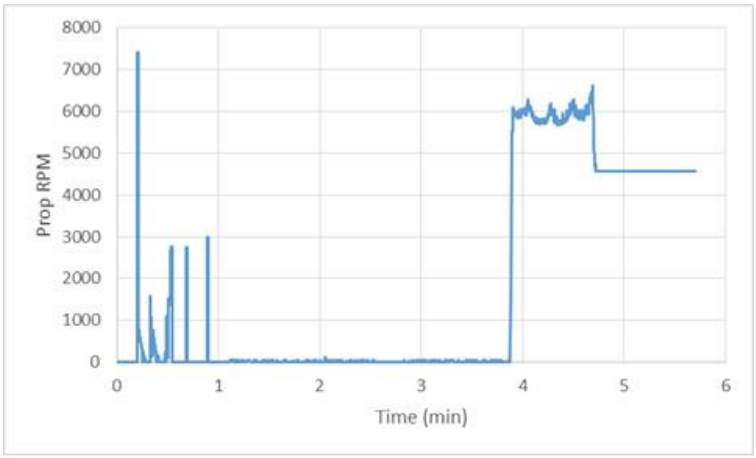

Figure 8. 6: Propeller RPM during mission 2 using Neu 1110 motor

Mission 3

Importance was focused on cumulative milliamp-hour to determine energy consumption throughout the final mission, the payload drop off. The longer the flight is with consecutive single ball drops per lap, the more points awarded. Aircraft had a cruise speed of 44 mph to optimize battery consumption and experienced average accelerations of 2.8 G's. To release the ball, our pilot had to maneuver full down elevator and then full up elevator to actuate the payload release system. This maneuver caused the aircraft to experience 3-3.5G's.

The Neu 1110 motor had excess energy in comparison to the Neu 1105 motor according to the graph below.

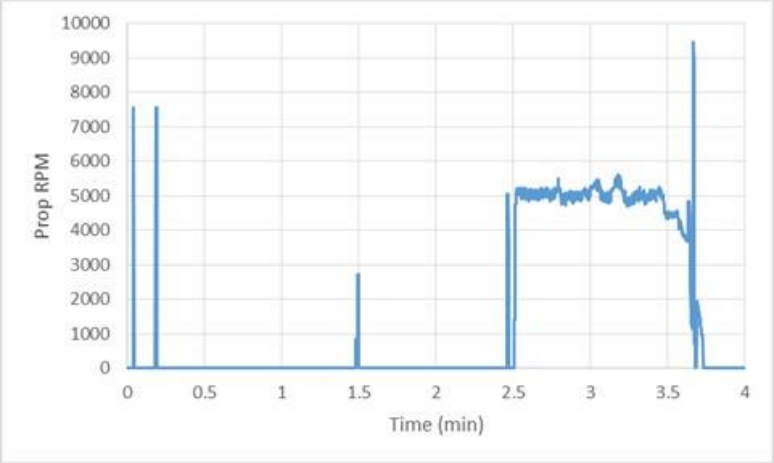

Figure 8. 7: Cumulative mAh during mission 3 using 1105 Neu motor

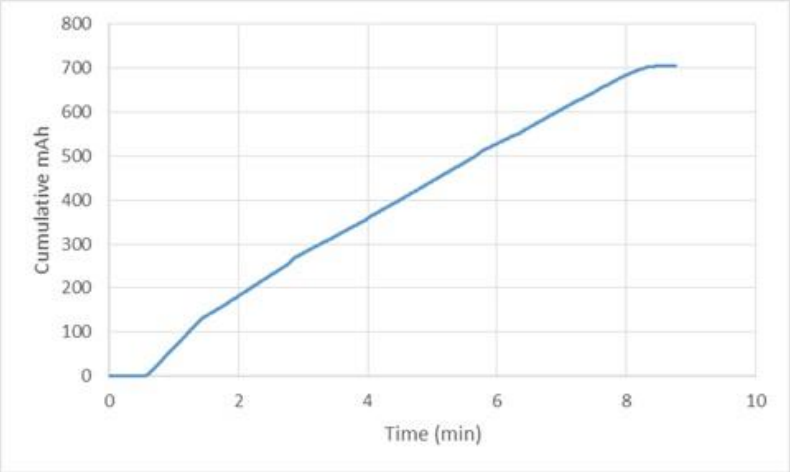

Figure 8. 8: Cumulative mAh during mission 3 using 1110 motor

Flight Pattern

GPS data log of flight pattern shown in Figure

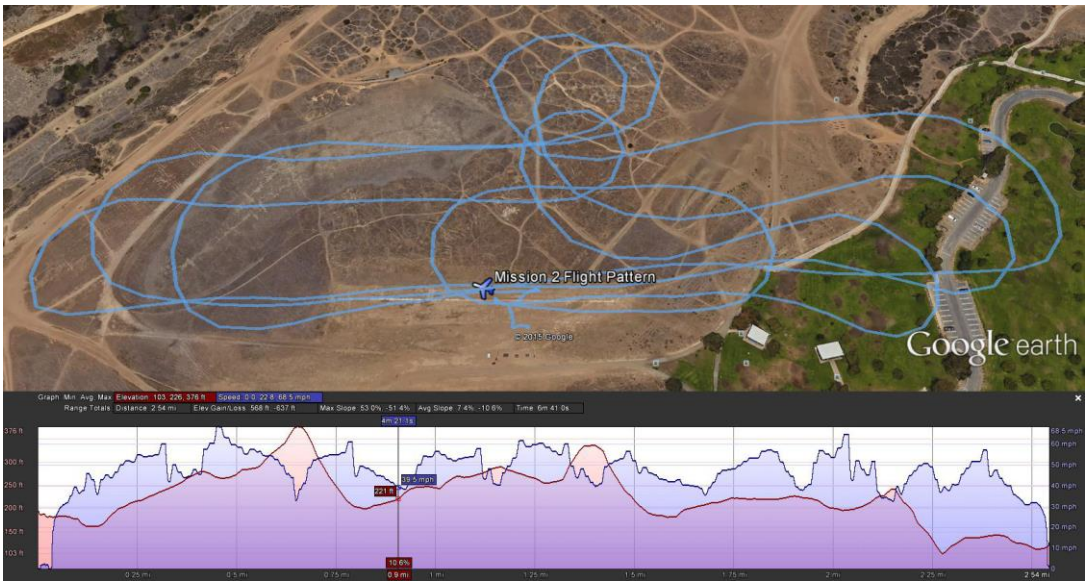

Figure 8. 9: Prototype Flight via Google Earth

Figure 8. 10: Prototype 2 in Flight

9.0 References

[1] “AIAA Design/Build/Fly Competition - 2014/2015 Rules”, 31 Oct. 2014, <http://www.aiaadbf.org/>.

[2] Drela, Mark & Harold Youngren. Athena Vortex Lattice, v. 3.27. Computer Software. MIT, 2008.

[3] Foster, Tyler M. Dynamic Stability and Handling Qualities of Small Unmanned-Aerial-Vehicles, Brigham Young University, April 2005.

[4] MichaelS. Selig, J. J. (1995). Summary of Low-Speed Airfoil Data. Virginia Beach: SoarTech Publications.

[5] MIL-F-8785C. Military Specification: Flying Qualities of Piloted Airplanes, November 1980.

[6] M.V. Cook. Flight Dynamics Principles, Reprinted 2008

[7] Simmons, M. (2000). Model Aircraft Aerodynamics. Chris Lloyd Sales & Marketing.

[8] Shevell, Richard. Fundamentals of Flight. 2nd Edition. Prentice Hall. 1988.

[9] Drela Mark. XFoil Subsonic Airfoil Development System. 28 January. 2012

[10] Page, Mark. Airplane Design. 2nd Edition. 2002.

[11] Hoerner, Sighard F. Fluid – Dynamic Drag. Great Britain. 1965

UC IRVINE DESIGN/BUILD/FLY

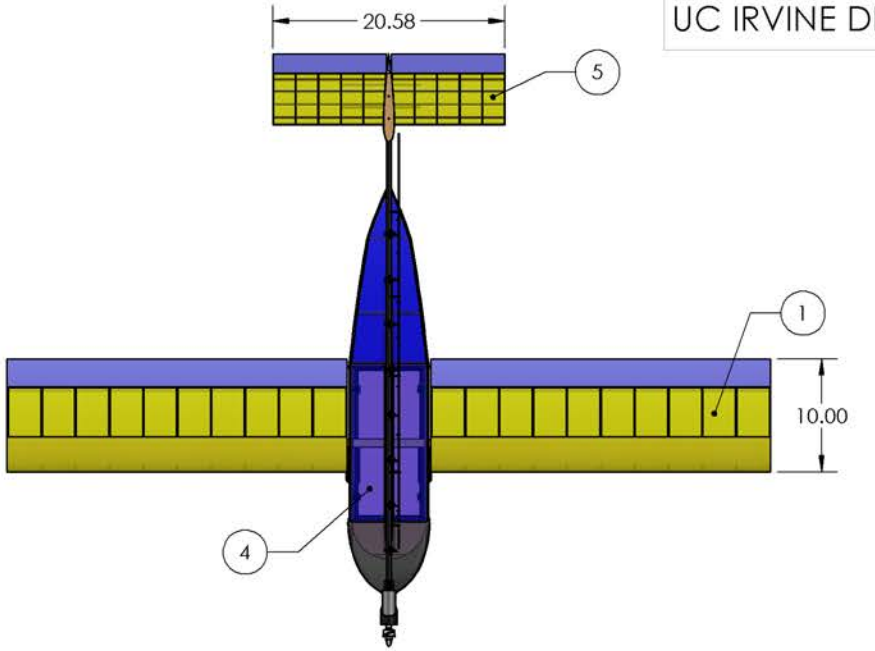

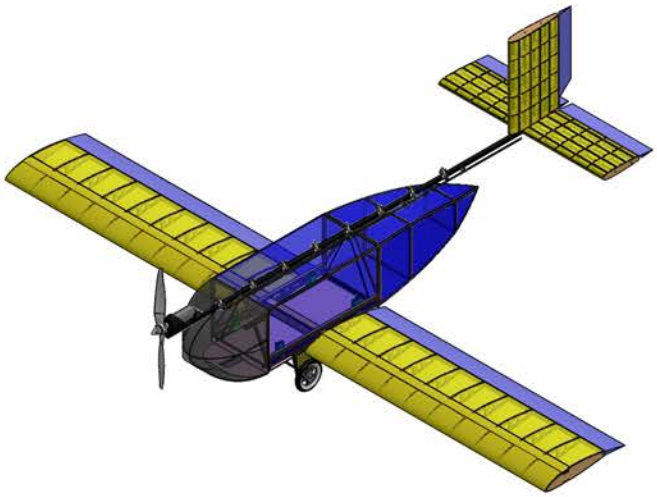

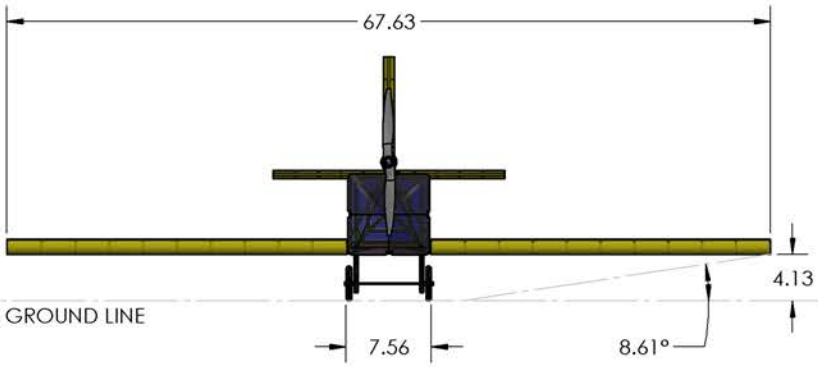

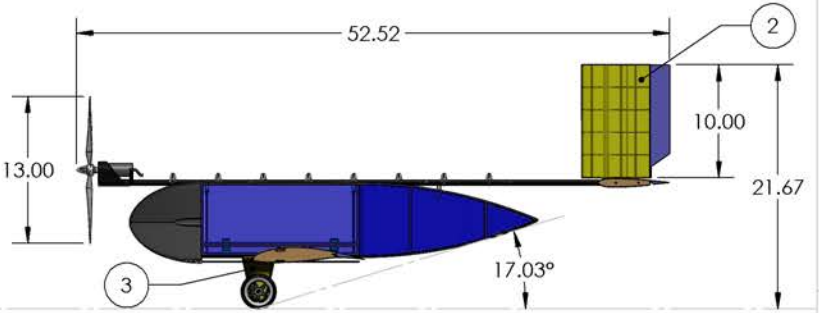

ITEM NO.	NAME
1	WING ASSEMBLY
2	VERTICAL STABILIZER
3	LANDING GEAR
4	FUSELAGE
5	HORIZONTAL STABILIZER

UNLESS OTHERWISE SPECIFIED:
DIMENSIONS ARE IN INCHES
TOLERANCES:
ANGULAR: BEND ± .5°
ONE PLACE DECIMAL ±.100
TWO PLACE DECIMAL ±.030
THREE PLACE DECIMAL ±.005

SAMUELI

	NAME	DATE
DRAWN BY:	A. HE	2/21/2015
CHECKED BY:	A. KWOK	2/22/2015
CHIEF ENGINEER:	C. POBLETE	2/22/2015

UNIVERSITY OF CALIFORNIA IRVINE

CESSNA-RAYTHEON-DESIGN/BUILD/FLY 2014-2015

DOCUMENT TITLE: AIRCRAFT 3-VIEW

SIZE B | APPROVAL DATE: 2015-02-22 | REPORT TITLE: DRAWING PACKAGE | REV NC

SCALE: 1:11 | PAGE 1 OF 5

Buzz Killington

AIAA Design/Build/Fly
2013-2014
Design Report

Georgia Institute of Technology®

TABLE OF CONTENTS

ACRONYMS AND NOMENCLATURE

C.G.	–	Center of Gravity
RAC	–	Rated Aircraft Cost
TFS	–	Total Flight Score
GS	--	Ground Score
EW	–	Empty Weight
TMS	–	Total Mission Score
M1	–	Mission One
M2	–	Mission Two
M3	–	Mission Three
FOM	–	Figures of Merit
FS	–	Flight Score
TOFL	–	Takeoff Field Length
s_g	–	Takeoff Roll Distance
NiCad	–	Nickel-Cadmium
NiMH	–	Nickel-Metal Hydride
AVL	–	Athena Vortex-Lattice
$\tilde{C}_L$	–	Airfoil Section Lift Coefficient
$\tilde{C}_D$	–	Airfoil Section Drag Coefficient
$\tilde{C}_m$	–	Airfoil Section Moment Coefficient
C_L	–	Aircraft Lift Coefficient
C_D	–	Aircraft Drag Coefficient
C_f	–	Skin Friction Coefficient
C_Y	–	Aircraft Side Force Coefficient
C_n	–	Aircraft Yawing Moment Coefficient
C_m	–	Aircraft Pitching Moment Coefficient
C_l	–	Aircraft Rolling Moment Coefficient
$C_{D,i}$	–	Aircraft Induced Drag Coefficient
$C_{D,0}$	–	Aircraft Zero-Lift Drag Coefficient
L’	–	Wing Thickness Location Parameter
e	–	Oswald Efficiency
P	–	Power
S	–	Area
Kv	–	Motor Voltage Constant (V)
K_D	–	Wing Loading Dissipative Constant
K_T	–	Thrust Loading Dissipative Constant
K_A	–	Regressive Constant
$\dot{x}$	–	Position Derivative with respect to time
V	–	Velocity
$\dot{V}$	--	Velocity Derivative with respect to time
m	–	mass
T	–	Thrust
D	–	Drag
$\bar{p}$	–	Dimensionless Rolling Rate
$\bar{q}$	–	Dimensionless Pitching Rate
$\bar{r}$	–	Dimensionless Yawing Rate
AR	–	Aspect Ratio
R_e	–	Reynolds Number
R_T	–	Taper Ratio
S_w	–	Wing Area (ft^2)
T_S	–	Settling Time (s)
ρ	–	Density
T_d	–	Doubling Time (s)
W	–	Weight, lbs
α	–	Angle of Attack (degrees)
β	–	Sideslip Angle (degrees)
μ_r	–	Rolling Coefficient of Friction
R_{ls}	–	Wing Sweep
R_{wf}	–	Wing Fuselage Interference

1. EXECUTIVE SUMMARY

This report details the design, testing, and manufacturing of the Georgia Institute of Technology *Buzz Killington* entry in the 2014-2015 AIAA Design/Build/Fly (DBF) competition. This aircraft was designed to successfully complete four tasks: a speed loading mission and three flight missions. The first flight mission consists of a high speed ferry flight with no payload. The second mission models the delivery of a sensor package and tests the maximum load capabilities of the aircraft by carrying a five pound payload internally through three laps. The third mission is a drop mission where a number of balls have to be carried externally and dropped one by one every lap.

1.1 Design Process

The primary objective for *Buzz Killington* is victory. This is achieved through the development of a light, fast aircraft that maximizes the flight score. Conceptual design of a winning aircraft began by translating the key mission requirements and scoring criteria into design requirements. These design requirements were used to determine an aircraft configuration that maximized the total flight score. The configuration was further defined in the preliminary design phase by comparing different motors, batteries, and propellers to achieve the required propulsion for the designed aircraft. Weight, drag, and aerodynamic coefficients were calculated and introduced into a flight simulation environment that estimated mission performance. The team used this data to conduct trade studies of wing loading, the propulsion system, payload capability, and takeoff distance to estimate the aircraft's maximum flight score. *Buzz Killington* then completed a detailed design by finalizing all dimensions, propulsion system components, and methods for component integration.

1.2 Key Mission Requirements and Design Features

A successful system design and score arise from the successful balance of key mission requirements. Specific design requirements were developed for each mission requirement and scoring element to maximize system performance and the overall competition score.

Empty Weight: The aircraft's empty weight is a significant driver of total score. Empty weight is comprised of the weight of the airframe and propulsion system. The entire aircraft was designed to be as minimalistic as possible without compromising the ability to complete all three flight missions. This was accomplished by determining the most efficient combination of airframe structure and propulsion system.

Number of Servos: The final flight score is inversely proportional to the number of servos on the aircraft. This competition defines a servo as any mechanical or electronic device used to control the airplane or payload release mechanism. Achieving the maximum flight score requires using the minimum number of servos required to control the aircraft. Various control surface configurations and drop mechanisms were analyzed to achieve the minimum number of servos.

Payload Requirement: Two of the three missions require the aircraft to carry a payload. Mission 2 (M2) requires a payload of five pounds to be carried internally. The access hatch for the internal payload must be easily accessible as this has a direct influence on the ground mission score. Mission 3 (M3) requires a number of balls to be carried externally. The number of balls carried in M3 has a large influence on the mission score, and define the number of laps required for the mission. The aircraft is designed to carry eight balls for M3.

Flight Time: Mission 1 (M1) requires that the aircraft complete as many laps along the designated flight path as possible within four minutes to maximize score, while M3 requires the aircraft to complete as many laps as the number of balls carried. For this reason, the propulsion system was designed to complete as many laps as balls carried while sustaining near full-throttle flight for the entire duration of the four minutes and minimizing propulsion system weight.

1.3 Performance Capabilities of the System

All of the specific design features created to maximize the performance of the system can be summarized by the following performance capabilities:

- Empty weight of 3 lbs.
- Reliable takeoff within 50 feet
- Four minute high-speed endurance
- Eight lap capability for M1
- 120 second flight time for M2
- Eight ball external capacity for M3
- Payload assembly in under 28 seconds
- Secure storage of required payloads
- Proven capability through two prototypes and seventeen test flights as shown in Figure 1.1
- Estimated RAC of 9.21 and a final score of 1.06

Figure 1.1: Aircraft in flight.

The final design was a conventional aircraft configuration with a low-wing placement, single motor, and tricycle gear. The aircraft was designed to simultaneously minimize weight, size, payload loading/unloading time, and takeoff distance, while maximizing speed and payload capabilities. The propulsion system was designed to provide enough power to fulfill ambitious performance characteristics, but weigh as little as possible. The aircraft's architecture and testing built on the teams' previous experience while continuing to push the envelope of practical, minimalistic design processes. *Buzz Killington* is confident that this design solution has been optimized to best accommodate all performance requirements and maximize total score.

2. MANAGEMENT SUMMARY

The *Buzz Killington* team consisted of twenty-six students: one graduate student, eight seniors, six juniors, three sophomores, and eight freshmen. Seventeen of the twenty-six students were returning members from the 2013-2014 Georgia Tech DBF entry. This team combines the right amount of manpower with the continued advantage of having a core of experienced members returning to build the team's knowledgebase and pass it on to newer members.

2.1 Team Organization

Buzz Killington used a hierarchal structure to establish leadership and responsibility amongst its senior members, where responsibilities flow down to the team's newer members. This hierarchy served as an outline only, as all team members collaborated extensively to reach deadlines, share ideas, learn various disciplines, and produce a more successful aircraft. The work was divided during the design phase into CAD and Structures, Aerodynamics, Electrical and Propulsion, Payload, and Manufacturing. During construction, testing, and report writing, all team members participated fully. Figure 2.1 shows the different positions and the roles of each member of the team.

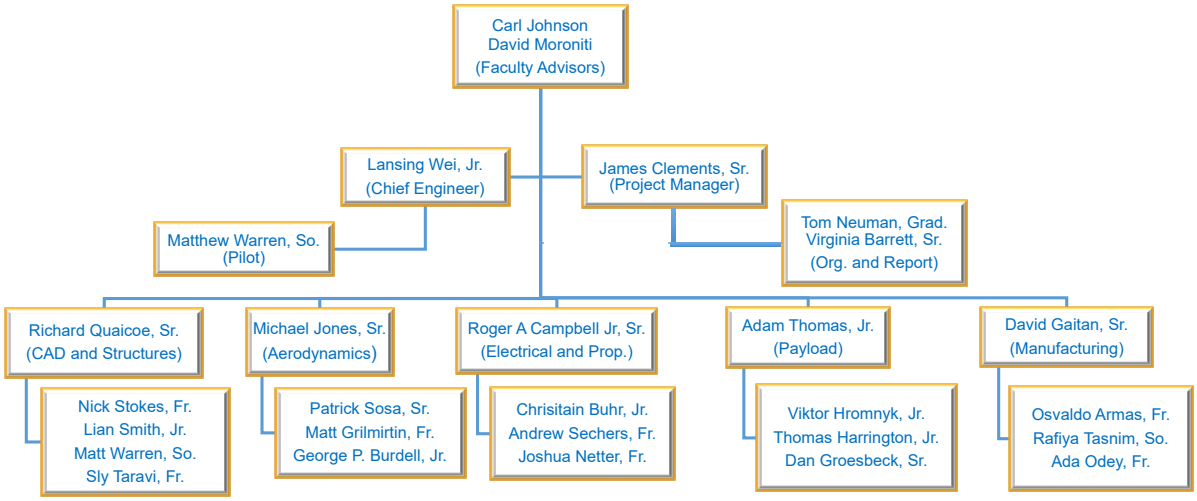

Figure 2.1: Organization chart.

2.2 Milestone Chart

A milestone chart was established at the beginning of the design process to capture major deadlines and design and manufacturing goals. Progress was monitored by team leaders to ensure all major milestones were met. The team worked throughout the entire academic year and established stringent deadlines early to gain testing and flight experience before the competition in April. The team met frequently with the faculty advisors to discuss progress. The milestone chart is shown below in Figure 2.2, capturing planned and actual timing of major events.

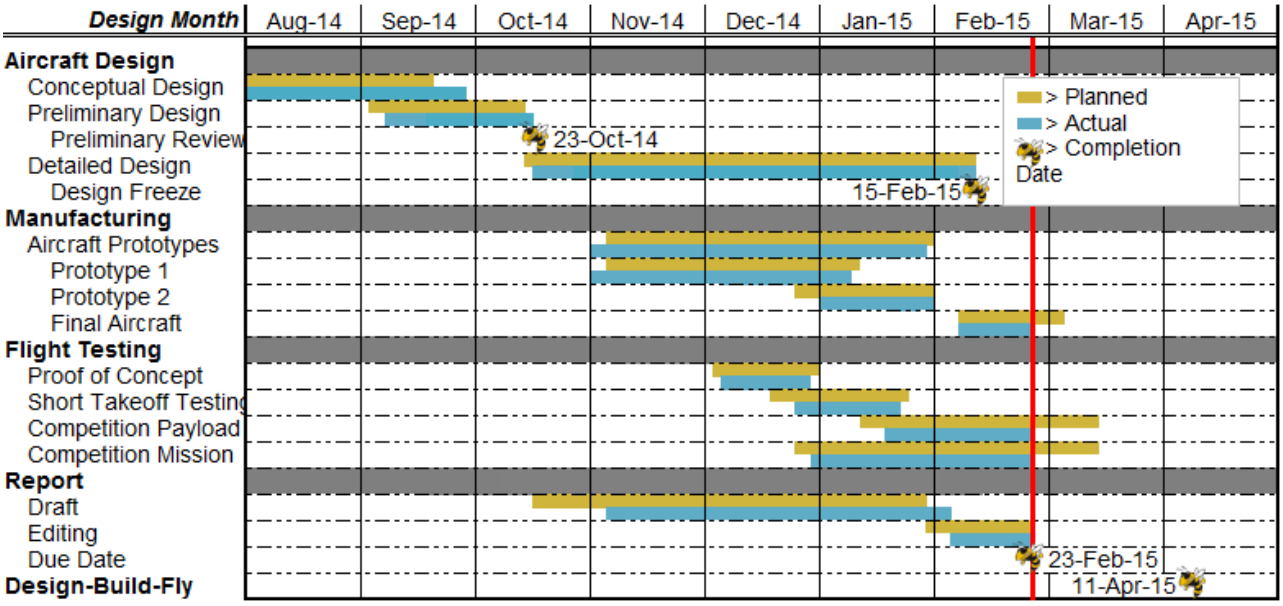

Figure 2.2: Aircraft design milestone chart showing planned and actual objective timings – major deadlines are marked by Buzz, Georgia Tech's mascot.

3. CONCEPTUAL DESIGN

The conceptual design phase was used to evaluate the competition rules, translate them into design metrics, and produce a feasible design configuration that maximized score. The team performed a quantitative scoring analysis in order to pinpoint key scoring drivers. In combination with the mission requirements, characteristics for a successful aircraft were derived. These were translated into Figures of Merit (FOMs), a metric applied to weigh different design choices against each other. The FOMs were applied to a design space of 41,472 possible aircraft configurations and yielded a single conceptual design that *Buzz Killington* is confident will be the best aircraft. The resulting configuration is a conventional airplane with tricycle landing gear, a low wing, and a single engine.

3.1 Mission Requirements

3.1.1 Mission and Score Summary

The AIAA Design/Build/Fly 2014/2015 competition consists of a ground payload loading mission, three flight missions and a design report. The total score for each team is calculated as shown in Equation 3.1:

$$Score = Written\ Report\ Score \times (TMS/RAC) \tag{3.1}$$

Where *TMS* stands for the Total Mission Score from all three missions, calculated using Equation 3.2:

$$TMS = GS \times (M1 + M2 + M3) \tag{3.2}$$

The flight score (FS) is the sum of M1, M2, and M3 scores, which are explained further below. GS is the score gained from payload loading. RAC, or Rated Aircraft Cost, is a term describing the highest empty weight (EW) of the aircraft in any of the flight missions multiplied by the number of servos (N_{servo}) and is seen in Equation 3.3 and Equation 3.4:

$$RAC = EW * N_{servo} \tag{3.3}$$

$$EW = Max(EW1, EW2, EW3) \tag{3.4}$$

Equations 3.1 through 3.4 show that empty weight and number of servos are the main score drivers, whereas various performance points of the design affect only the flight scores.

The ground mission will take place before any flying mission. The GS is driven by the loading time. For a rapid loading time, the aircraft must have an easily accessible payload bay to load M2 payload as well as a system to quickly accept balls for M3. The loading time is measured in two sections: the time required to load the payload for M2 and secure the aircraft, and the time required to remove the M2 payload and then load the M3 payload. The sum of these sections is the total loading time. The final ground score is the ratio of the fastest loading time in the competition to the loading time of the team, as shown in Equation 3.5. The ground mission must be completed in 5 minutes or a score of 0.2 is used for intermediate scoring calculations. Once the ground mission is completed, the flight missions commence.

$$GS = \left\{ \begin{matrix} 0.2 \; if \; incomplete \\ \frac{Fastest \; Loading \; Time}{Loading \; Time} \; If \; complete \end{matrix} \right\} \tag{3.5}$$

All flight missions are flown along the same distance and pattern per lap. For flight missions, the individual portions of the flight pattern seen in Figure 3.1 are as follows:

1. Successful Takeoff within 60 ft.
2. Climb to Safe Altitude
3. 180º U-turn, 500 ft. Upwind from the Start/Finish Line
4. 1000 ft. Downwind
5. 360º Turn Along the Backstretch
6. 180º U-turn
7. 500 ft. Final with a Successful Landing

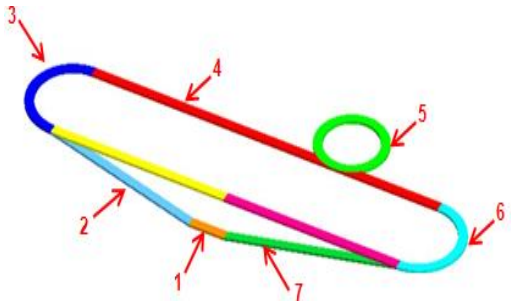

Figure 3.1: Competition flight course.

Each lap is at least 2000 ft. long, or roughly 2500 ft. when accounting for the three turns involved. A complete successful lap is defined as beginning and ending at the start/finish line while still in the air. The required number of laps is defined by the mission.

Mission 1 Ferry Flight: The aircraft must take off within the designated field length and fly as many laps as possible in 4 minutes. Time starts when the aircraft is throttled up and a lap is complete when the aircraft passes the start/finish line. The score is determined by dividing the number of laps for each team by the maximum number of laps completed by any team flying M1 and multiplying by 2, as seen in Equation 3.6:

$$M1 = 2 \times \frac{Number\ of\ Laps}{Maximum\ Numberof\ Laps} \tag{3.6}$$

Mission 2 Maximum Load: The aircraft must take off in the designated field length, complete three laps carrying wooden blocks in as little time as possible, and then land successfully. The dimensions and weight of the blocks are detailed in Table 3.1. The blocks are required to be secured to prevent in-flight shift. The scoring of M2 is shown in Equation 3.7:

$$M2 = 4 \times \frac{Fastest\ Time\ Flown}{Time\ Flown} \tag{3.7}$$

Table 3.1: Payload composition for Mission 2.

Payload	Size				Number Carried
	Length	Width	Height	Weight (lbs)	
Wooden Blocks	10”	5.5”	1.5”	~1.6	3

Mission 3: Sensor Drop Mission: The aircraft must take off in the designated field length. The external payload is a team-selected number of Champro 12" Plastic Balls. The size and dimensions of the balls are listed in Table 3.2. On each lap, while airborne, the aircraft will remotely drop a single ball. Each drop will occur within a drop zone on the upwind leg of the lap. If more than one ball is dropped in one lap, that lap will be invalidated.

Table 3.2: Payload composition for Mission 3.

Payload	Size				Number Carried
	Length	Width	Height	Weight (lbs)	
12” Champro Balls	3.8”	3.8”	3.8”	~0.1	Team Determined

The score is computed by the number of team laps flown divided by maximum number of laps flown by any team as shown in Equation 3.8:

$$M3 = 6 \times \frac{Number\ of\ Laps\ Flown}{Maximum\ Number\ of\ Laps\ Flown} \tag{3.8}$$

3.1.2 Aircraft Constraints

The competition rules stipulate specific constraints on the aircraft's takeoff distance, propulsion system, and payload:

Takeoff Distance: The aircraft must have the ability to start and take off completely within a 60 foot runway for all three flight missions.

Propulsion System: The aircraft must be propeller driven and electrically powered, with all components of the propulsion system commercially available. These include the motor, propeller, speed controllers, receivers, and batteries. The battery selection is limited to NiCad or NiMH, but may be of any cell count, voltage, or capacity. The entire propulsion battery may weigh no more than 2.0 lbs and must be armed by an external safety plug or fuse. The arming device must be mounted on the exterior of the aircraft and must be accessible from behind in a tractor propeller configuration.

Payload: The aircraft's wooden block payload must be stored internal to the aircraft, and the ball payload must be secured externally and be dropped only due to pilot command. All payloads must be securely fastened to the aircraft's structure so that they do not shift or come loose during flight.

3.1.3 Flight Score Sensitivity Analysis

A sensitivity analysis on the flight scoring drivers was performed to understand the design trades and mission objectives that maximize the flight score (FS) as divided by the empty weight (EW). A conventional sensitivity analysis entails plotting scoring drivers, such as weight or speed, on multiple axes and visualizing the effect on score to determine the maximum. This analysis would show how speed and weight trade in terms of points, and indicate that the aircraft should be as light and fast as possible. In reality, speed and weight are strongly correlated, and it is unlikely for the fastest aircraft to also be the lightest due to a heavy propulsion system. It is also possible for the optimum design to be neither the lightest nor the fastest, but the optimum point is not known when physical aircraft parameters are varied independently. Another deficiency of the conventional scoring analysis is that the team is left to guess the best possible lap count, speed, and ball count for the three missions, since the team's score depends on other aircraft. In all, a conventional scoring analysis does not inform realistic design tradeoffs or scoring goals, therefore, the team sought a more detailed, physics-based approach to the scoring analysis.

Aircraft weight and speed are the main factors that affect flight score, but they cannot be varied independently as described previously. By contrast, aircraft size and propulsion system power are independent design parameters and govern the weight and speed. These two design parameters were varied by two parameters. These two parameters were (1) wing area, assuming a baseline fuselage size required for the M2 payload, and (2) number of battery cells, assuming propulsion power is governed by

the cell count. Aircraft weight and performance were then calculated as functions of the wing area and cell count using the procedure detailed below.

Empty Weight: The aircraft empty weight was divided into propulsion and structural components. The propulsion system weight is proportional to the number of battery cells used. Based on previous team experience, 1,500 mAh NiMH cells were selected as representative batteries, weighing 0.05 lbs each. To fly for four minutes during M1, the average current draw cannot exceed 22 amps without draining the batteries. The electric motor weight was estimated at 0.5 lbs / kW from past experience, and speed controllers that met the pack voltage were cataloged. The propulsion weight assessment is summarized by Equations 3.9-10:

$$P_{electric} = n_{cells}\left(1.2\frac{V}{cell} \times 20amps\right) \tag{3.9}$$

$$W_{propulsion} = n_{cells}\left(0.05\frac{lbs}{cell}\right) + P_{electric}\left(0.5\frac{lbs}{kW}\right) + W_{ESC} \tag{3.10}$$

Structural weight was estimated using the team's experience, with a baseline minimum weight which increases with wing area. The coefficients K_A and K_B in Equation 3.11 were adjusted to match past years' Design/Build/Fly planes, and Equation 3.12 summarizes the empty weight assessment:

$$W_{struct} = W_{baseline} + K_A\left(S_{wing} - S_{baseline}\right)^{K_B} \tag{3.11}$$

$$EW = W_{struct} + W_{propulsion} \tag{3.12}$$

Mission 1 and 2 Speed: The number of laps for M1 and the time to complete 3 laps for M2 were estimated based on the aircraft's maximum velocity and 2,500 ft lap lengths. The maximum speed was calculated using simple power-required calculations that stem from the drag polar, and the power-available from the propulsion system, as seen in Equation 3.13. Lap numbers were truncated down, since only integer numbers of laps count towards the score.

$$P_{req} - P_{av} = \left(\frac{1}{2}\rho V_{max}^3 S C_{D,0} + \frac{2W}{\rho V_{max} S \pi A R e}\right) - P_{electric}\eta_{prop} = 0 \tag{3.13}$$

Mission 2 Takeoff: Aircraft must be able to take off with the 5 lbs payload within 60 ft to receive an M2 score and advance to M3. This constraint was important because it eliminated infeasible designs that have too little wing area or power to take off. The takeoff constraint was solved for a given wing area and power level, with the governing relation shown in Equation 3.14. The K_D term is a function of dissipative forces and wing loading (W/S), while K_T is a function of propulsive forces and thrust loading (T/W).

$$s_g = \frac{1}{2gK_D} + \ln\left(1 + \frac{K_D}{K_T}V_{LO}^2\right) \leq 60\ feet \tag{3.14}$$

Mission 3: The number of balls carried for M3 dictates the number of laps flown, since only one ball can be dropped during a single lap. However, the team could not select a number of balls (laps) that would exceed the aircraft's maximum range. It was assumed that the vehicle would operate near maximum L/D to maximize range since there is no time limit for M3. The one-ounce balls were added to the aircraft weight to affect the range and also ensure the aircraft can still take off according to Equation

3.14 above. The propulsion energy available from the batteries dictates the range, so the total energy was calculated from the system efficiency (η) and battery ratings as seen in Equation 3.15. Finally, the maximum number of laps was calculated according to Equation 3.16.

$$E_{av} = \eta_{total}\left[n_{cells} \times 1.2\frac{V}{cell} \times \left(0.90_{maximum\ discharge} \times 1500mAh\right)\right] \quad (3.15)$$

$$Maximum\ M3\ Laps = \frac{E_{av}\left(L/D\right)_{max}}{2500ft \times (EW + n_{balls} \times 1oz)} \quad (3.16)$$

The physics-based analysis revealed that neither takeoff nor maximum range constrain the balls to a practical number that could be loaded quickly and fit on the aircraft, so the ball count objective was chosen using the sensitivities in the next report section. This means that the aircraft design point and objectives for M1 and M2 are mostly independent of M3. As a result, the scoring sensitivity in Figure 3.2 below only shows the flight score from M1 and M2 divided by empty weight. The scores seen in the figure depend on the best-performing aircraft resulting from the simulation: 9 laps in M1 and 93 seconds in M2. The plot represents a physics-based tradeoff between speed and aircraft weight, as governed by wing area and battery count.

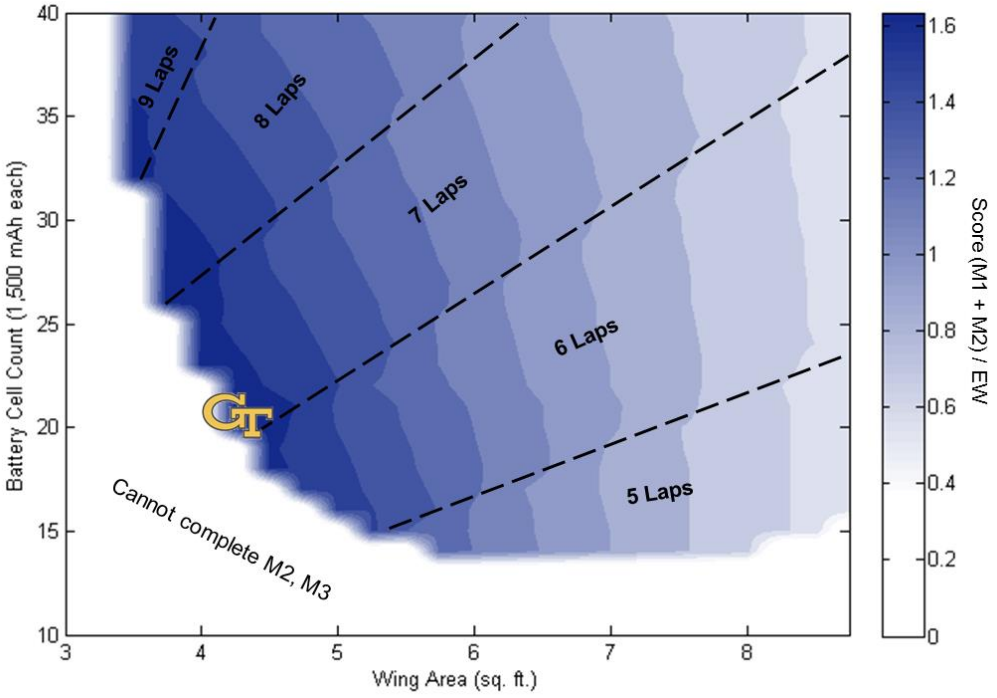

Figure 3.2: A physics-based scoring analysis of the design space for Missions 1 and 2. The team's chosen conceptual design point is noted by the Georgia Tech logo.

Aircraft that could not complete M2 and advance to M3 were assigned a score of zero. In general, smaller and more powerful aircraft are capable of faster flight and thus have higher scores for M1 and M2, but these designs suffer when normalized by EW. Inside of each Lap region, the best-scoring design is

typically the smallest and lightest one and can take off with the M2 payload. Figure 3.2 demonstrates that the highest scoring-potential design must complete 7 laps in M1, have a roughly 2-minute flight in M2, and weigh less than 3 lbs with the best balance of wing area and propulsion system. This was the conceptual design point choice for the team. The optimal design is neither the lightest nor the fastest but represents a good combination of weight and speed, as hypothesized prior to the physics-based analysis.

It should be noted that the analysis performed for this study was simplified, and the boundaries defining laps and ability to complete M2 are not exact. The weight estimates, wing area sizing, and propulsion system selection were also simplified. Therefore, the results were used to realistically assess the scoring space and guide the team's design and objectives, with the aircraft design and sizing pending further refinement and analysis during Preliminary Design.

3.1.4 Ground Score Sensitivity Analysis

The physics-based analysis of the missions indicated that the battery endurance and takeoff do not constrain the number of balls carried in Mission 3. The team decided that a practical volumetric constraint is 10 balls, beyond which the external payload restraint would become too cumbersome and approach the size of the entire aircraft. The best number of balls to carry was determined using two important scoring aspects that could not be modeled in the physics-based method: the number of servos and the loading time.

Number of Servos: The minimum number of servos for safe flight is three: the motor's ESC, the elevator, and either a rudder or ailerons. An additional servo can be added for the payload release mechanism. The addition makes triggering the ball release more straightforward than having to connect a flight servo to the release; however, as the score is divided by the number of servos, the GS would have to be offset by faster loading time.

Loading Time: The loading procedure includes both M2 and M3 payloads. Each payload type has to be loaded and timed separately, with the process also including some time to shuttle back and forth to the aircraft. The team estimated the minimum time for each shuttle and brief loading to be 6 seconds, resulting in a baseline minimum loading time of 12 seconds. Loading time is likely to increase if the team elects to carry more balls, but the additional loading time could be offset by a higher M3 score.

The tradeoff between loading time, number of balls, and number of servos needed to be quantified before significant detail was known about the ball loading mechanism. As a result, the loading time was calculated by simply assigning an average loading time per ball, multiplying by the number of balls, and adding the ball loading time to the baseline time of 12 seconds. The total effect on the score is shown in Figure 3.3 below. The sensitivity analysis shows a distinct break in the scoring at 1.5 seconds per ball: the team should carry as many balls as possible if the average time is faster, or carry only one ball if the

average time is slower. For an equivalent aircraft weight, adding a servo can only be justified if it is 1.0 seconds faster per ball, otherwise the decrease in score is substantial. A quarter-pound increase in the payload mechanism weight can only be justified if it decreases loading time by 0.5 seconds per ball.

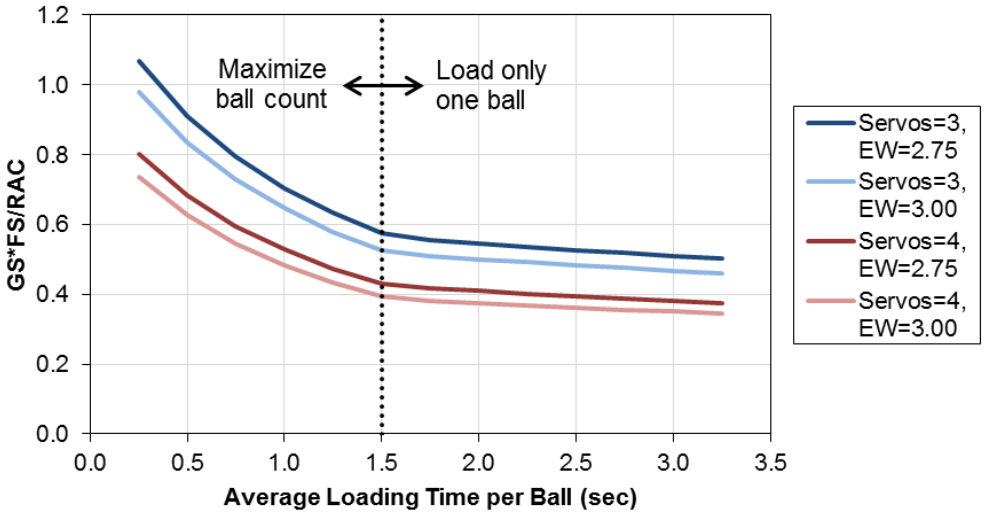

Figure 3.3: The best score obtainable for aircraft with different weights and servo counts, as a function of the average loading time per ball.

Based on this analysis, it was the team's objective to carry as many balls as possible with an average loading time less than 1.5 seconds per ball, without adding a fourth servo, and with the lightest possible external payload support. It can be seen that fast shuttling, M2 loading, and efficient ball loading can nearly double the total score. The loading time and ball capacity for M3 are the top priorities for the team because they constitute approximately two-thirds of the total score. The weight and flight performance for M1 and M2 are lower priorities, but are still critical to fielding a winning design.

3.2 Translation into Design Requirements

The scoring analysis revealed four main components that drive the overall flight score:

Loading Time: Any competitive configuration must be designed for quick loading while withstanding any stresses caused by rapid loading of the wood and balls. In addition the loading device must maximize the external payload without a significant increase in loading time. A balance must be struck between maximum external payload and minimum loading time through testing and engineering judgment.

Servo Count: A servo is defined as any mechanical or electronic device used to control the airplane or payload release mechanism. For the maximum achievable score, the servo count needs to be the absolute minimum number of servos required to control the aircraft and release the M3 payload.

Empty Weight: Any configuration that fails to be as light as possible will not be competitive. Effort must be made to reduce the aircraft empty weight. However, loading time is a critical factor in success. Such considerations must be made carefully to balance loading time and empty weight.

Speed: More flight speed leads to more M1 laps and a lower M2 time. There is also a strong correlation between the number of laps flown in M1 and the number of balls dropped in M3. Both the drag of the configuration and the useful power available via the propulsion system will impact the speed. A balance must be established since increasing power available implies increasing empty weight.

3.3 Configurations Considered

The analysis conducted in Sections 3.1 and 3.2 were translated into qualitative design metrics that were used to evaluate and select an aircraft configuration, as summarized in Table 3.3:

Table 3.3: Rules and requirements translated into design requirements.

Mission/Scoring Requirement	Design Requirement
Minimal Loading Time	High accessibility
Minimal Servo Count	Simple, Robust Design
Low Weight	Efficient Structure
High Speed	Optimized Propulsion

These requirements show that minimizing loading time is the most critical design consideration, followed closely by design simplicity. If a design has the smallest possible loading time and has the least number of servos, it is also likely to have low weight.

After determining the requirements, the next step of conceptual design was establishing a design space that considered all possible aircraft concept configurations. The matrix of alternatives contained five major categories: wings, fuselage, empennage, propulsion, and landing gear. With all component alternatives considered, the design space shown in Table 3.4 contained 41,472 different potential configurations.

Table 3.4: Complete Matrix of Alternatives.

Components	Alternatives			
Wing Layout	Flying Wing	Biplane	Conventional	Tandem Wing
Wing Attachment	Low	Middle	High	Blended
Fuselage Shape	Blended	Rounded	Circular	Square
Number of Fuselages	0	1	2	
Tail Type	V-tail	Conventional	H-Tail	T-Tail
Tail Attachment	One Boom	Two Booms	On Fuselage	
Number of Engines	1	2		
Engine Location	Pusher	Tractor	Both	
Landing Gear	Skids	Tricycle	Taildragger	

3.4 Component Weighting and Selection Process

Figures of Merit (FOM) were created based on the most important configuration factors. The FOM are shown in Table 3.5. The FOMs were assigned an importance of 0 through 5, with 5 being the most important factor and 0 being a non-factor in design.

Table 3.5: Figures of Merit.

Figure of Merit	0	1	2	3	4	5
Mission 2 Accessibility						**5**
Mission 3 Accessibility						**5**
Weight					**4**	
Drag			**2**			

To reduce the design space from all possible configurations presented in the matrix of alternatives, aircraft components were measured against each other with the relevant FOM. Each configuration was given a scoring value for each figure of merit, and that rating was then multiplied by the FOM value. The scoring values are shown in Table 3.6. The configuration with the highest total quality was then selected for further analysis in the design process.

Table 3.6: Configuration Scoring Values.

Score	Value
1	Inferior
3	Average
5	Superior

3.4.1 Aircraft Configuration

The team examined three basic configurations: a flying wing, a biplane, and a conventional monoplane as shown in Table 3.7.

Table 3.7: Aircraft configuration Figure of Merit.

		Aircraft Configurations		
				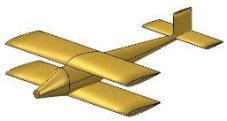
FOM	**Value**	**Conventional**	**Flying Wing**	**Biplane**
Mission 2 Accessibility	**5**	5	1	1
Mission 3 Accessibility	**5**	3	1	5
Weight	**4**	4	1	2
Power	**3**	4	3	4
Drag	**2**	4	2	2
Value	**20**	76	27	54

The biplane was deficient in Mission 2 accessibility due to the top win interfering with loading the pine blocks. The flying wing was ill suited for either Mission 2 or Mission 3 payloads due to its sensitive C.G. range and short body. The conventional monoplane configuration had the highest total score, and was therefore chosen as the basic configuration for this year's DBF competition.

3.4.2 Wing Placement

Two possible wing locations on the conventional monoplane were considered: a high wing and a low wing. These are shown in Table 3.8, below.

Table 3.8: Wing placement Figure of Merit.

		Wing Placement	
			
FOM	**Value**	**Low Wing**	**High Wing**
Mission 2 Accessibility	**5**	5	1
Mission 3 Accessibility	**5**	4	5
Weight	**4**	4	4
Total	**14**	**61**	**51**

The high wing and low wing configurations both present similar levels of structural efficiency and Mission 3 accessibility. The deciding factor is Mission 2 accessibility. The high wing configuration makes it difficult to maintain a solid wing spar and still load the wooden blocks from the top. As a result, the wing must be placed in a low wing configuration.

3.4.3 Payload Configuration

The ball payload attachment method is critical for reduction of loading time. Three possible locations were considered. The first location was under the wing along the span. However, attaching the payload at this location would increase drag and complicate the release mechanism, reducing speed and increasing loading time. The second location was underneath and along the fuselage. While this location reduces drag, the loading procedure would still be time intensive. The final location considered was on top of the fuselage. This location makes it easy to load while having as low drag as possible and was chosen for these reasons.

3.4.4 Tail Configuration

The ball attachment location above the fuselage could interfere with a conventional T-tail configuration. As a result, the two tail configurations considered were an H-tail and a V-tail, shown in Table 3.9. Both the

H-tail and V-tail move the vertical control surface away from the centerline of the vehicle, minimizing the potential for interference between the vertical surface and the top-mounted M3 payload mechanism.

Table 3.9: Tail Configuration Figure of Merit.

		Tail Configuration	
			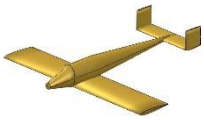
FOM	**Value**	**V-Tail**	**H-tail**
Mission 3 Accessibility	**5**	5	5
Weight	**4**	2	5
Total	**9**	**33**	**45**

Selection of a V-tail however requires the use of two servos, one per surface. When considering the requirement for the fewest number of servos, the decision between the empennage choices becomes a choice between Rudder-Elevator and Aileron-Elevator control. Consultation with the team's test pilots indicated that roll control was preferable to yaw control for minimizing lap times. Therefore, the H-tail was selected and would provide elevator control only.

3.4.5 Landing Gear Configuration

The two landing gear options for the chosen wing, tail, and fuselage combination are a tail-dragger configuration and a tricycle configuration as shown in Table 3.10.

Table 3.10: Landing gear configuration Figure of Merit.

		Landing Gear Configuration	
			
FOM	**Value**	**Tail-dragger**	**Tricycle**
Mission 2 Accessibility	**5**	3	5
Mission 3 Accessibility	**5**	3	5
Weight	**4**	5	4
Drag	**2**	5	3
Total	**16**	**60**	**72**

The tail-dragger is the lighter and has the least drag of the two options, because it allows for minimization of landing gear height. However, this configuration places the aircraft at an angle relative to the ground, which complicates loading procedure and increases loading time. As a result, the tricycle landing gear configuration was chosen.

3.4.6 Propulsion Placement

Since the number of servos includes motors, only one engine was considered. A pusher-mounted motor would interfere with the Mission 3 payload drop. Therefore, a tractor mounting was chosen.

3.5 Final Conceptual Design Configuration

The final configuration is a low wing, H-tail aircraft with a single-engine tractor propulsion system as shown in Figure 3.4. It offers minimum loading time and servo count, while allowing for greater speed by reducing drag. The empty weight of the aircraft is more heavily influenced by structural design, and is discussed later in this report.

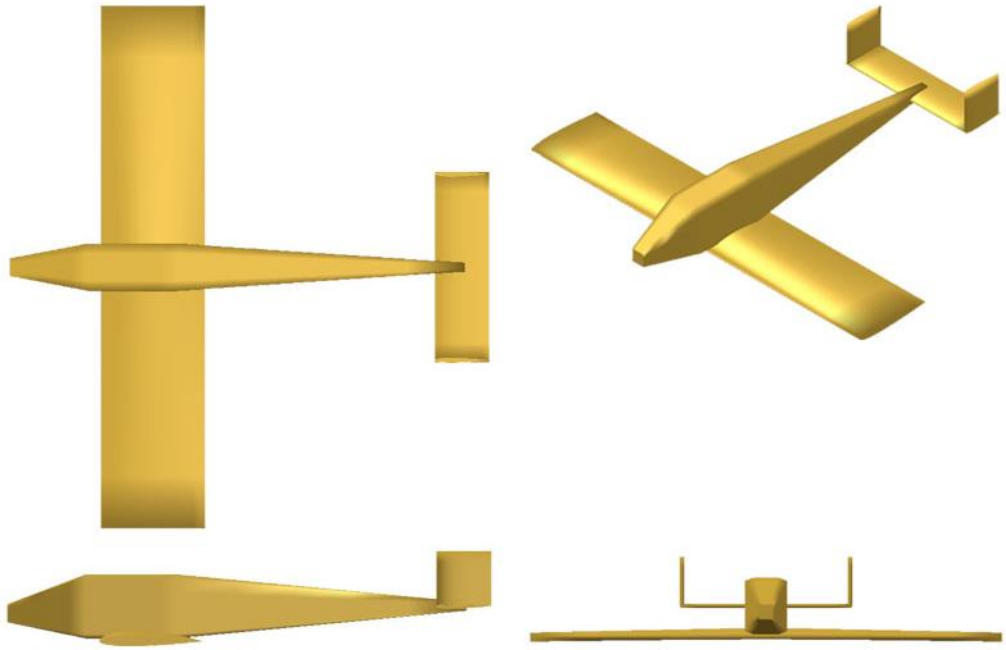

Figure 3.4: Final Configuration.

This configuration used three servos with a predicted empty weight of 2.75 pounds. This corresponds to a RAC score of 8.25. Using the assumed best capabilities of the other aircraft in the competition, this aircraft would be capable of achieving the mission scores tabulated in Table 3.11. Loading time of 1 second per ball and a total loading time of 20 seconds yields a potential TMS of 0.6836.

Table 3.11: Predicted flight scores.

Aircraft	M1	M2	M3
Buzz Killington	7	120	8
Assumed Best	10	96	10
Score	1.4	3.2	4.8

4. PRELIMINARY DESIGN

The objective of the preliminary design phase was to further narrow the design space. To do this, design/sizing trades for the system were evaluated by examining propulsion system options and wing area sizing for takeoff distance. Then weight, drag, motor, propeller and battery data, and aerodynamic coefficients were calculated and combined to estimate mission performance for all three flight missions.

4.1 Design Methodology

The *Buzz Killington* team designed the aircraft configuration using an iterative performance-focused multidisciplinary analysis. The team used constraint sizing to select a weight-normalized design point that could satisfy objectives for all three missions. From this design point, the team analyzed possible propulsion systems, aerodynamic characteristics, built the mission model, and compared them to estimates generated as part of the sizing process. After this analysis, the mission performance and stability of the sized aircraft configuration were computed. The design process detailed in sections below is written as sequential, but iterations occurred throughout, as seen in Figure 4.1. An example of iteration would be updating wing area at a constant wing-loading if propulsion weight is found to be lower, re-evaluating stability and mission performance, and re-adjusting the wing or propulsion system if needed. All iterations were performed with the ultimate goal of maximizing overall score. Therefore, the design shown in this report is the final product of a more complex, iterative procedure.

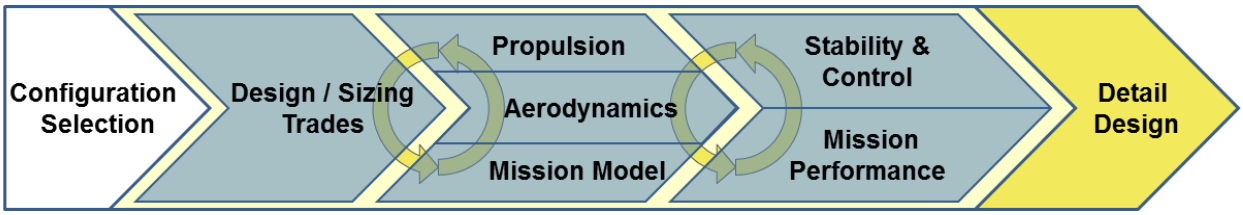

Figure 4.1: The team's preliminary design methodology highlighting multidisciplinary iterations.

4.2 Design Trades

Two trade studies were conducted to determine the size of the aircraft and the propulsion system.

4.2.1 Constraint Sizing

A constraint sizing study allowed the team to analyze the impact of changing wing area, weight, and power required on the various mission parameters to ultimately maximize the total flight score. The trends of Figure 4.2 show that for a given power to weight ratio, increasing wing loading on this graph has three effects: increases the number of achievable laps, decreases the ability to take off, and reduces lifting area. Alternately, increasing power to weight increases the number of achievable laps, increases the ability to take off, and increases the weight of the battery and propulsion system.

The sixty foot takeoff distance requirement gave the first of two lower bounds on the power to weight and wing loading plane. Desired number of laps gave the second lower bound. A takeoff distance of fifty feet

was chosen as a conservative starting point, ensuring that the aircraft would be more than able to meet the sixty feet requirement. This shorter takeoff distance requires a higher power to weight ratio and a higher wing loading. The ideal scoring point will be located close to the intersection of these two bounds without falling below either.

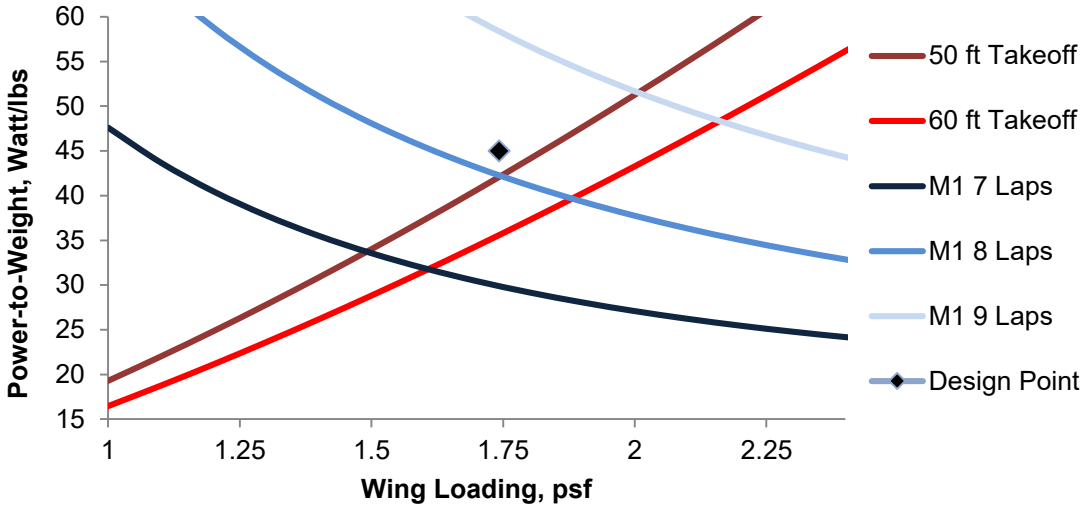

Figure 4.2: Selecting the design point from the constraint plot, marked by the point.

The design point chosen was marked on Figure 4.2. It surpasses the constraint lines for a 50-foot takeoff distance and approximately an 8 lap capability for Mission 1. The point selected has a wing loading of 1.75 psf, and a power to weight of 45 W/lb. Implied in this analysis is an assumption of flying the same number of laps in M3 as M1, since as an endurance-focused M3 can be flown slower to account for higher drag. Next, the impact of the number of laps was analyzed to maximize score. Figure 4.2 shows that the difference between 7 laps and 8 laps is fairly substantial. Choosing 8 laps instead of 7, and thus moving up along the takeoff constraint line, would increase wing loading and the power to weight ratio. The higher weight of the battery and propulsion were chosen to be acceptable because the extra power to weight would add considerable speed to the aircraft during the lightweight M1, as well as increase the performance of the plane during M2.

4.2.2 Propulsion System Selection

The process to select the best motor for the aircraft involved multiple stages. First, a motor database was created subject to several constraints. The motor constant, Kv, was limited to a low value, as a low Kv can drive a larger diameter, more efficient propeller. An upper limit on motor weight of 0.5 lb was chosen to minimize overall empty weight. The database contained over 50 motors from various companies, including Hacker, Tiger, Scorpion, Cobra and AXI.

Next, a propeller database was generated. The propellers were sorted by their pitch to diameter (P/D) ratio. Any propellers with a P/D less than 0.60 were removed from this database. This P/D ratio limit was chosen to ensure that higher thrust levels could be maintained at high speeds. MotoCalc, a commercially available motor analysis tool, was then used to estimate the motor efficiency, static thrust, and thrust at 60 mph for each motor with multiple battery and propeller combinations.

The team sorted the motor, propeller, and battery combinations by weight from least to greatest. The top ten motor combinations were chosen to undergo further testing. The top motor-battery-propeller combinations were analyzed and their variation with speed was graphed. This allowed the team to visualize how various combinations would work under different flight conditions, and to evaluate the most effective combination to meet the competition's needs given the current aircraft's capabilities.

Two motor combinations were chosen to purchase and test, as shown in Table 4.1. The former, although heavier, was selected as the primary motor because it had greater static thrust. However, both motors were purchased and extensively tested to see if the theoretical results would match the actual outcomes. Section 5.3 will go into further detail regarding these tests.

Table 4.1: Final propulsion alternatives.

Motor	Kv	Battery (Cells)	Current (Amps)	Best Propeller	Static Thrust (lb)	Propulsion System Weight (lb)
Tiger 3510-13	700	20 (2,000 mAh)	0.50	11x7	3.81	1.464
Tiger 4010-11	475	20 (1,500 mAh)	0.80	13x10	3.49	1.255

4.3 Mission Model

4.3.1 Description and Capabilities

The three missions were simulated via a set of first order differential equations (Equations 4.1-4.3) defining the position and orientation of the vehicle throughout the flight. By integrating these equations over time using a 4th Order Runge-Kutta approach in MATLAB with some simple logic defining each of the required mission segments, it is possible to define the position, velocity, and orientation of the vehicle over time. The thrust (T) was defined as a function of velocity with the relationship defined by MotoCalc, the analysis tool used in the propulsion system selection. The drag (D) was represented via a parabolic drag relationship. The load factor was explicitly defined for each turn segment, but if it exceeded the estimated maximum lift coefficient, it was limited to that value.

$$\dot{x} = V \tag{4.1}$$

$$\dot{V} = \frac{T-D}{m} \tag{4.2}$$

$$\dot{\psi} = \frac{g\sqrt{n^2-1}}{V} \tag{4.3}$$

4.3.2 Uncertainties

The approach described above has specific limitations and uncertainties. The lack of a vertical dimension means that it cannot capture any aerodynamic effect due to altitude changes, or for the energy required or saved due to climbing or diving. The lack of any wind model discounts any additional drag due to sideslip in flight, or changes in velocity depending on traveling with or against the wind. The flight path defined for each lap assumes an idealized flight path, with the pilot turning perfectly after each 1000 ft. leg and the turns being optimal turns. Finally, there are additional uncertainties in the mission predictions due to any errors or inaccuracies in the thrust and drag predictions.

4.4 Aerodynamic Characteristics

4.4.1 Airfoil Selection

Using the correct airfoil for the aircraft is key to achieve the aerodynamic characteristics required to compete in this competition. Hundreds of airfoils were analyzed through a MATLAB script at an estimated Reynolds number of 200,000 to choose an airfoil that could provide the requisite lift and moment coefficients. These airfoils were also filtered based on their thickness and manufacturability.

Manufacturability: Complex airfoil geometry, as shown in Figure 4.3, can result in manufacturing error. These imperfections can negatively impact the aerodynamics of the vehicle and therefore its performance. The airfoil must not have a highly cambered or sharp trailing edge while maintaining sufficient thickness to reduce these manufacturing difficulties and obtain the desired performance from an airfoil.

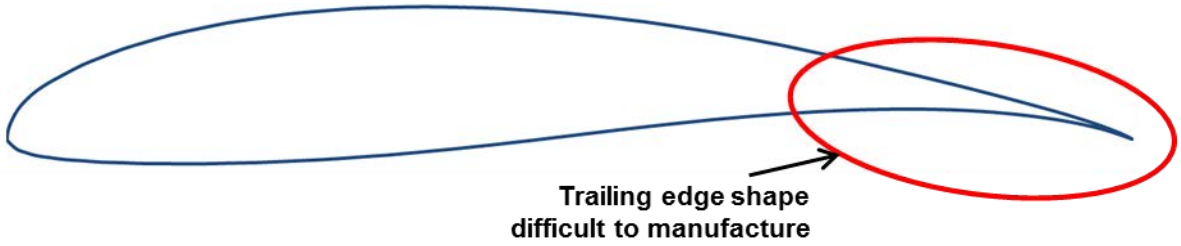

Figure 4.3: Wortmann FX 63-137 showing poor manufacturability.

Thickness: Low thickness airfoils typically have a small leading edge radius that results in abrupt stall at lower angles of attack. Increasing airfoil thickness increases the space for internal structural members that increase the structural rigidity of the airfoil while reducing structural weight. After testing multiple airfoil types, a thickness greater than 12% was preferred to achieve the space for these members.

Afterwards, the filtered airfoils were further analyzed based on maximum section lift coefficient and lift to drag ratio. Drag and lift curves for the final four airfoils were constructed using airfoil data obtained from wind tunnel test results from UIUC as shown in Figure 4.4.

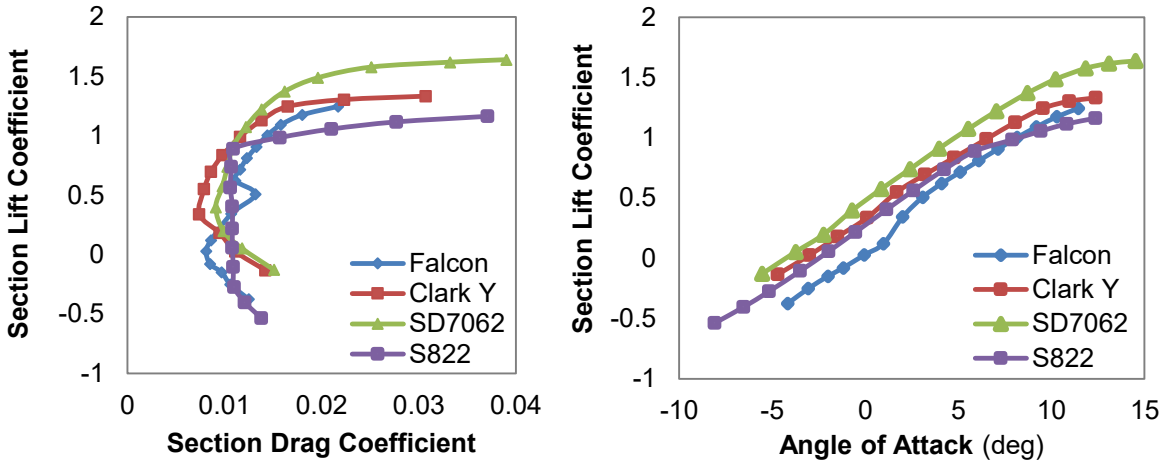

Figure 4.4: Experimental lift and drag characteristics for selected airfoils from UIUC data.

Examination of the drag polar shows that the SD7062 and S822 airfoils have a more stable sectional drag coefficient ($\tilde{C}_D$) over longer ranges of $\tilde{C}_L$ than the other airfoils. This indicates that for a given range of $\tilde{C}_L$ values, namely those around a $\tilde{C}_L$ of 0.5, the $\tilde{C}_D$ remains relatively low and constant. This is important due to the variance of $\tilde{C}_L$ over the wings caused by downwash due to wingtip vortices and environmental variables such as local wind. A high maximum $\tilde{C}_L$ is a desirable airfoil characteristic as it enables good STOL performance, which is critical due to the sixty foot takeoff requirement.

The SD7062, shown in Figure 4.5, has a thickness to chord ratio of 14% which aids in both the manufacturing process and increases the geometric stiffness of the wing. The SD7062 also had a maximum $\tilde{C}_L$ and lift-to-drag higher than the other airfoils considered, enabling the team to select the best combination of takeoff performance and speed. In summary, the SD7062 airfoil was selected for its combination of high maximum $\tilde{C}_L$, manufacturability, thickness to chord ratio, and favorable lift to drag ratio.

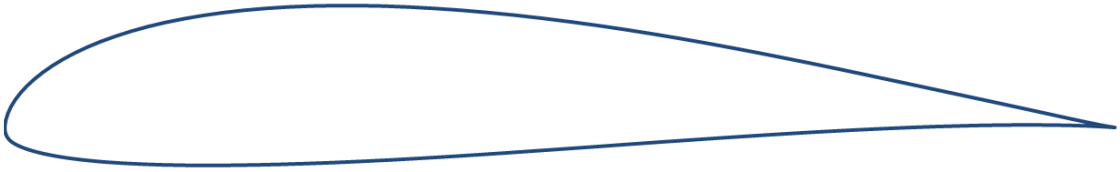

Figure 4.5: SD7062, the team's selected airfoil.

4.4.2 Lifting Surface Analysis

Athena Vortex Lattice (AVL), an aerodynamic tool developed by Dr. Mark Drela at MIT, was used to model the lifting surfaces of the aircraft to compute the aerodynamic characteristics of the entire aircraft. AVL models lifting surfaces as an infinitely thin sheet of discrete vortices, and models their interactions. The aircraft's tail and control surfaces were sized in AVL to provide desired static stability and trim characteristics. The aircraft configuration and paneling in AVL is seen in Figure 4.6. The lift distribution

shown in Figure 4.7 was generated in AVL using elevator trim to maintain flight at a moderate angle of attack on approach and landing. Due to the distribution shape, stall is expected to occur at the wing root, allowing the pilot to maintain roll control using the ailerons that are mounted outboard.

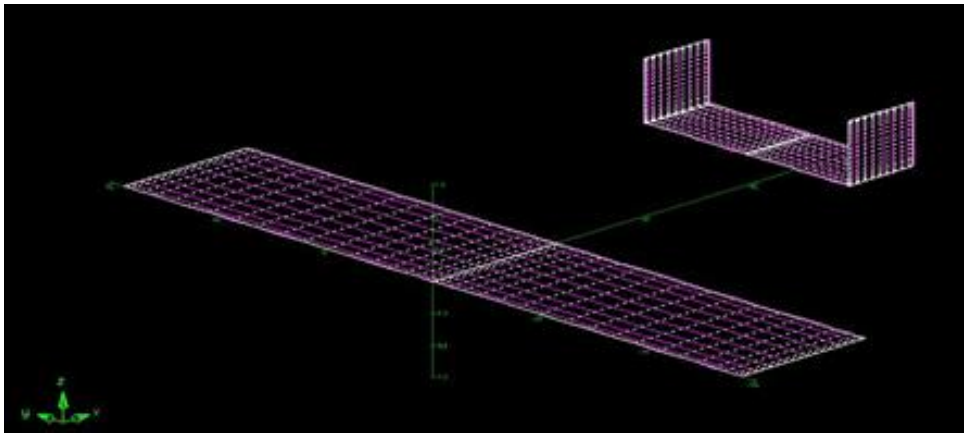

Figure 4.6: AVL model of aircraft.

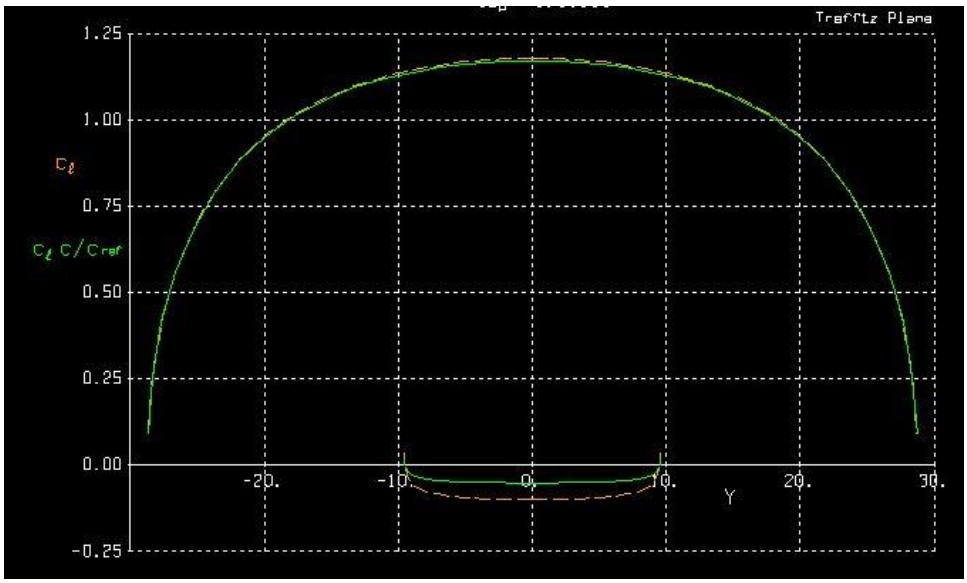

Figure 4.7: AVL predicted lift distribution of the aircraft.

4.4.3 Drag Analysis

A preliminary parasitic drag estimate was computed by summing each component's drag contributions, approximated using the semi-empirical methods from Hoerner's *Fluid Dynamic Drag*, and then normalizing each component according to the wing reference area. Table 4.2 shows the contributions of the main aircraft components, with Figure 4.8 displaying the same data as a percentage breakdown.

Table 4.2: Aircraft zero lift drag estimates.

Component	$C_{D,0}$
Wing	0.0137
Landing Gear	0.0085
Payload Release	0.0064
Fuselage	0.0059
Tail	0.0013
Total	**0.0358**

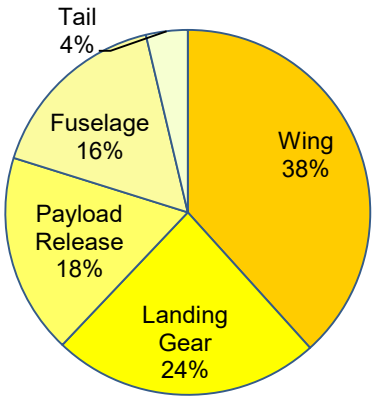

Figure 4.8: Graphical representation of drag estimates.

The main components of the parasitic drag are detailed below:

Wing: The drag coefficient for the wing was calculated using Equation 4.4 from Hoerner:

$$C_{D,0} = R_{wf} R_{LS} C_{f_w} \left(1 + L'\left(t/c\right) + 100\left(t/c\right)^4\right) \cdot \frac{S_{wet_w}}{S} \tag{4.4}$$

Equation 4.4 contains terms correcting for wing thickness location, sweep, and wing-fuselage interference (L', R_{LS}, and R_{wf}, respectively). The flat-plate skin friction coefficient (C_f) is a function of Reynolds number approximated for fully turbulent flow. The wing was found to be the largest contributor to zero-lift drag, with a total $C_{D,0}$ contribution of 0.0137, which is about 38% of the total drag.

Landing Gear: The landing gear components are significant contributors to the overall drag of the aircraft. The main gear and nose gear drag contributions were calculated separately, but both were modeled as a wheel and a flat plate added for the strut. The overall contribution of the landing gear to the drag was about 24%.

Payload Release: The drop mechanism significantly increased the overall drag of the aircraft. The drag of the drop mechanism was modeled as a flat plate, with a wedge nose to reduce drag. Knowing the relation between drag of a wedge compared to a flat plate, the zero-lift drag contribution was found to be 0.0064, or 18% of the overall drag.

Fuselage: The drag coefficient for the fuselage was determined using Hoerner's method, which computes drag as a function of the body fineness ratio, the Reynold-adjusted skin friction coefficient, and

lifting-surface/fuselage interference. The total $C_{D,0}$ contribution by the fuselage was calculated to be 0.0059, which accounted for about 16% of the drag.

Tail: The tail surfaces were modeled as wings and the drag contributions were calculated using the same method as the wing calculation. Overall, the contribution of the tail to the drag was 4% due to their small size.

With parasitic drag computed, the team used AVL to model the lifting surfaces of the aircraft to estimate induced drag. The estimated span efficiency was 80% for the full configuration. Sub-optimal efficiency was preferred to manufacturing complexity added by sweeping, twisting, or tapering the wing. The full drag polar is displayed in Figure 4.9 and was calculated by adding the induced drag from AVL and the parasitic drag from above. The drag polar indicated lift-to-drag ratios around 8 for the majority of lift coefficients, a relatively low value that can be attributed to the large fuselage driven by Mission 2 and 3 payload volume.

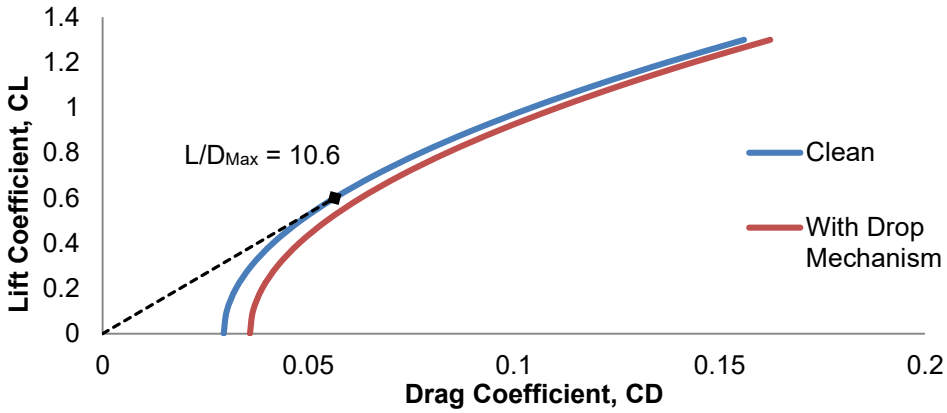

Figure 4.9: Full drag polar.

4.5 Stability and Control

Static and dynamic stability were analyzed to ensure that the aircraft would be able to successfully complete the flight missions. The fastest speeds, slowest speeds, heaviest weights, lightest weights, cruise, climbs, and turns were all considered, with results presented only for the critical flight condition.

4.5.1 Static Stability Analysis

Static stability was evaluated using the vortex lattice method implemented in AVL. The most demanding flight condition for trim was at the highest weight and lowest speed in Mission 2. Stability derivatives are given for this flight condition in Table 4.3. The aircraft is trimmed at this condition with a small elevator deflection and no extreme deflections were required for any of the cases analyzed. All cases indicate the aircraft is longitudinally, statically stable with a static margin of 9.3%. All pitch, roll, and yaw derivatives are stable and within the acceptable range based on previous years' pilot feedback.

Table 4.3: Relevant stability coefficients and derivatives for static stability.

Parameter	AVL Results	
Inputs	W_{total} (lbs.)	8.0
	V (ft/s)	35.3
Aerodynamic Parameters	C_L	0.97
	α (deg.)	10.0
	β (deg.)	0.0
Deflections	$\delta_{elevator}$ *(deg)*	-8.9
	$\delta_{aileron}$ *(deg)*	0.0
Stability Derivatives	$C_{l,\beta}$ (rad^{-1})	-0.13
	$C_{L,\alpha}$ (rad^{-1})	4.04
	$C_{m,\alpha}$ (rad^{-1})	-0.38
	$C_{n,\beta}$ (rad^{-1})	0.11
Damping Derivatives	$C_{l,p}$ (rad^{-1})	-0.37
	$C_{m,q}$ (rad^{-1})	-7.35
	$C_{n,r}$ (rad^{-1})	-0.077
Static Margin	% Chord	9.3

4.5.2 Dynamic Stability Analysis

Knowing the trim conditions from the static stability analysis, the next step was to use the aerodynamic derivatives about the trim conditions to investigate the dynamic behavior of the airplane. The stability and control derivatives were obtained using AVL, the mass properties were obtained from the CAD file, and the stability characteristics were calculated using the six degrees of freedom linearized differential equation matrix found in Phillips' *Mechanics of Flight*, Section 9.8. The eigenvalues and eigenvectors of the matrix revealed that the aircraft is stable in the Short Period, Dutch Roll, and Roll modes, unstable in Spiral mode, and neutrally stable in Phugoid mode. The Spiral mode has a 4.2 second doubling time, which is in line with past year's airplanes that flew without issue. The flight conditions used for this calculation were the same ones used in the static stability section, listed in Table 4.3. The dynamic stability characteristics are tabulated in Table 4.4.

Table 4.4: Dynamic stability analysis for least stable case.

	Longitudinal Modes		Lateral Modes		
Mode	Short Period	Phugoid	Dutch Roll	Roll	Spiral
Damping Rate (s^{-1})	4.00	-0.053	0.62	8.46	-0.16
Time to double/half (s)	0.17	13.03	1.10	0.08	4.17
Damping Ratio (~)	0.72	-0.061	0.13	-	-
Damped Natural Frequency (s^{-1})	3.88	0.87	4.66	-	-
Undamped Natural Frequency (s^{-1})	5.57	0.87	4.70	-	-

4.6 Mission Performance

The lap trajectory was calculated using the mission simulation described in Section 4.3 in conjunction with propulsion characteristics from MotoCalc and aerodynamic characteristics of the airplane. The velocity profile for the first lap of Mission 1 using an 11x7 propeller and a Tiger MN 3510-13 motor is shown on the left of Figure 4.10, and the profile for M2 also using an 11x7 propeller and Tiger MN 3510-13 is shown on the right of Figure 4.10. Both figures show the first lap of each mission and include the initial acceleration after takeoff. Velocity deficits in the plots correspond to the required turns over the course of each lap. The maximum velocity estimated for M1 is 70.0 mph (102.7 ft/s), and the maximum velocity for M2 is 63.3 mph (92.8 ft/s). The estimated lap times using optimal propellers for each mission are shown in Table 4.5, and correspond to a lap started and finished in the air. The analysis indicates that M1 and M2 performance targets of 8 laps and 120-second flight time, respectively, are achievable. It should be noted again that the analysis is likely optimistic, as detailed in Section 4.3, and true lap times will be verified through flight testing.

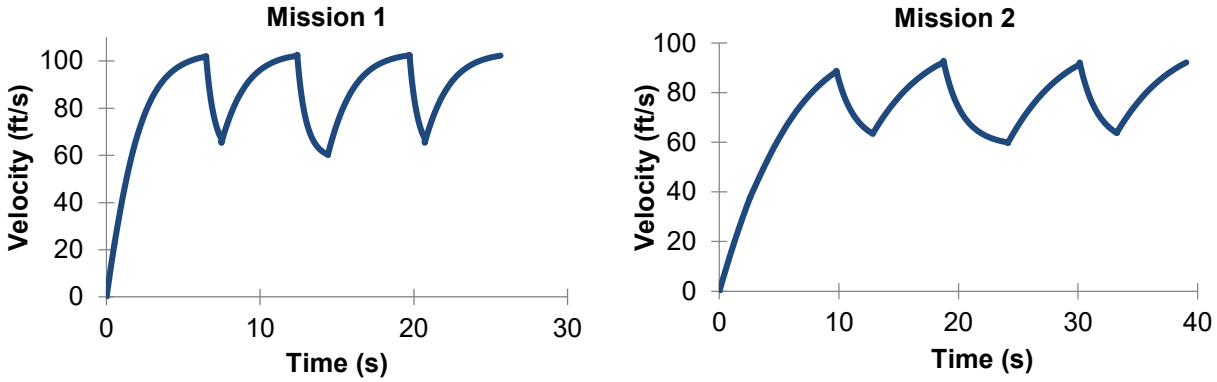

Figure 4.10: Simulation of Mission 1 and 2 lap trajectory.

Table 4.5: Predicted mission performance for each mission-propeller combination.

Mission	Propeller	Lap Time(s)
M1	11x7	25.6
M2	11x7	39.1

5. DETAIL DESIGN

5.1 Final Design

The aircraft dimensions did not vary between the preliminary and detailed design stages because the structural analysis and layout, component selection, and weight-balance calculations did not indicate major changes were needed. With the sizing completed, the final dimensional parameters are listed in Table 5.1. All wing and control surface chords were chosen to allow sufficient thickness for structure and embedded servos, and then sized to provide stability at the constraint-derived wing area, leaving aspect

ratio as a fallout variable. In summary, the final aircraft was designed for flight stability, simplicity, and structural efficiency.

Table 5.1: Final aircraft dimensional parameters.

Overall Dimensions		
Length	49	in.
Wing L.E. X-Location	10.7	in.
C. G. X-Location	12	In.
Static Margin	9.3%	chord

Wing		
Span	57.5	in.
Mean Chord	11.5	in.
Aspect Ratio	5	~
Wing Area	661.25	$in.^2$

Horizontal Tail		
Span	19	in.
Chord	6	in.
$\delta_{e,\,max}$	30	deg.
Reference Area	114	$in.^2$

Vertical Tail (x2)		
Span	5	in.
Chord	6	in.
$\delta_{r,\,max}$	0	deg.
Reference Area	30	$in.^2$

5.2 Structural Characteristics

5.2.1 Layout and Design

The primary goal for the structural layout was to ensure that all loads were accounted for and have an adequate load path to the major load-bearing components. The team divided all the loads the aircraft would see into three categories:

Motor Loads: Includes thrust, torque, and sustained vibrations. Components should be made of harder, quasi-isotropic materials such as plywood, and all fasteners must be locked.

Aerodynamic Loads: Includes wing and control-surface lift, drag, and moment, which translate to bending and torsion. Components can be anisotropic for added strength in the load direction.

Ground Loads: Includes aircraft weight and landing impact. Struts should be metal, which sustains impact by bending, not breaking.

The loads on the aircraft need to transfer into the major load bearing components, which includes the wing spar and fuselage attachment point. In flight, the wing may sustain up to a 2.5g load at maximum weight, based on the requirement of the wing tip test, therefore all loads from components not on the wing, such as payload and the empennage, traverse to the spar attachment point via the fuselage, as demonstrated in Figure 5.1. The fuselage is geometrically stiff due to the size required to accommodate the payload, making it an adequate load path. For the ground loads the fuselage has hard-points at the gear attachment locations to ensure impact loads do not damage any components.

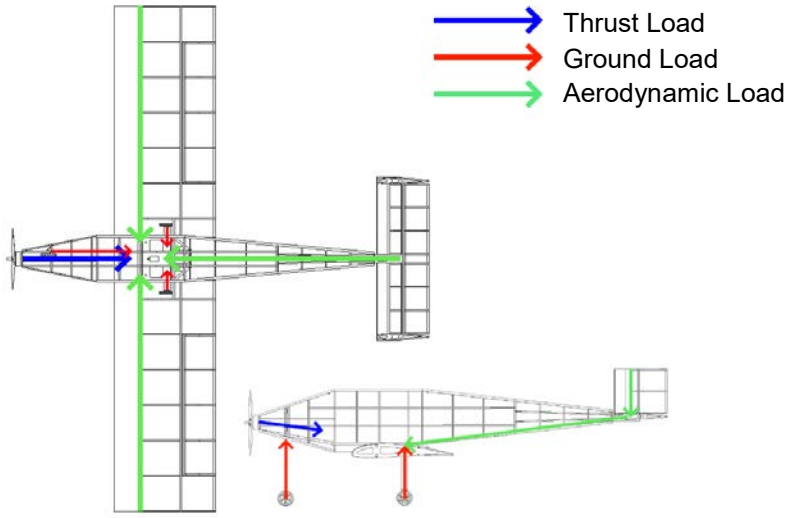

Figure 5.1: Load paths of major forces.

5.2.2 Operating Envelope

With the loads mapped and layout complete, the structure of the airplane was designed to withstand the design load of 2.5g at the maximum gross weight of 8 lbs. This translates to a 66-degree bank angle for sustained level turns. The ultimate load could not be well quantified because balsawood has significant variation in ultimate strength, thus the 2.5g design load-limit at small deflections was retained as the maximum positive load envelope for Mission 2. Since M1 and M3 fly at lower weights than M2, the structural limit increases to 6.25g. The negative load limit was defined at -1g for M2 to prevent the wing attachment area from failing in compressive buckling. This translated to greater negative loads for M1 and M3 due to their load limits. The defining structural limits were combined with aerodynamic performance limits at each mission to construct the V-n diagram displayed in Figure 5.2.

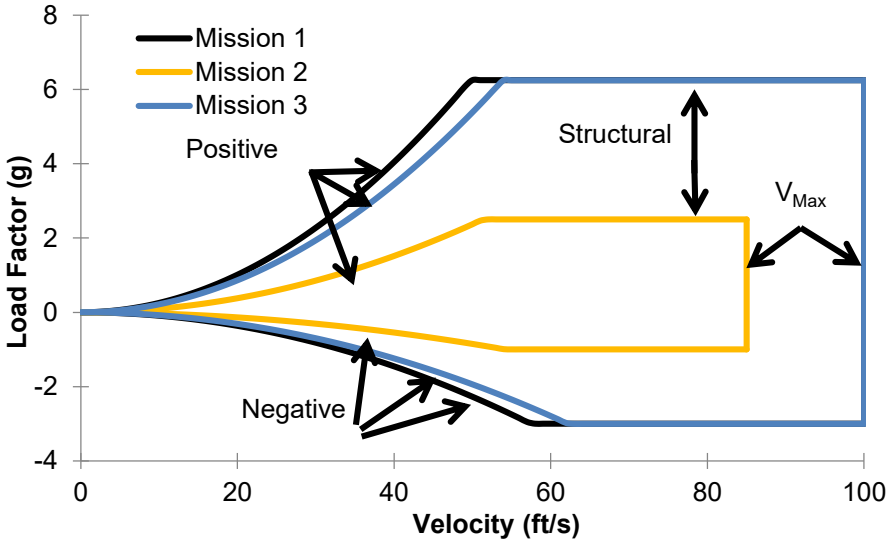

Figure 5.2: V-n Diagram showing loading as a function of velocity for Missions 1, 2 and 3.

5.3 System and Subsystem Design/Component/Selection/Integration

To finalize the aircraft design, the following subsystems were analyzed with greater detail: radio controller, servos, main wing, propulsion system, landing gear, and the structural architecture/assembly for each of these components.

5.3.1 Fuselage/Payload Bay

The fuselage of the aircraft is of a bulkhead and stringer design, using balsa wood for the majority of the structural members, with plywood being used to reinforce critical areas. The geometry of the fuselage design was primarily driven by enclosing an internal payload bay that could contain the payload for Mission 2. This led the team to design around the volume and weight requirements for the five pound payload block with a single open volume for the entire payload. Bulkhead placement was based on providing structural support to the payloads.

The CAD model was developed such that the bulkheads had interlocking slots, so that the parts fit together like a jigsaw. This interlocking method allows for the grain direction of the balsa wood to be in the proper direction for load transfer and more efficient manufacturing. The interior of the fuselage is open to allow for free arranging of the payload, the batteries, receivers, controllers and wires for the electronic components.

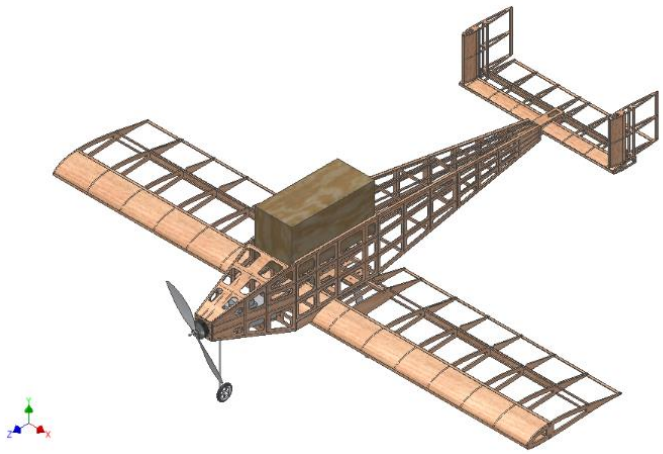

Figure 5.3: Payload loading method.

The fuselage was designed with a top lid that can easily open to allow rapid and simple access to the payload, and to provide a solid base to mount the payload drop mechanism for Mission 3. This is shown in Figure 5.3.

5.3.2 Wing

The wings were designed in a conventional scheme, with a rib and spar layout. The main load bearing structure was a balsa spar located at the quarter chord, which was reinforced with carbon fiber flat rectangular rods, and supplemented with an aft spar located at the three-quarter chord for the aileron attachment, as shown in Figure 5.4. Balsa wood was selected as the material for the spars and ribs, due to the strength, weight, and ease of manufacturability.

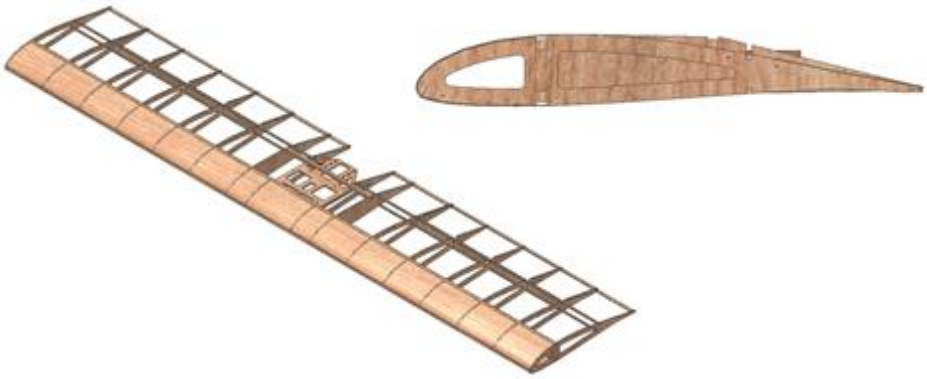

Figure 5.4: Wing design and structural layout.

The middle of the wing was designed around a central plate that integrated the aileron servo as well as acting as the attachment point to the main fuselage. The servo was connected to push rods and control horns to move both ailerons, which were then attached along the aft spar of the wing. Several ribs were modified to allow these push rods to pass from the center of the plane out into the wings. The hinges of the ailerons were fabric hinges, which are both small and lightweight.

5.3.3 Motor Mount

In keeping with the team design goal of minimizing system weight to maximize overall score, the motor mount is connected directly to the front section of the main fuselage. The motor attaches directly to a plate of 1/8th inch thick poplar plywood, shown in Figure 5.5, which was selected for its ability to withstand the torque and static thrust of the motor.

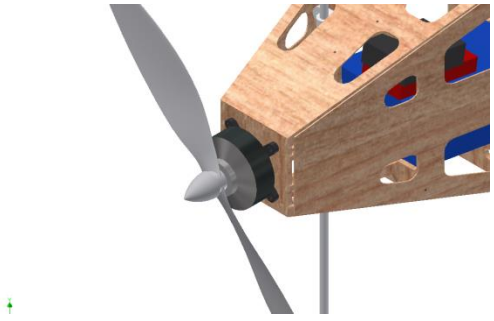

Figure 5.5: Motor mount assembly.

5.3.4 Empennage

The empennage, seen in Figure 5.6, was designed in CAD to be a lightweight and effective control surface. The construction uses similar materials and construction techniques as the wings, with balsa wood used for the majority of the structure, augmented by plywood members in key locations.

The tail was constructed as a separate unit from the fuselage and was attached to the aft of the fuselage with a box that fit into the back two bulkheads on the fuselage. This would allow removal and replacement of the tail, as new iterations of the tail or modifications were made. Wiring for the control servos runs through the tail box and into the fuselage.

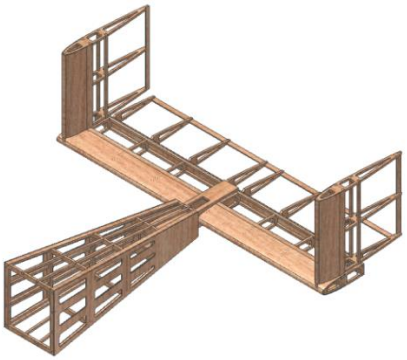

Figure 5.6: Empennage assembly.

In addition to providing stability and control authority in flight, the tail also supports part of the ball drop mechanism, which is connected to the elevator to allow commanded ball drops to avoid the added complexity, weight, and RAC of a dedicated drop servo.

5.3.5 Ball Deployment Mechanism

The ball deployment mechanism system was designed to reliably deploy the balls for Mission 3 without performing a maneuver dangerous to the aircraft or requiring an additional servo. This system consists of a series of 3D printed shuttles which slide along carbon fiber rods mounted to the top of the aircraft. A small lever arm placed near the tail of the aircraft uses the elevator servo to force the ball off the shuttle and away from the aircraft. The mounted deployment mechanism is shown in Figure 5.7.

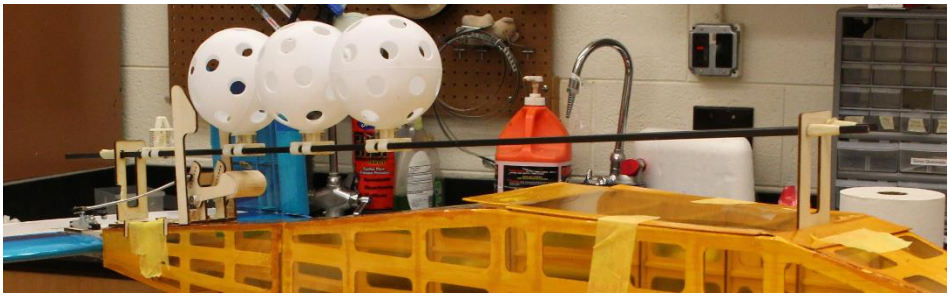

Figure 5.7: Ball deployment mechanism.

The 3D-printed shuttle was designed to hold the balls in place utilizing three linked arms that fit into one of the holes in the ball. A set of springs is compressed during the loading procedure, locking the arms into an extended position which locks the ball in place. A lever connected to the aircraft's elevator pushes a pin underneath the carriage which contracts these arms and releases the ball. The lever is connected to the elevator such that an elevator deflection above 35 degrees will force the lever arm to push the pin. Normal flight would not require an angle of 35 degrees preventing a premature ball release. The drag acting on the unreleased balls forces them to slide back onto the release arm after a drop, effectively reloading the mechanism.

The system works in a binary manner; the balls are either released or not. This increases the system reliability, as the transmitter can be set to limit servo travel during the lap to be below the deployment threshold, until the pilot flips a switch and enables full travel. Below are images of the ball holder and lever devices in Figure 5.8.

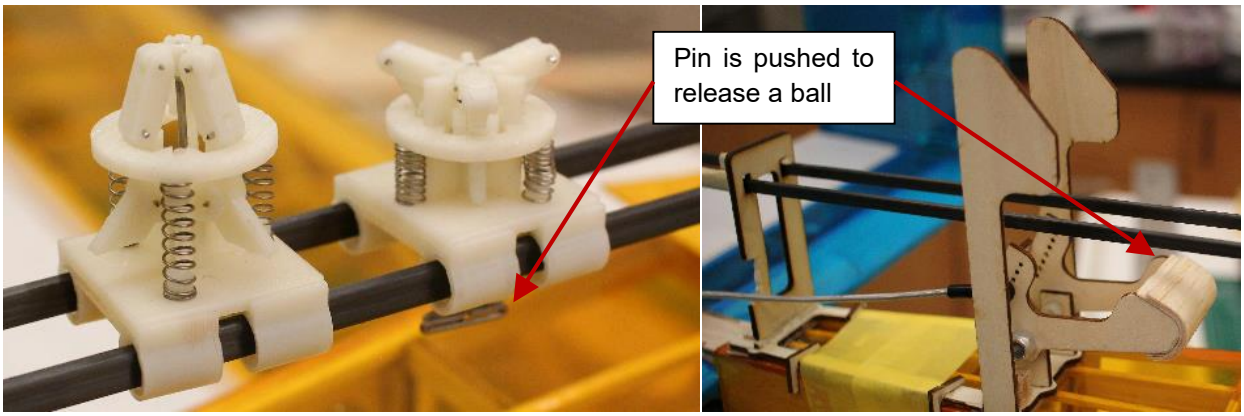

Figure 5.8: The shuttle for the drop mechanism and the lever system.

5.3.6 Receiver and Transmitter Selection

The receiver selected is the Futaba R6008HS, as it provides the required failsafe mechanism with minimum weight. *Buzz Killington* used a Futaba T8FG 2.4 GHz radio transmitter to communicate with the Futaba receiver.

5.3.7 Propulsion System

The propulsion system components were initially selected using the analysis from the MotoCalc program, as described in Section 4, but were changed after the results of wind tunnel testing described in Section 7 and 8. Originally, the Tiger MN 3510-13 motor was selected, but based on the data described in Section 8, it was found that the initial motor thrust was over predicted and that the Tiger MN 4010-11 was a better choice. The final selected propulsion system consists of a Tiger MN 4010-11 motor, 20 cell Elite 1500 mAH NiMH battery pack, a Phoenix Edge Lite 50 speed controller, and different propellers for each mission. The chosen propellers are APC 12x10 for Missions 1 and 3 and APC 13x10 for Mission 2.

5.3.8 Servo Selection and Integration

The Turnigy 380MAX was selected as the servo for the aileron and nose-gear as well as the servo for elevator and release mechanism. These servos were selected by analyzing hinge-moments for each control surface using AVL and then finding servos that had sufficient control power to handle the calculated moments, with the lightest weight possible. The selected components are tabulated in Table 5.2:

Table 5.2: Selected components.

Components	Description
Motor	Tiger MN 4010-11
Battery	20 cell ELITE 1500
Speed Controller	Phoenix Edge Lite 50
Receiver	Futaba R6008HS
Transmitter	Futaba T8FG
Aileron and Nosegear Servo	Turnigy 380MAX
Elevator and Release Servo	Turnigy 380MAX

5.4 Weight and Balance

An important aspect of stability is correct center of gravity (C.G.) measurements. To measure the C.G., a simple calculator was created that consisted of a list of all components, their weights, and their locations along the x-axis and z-axis. Component weights were first estimated using the CAD model and then confirmed with the physical vehicle. The results for all scenarios are given in Table 5.3. The x-axis was measured positive aft of the nose of the aircraft and the z-axis was measured positive above the chord-line of the wing. The predicted C.G. location from the CAD is shown in Figure 5.9.

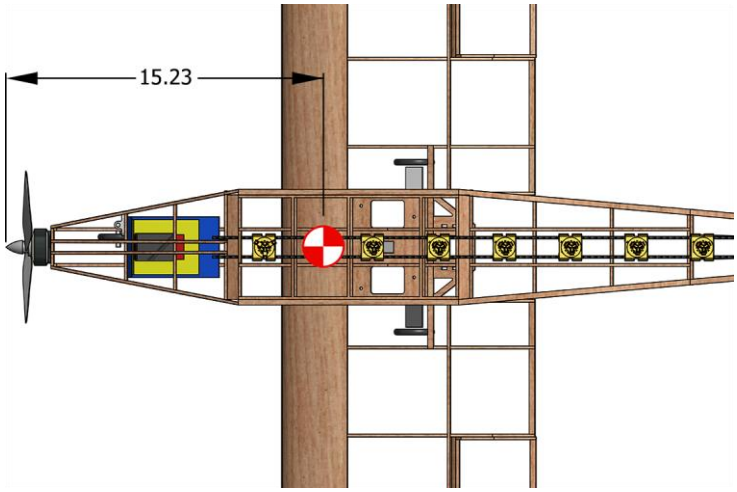

Figure 5.9: C.G. location on CAD model.

Table 5.3: Weight and balance chart.

Empty Weight					
Component	**Weight (lbs)**	**C.G. loc.(in, x-axis)**	**Moment (in-lbs, x-axis)**	**C.G. loc. (in, z-axis)**	**Moment (in-lbs, z-axis)**
Fuselage	0.18	18.00	3.28	2.00	0.36
Empennage	0.11	44.00	4.77	4.00	0.43
Speed Controllers	0.02	8.00	0.16	2.13	0.04
Receiver	0.03	3.00	0.09	2.13	0.06
Propeller	0.04	1.00	0.04	3.75	0.15
Wing	0.49	18.00	8.91	0.00	0.00
Aileron Servo	0.04	18.00	0.72	1.50	0.06
Tail Servo	0.04	45.00	1.80	4.13	0.17
Main Gear	0.19	19.50	3.66	-4.00	-0.75
Nose Gear	0.06	6.00	0.33	-3.50	-0.19
Motor	0.24	3.00	0.73	3.75	0.91
Receiver Battery	0.28	6.00	1.65	1.75	0.48
Aircraft Totals	**1.72**	**15.23**	**26.15**	**0.99**	**1.73**
Mission 1					
Battery	1.36	15.00	20.35	2.00	2.71
Payload	0.00	0.00	0.00	0.00	0.00
Aircraft Totals	**3.07**	**15.13**	**46.49**	**1.45**	**4.44**
Mission 2					
Battery	1.36	8.00	10.85	2.00	2.71
Payload	5.00	16.00	80.00	4.00	20.00
Aircraft Totals	**8.07**	**14.49**	**117.00**	**3.03**	**24.44**
Mission 3					
Battery	1.36	6.00	8.14	2.00	2.71
Payload	0.52	38.00	19.69	4.00	2.07
Aircraft Totals	**3.59**	**15.03**	**53.98**	**1.81**	**6.52**

The table shows that the battery must move significantly in order to balance C.G. for each mission. This is non-ideal, but necessary due to the large change in the nature of the payloads between Mission 2 and Mission 3.

5.5 Flight and Mission Performance

5.5.1 Flight Performance

The flight performance of the aircraft may be described by the point performance of the vehicle. Key aspects include the velocity envelope and turn performance, as well as takeoff distance and stall speed. These are given below in Table 5.4.

Table 5.4: Aircraft flight performance parameters for each mission.

	Mission 1	Mission 2	Mission 3
Weight (lb.)	3.07	8.07	3.59
W/S (psf)	0.653	1.742	0.828
TOFL	6.72	53.2	10.76
V_{stall} (ft/sec)	21.93	35.80	24.06
V_{max} (ft/sec)	95.0	81.78	93.0
Load Factor	6.67	2.5	6.5
Turn Radius (ft.)	42.52	90.65	17.2
Time for 360° (s)	3.49	7.45	3.03

Weight represents the Mission 1, 2, and 3 gross take-off weights. Both wing loading and stall speed are calculated at 1g assuming steady level flight while using an estimation of C_{Lmax} created with AVL modeling and section lift data. Takeoff field length (TOFL) was computed via numerical integration in MATLAB using the drag polar, friction coefficients, and thrust available from the wind tunnel test data.

Load factor for each mission was calculated based on the wing-tip test requirement. A point load on the tip of the wing is equivalent to a 2.5g distributed load on the wing. Expected lift at this load factor was calculated based on estimated system weight, and then used to calculate load factor for Mission 1. In both cases, the value for load factor is intended to represent a maximum. Flight test data indicates that in-flight loads will be lower.

Mission 3 load factor was calculated with the expectation that the aircraft would not experience high loads. This arises because M3 does not require high speed flight, giving preservation of battery power a higher importance and allowing the mission to be flown as close to stall as possible. The relation between RPM and power consumption is more important than the increase in induced drag at high angles of attack. Low flight speed implies reduced lift over the wing so the load factor is reduced for a weight similar to M1.

The turn radius and time to complete a 360 degree turn were calculated for each mission using the mission's expected maximum velocity and allowable load factor.

The maximum velocity of the aircraft occurs at the point when the thrust required is equal to the thrust available. Thrust required is calculated using Equation 5.1 where $C_{D,0}$ and e are calculated in Section 4.4.3.

$$T_R = \frac{1}{2}\rho V^2 S C_{D,0} + \frac{2W}{\rho V^2 S \pi A R e} \quad (5.1)$$

Thrust available is taken from wind tunnel data gathered on the propulsion system chosen and is plotted in Figure 5.10 as discrete data points. A best-fit curve was calculated using Excel and extended to show the intersection of thrust available and thrust required.

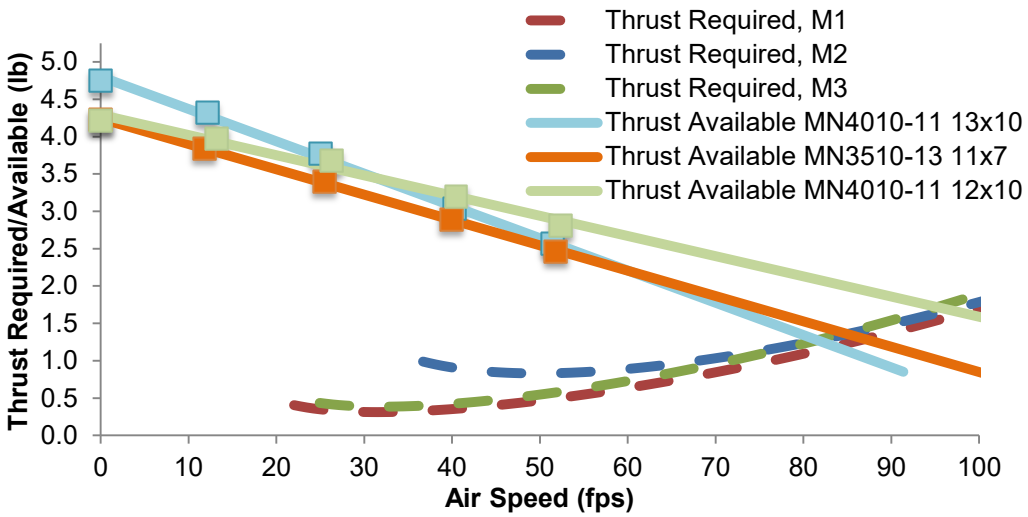

Figure 5.10: Thrust available and thrust required versus velocity. Solid lines are extrapolations of the wind tunnel data.

Figure 5.10 shows that the MN 3510-13 motor is inferior at all points along the expected flight regime. As a result, the motor selected was the MN 4010-11. Propeller selection was dependent on the specific mission. Since competition rules make it possible for teams to change the propeller used for each mission, the 12x10 propeller was chosen for M1 and M3. This combination has the highest thrust at speed, allowing for a higher maximum velocity. This is especially relevant for M1, where lap times are important. The 13x10 propeller was chosen for M2, as the 13x10 provides higher low end thrust, allowing for greater acceleration at low velocities and therefore reduced takeoff distance for the heaviest mission.

5.5.2 Mission Performance

The mission model described in Section 4.3 was used to estimate the final mission performance of the aircraft. The computed lap times represent an estimate that combines aerodynamics from AVL, power and current characteristics from wind tunnel data, and the physics of the mission model as described in Section 4.3. Figure 5.11 displays the projected first lap trajectories for Missions 1 and 2, with an initial ramp-up following takeoff and dips in velocity occurring at the turns. The remaining laps for Missions 1 and 2 are faster because they do not include takeoff. Table 5.5 shows the resulting estimated performance for each of the three missions with the selected propellers. The table also includes scoring estimates based on the updated analysis.

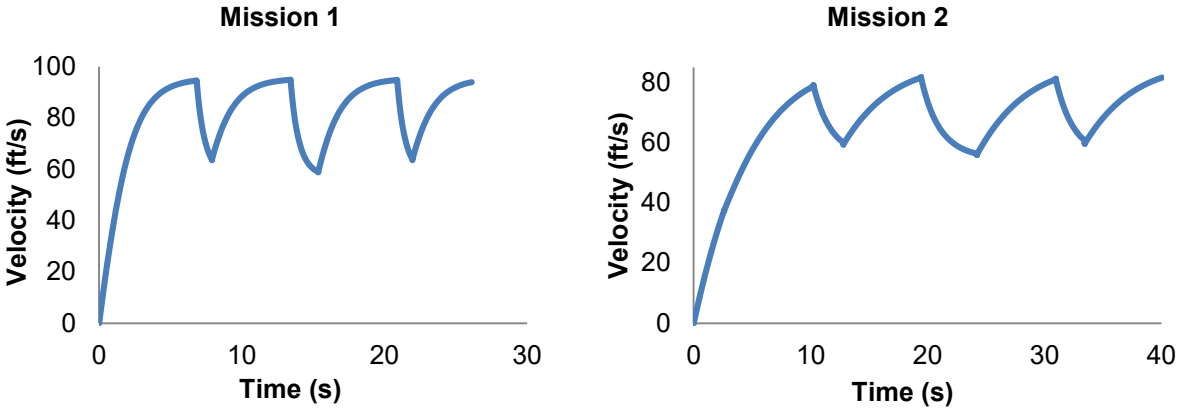

Figure 5.11: Simulation of Mission 1 and 2 lap trajectory.

Table 5.5: Aircraft mission performance parameters.

Mission Parameter	Mission 1	Mission 2	Mission 3
W/S (psf)	0.653	1.742	0.828
Propeller Selection	12x10	13x10	12x10
Max Current (Amp)	19	19	19
Static Thrust (lbs)	2.30	2.30	2.30
1st Lap Time (sec)	27.4	40.07	N/A
Mission Performance	8 laps in 4 minutes	120 seconds for 3 laps	8 balls
Mission Score	1.6	3.2	4.8
RAC	9.0	9.0	9.0

Based on the updated mission performance estimates shown in Table 5.5, the estimated FS is 9.6 while after normalization by RAC the score stands at 1.06.

5.6 Drawing Package

The following four pages illustrate the detailed CAD of *Buzz Killington*. The first sheet has the three-view diagram with relevant dimensions. The second sheet shows the structural arrangement of all major components. The third sheet displays the systems layout and location. The fourth sheet displays the payload arrangement for the internal and external payloads.

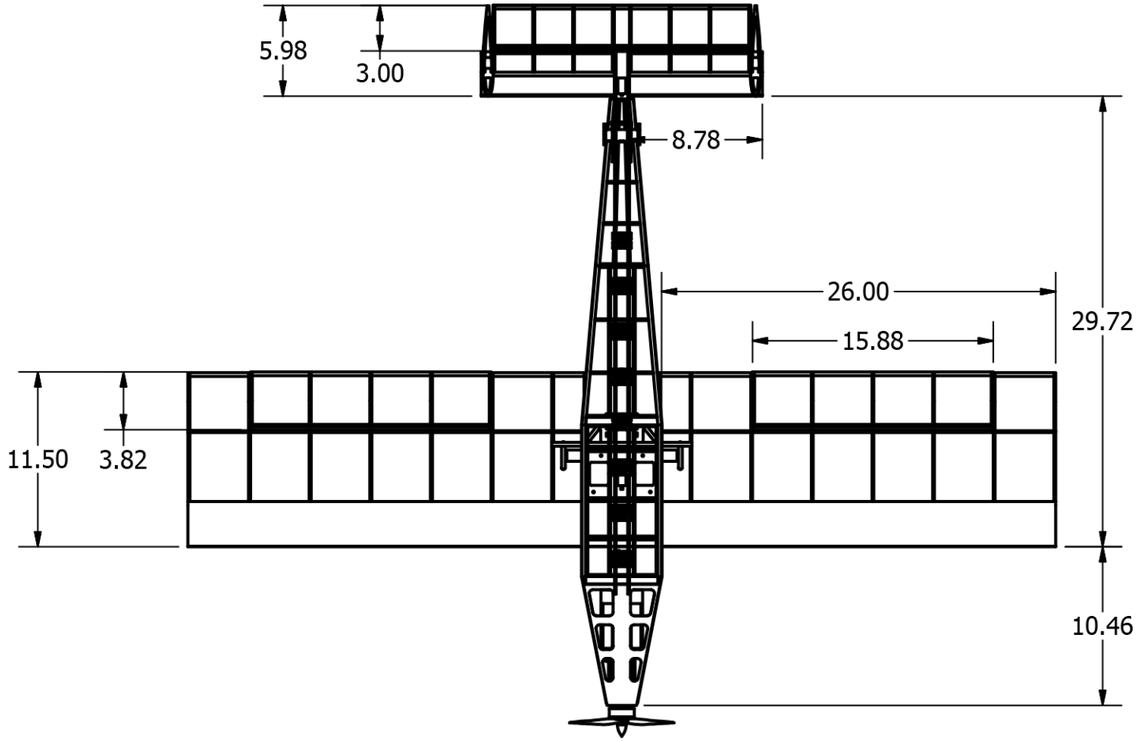

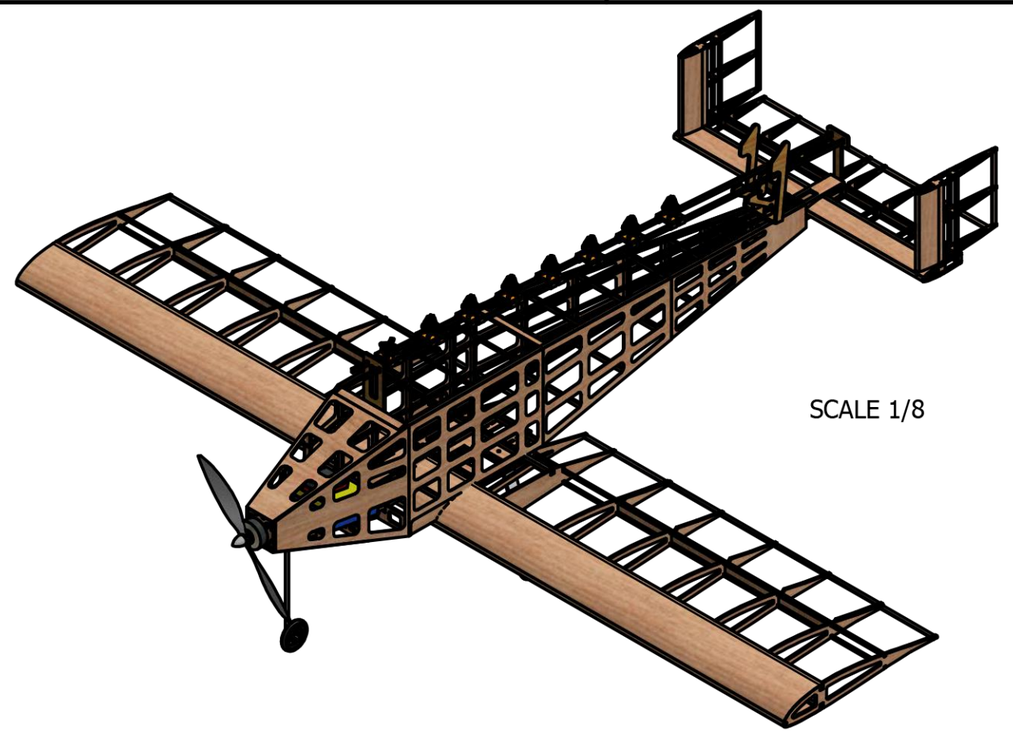

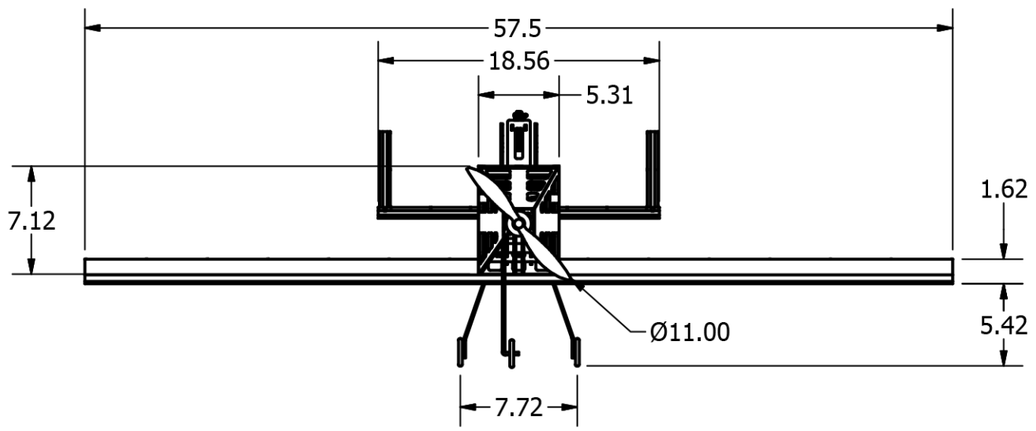

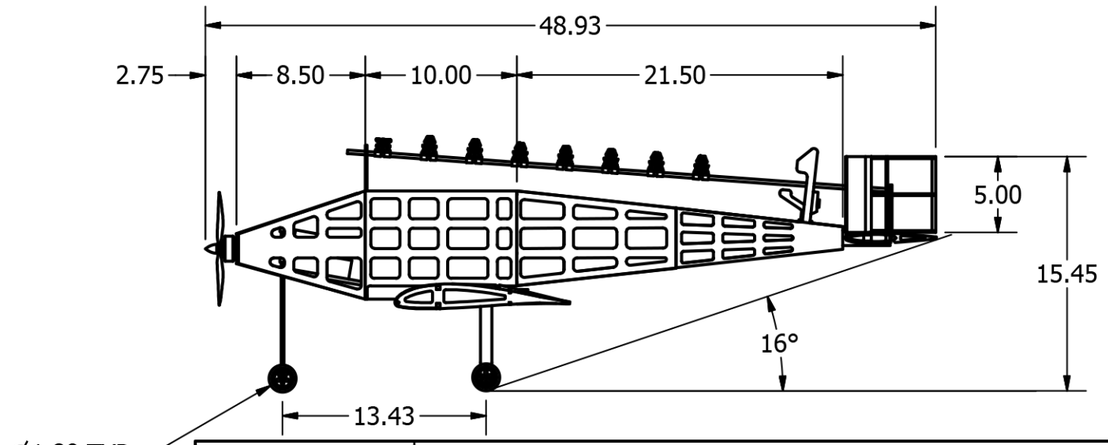

DRAWN	David Gaitan
CHECKED	George P. Burdell
	2/19/2015

Georgia Institute of Technology

Buzz Killington

SIZE	DWG
B	Three View Drawing with Dimensions, M1 Configuration

SCALE 1/10 | All Dimensions in Inches | SHEET 1 OF 4

Parts List			
Item	Quantity	Part Name	Material
1	1	Motor Mount	Plywood
2	1	Nose Gear	Aluminum
3	9	Fuselage Sheeting	Balsa
4	12	Bulkhead	Balsa
5	2	Wing Sheeting	Balsa
6	2	Aileron	Balsa
7	1	Wing/Fuselage Joint	Plywood
8	2	Main Bulkhead	Plywood
9	1	Tail Attachment	Balsa
10	1	Empennage	Balsa
11	2	Horizontal Tail Sheeting	Balsa
12	1	Elevator	Balsa
13	1	Shuttle Retainer	Plywood
14	10	Horizontal Tail Ribs	Balsa
15	2	Vertical Tail	Balsa
16	6	Vertical Tail Ribs	Balsa
17	2	Vertical Tail Sheeting	Balsa
18	1	Ball Retainer	Plywood
19	2	Shuttle Rail	Carbon Fiber
20	1	Rail Holder	Plywood
21	16	Wing Rib	Balsa
22	2	Nose Gear Mount	ABS Plastic
23	1	Main Landing Gear Strut	Aluminum
24	2	Wing Attachment Bolts	No. 4 Steel Bolts

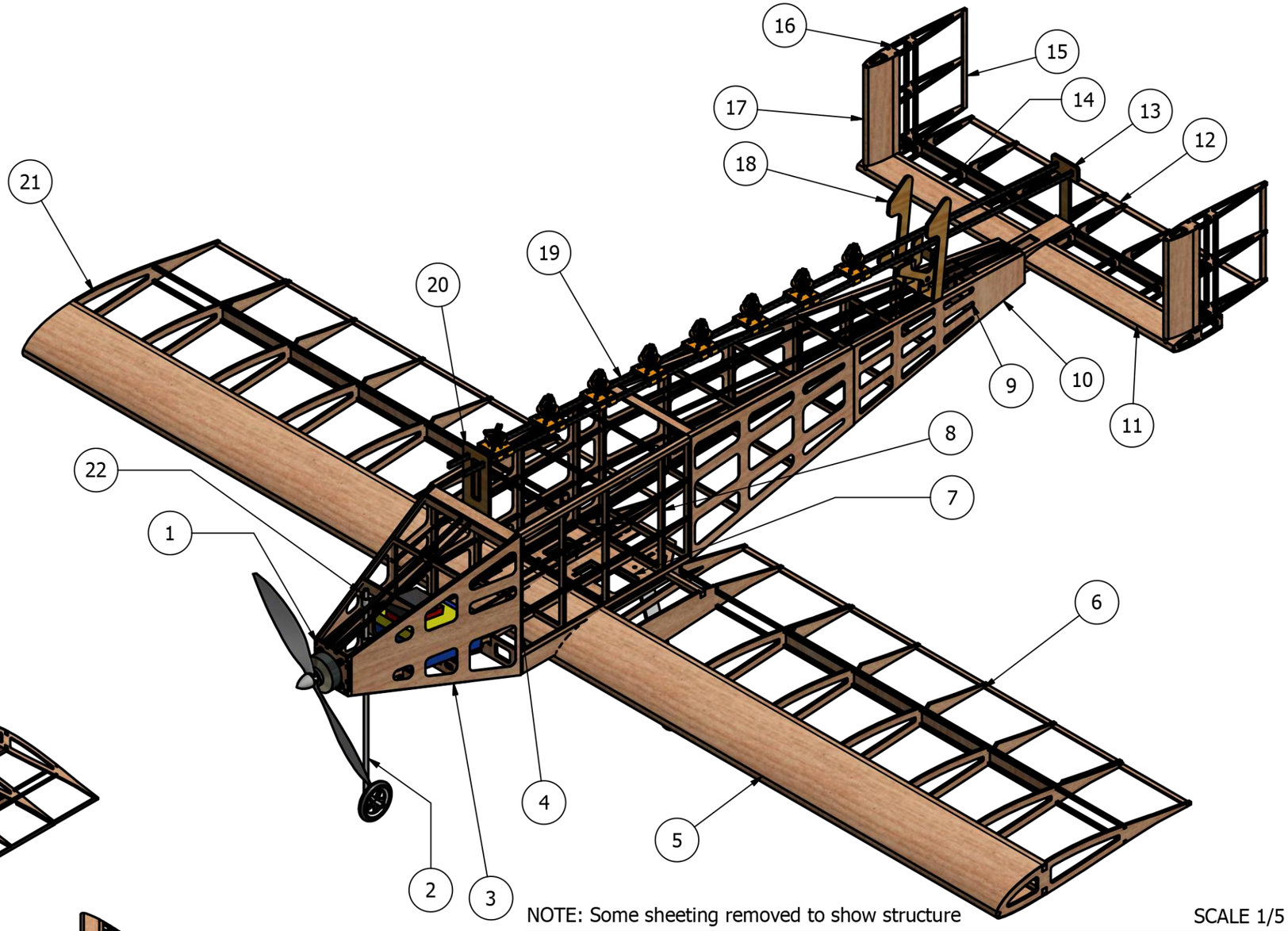

NOTE: Some sheeting removed to show structure

SCALE 1/5

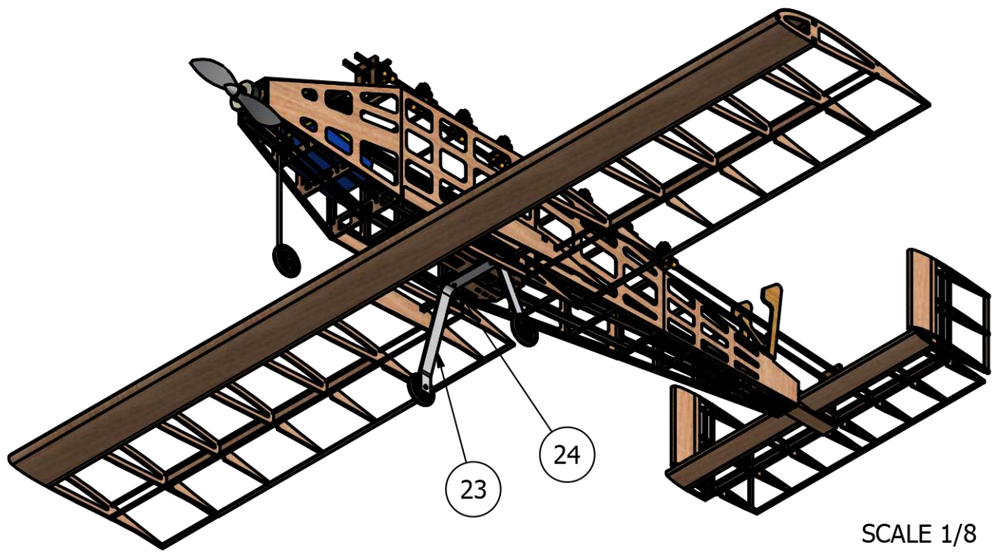

SCALE 1/8

DRAWN David Gaitan	Georgia Institute of Technology
CHECKED George P. Burdell	Buzz Killington
2/19/2015	SIZE B · DWG Structural Arrangement Drawing
	SCALE VARIES · SHEET 2 OF 4

Systems List			
Item	Quantity	Item Name	Description
1	1	Propeller	APC 11 x 7
2	1	Motor	MN4010-11
3	3	Wheel	Rubber Tires
4	1	Main Battery	20 Cell NiMH, 1,500 mAh
5	1	Receiver Battery	4 Cell NiMH
6	1	Receiver	Futaba
7	1	Speed Controller	Phoenix 50
8	1	Aileron/Nose Gear Servo	BMS 380 Max
9	1	Ball Release Lever	Balsa
10	1	Elevator/Ball Release Servo	BMS 380 Max
11	8	Ball Shuttle	ABS Plastic

NOTE: Some sheeting removed to show details

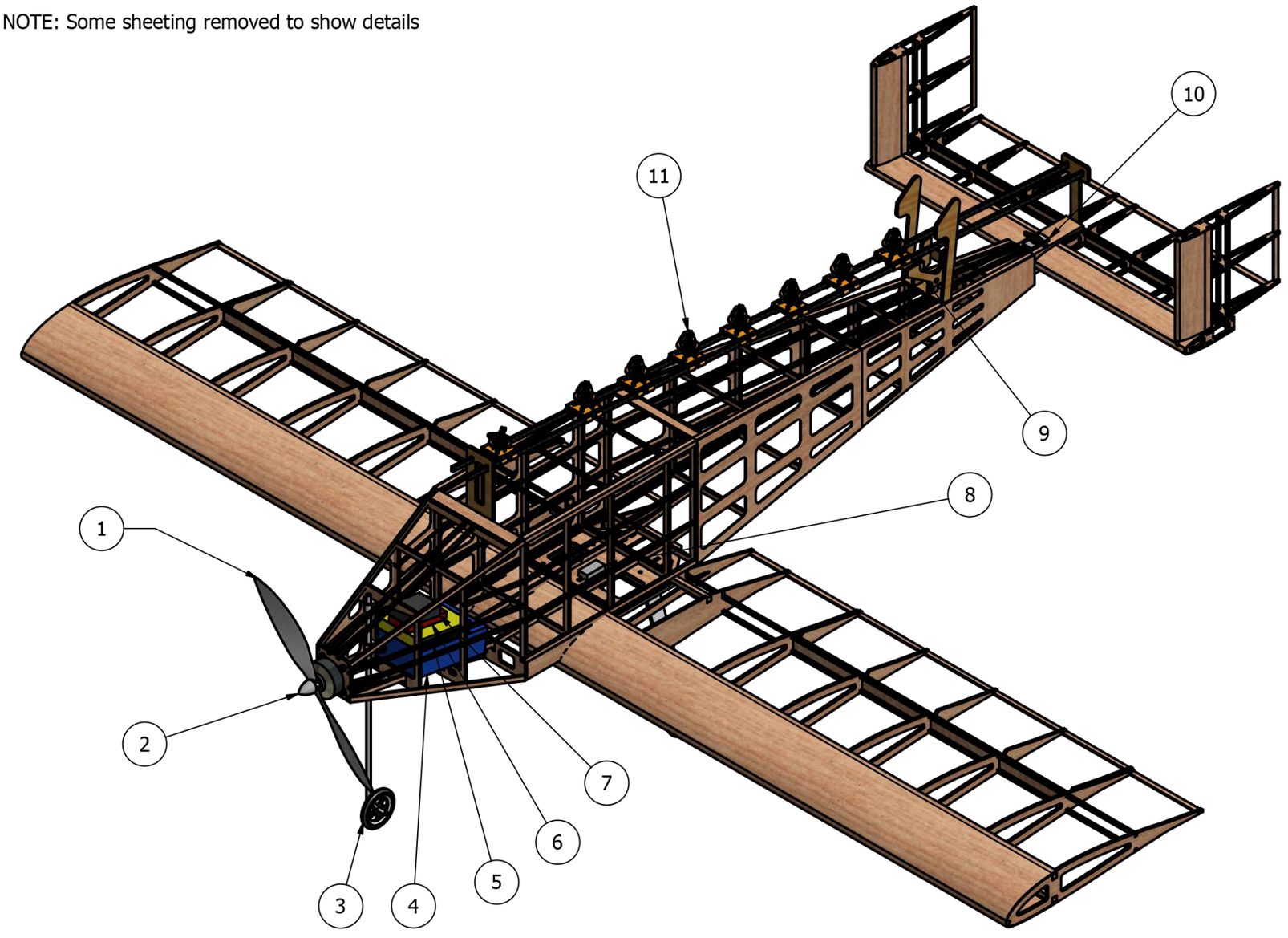

DRAWN David Gaitan	Georgia Institute of Technology
CHECKED George P. Burdell	Buzz Killington
2/19/2015	SIZE B | DWG Systems Layout Drawing
	SCALE 1/5 | SHEET 3 OF 4

SCALE 1/5

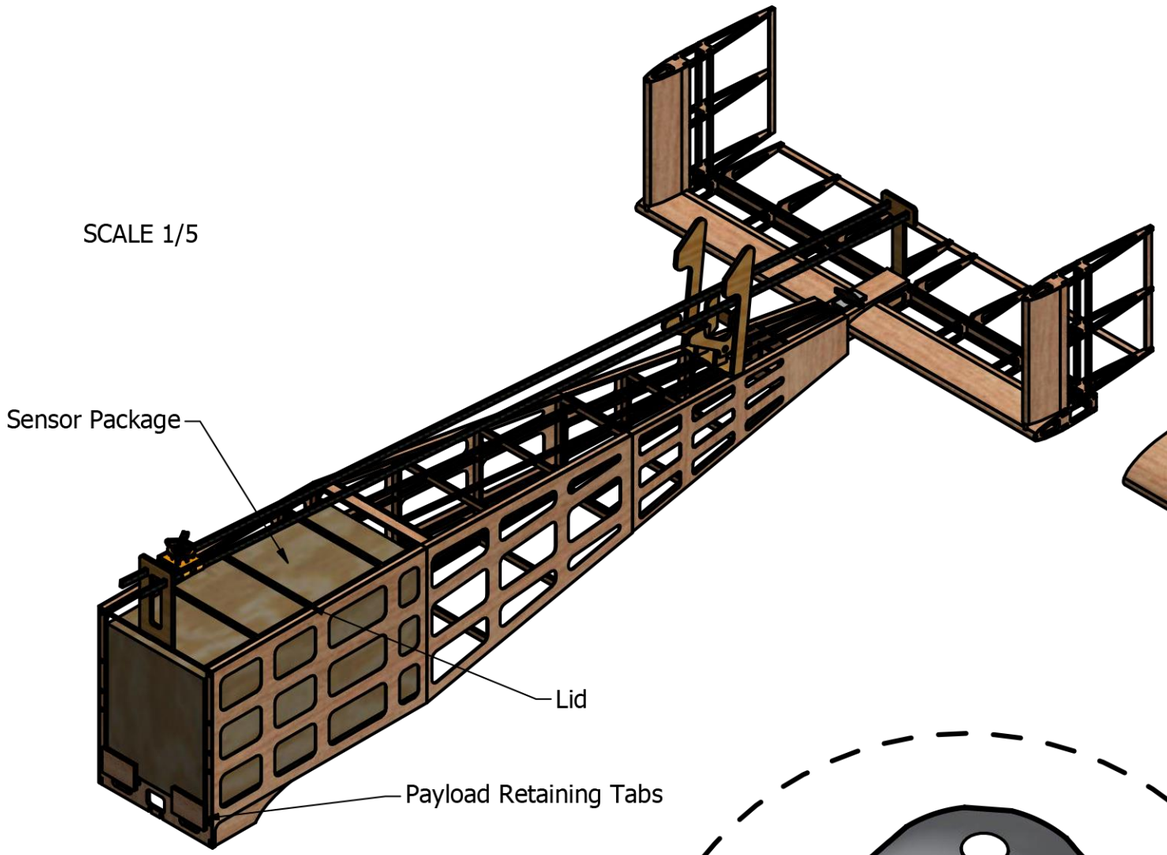

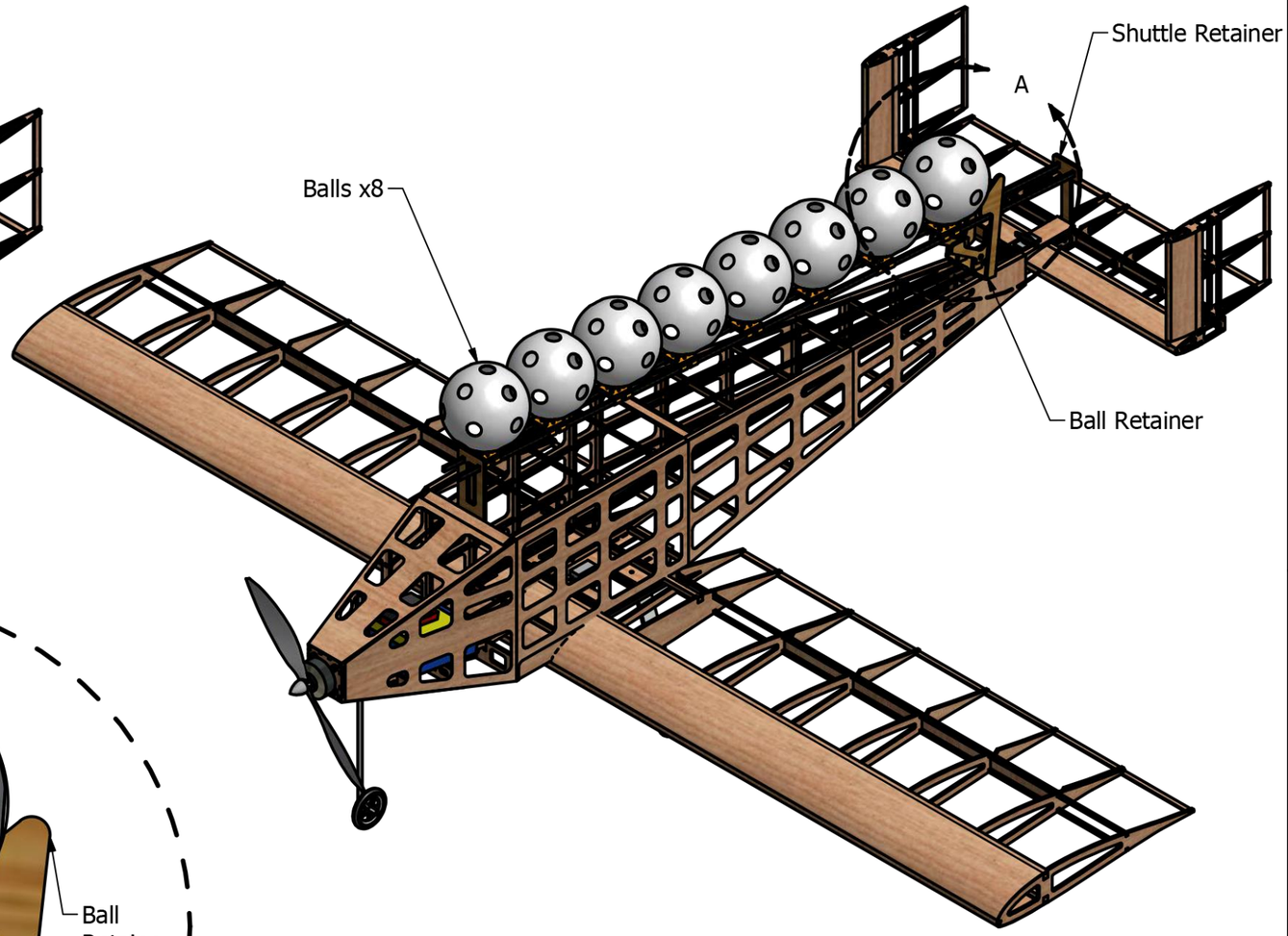

SCALE 1/6

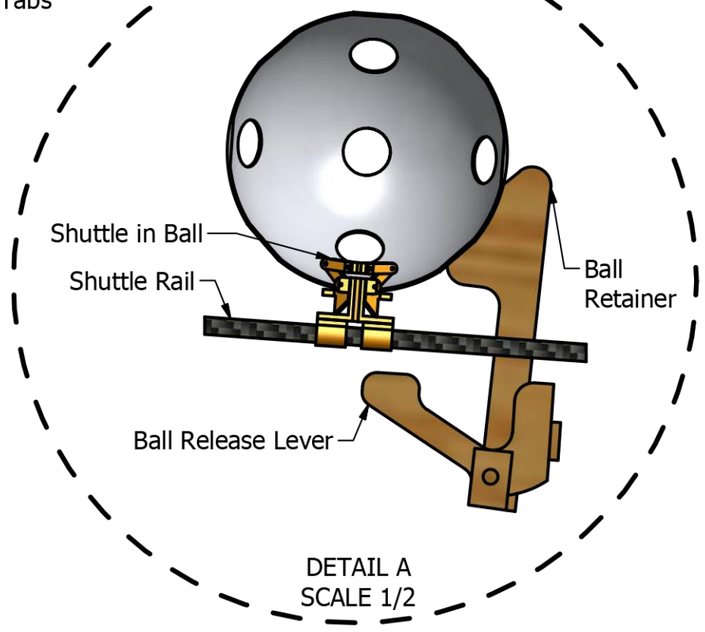

DETAIL A
SCALE 1/2

DRAWN David Gaitan	Georgia Institute of Technology
CHECKED George P. Burdell	Buzz Killington
2/19/2015	SIZE B · DWG Payload Accomodation Drawing, M2 and M3
	SCALE VARIES · SHEET 4 OF 4

6. MANUFACTURING PLAN AND PROCESSES

In order to design and build a competitive aircraft, the team considered various manufacturing processes and materials. The manufacturing process selected represented the best combination of weight, reparability, ease of manufacturing, team experience with the process, and cost.

6.1 Manufacturing Processes Investigated

The team had a wealth of experience using the well-established technique in built-up balsa wood manufacturing. However there were other viable manufacturing processes that could be superior. These processes were considered and qualitatively compared to the built up balsa technique using Figures of Merit, detailed below and summarized in Table 6.1.

Weight: similarly to conceptual design, weight is still the most important factor for any design decision, and is assigned a FOM of 5.

Reparability: With ever-present unknown factors, the reparability of the aircraft in case of an accident or a crash has to be accounted for, and was assigned a FOM of 2.

Ease of Manufacture: The ability to produce the aircraft to specification is critical to it performing according to predictions, and is directly related to Ease of Manufacture; it was therefore assigned a FOM of 3.

Experience: The team's knowledge was given some weighting because it relates to the ability of team members to produce quality results, as well as to refine existing techniques. However, since the team is always willing to learn new techniques, experience was only assigned a FOM of 2.

Cost: Keeping in mind that the team had limited resources, cost was inevitably added as a FOM. However, since the team emphasizes winning above all, cost was assigned a FOM of 1.

Table 6.1: Manufacturing FOM weighting.

Figure of Merit	0	1	2	3	4	5
Weight						5
Ease of Manufacture				3		
Reparability			2			
Experience			2			
Cost		1				

These Figures of Merit were used to investigate the manufacturing processes and materials common to remote control aircraft construction that were investigated detailed below.

Built-up Balsa: Stocks of competition grade balsa wood are laser cut from CAD models and glued together using cyanoacrylate (CA) adhesive to form the skeleton of the aircraft. It is then locally reinforced with more balsa or carbon fiber if necessary, and coated with Ultracote heat shrink film.

Foam Core Composite: Large blocks of foam are cut with a hot-wire or Computer Numerically Controlled (CNC) router to form the basic shape of the aircraft. Structural reinforcements are locally added if needed, and the entire foam-core is coated in fiberglass or carbon fiber, adding strength while providing an aerodynamic skin.

Molded Composite: This process is similar in principle to a foam core; however, the foam parts are only used to mold the composites and are then removed, with the fiberglass or carbon fiber acting as the primary structure.

The processes were evaluated against each other by assigning each one a FOM score, with a score of five indicating a superior choice, three an average choice, and one equaling an inferior choice. All methods were assumed to result in an aircraft designed for an identical load. The results of the comparison are summarized in Table 6.2.

Table 6.2: Weighting for various manufacturing techniques.

		Manufacturing Process		
FOM	**Value**	**Built-up Balsa**	**Foam Core Composites**	**Molded Composites**
Weight	**5**	5	3	5
Ease of Manufacture	**3**	3	3	1
Reparability	**2**	3	1	1
Experience	**2**	5	3	3
Cost	**1**	5	3	1
Total	13	55	35	37

Based on the Figures of Merit, built-up balsa was considered the best method for the plane manufacturing. To further confirm this choice, the team laid-up a molded composite wing section, the second-best candidate of the assessment above. The section consisted of 3 oz/yd^2 fiberglass with 1/32" balsa core, and resulted in an area density of 0.12 lbs per square foot of skin. With nearly 10 ft^2 of wetted area, the wing alone would weigh 1.2 lbs, more than the entire balsawood structure of the aircraft as-built. Therefore, the built-up balsa technique was used to construct the aircraft.

6.2 Manufacturing Processes Selected

The team used the above comparison to optimize the built-up balsa technique to achieve the most competitive aircraft by having the lightest structure possible in accordance with competition rules without sacrificing structural integrity. This optimized technique is detailed in Table 6.3:

Table 6.3: Built-up balsa manufacturing technique.

Manufacturing Component	Material / Technique
Principal material	Competition Grade balsa wood
Other materials	Local fiber reinforcements
Adhesive	CA, or epoxy if needed
Coating	Ultracote
Part manufacture	CAD-guided laser cutting
Part assembly	Designed-to-fit jigsaw pieces

Of the many different ways to apply built-up balsa, the team chose specific techniques and materials that would minimize the aircraft structure's weight without compromising its strength. These strategies are:

Selective Material Use: Since balsa wood can vary significantly in density and strength, the team sorted its entire stock of balsa by weight. The lightest pieces were selected for construction and were sent to the team's laser cutter, with the lightest of the cut parts reserved for the final competition aircraft.

Local Reinforcements: Due to the very low density of balsa used, the aircraft structure lacked strength in several key locations. Rather than compensate by over-building the entire aircraft, these locations were reinforced with composite or additional balsa, increasing strength with minimal penalty in weight.

Selective Shear Webbing: The wing for this aircraft provided an uncommon structural challenge for the team due to the requirement of containing the minimum amount of servos. The need for the servo that controls the ailerons of the wing to also control the nose gear introduced a large amount of torque on the wing. The team employs shear webbing in the bays adjacent to the servo attachment points to provide additional stiffness. The wing structure can be seen in Figure 6.1.

Figure 6.1: Prototype aircraft wing in production.

Lightening Holes: The use of a concentrated and localized structure caused most structural members to not experience significant loading. Where possible, the team laser-cut lightening holes into ribs and bulkheads to reduce weight with little losses in the overall stiffness and strength of the aircraft.

3-D Printing: Traditionally, parts are laser cut from balsa wood or milled from aluminum. However, the integration of additive manufacturing techniques allowed for the creation of light, custom, components that maintain torsional stiffness and resistance to shear stress. Additive manufacturing is becoming a more important part of aerospace manufacturing; the use of these techniques also provides valuable experience for team members. 3-D printing was used to create a reliable drop mechanism.

Coating: Most balsa aircraft are coated with a heat shrink adhesive infused plastic covering material called Monokote, which is durable and easy to handle. However, the team chose to use a more delicate plastic covering, Ultracote, because it is significantly lighter.

6.3 Manufacturing Milestones

A milestone chart was established at the beginning of aircraft manufacturing to ensure a logical, consistent order was followed during construction. Progress was recorded and monitored by the team leader to ensure all major milestones were met. The milestone chart is shown below in Figure 6.2, capturing the planned and actual timing of major events.

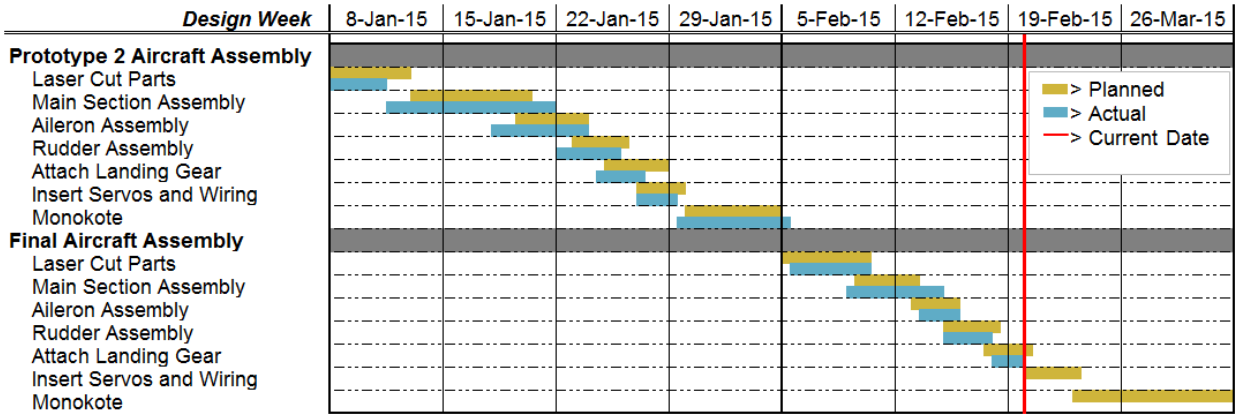

Figure 6.2: Aircraft manufacturing milestone chart showing planned and actual timing of objectives.

7. TESTING PLAN

A plan for an extensive testing campaign to validate the aircraft, and its components, was created to determine what configurations and subsystems would be the most capable. Testing culminates in test flying a full round of competition flights on the final competition airframe.

7.1 Objectives and Schedules

The testing was broken up into three main categories: propulsion, structures, and performance. The propulsion and structures subsystems were tested before flying the whole aircraft to gain knowledge and set realistic and useful objectives at each test flight. A breakdown of the testing schedule is displayed in the following Gantt chart, shown in Figure 7.1:

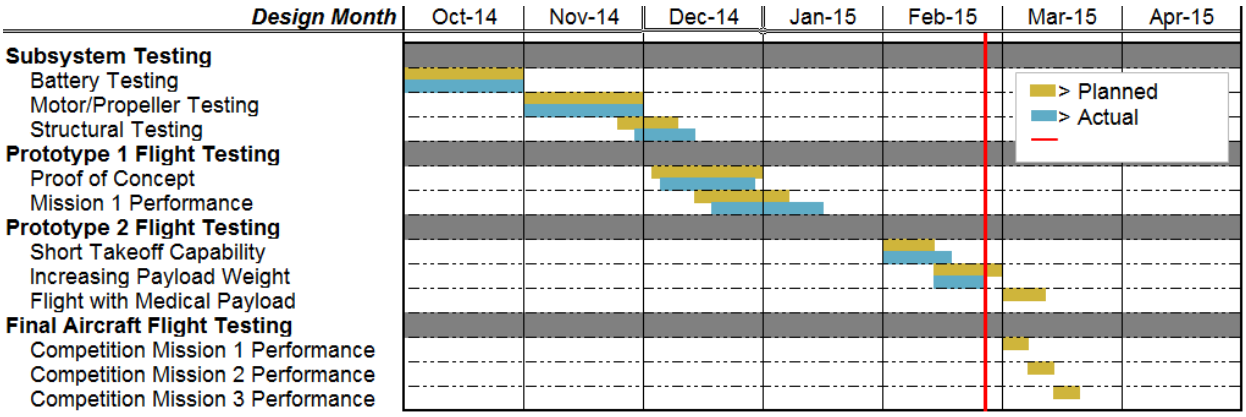

Figure 7.1: Aircraft and subsystem testing milestone chart showing planned and actual timing of objectives.

7.2 Propulsion Testing

The objectives for the propulsion testing were to determine which of the two motors would be best for the flight missions. The motors and propellers tested were based on MotoCalc predictions as expressed in Section 4.2. Thrust versus velocity for vehicle performance and power draw for motor performance for each motor propeller combination were determined using measurements of thrust, torque, RPM, voltage, and current draw. Using data obtained from testing, the team was able to compare the actual performance of the motors to the MotoCalc predictions in order to gather a better estimate of actual performance. This information allowed the team to select the best propulsion system to achieve the best score possible.

A rig that included load cells to calculate thrust and torque as well as an electric motor measurement system was constructed for the wind tunnel testing, and is shown in Figure 7.2. The electric motor parameters were monitored with an EagleTree system that records the RPM, voltage, and current draw of the motor. Custom written software was used to collect the torque and thrust values as well as to remotely control the motor for 30-second intervals with 10-second full thrust intervals and 10-second acceleration and deceleration intervals.

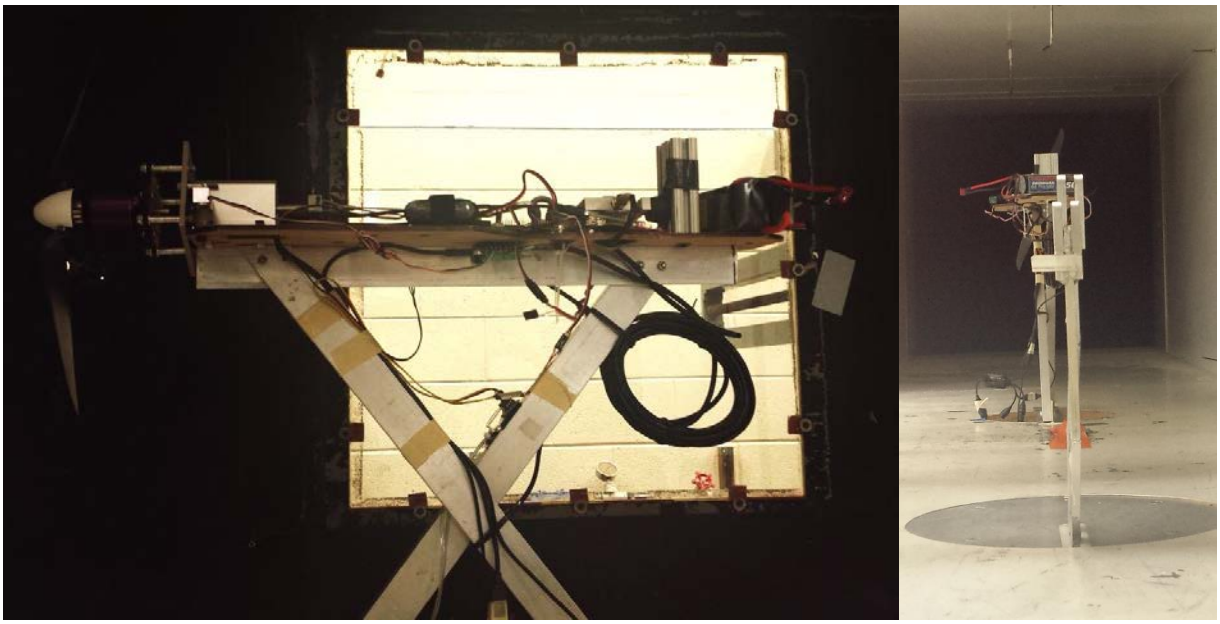

Figure 7.2: Picture of thrust test rig in wind tunnel.

The team utilized the Georgia Tech Low Turbulence Wind Tunnel to conduct its wind tunnel tests. The wind tunnel is powered by a fan which forces air through a series of honeycombed grates creating a smooth, even flow of air. The fan creates airflow with a maximum airspeed of about 52 feet per second. The wind tunnel creates an environment closely resembling actual flight conditions and thus providing accurate motor and propeller efficiencies. By testing different combinations of motors and propellers, these efficiencies were contrasted to find the best combinations for each mission. The results are described in Section 8.1.

7.3 Payload Loading and Release Testing

An experimental trade study was performed to determine the relationship between the amount of payload and total loading time. The GS was simulated using a team of three individuals. One team member would hold the aircraft while the other two loaded the payload. Since the distance from the safe zone to the loading area was not specified, the team did all test runs starting 20 ft. from the loading zone. This distance was chosen due to it being the distance to the loading zone at the 2013-2014 AIAA DBF competition GS. The team conducted a timed loading sequence in which the M2 payload was installed into the aircraft. The team then conducted a second timed sequence in which it unloaded the M2 payload and installed the M3 payload. Using the times found in this study it was determined the greatest time cost in the GS was due to the number of balls used in M3.

The most important aspect of the drop mechanism is its reliability. The goal of M3 is to drop a single ball for each lap flown, and if multiple balls are dropped in the drop zone during one lap, the lap is invalidated.

Therefore extensive testing was conducted in order to validate the reliability of the drop mechanism. The drop testing mechanisms was initially tested in a controlled static case for proof of concept. The team utilized the Georgia Tech Low Speed Wind Tunnel in order to test how the drop rig acted in air flow at different angles of attack and sideslip, to determine all possible orientations the drop mechanism could perform at. Finally the aircraft was flight tested with the drop mechanisms to validate the reliability in true flight.

7.4 Structural Testing

To validate the design of the wings, the aircraft was subjected to a wing tip test. A wing tip test simulates the maximum loading the wings would experience in flight by loading the payload bay with the maximum weight and lifting the plane by the wing tip. The tip test simulates a maneuver resulting in a root bending moment of 2.5g.

7.5 Flight Testing

Flight testing was conducted across two airframes. Each airframe represents an iteration of the design. The first airframe, the initial prototype, was used to determine the flying qualities of the aircraft design. Verification of structural layout and load estimates were also conducted. Initial testing of a simulated M1 profile was flown.

The second airframe is currently being used as a testing platform. Changes were made to the design based on pilot feedback about Airframe One. These included modifications to the fuselage and vertical tail to improve handling qualities and optimization of M2 and M3 payload integration. After initial evaluation of flight qualities, both M2 and M3 were simulated.

Evaluation of M2 and M3 mission performance of Airframe Two is ongoing. Experience and data gained from Airframe Two will be used to improve the design for Airframe Three, which is intended to be the final competition aircraft. Airframe Three will then fly simulations of all three flight missions to determine the performance. The schedule and flight order is displayed in Table 7.1, seen below.

Table 7.1: Flight test goals and order.

Flight Test	Aircraft	Goal
1	Prototype	Maiden flight, determine flying qualities
2	Prototype	Takeoff distance, stall and recovery tests
3	Prototype	Mission 1 simulation
4	Prototype 2	Determine flying qualities, takeoff distance tests
5	Prototype 2	First flight with payload
6	Prototype 2	Maximum payload test
7	Prototype 2	Ball payload test
8	Final	Mission 1 performance
9	Final	Mission 2 performance
10	Final	Mission 3 performance

7.6 Checklists

Various tests have specific procedures which must be followed accurately to produce the desired objectives and ensure safety. This section lists the checklists utilized by *Buzz Killington* while conducting tests that required a significant amount of steps, such as propulsion and flight testing.

7.6.1 Propulsion Test Checklist

The checklist in Table 7.2 was created to ensure safety while dealing with propellers and electrical equipment, and to make sure the test is not wasted due to some mistake in preparation. This checklist was used in the testing of all motor, battery and propeller combinations.

Table 7.2: Propulsion testing checklist.

Propulsion Test Checklist		
1. Propeller secured? ☐	2. Motor mount secured? ☐	3. All plugs secured? ☐
4. Batteries peaked? ☐	5. Throttle down? ☐	6. Data system on? ☐
7. Custom code running? ☐	8. All clear of testing rig? ☐	9. Wind tunnel closed? ☐

7.6.2 Flight Test Checklist

The checklist in Table 7.3 was created with the important goal of preventing any system from malfunctioning in mid-air, which could lead to the aircraft crashing; its thorough execution is paramount to the team's success, and it will be used at the DBF event as well.

Table 7.3: Pre-flight checklist.

General System Checks					
Structural Integrity	**Center of Gravity Location**			**Time**	**Date**
	X:		Y:		
Payload					
Internal					
Primary Bay			**Propulsion Bay**		
Laterally Secure?	**Hatch Secure?**		**Battery Pack**	**Receiver Pack**	**Secure?**
External					
Attachment secure?	**Pins locked?**			**Clear of Jams?**	
Control Surfaces					
Ailerons			**Elevator**		
Deflects?	**Glued?**	**Slop?**	**Deflects?**	**Glued?**	**Slop?**
Electronics and Propulsion					
Receiver Battery Charged?	**Primary Battery Charged?**	**Receiver/Transmitter Go?**	**Wires secure?**	**Battery hot?**	**Prop secure?**	**Prop direction?**
Weather					
Wind speed	**Wind Direction**			**Temperature**	
Initials for Approval					
Chief Engineer	**Pilot**			**Advisor**	

8. Performance Results

8.1 Component and Subsystem Performance

8.1.1 Propulsion

Batteries: A 10-cell, 1500mAh NiMH battery pack was discharged at 5 amps (3.3 times its capacity) and at 15 amps (10 times its capacity) to characterize the discharge capabilities of the NiMH batteries. The resulting data is shown in Figure 8.1 on a per cell basis. NiMH battery cells have a nominal voltage of 1.2V, and the 5 amp discharge curve is capable of maintaining this voltage. However, at the higher discharge rate of 15 amps the cell voltage continuously drops. The result of this is a small decrease in the effective power that can be drawn from the batteries. However, the higher current draw of the 15 amp discharge is necessary for the propulsion system to generate the power required for the aircraft.

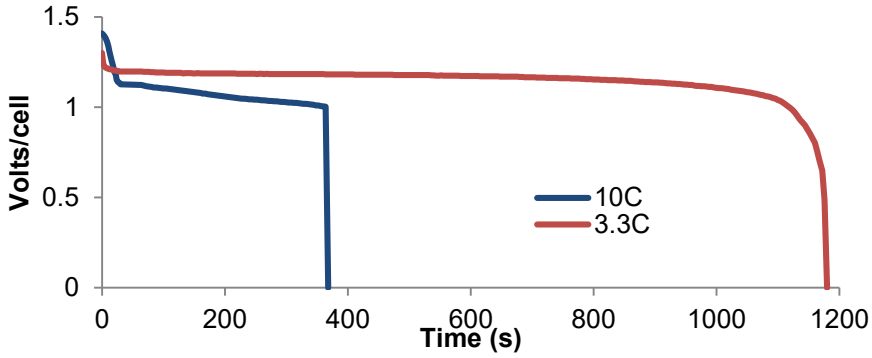

Figure 8.1: Battery discharge rates.

Motors and Propellers: Three motor-prop combinations were tested, based on the calculations described in Section 4. These combinations were modeled within MotoCalc, then the results verified against wind tunnel data. Figure 8.2 gives the efficiency curves for all three motor-prop combinations. Figure 8.3 gives the thrust curves for all three motor-prop combinations.

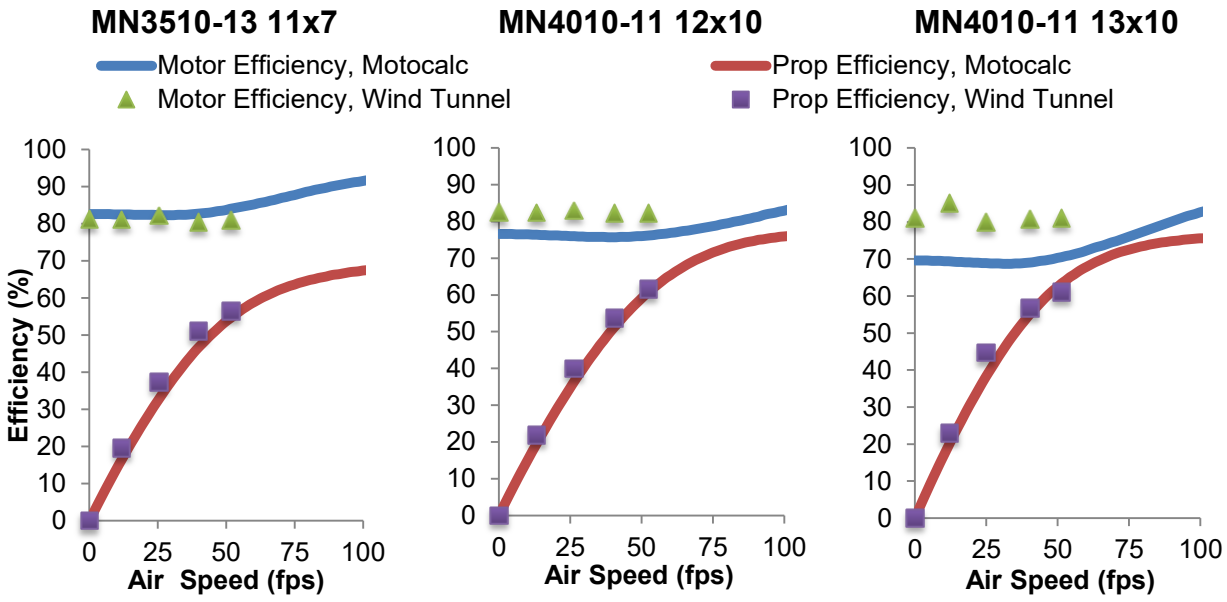

Figure 8.2: Motor efficiencies predicted by MotoCalc and wind tunnel testing.

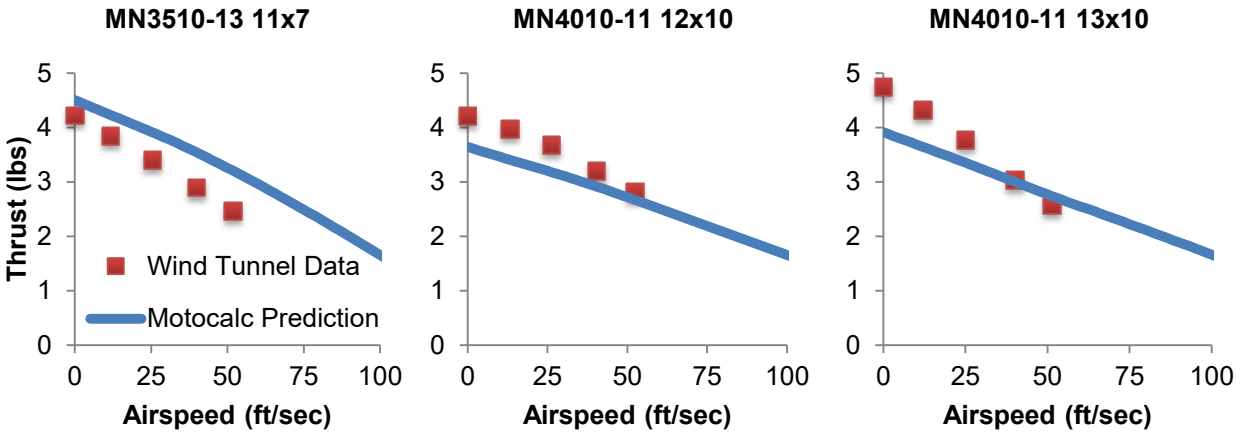

Figure 8.3: Error between motor efficiencies predicted by MotoCalc and wind tunnel testing.

Figure 8.2 shows that the motor and propeller efficiencies predicted by MotoCalc are largely corroborated by the wind tunnel data. Figure 8.3, however, demonstrates significant discrepancies in the thrust prediction. MotoCalc over predicts the thrust for the Tiger MN 3510-13, but under predicts thrust for the MN 4010-11. This drove the selection of the latter as the final propulsion system. The difference between the two data sources potentially arises from the propeller model used in MotoCalc. While the efficiency curves are well aligned, it is possible that MotoCalc's propeller calculation method causes the error in thrust. Further investigation is necessary to determine the exact cause of the discrepancy, and to evaluate alternative propulsion analysis methods.

8.1.2 Structural Tests

Wing Testing Results: The full size airplane was subjected to the required wing tip testing specified in the rules as part of the technical inspection process. This was done by loading the full internal Mission 2 payload of three blocks into the payload bay, then lifting the airplane by the wing tips. The successful wing tip test is shown in Figure 8.4.

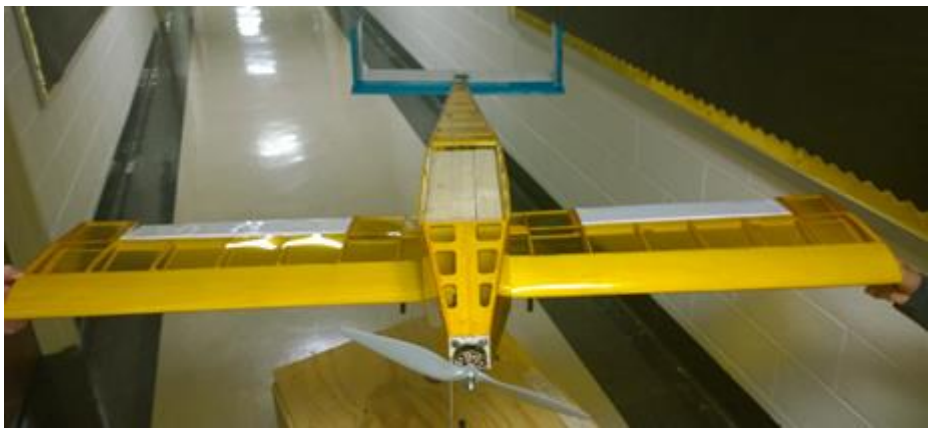

Figure 8.4: Wingtip Structural Test with Full Payload.

8.2 System Performance

A loading time test determined the time required to run from the safe zone to the aircraft and load the M2 payload was 12 seconds. This time was assumed to be constant for each run. The M3 loading time was then timed using the method described in Section 7.3. Initially the time required to load a single ball was 2.0 seconds. The team believes the time to load a single ball can be decreased to the predicted time of 1.5 through practice. Summing the floor M2 payload time of 12 seconds with the fastest ball loading time of 2.0 seconds per ball, it was found that the team could achieve a total loading time of 28 seconds with a minimum possible time of 24 seconds. A picture taken during a loading test is shown in Figure 8.5.

Figure 8.5: Payload Loading Time Testing.

Flight tests of *Buzz Killington* were performed to evaluate the performance of the aircraft and validate the performance predictions. The results indicate the performance predictions were realistic. Further optimization and increasing pilot familiarity with the system should improve system performance to meet or exceed the predicted performance.

To evaluate system performance during flight testing beyond simple lap timing and takeoff performance, the team equipped the aircraft with a data collection system that could be used to compare to the estimated mission performance in Section 5. The team purpose-built an Arduino-based telemetry system with a live data feed. On a number of test flights, the Arduino was mounted to the aircraft and recorded

GPS at 1 Hz to yield trajectory data. An example of a full lap trajectory is displayed in Figure 8.6 superimposed on satellite imagery using Google Earth.

Figure 8.6: Trajectory of aircraft during competition laps from GPS data.

The results of flight testing are shown in Table 8.1:

Table 8.1: Comparison of Predicted and Actual Performance Averages.

	1st Lap Time (s)		Time for 360		Balls Carried		TOFL	
	Predicted	**Actual**	**Predicted**	**Actual**	**Predicted**	**Actual**	**Predicted**	**Actual**
M1	27.4	33.1	3.49	3.15	-	-	6.72	17
M2	40.07	54.2	7.45	8.46	-	-	53.2	57
M3	-	-	-	-	8	2	10.76	15

Discrepancies between predicted and actual times for a 360 degree turn are low. Much of the difference between the two figures can be explained by pilot behavior. In all cases, time for a 360 degree turn was predicted assuming maximum velocity. However, during testing, the pilot tended to reduce speed slightly when going into a turn, which reduced the turn radius. For M3, the discrepancy was due to the test pilot flying conservatively so as not to inadvertently over stress the aircraft in a turn. These discrepancies could be caused by inconsistent turning radii of the pilot compared to an ideal turn.

Discrepancies between predicted and actual TOFL vary significantly for M1 and M3, and slightly for M2. While M2 takeoff distance is currently within competition bounds, a reduction in weight to increase the safety margin is necessary. M1 and M3 discrepancies are a result of differences between pilot actual behavior and assumed behavior. The model used for calculating TOFL assumes that the pilot immediately advances to maximum throttle, but the pilot has been taking off more conservatively to maintain ground steering.

Buzz Killington can achieve at total of 7 laps in four minutes for M1 based on the recorded flight times. Further optimization of the system is required to achieve 8 laps. The team plans to accomplish this by decreasing the landing gear height to reduce weight and drag. In addition, increasing pilot familiarity with the system will allow for a reduction in lap times. The team believes with these optimizations, 8 laps can be achieved as predicted.

Flight testing was also used to validate M3 feasibility. Testing has not completed full M3 laps at this time, but it is expected that the aircraft will be able to complete all laps required for M3 without exhausting the batteries. Testing demonstrates that the drop mechanism described within Section 5.3.5 is fully capable of dropping one ball, on command, without requiring an unsafe acrobatic maneuver. The aircraft is shown dropping a ball during a test flight in Figure 8.7.

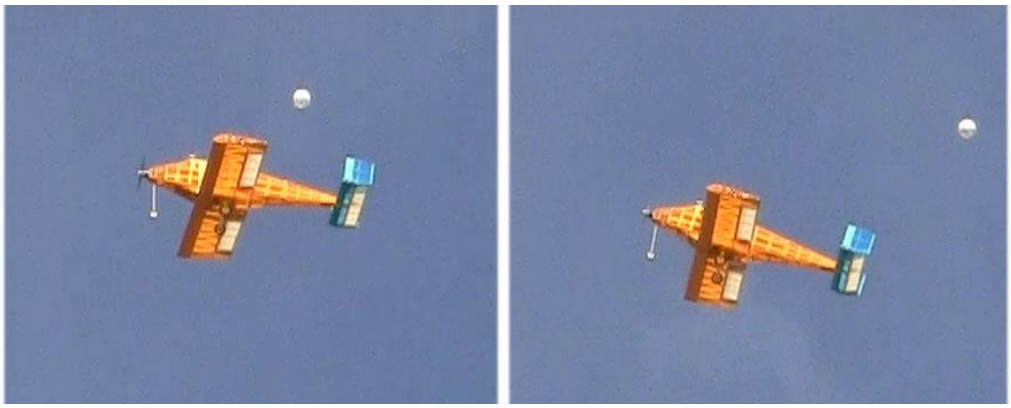

Figure 8.7: In flight release of payload.

In summary, as of the time of this report, seventeen flight tests have been performed on two different prototypes. Although flight testing revealed Mission 1 scores may be lower at the competition than analysis predicted, the research, component selection, and testing that fed into the design process resulted in a lightweight aircraft capable of lifting three blocks for Mission 2, drop payload successfully for Mission 3, all without suffering major losses to speed. The concept of a single-engine, low wing, conventional aircraft proved to be successful in completing the loading mission and all flight missions, and was proven through laboratory testing to be lighter than other designs of an equivalent power level. The *Buzz Killington* team is eagerly awaiting more testing opportunities to ensure success during all missions at the competition and hone pilot familiarity with the aircraft. The team is confident that the overall configuration for *Buzz Killington* as shown in Figure 8.8 has the best scoring potential, and is positioned to place well in Tucson.

Figure 8.8: Final Aircraft.

9. REFERENCES

Anderson. J. D. *Fundamentals of Aerodynamics,* 4th edition, McGraw Hill.

Bauchau, O. A., & Craig, J. I. (January 7, 2009). *Aerospace Structural Analysis.* Springer.

Drela, M., & Youngren, H. (2008, 08 04). *AVL.* Retrieved 01 10, 2009, from [http://web.mit.edu/drela/Public/web/avl/].

Drela, M., & Youngren, H. (2008, 04 07). *XFOIL.* Retrieved 10 01 2008, from Subsonic Airfoil Development System: [http://web.mit.edu/drela/Public/web/xfoil/].

Hoerner, Sighard F. *Fluid Dynamic Drag*. 2nd. Published by author, 1965.

Katz, Joseph and Maskew, Brian. "Unsteady low-speed aerodynamic model for complete aircraft configurations," *Journal of Aircraft.* Vol. 25, pp. 302-310. Apr. 1988.

McDaniel, Katie et al. (2008). *Georgia Institute of Technology Team Buzzed*. Editor: Johnson, Carl.

Phillips, Warren F. *Mechanics of Flight*. 1st. Hoboken, NJ: Wiley, 2004.

Roskam, Jan. *Airplane Design Part VI*. Darcorp, 2000.

Roskam, Jan. *Airplane Flight Dynamics and Automatic Flight Controls Part I*. Darcorp, 2007.

Selig, M. (2008, 02 19). *UIUC Airfoil Data Site*. Retrieved 10 01, 2008, from [www.ae.uiuc.edu/m-selig/ads.html].

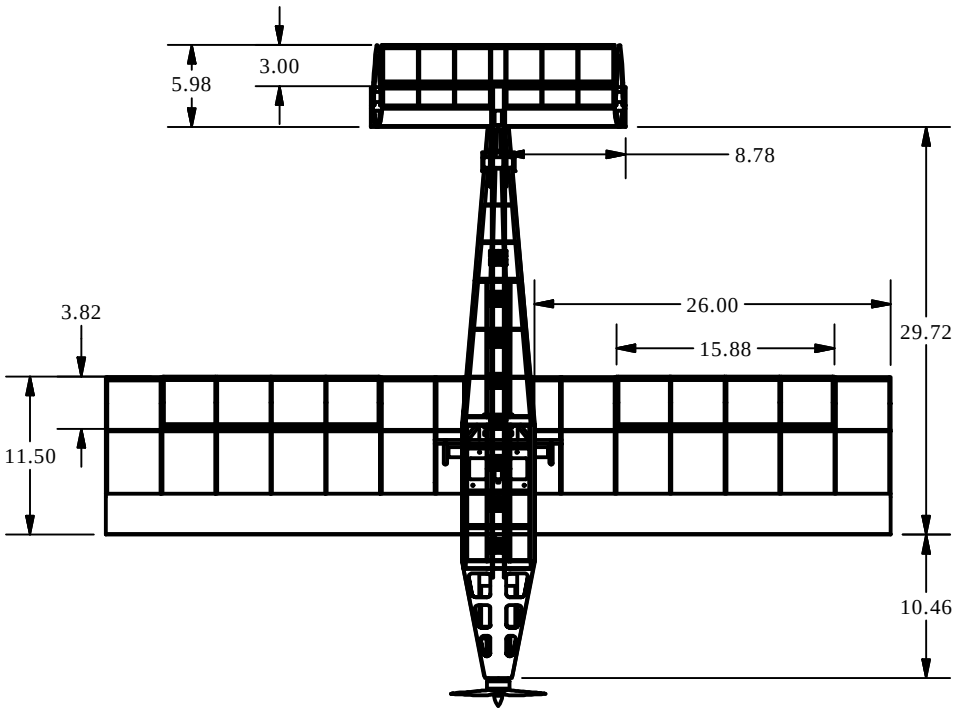

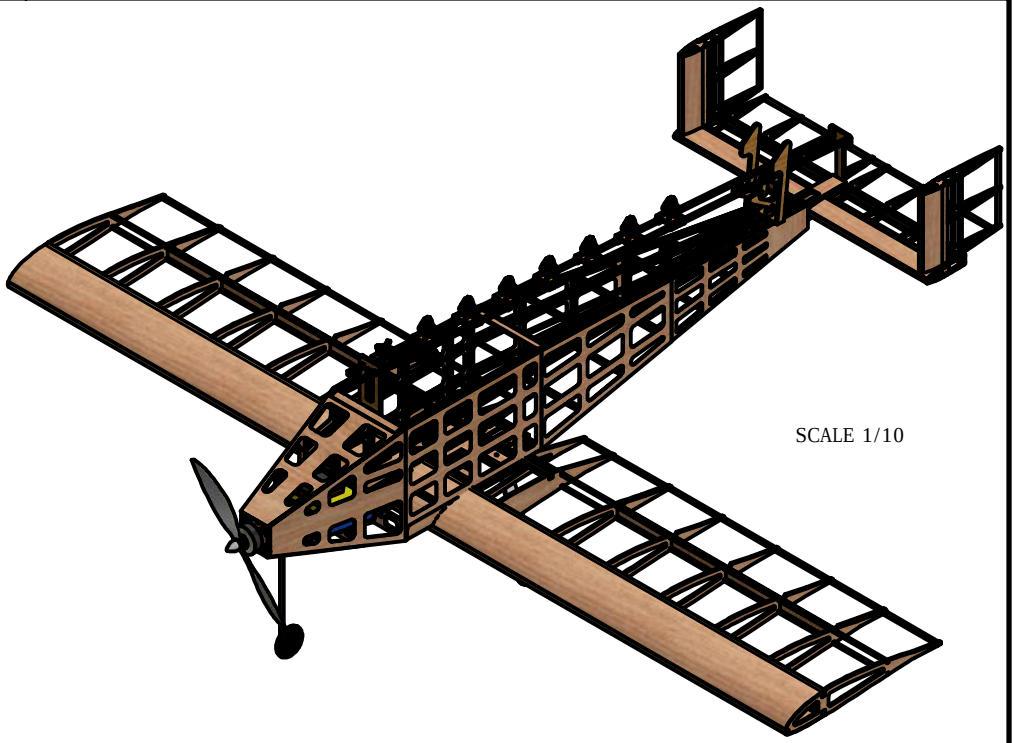

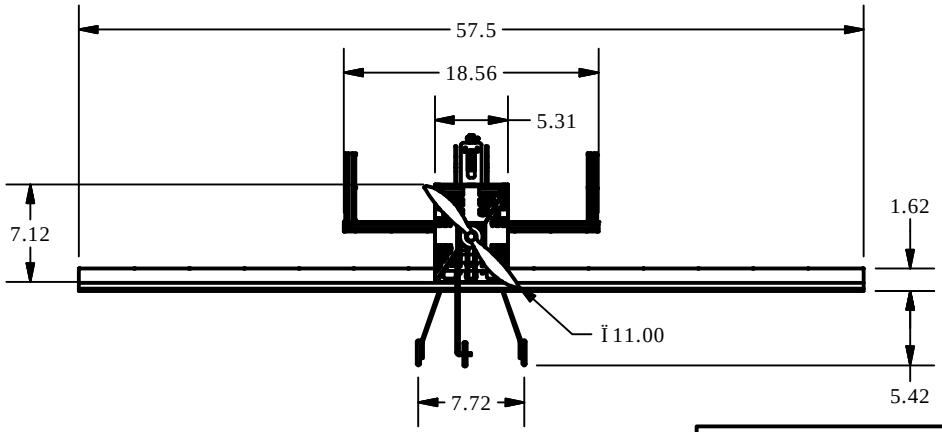

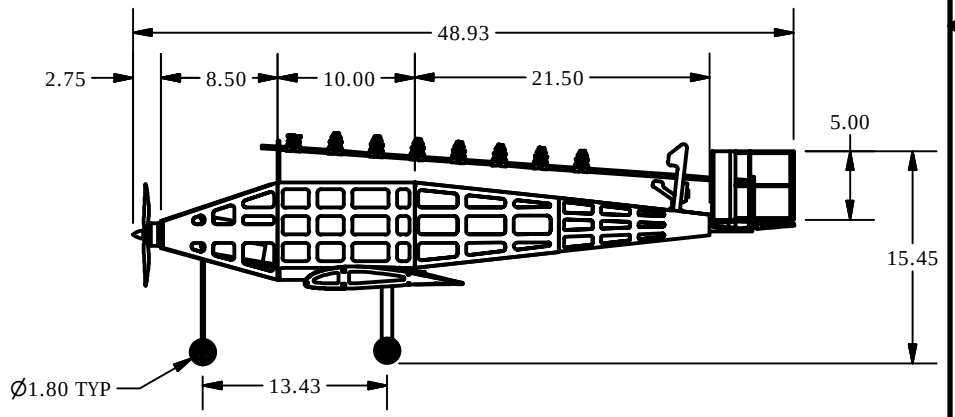

DRAWN	David Gaitan
CHECKED	George P. Burdell
	2/19/2015

Georgia Institute of Technology

Buzz Killington

SIZE	DWG	
A	Three View Drawing with Dimensions, M1 Configuration	
SCALE 1/14	All Dimensions in Inches	SHEET 1 OF 1